UNIVERSITY OF CALIFORNIA SAN DIEGO

A multi-scale analysis of coral reef resilience in the Hawaiian Islands

A Dissertation submitted in partial satisfaction of the requirements
for the degree Doctor of Philosophy

in

Marine Biology

by

Orion Stefan McCarthy

Committee in charge:

Jennifer E. Smith, Chair
Eric Conklin
Lisa A. Levin
Katharine Ricke
Stuart A. Sandin

2024

The Dissertation of Orion Stefan McCarthy is approved, and it is acceptable in quality and form for publication on microfilm and electronically.

University of California San Diego

2024

DEDICATION

This dissertation is dedicated to the people of Maui, especially the community of Lāhainā, whose generosity, insights, and hospitality made this research possible. It is fitting that this dissertation chronicles the resilience of Maui's benthic communities to climate change. Above the waves, a climate-induced inferno has demonstrated the remarkable resilience of Maui's human communities as well. Faced with unimaginable hardship and loss, their unflinching tenacity and commitment to one another has carried them through. To my friends and colleagues on this beautiful island, I commend your resilience and have faith for a prosperous future for Maui, from mauka to makai.

TABLE OF CONTENTS

LIST OF FIGURES

LIST OF TABLES

LIST OF ABBREVIATIONS

AUV	Autonomous underwater vehicle
CAP	Canonical analysis of principal coordinates
CCA	Crustose coralline algae
COTS	Crown of thorns starfish
CRAMP	Hawai'i Coral Reef Assessment and Monitoring Program
D	Fractal dimension
DAR	Hawai'i Division of Aquatic Resources
DEM	Digital elevation model
DHW	Degree heating weeks
FFS	French Frigate Shoals
FNU	Formazin Nephelometric Unit
GAM	Generalized additive model
HAW	Hawai'i Island
KAH	Kaho'olawe Island
K-S test	2-sample Kolmogorov-Smirnov test
KUR	Kure Atoll
LAI	Large-area imagery
LAN	Lāna'i Island
LIS	Lisianski Island
MAI	Maui Island
MHI	Main Hawaiian Islands

MOL	Moloka'i Island
NGO	Non-governmental organization
NMDS	Non-metric multidimensional scaling
NOAA	National Oceanic and Atmospheric Administration
NWHI	Northwest Hawaiian Islands
OAH	Oah'u Island
PERMANOVA	Permutational multivariate analysis of variance
PHR	Pearl and Hermes Reef
RMS	Root mean square height
SD	Standard deviation
SE	Standard error
SfM	Structure from Motion
SIO	Scripps Institution of Oceanography
TNC	The Nature Conservancy
VPG	Virtual profile gauge tool
VPI	Virtual point intercept tool

ACKNOWLEDGEMENTS

When I think about my time at the Scripps Institution of Oceanography, the primary emotion I feel is gratitude. As a child, I used to dream about exploring the ocean, “saving” nature, and uncovering secrets about the natural world. The life changing opportunities I’ve had access to while at Scripps have exceeded even my wildest childhood dreams and curiosity. From diving in Maui, Palmyra, and Micronesia to attending the UN Global Climate COP in Egypt, I’ve been able to experience marine science and policy up close and hands on. Equally as impactful have been opportunities to manage a monitoring program, organize and lead multiple field expeditions, teach and mentor students, and learn from and collaborate with world-class researchers. These collective opportunities have undoubtedly shaped my development as a scientist. My sense of gratitude extends beyond this formal training to the life-long friendships I’ve had the fortune of making as part of the Scripps community.

These formative years and opportunities would not have been possible without the support, collaboration, and friendship of so many. First, I would like to thank my advisor Jennifer Smith, who brought me into the Smith-Sandin lab family nearly six years ago. Jen is an incredibly accomplished researcher and has shaped countless students, myself included, by challenging us to carefully observe the natural world, develop and refine our ecological questions, and broadly communicate our findings. Jen encouraged me to pursue opportunities such as the QUEST field school and field work in Palmyra, and her decades of prior work in Hawai'i informed nearly every aspect of my research. I am extremely grateful for the trust and autonomy she has afforded me by letting me take ownership of our lab’s Maui Nui long-term monitoring program, which has been an incredibly rewarding and informative experience. Jen also helped to broaden my horizons by introducing me to the hidden world of seaweed and

temperate marine ecology, which allowed me to better appreciate ecosystems in my own backyard.

In addition to Jen's mentorship, I would like to thank my other committee members for guiding my Scripps journey and shaping this dissertation. Stuart Sandin has always been an enthusiastic thought partner, and I've enjoyed our many brainstorming sessions about statistics, rugosity, and large-area imaging. I admire Stuart's creative and lofty visions for coral reef monitoring and conservation technology, and am grateful for the opportunity to work closely with him and his entire lab on one of those visions, the 100 Island Challenge. I am grateful to Lisa Levin for her insight into the world of ocean and climate policy, and I feel privileged to have been able to discuss these topics with her both in a classroom setting and halfway across the world at COP 27 in Egypt. Similarly, Kate Ricke and Eric Conklin both encouraged me to thoughtfully consider the policy applications of my research as well as its relevance to practitioners. Their focus on policy and applied conservation have helped increase the potential impact of the results presented here.

Beyond my committee, my graduate school experience was profoundly shaped by those in the Scripps community. First and foremost, I can confidently say that my time at Scripps would not have been the same without the Hubbs Homies: Erik Saberski, Anela Akiona, Ivan Moreno, Carol Contreres, Emma Choi, Onyx, and Lava. Their unconditional friendship felt like family. I will cherish our countless hangouts playing Jackbox or AmongUs at the Beach House, walks to Brick and Bell, pint nights at Shore Rider, and outings for tacos, ramen, and Salt and Straw. Erik and Onyx kept me entertained, Anela kept me alive in the field, Emma ensured that I never won a board game, and Ivan and Carol's generosity ensured that good vibes were always in abundance.

The Smith and Sandin Labs were another wonderful source of community for which I am incredibly thankful. First, I am grateful to Jill Harris, one of Jen's earliest PhD students who happened to be my supervisor while I was an intern at the World Wildlife Fund in 2016. I would not have made it to Scripps without Jill's mentorship: she helped introduce me to coral research and put Jen's lab and Scripps on my radar in the first place. I am also indebted to Emily Kelly, another of Jen's early PhD students who pioneered our lab's research in Maui. Emily's foresight to start using large-area imaging to document Maui's reefs back in 2014 (one year before a major bleaching event) made it possible to consider the research questions in this dissertation. Furthermore, Emily formed a nurturing community of collaborators in Maui that welcomed me with open arms. Even though we never directly overlapped at Scripps, Emily always made herself available to share insights and talk through challenges, and her unbridled enthusiasm helped to keep me excited and engaged. Our chance encounter at COP 27 and impromptu snorkeling adventure in the Red Sea was the perfect capstone to years of virtual collaboration.

The Smith and Sandin lab family has been the keystone of my graduate experience. I am grateful to Samantha Clements for training me in all aspects of Maui field work, and for her tireless effort behind the scenes to keep the Smith Lab functioning. Maui field work also offered me the opportunity to train the next generation of Smith Lab researchers, including Sarah Romero and Mitchell Smelser. Watching them mature as scientists over the past few years has been a delight, and I cherish our time spent together on and under the water in Maui. Special thanks to the 100 Island Challenge team for routinely lending us equipment for our Maui surveys, especially Brian Zgliczynski, Chris Sullivan, and Nathaniel Hollaway for expertly organizing and prepping field gear. I'm also grateful for field work buddies Clinton

Edwards and Ahmyia Cacapit, who I accompanied to Palmyra and Micronesia, respectively. Clint has been a gracious mentor, and I admire his intense passion for ecology and thoughtful insights. Thank you, Ahmyia, for always exuding good vibes and for being my submersible buddy on Oroluk Atoll – the Pristine Seas expedition wouldn't have been the same without your cheery presence. I am also grateful to Bella Doohan, Danielle McHaskell, and Mohammad Sedarat for the opportunity to participate in their local field work, in the intertidal, rocky reefs, and kelp forests respectively. Throughout my time at Scripps, I relied heavily on Nicole Pedersen and Vid Petrovic for technical support and training. Thank you, Vid, for your creative vision and dedication to developing Viscore into such a unique and useful piece of ecological software. Nicole, thank you for the many hours spent building 3D coral reef models, organizing data, and walking me through Viscore's intricacies. I also want to thank Beverly French and Adi Khen (and Kiwi) for creating a warm and welcoming environment in our lab family. Special thanks to Adi for her amazing graphic design (which is heavily featured in this dissertation). I also want to thank all past lab members for their general mentorship and collaboration, especially Lindsay Bonito, Sho Kodera, Jonny Charendoff, Corinne Amir, and Esmerelda Alcantar. Amanda Carter, thank you for suggesting that I focus my research on Maui during my first quarter at Scripps – that advice proved to be formative.

Studying Maui Nui's reefs has been a major highlight of my career, and this experience wouldn't have been possible without the generosity of local partners, our lab's Maui family. Special thanks to George and Donna Brown and to Will and Meghan Dailer for opening your homes to us and our van-load of gear, and to Lee James, Craig and Amy Venema, and Peter and Toni Colombo for captaining us safely from Lāhainā to our sites and

back again each day. Thank you, Don McLeish, for your snorkeling insights and generous use of your beach cart. This work would not have been possible without local businesses in Lāhainā, including Ultimate Whale Watch, Maui Divers, Dive Maui, and Aina Nalu. I especially want to thank the staff of the Division of Aquatic Resources and the Kaho'olawe Island Reserve Commission for their partnership, permitting, and support, especially Russell Sparks, Kristy Wong Stone, Cole Peralto, Tatiana Martinez, and Itana Silva, Catherine Gewecke, Dean Tokeshi and Michael Naho'opi'i. I would also like to thank Anna Rothstein, Maya deVries, and their team from San Jose State University for inviting me to join their 2022 field season in Maui. Anna's enthusiastic camp counselor energy carried us through. Thank you as well to the broader Hawai'i marine science community. In particular, I would like to thank my collaborator Morgan Winston for her partnership on Chapter 4, including the countless hours spent tracing corals and troubleshooting DEMs. In addition, I'd like to thank Ray Boland, Courtney Couch, Mary Donovan, Michael Iacchei, Jeff Kuwabara, Tom Oliver, Darla White, and the staff of QUEST and the UH Marine Option Program for their advice, support, and mentorship. Beyond Hawai'i, I would like to thank the Nature Conservancy's Palmyra Team and the National Geographic's Pristine Seas team for allowing me to broaden my horizons via incredible field work experiences.

The research presented in this dissertation wouldn't be possible without the hard work of numerous undergraduate volunteers, including Andre Lai, Conor Elliott, Elise Gonzales, Kanisha Contractor, Miles Kaufman, Mitchell Smelser, Sabrina Sauri, Solomon Chang, Varun Sachin Shirhatti, and Victoria Vasquez. Special thanks to Kanisha Contractor for going above and beyond to support research in Chapter 1, including by taking notes on late night zoom calls and combing through the coral reef literature. I would also like to thank Queer@Scripps

for providing a valuable source of community amidst the challenging environment of graduate school, particularly Austin Carter, Hannah Adams, and Noel Gutierrez-Brizuela. I am grateful to past Scripps students who have served as mentors, particularly Yui Takeshita, Garfield Kwan, Erica Ferrer, and Kayla Blincow. Finally, I would like to thank the 2018 Scripps cohort for their support and friendship, particularly Vanessa ZoBell, Athina Lange, Bethan Wynne-Cattanach, Alex Andriatis, Tricia Light, Pascal Polonik, Alli Ho, Max Rintoul, Gabby Negrete-Garcia, Monica Thukral, Duncan Wheeler, Emelia Chamberlain, Anne Schulburg, Rob Lampe, Ariel Rabines, and Philipp Arndt.

In addition to Scripps students, I want to thank the staff at Scripps who elevate our research and make it possible to pursue such amazing opportunities. In particular, thank you to the Scripps Dive Office (Christian McDonald, Rich Walsh, Ashleigh Palinkas, Jessica Hallisey, and Phil Zerofski) for your training, technical expertise, watchful oversight, and safety ethos. Special thanks to Melissa Torres for welcoming me into the Birch's volunteer program, allowing me to fulfil my childhood dream of diving in an aquarium. Thank you to the Scripps Grad Office, the Scripps Communications Office, and the Center for Marine Biodiversity and Conservation for answering my questions, elevating my research, ensuring I had the means to pursue cool opportunities and got paid every month. In this regard, I'd like to specifically thank Gilbert Bretado, Shelly Weisel, Keiara Auzenne, Dejan Ristic, Allison Kellum, and Rob Monroe. Thank you to Samantha Murray, Brice Semmens, Peter Franks, and Jenni Brandon for their engaging instruction about ocean law and policy, statistics, writing, and science communication. Finally, I'd like to thank the National Science Foundation, the Scripps department, Michael Joo, and the Ferguson Family for providing funding to support my research.

Beyond the Scripps community, I want to acknowledge the years of mentorship and support that enabled me to attend Scripps in the first place. Thank you to the teachers who went above and beyond to inspire me: Megan Dieckman, Chris Brown, Charlie Demma, Jennifer Edwards, Laura Flicker, John Giles, Jennifer Murrow, Kelly O'Connor, and Jonathon Verock. Outside of an academic setting, I would also like to thank my amazing colleagues and mentors from the Meridian Institute, the International Pacific Halibut Commission, the World Wildlife Fund, and the Smithsonian National Zoo. You not only worked alongside me, you took a vested interest in my success and showed me what a career in marine science, conservation, and environmental policy could look like. Specific thanks to Gabby Ahmadia, Mallorie Bruns, Laura Cantral, Gwendolyn Cooper, Gary Decker, John Ehrmann, Helen Fox, Kiera Givens, Sophie Gunderson, Ingrid Irigoyen, Heather Lair, Meghan Massaua, Jeff Maynard, Tim Mealy, Molly Mayo, Marielena Octavio, Robyn Paulekas, Diana Portner, Lauri Sadorus, Annie Shapiro, Lucas Smith, Isabella Soparkar, and Ian Stewart. Thank you to my Meridian colleagues in particular for proofreading my NSF Graduate Research Fellowship Application back in 2017. My attendance at Scripps (and all of the research presented here) was predicated on the success of that GRFP application. You helped push me over the finish line, and I will be forever grateful for that.

Finally, I wouldn't be where I am today without my family and friends. I feel incredibly lucky to come from a large extended family and have a close-knit group of friends, the Condor Alliance. Their unconditional love and support encouraged me to take this journey and have kept me afloat through good times and bad. I'd specifically like to thank my parents, Roula and Brian, for recognizing my love of nature at an early age and providing me with countless opportunities to pursue this passion, from snorkeling excursions to summer camps

at the zoo. You've always encouraged me to think creatively, be open minded, foster community, and to someday change the world. Every day I try my best to live up to that tutelage. To my sister Zoe, thank you for your companionship, passion, and curiosity over the last three decades. Your genuine interest in this research informed my approach to writing, and you were the first (and perhaps only) person to read this dissertation cover to cover. I'm excited by the prospect of working together to develop this dissertation into an interactive animation. Finally, I want to thank my partner Chance Dunbar for being at my side through the highs and lows of graduate school. Much like Zoe, Chance has taken a real interest in my research, nurtured my passion for the ocean, pushed me to think critically, and even helped me refine several of my research ideas (how does one define resilience anyways?). More importantly, he has been a reliable partner, a constant cheerleader, a source of entertainment, my literal dive buddy, and a steadfast friend. I can't thank him enough for his support these last four years, and look forward to many more.

Chapter 1, in full, is a reprint of the material as it appears in Conservation Biology. McCarthy, Orion S.; Contractor, Kanisha; Figueira, William F; Gleason, Arthur C. R.; Viehman, T. Shay; Edwards, Clinton B; Sandin, Stuart A. 2023. The dissertation author was the primary investigator and author of this paper.

Chapter 2, in full, is a reprint of the material as it appears in Marine Ecology Progress Series. McCarthy, Orion S.; Smith, Jennifer E.; Petrovic, Vid; Sandin, Stuart A. 2022. The dissertation author was the primary investigator and author of this paper.

Chapter 3, in part, is currently being prepared for submission for publication of the material. McCarthy, Orion S.; Kelly, Emily L. A.; Akiona, Anela K.; Clements, Samantha M.; Martinez, Tatiana; Pedersen, Nicole E.; Peralto, Cole; Ricke, Katharine; Romero, Sarah L.;

Silva, Itana F.; Smelser, Mitchell H.; Stone, Kristy W.; Sparks, Russell T; Smith, Jennifer E. The dissertation author was the primary researcher and author of this material.

Chapter 4, in part, has been submitted for publication of the material as it may appear in PLoS ONE, McCarthy, Orion S.; Winston, Morgan; Smith, Jennifer E., 2024. The dissertation author was the primary researcher and author of this paper.

Chapter 5, in part, is currently being prepared for submission for publication of the material. McCarthy, Orion S.; Conklin, Eric; Ricke, Katharine; Sparks, Russell T.; Smith, Jennifer E. The dissertation author was the primary researcher and author of this material.

VITA

2015 Bachelor of Science in Ecology and Evolution, University of Maryland, College Park

2018 William Ruckelshaus Fellowship, Meridian Institute, Washington DC

2024 Doctor of Philosophy in Marine Biology, University of California San Diego

PUBLICATIONS

Edwards CB, Viehman TS, and 20 other co-authors, including **McCarthy OS**. 2023. Large-area imaging in tropical shallow water coral reef monitoring, research and restoration: A practical guide to survey planning, execution, and data extraction. NOAA National Ocean Service, National Centers for Coastal Ocean Science. NOAA Technical Memorandum NOS NCCOS 313. https://repository.library.noaa.gov/view/noaa/55814

McCarthy OS, Contractor K, Figueira WF, Gleason ACR, Viehman TS, Edwards CB, Sandin SA. 2023. Closing the gap between existing large-area imaging research and marine conservation needs. *Conservation Biology*, e14145. https://doi.org/10.1111/cobi.14145

McCarthy OS, Smith JE, Petrovic V, Sandin SA. 2022. Identifying the drivers of structural complexity on Hawaiian coral reefs. *Marine Ecology Progress Series*, 702: 71-86. https://doi.org/10.3354/meps14205

Loher T, **McCarthy OS**, Sadorus LL, Erikson LM, Simeon A, Drinan DP, Hauser L, Planas JV, Stewart IJ. 2022. A test of deriving sex-composition data for the directed Pacific halibut (*Hippoglossus stenolepis*) fishery via at-sea marking. *Marine and Coastal Fisheries*. 9999:e10218. https://doi.org/10.1002/mcf2.10218

Surowidjojo A and 19 co-authors, including **McCarthy OS**. 2019. *The Legal Framework and Government Institutional Landscape of the Fisheries Sector in Indonesia*. Jakarta, Indonesia. https://bit.ly/3Yrw2HM

Harris JL, Estradivari E, Fox HE, **McCarthy OS**, Ahmadia GN. 2017. Planning for the future: incorporating global and local data to prioritize coral reef conservation. *Aquatic Conservation: Marine and Freshwater Ecosystems*, 27(S1): 65-77. https://doi.org/10.1002/aqc.2810

LaBelle R, Leonard K, Schultz G, and 172 co-authors and contributors, including **McCarthy OS**. 2017. *Mid-Atlantic Regional Ocean Action Plan*. https://www.boem.gov/environment/mid-atlantic-regional-ocean-action-plan

ABSTRACT OF THE DISSERTATION

A multi-scale analysis of coral reef resilience in the Hawaiian Islands

by

Orion Stefan McCarthy

Doctor of Philosophy in Marine Biology

University of California San Diego, 2024

Jennfier Smith, Chair

Coral reefs hold immense ecologic, economic, and social value, yet these important ecosystems face an existential threat from global climate change. Coral reef conservation is thus an urgent international priority, yet it can be challenging to design and implement effective conservation measures due to the innate complexity of coral reef ecosystems. Coral reef "resilience" is shaped by numerous environmental, biotic, and anthropogenic processes that operate across a range of scales. A particular conservation strategy might be appropriate for one set of conditions but fail to adequately protect reef health in another. Robust coral reef

monitoring data can help natural resource managers identify the key processes impacting a given reef and design appropriate management interventions.

We demonstrate how new conservation technology, specifically large-area imagery (LAI), can enhance our ability to study ecosystem processes across multiple scales in space and time, identify drivers of ecosystem condition, and inform site-specific decision making. Here, we use Hawaiian coral reefs as a case study to investigate multiple reef processes using multi-scale LAI data, specifically 1) habitat structural complexity, 2) benthic community succession, and 3) coral bleaching, growth, and survivorship in response to thermal stress. We apply these findings to quantify "resilience" (specifically patterns of resistance and recovery) at multiple scales for forereefs in leeward Maui. We use this multi-scale data to critically evaluate the predictive accuracy of coral reef resilience assessments, a popular conservation triage and marine spatial planning tool. In doing so, we demonstrate the potential of LAI to inform conservation decision making, and we recommend steps that can be taken to make this conservation technology more accessible to practitioners.

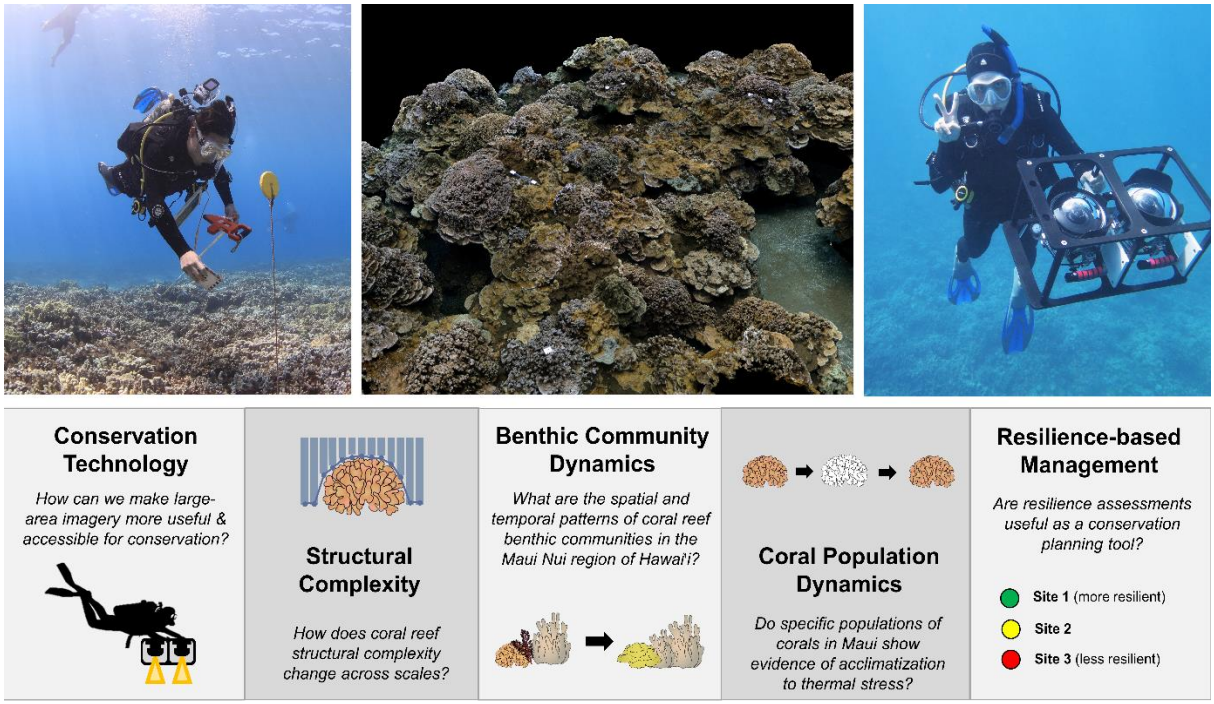

INTRODUCTION

Coral reefs are among the most important ecosystems on the planet. Even though they constitute less than 1% of the ocean's total area, they provide habitat for 25% of known marine species (Plaisance et al. 2011). Due in part to their biodiversity, coral reef fisheries provide sustenance to approximately one billion people worldwide, primarily those residing in coastal communities in the Global South (Wong et al. 2022). Coral reefs also generate revenue through ecotourism, form a naturally regenerating barrier that protects communities from storm damage, and provide cultural value to nearby communities (Woodhead et al. 2019; Giglio et al. 2023). In total, coral reefs are estimated to provide $9.9 trillion per year in ecosystem services (Costanza et al. 2014).

Despite their importance, coral reefs are rapidly transforming (Done 1992; Graham et al. 2011; Hughes et al. 2018). The corals that grow to build these reefs are vulnerable to changes in environmental conditions caused by humans at local and global scales (Good & Bahr 2021). Local impacts include overfishing, nutrient pollution and sedimentation from coastal development and agriculture, introduction of invasive species, and damage from irresponsible tourism (Donovan et al. 2021, 2023b; Andrello et al. 2022; Gove et al. 2023; Weng et al. 2023). At a global scale, widespread emissions of greenhouse gasses are changing the climate, leading to adverse impacts for coral reefs (van Hooidonk et al. 2016). These impacts include rising sea levels, ocean acidification and deoxygenation, increased frequency and severity of tropical storms, and frequent marine heatwaves that can lead to coral bleaching (Hoegh-Guldberg et al. 2007; Sully et al. 2019; Hughes et al. 2020; van Woesik et al. 2022). During the most recent global coral bleaching event, which lasted from 2014 to 2017, 75% of the world's coral reefs

experienced heat stress intense enough to cause coral bleaching, which led to widespread loss of corals on reefs around the world (Eakin et al. 2019).

Given the value of coral reefs for both people and wildlife, as well as the rapid environmental shifts that are already occurring under climate change, we must deploy the best science available to inform conservation that can target and alleviate sources of coral degradation. This requires us to understand the current status of coral reefs around the world so that we can identify where reefs are declining, which reefs are doing better than expected, and what drivers are responsible for those trends (Cinner et al. 2016; Camp 2022; Sully et al. 2022). With this information in hand, we can recommend targeted actions to improve coral reef health and persistence (McClanahan et al. 2012; McLeod et al. 2021). To accomplish this goal, we need baseline data on coral reef condition, repeat surveys to see how reefs have changed, and environmental data to contextualize our observations (Dixon et al. 2021; Sandin et al. 2022).

Emerging technology has the power to expand our access to baseline data and our ability to study ecological processes across multiple scales in space and in time (Foo & Asner 2019; Ferrari et al. 2021; Speaker et al. 2021; Donovan et al. 2023a). The Smith and Sandin Labs at the Scripps Institution of Oceanography (SIO) have amassed an unprecedented dataset of coral reef condition through years of field surveys. This includes a global dataset of reef condition collected as part of the 100 Island Challenge, as well as a long-term annual coral reef timeseries from the island of Maui that dates back to 2014. For both Maui and the 100 Island Challenge, we use novel technology called large-area imaging to document reef condition. When we visit a reef, we use underwater cameras to take thousands of pictures of the benthos. Using the overlap between images, we are able to generate a composite 3D model that accurately reconstructs stationary objects in the environment (Westoby et al. 2012). These models form the basis of

"virtual fieldwork", or the process of extracting ecological data from the 3D models, unencumbered by the constraints of SCUBA (Edwards et al. 2023). This approach has made it easier to collect more detailed and multi-scale ecological metrics and to document subtle but important changes in reef condition over time that would be easily missed by divers in the water. Furthermore, we can use the 3D models to create visuals that convey changes in coral reef condition, be they degradation or recovery, to a broad audience.

This dissertation uses large-area imagery from Hawaiian coral reefs to address novel ecological questions across a range of scales, evaluate the efficacy of existing conservation approaches, and recommend steps for improving conservation and access to conservation technology. First, I describe how large-area imagery has been used to date to study coral reefs, identify systemic barriers that hinder access, and provide recommendations for how to make this technology more accessible for coral conservation efforts. In the subsequent chapters, I utilize large-area imagery to address gaps in the coral reef literature that I identified in chapter 1. Specifically, I document the role of abiotic and biotic factors on coral reef 3D habitat structure across the Hawaiian islands (chapter 2), investigate the impact of successive environmental disturbances on coral reef succession in Maui Nui (chapter 3), document evidence of selection for thermal tolerance and acclimatization following repeated bleaching events on Maui (chapter 4), and evaluate the predictive accuracy of a conservation planning method known as "resilience-based management" using multi-scale data collected from 3D reef models on Maui (chapter 5). Taken together, this body of research demonstrates how a new technology can be applied to inform conservation while faithfully accounting for myriad ecological processes across multiple scales. A brief summary of each chapter is enclosed below.

Chapter 1 – Closing the gap between existing large-area imaging research and marine conservation needs

As described above, large-area imagery allows researchers to study environmental change across novel scales in time and space, and creates compelling visuals for science and conservation outreach. While large-area imagery has potential as a form of conservation technology, barriers to adoption such as equipment cost, technical expertise, and staff capacity hinder broad, equitable use of this technology. Through a literature review and survey of coral reef scientists and conservation practitioners, we documented barriers to adopting large-area imagery and identified a mismatch between current applications (mainly by scientists from wealthy countries) and the interests of conservation practitioners. The applied conservation research described in later chapters is a first step toward closing this gap. Finally, to help address equity concerns around applications of this novel technology, we collaborated with survey participants to develop recommendations for making large-area imaging more accessible. This chapter was published in *Conservation Biology* in July 2023 (McCarthy et al. 2023).

Chapter 2 – Identifying the drivers of structural complexity on Hawaiian coral reefs

Coral reefs consist of a matrix of different microhabitats, from the interstitial space within coral branches to the crevices, overhangs, and channels formed within the reef substrate. These many microhabitats are part of the reason why coral reefs are hotspots of biodiversity, and are created by biotic and abiotic processes that operate across different scales. To track changes in reef habitat structure that are driven by coral growth or decline, we need to know what scales to focus on. Using reefs in Hawai'i as a case study, we quantified coral reef structural complexity at multiple different scales by measuring the fractal dimension of 3D reef models. We found that coral cover is the primary driver of structural complexity on Hawaiian coral reefs at small scales (mm to cm), while the geomorphology of the reef shapes structural complexity at larger scales

(meters). We found that reefs in the Main Hawaiian Islands had more fine-scale habitat structure associated with corals than reefs in the remote Northwest Hawaiian Islands. This chapter was published in *Marine Ecology Progress Series* in 2022 (McCarthy et al. 2022).

Chapter 3 – Fine-scale variation in community composition shapes ecosystem response to disturbance

Coral reefs in the Maui Nui region of Hawai'i demonstrate remarkably high levels of coral cover, but have recently been impacted by multiple disturbance events; a tropical cyclone sideswiped the region in 2018, a marine heatwave caused coral bleaching in 2019, and COVID-19 lockdowns changed human use patterns in 2020. Using a dataset of coral reef 3D models from 36 sites revisited in 2017, 2019, 2021, and 2023, we identified distinct coral communities that may represent different successional stages of leeward forereefs in the region. Each of these communities displayed unique trajectories over our timeseries in response to disturbance events. In particular, reefs with low coral cover dominated by the stress-tolerant coral *Porites lobata* experienced promising signs of recovery, while reefs with high coral cover dominated by the competitive coral *Montipora capitata* exhibited signs of degradation over time. Furthermore, community composition was highly variable at fine spatial scales, even on reefs exposed to similar environmental conditions. Taken together, these results suggest that coral reef management and conservation should account for site-specific factors such as a reef's disturbance history, local environmental impacts, and species composition.

Chapter 4 – Corals that survive repeated thermal stress show signs of selection and acclimatization

Targeted coral restoration is one of several methods for recovering degraded coral reefs, but to be successful, outplanted corals must be thermally tolerant so that they aren't lost to bleaching during future marine heatwaves. Identifying populations of thermally tolerant corals

that can serve as a source of outplants can help improve the success of restoration efforts. Using a timeseries of 3D coral reef models from Maui that spans two successive bleaching events (2015 and 2019), we tracked the bleaching response of hundreds of individual coral colonies representing four different taxa. This allowed us to identify coral populations with significantly higher proportions of thermally tolerant or acclimatizing coral colonies. Yet, across all surviving corals, we found little impact of bleaching history on coral growth. Our findings suggest that coral age could be an important indicator of resilience, and suggests that restoration practitioners should target larger, older colonies as a source of outplants for restoration. Understanding the spatial patterns of thermal tolerance and acclimatization around Maui will help resource managers decide where to source outplants for restoration and identify at-risk coral populations in need of conservation action. This chapter was submitted to PLoS One in January 2024.

Chapter 5 – Evaluating the predictive capacity of coral reef resilience assessments

As mentioned previously, coral reefs are threatened by both global stressors (climate change) and local stressors (i.e., overfishing, sedimentation, tourism, development, etc.). One approach to coral reef conservation, known as resilience-based management, aims to identify "resilient reefs" where local management actions can have the greatest conservation impact. This approach uses ecological indicators to predict the relative resilience of specific sites to climate change so that resilient reefs can be prioritized for management, thereby ensuring their persistence. This conservation approach is widely used on coral reefs but has rarely been validated following a disturbance event. We used our large-area imagery timeseries in Maui to recreate a resilience assessment conducted by the Nature Conservancy 2018. This research represents the first application of large-area imaging to conduct a resilience assessment and one of the only applications of large-area imaging to address applied conservation questions. By

using large-area imaging to conduct resilience assessments in five different years at sites used by the Nature Conservancy, we were able to test whether resilience predictions were consistent across survey years and methodologies. Furthermore, we validated the accuracy of these predictions by comparing them to observed patterns of resistance and recovery following the 2015 bleaching event. Importantly, we found that resilience assessments are capable of producing consistent predictions over time and across methods, but that these predictions did not align with observed resistance or recovery in leeward Maui. Additional research to identify appropriate functional indicators of resistance and recovery would improve future resilience assessments. For those planning or implementing resilience assessments, we encourage long-term monitoring to validate resilience predictions.

Chapter 1 – Closing the gap between existing large-area imaging research and marine conservation needs

Orion S. McCarthy, Kanisha Contractor, Will F. Figueira, Arthur C. R. Gleason,

T. Shay Viehman, Clinton B. Edwards, and Stuart A. Sandin

Abstract

Emerging technology has immense potential to increase the scale and efficiency of marine conservation. One such technology is large-area imaging (LAI), which relies on structure-from-motion photogrammetry to create composite products, including 3D environmental models, that are larger in spatial extent than the individual images used to create them. Use of LAI has become widespread in certain fields of marine science, primarily to measure the 3D structure of benthic ecosystems and track change over time. However, the use of LAI in the field of marine conservation appears limited. We conducted a review of the coral reef literature on the use of LAI to identify research themes and regional trends in applications of this technology. We also surveyed 135 coral reef scientists and conservation practitioners to determine community familiarity with LAI, evaluate barriers practitioners face in using LAI, and identify applications of LAI believed to be most exciting or relevant to coral conservation. Adoption of LAI was limited primarily to researchers at institutions based in advanced economies and was applied infrequently to conservation, although conservation practitioners and survey respondents from emerging economies indicated they expect to use LAI in the future. Our results revealed disconnect between current LAI research topics and conservation priorities identified by practitioners, highlighting the need for more diverse, conservation-relevant research using LAI. We provide recommendations for how early adopters of LAI (typically Global North

scientists from well-resourced institutions) can facilitate access to this conservation technology. These recommendations include developing training resources, creating partnerships for data storage and analysis, publishing standard operating procedures for LAI workflows, standardizing methods, developing tools for efficient data extraction from LAI products, and conducting conservation-relevant research using LAI.

1. Large-area imaging as conservation technology

Technology has the power to transform the way the environment is studied (Allan et al. 2018; Lahoz-Monfort et al. 2019). For instance, before the advent of scuba diving in the 1950s, marine scientists had limited access to underwater spaces. The rise of scientific diving revolutionized many fields of marine science, especially in shallow subtidal coastal ecosystems, by providing a means for conducting directed observations and performing experiments underwater. In-water field techniques supported by scuba opened new avenues of study and changed how much of marine ecological research is conducted (Witman et al. 2012; Cattaneo-Vietti 2021).

More recent technological advances have similar potential to transform the way researchers and practitioners access, monitor, and study marine environments. One such technology is large-area imaging (LAI), a form of multiview photogrammetry in which overlapping images are used to generate composite digital reconstructions of objects or environments. LAI reconstructions include 3D point clouds and meshes, 2D composite images (e.g., photomosaics), and digital elevation models (DEM). These data products are large relative to the footprint of the individual components used to generate them (i.e., individual photographs). The object being reconstructed with LAI may be as small as a single organism

(Olinger et al. 2019; Conley & Hollander 2021) or as large as an entire community or landscape (Westoby et al. 2012). Readers may be familiar with LAI as structure from motion, a term that technically refers to 1 of multiple steps required to generate 3D LAI reconstructions, or photogrammetry, a general term that refers to the entire field of image-enabled measurements. We prefer more targeted language and use the term large-area imaging to describe the overall workflow of imaging, assembly of 3D and 2D data products, and extraction of ecological information (Figure 1.1) (Edwards et al. 2017).

LAI has myriad potential applications for marine conservation (Johnston 2019; Bongaerts et al. 2021; Rossi et al. 2021). Among the most powerful applications is tracking and visualizing change in benthic ecosystems over time. Coregistered imagery of the same environment collected at different times provides unique information of organism- and community-level change that can transform the way researchers and practitioners document ecosystem recovery or decline (Thornton et al. 2016; Kaplanis et al. 2020; Sandin et al. 2020) and can inform restoration efforts and other management interventions (Voss et al. 2019; Merlino et al. 2020; Ferrari et al. 2021; Richaume et al. 2021). Importantly, these visual products can be used to communicate conservation needs or outcomes and help decision makers and the general public form a connection with an ecosystem they might never experience in person (van den Bergh et al. 2021). For researchers, LAI creates a powerful data set of virtual ecosystems that can be reused to answer a variety of research questions, creating an economy of scale that can reduce fieldwork costs (Couch et al. 2021). Furthermore, high-resolution imagery captured over the extent of 100s of square meters to several square kilometers can be used to answer novel scientific questions, develop new ecological metrics, create fine-scale habitat maps, and expand the footprint of long-term monitoring programs (Palma et al. 2017; Piazza et al. 2019).

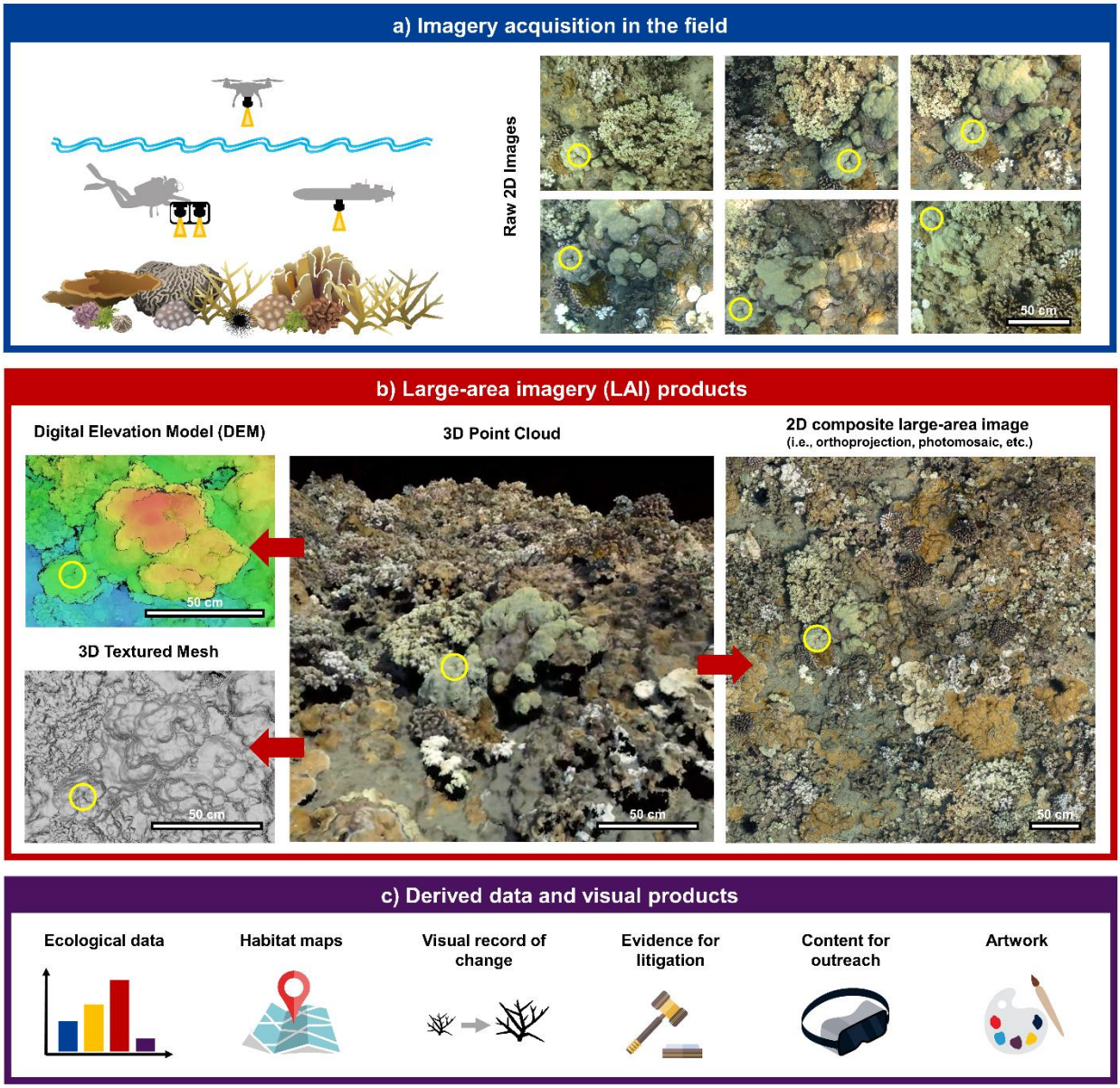

Figure 1.1: Large-area imagery (LAI) data products and their use. A) A collection of 100s to 1000s of component images of an object or environment are collected, typically using a digital camera operated by a diver, autonomous underwater vehicle (AUV), or airborne drone. B) Component images are used to create a 3D reconstruction called a point cloud, which covers a larger area than visible in any single image. The point cloud is computed using a process known as structure from motion (SfM), implemented with modern photogrammetric and computer vision software. This process relies on the position of fixed features that show up in multiple overlapping component images (represented here by a yellow circle). Multiple data products can be produced from the point cloud such as digital elevation models, 3D textured mesh surfaces, and 2D composite image products. C) A nonexhaustive representation of data and visual products that can be derived from LAI.

LAI 3D reconstructions are based on the principle of parallax, the apparent displacement of an object when viewed from 2 or more perspectives. Once images are collected, typically with a drone (Chirayath & Instrella 2019), autonomous underwater vehicle (AUV) (Parsons et al. 2018), or diver-operated camera (Bayley et al. 2019b), an algorithm identifies fixed features that appear in multiple photographs to first align the images relative to one another and then to create a geometrically accurate 3D reconstruction of the photographed object or environment (Figure 1.1). The 3D reconstruction, or point cloud, is a series of millions to billions of points with Cartesian coordinates and other associated information (e.g., RGB values). The point cloud can be converted into a 3D meshed surface or DEM or exported into a 2D composite image such as a photomosaic or orthoprojection (i.e., an orthographic projection of the point cloud). Users can conduct virtual field work by designing *in-silico* natural experiments and collecting data directly from LAI data products, which are digital archives of benthic ecosystems. Ecological data extracted from LAI may include species density and abundance, habitat structural complexity metrics, and the size and location of sessile organisms (Figure 1.1).

Throughout the 20th century, LAI was used for both terrestrial (Colwell 1983) and marine applications (Martin & Martin 2002), but widespread adoption of this technology for marine science was limited because images needed to be aligned to one another by hand, or at least with a great deal of human guidance. However, in the 2000s, improvements in underwater cameras, computing power, digital storage, and computer vision algorithms enabled automated construction of underwater image mosaics (Lirman et al. 2007). The ability to collect and process thousands of images without manual alignment enabled new uses of the technology that could exploit a “landscape view” of the seabed (Gleason et al. 2007; Lirman et al. 2010). Starting in the

2010s, commercial software made this technology widely available, expanding the types of studies and the number of people using LAI (Carrivick et al. 2016).

While use of LAI in marine science has increased over the last decade (Anderson et al. 2019; D'Urban Jackson et al. 2020), a number of factors have limited access to LAI in the marine conservation sector. These barriers include access to the equipment needed to collect and process imagery (e.g., cameras and computers) and the cost of computers and software required to construct 3D models (Raoult et al. 2016; Roach et al. 2021). Collecting the large volume of ecological data that can be extracted from LAI products requires specialized training and personnel time, which can create staff capacity bottlenecks. These challenges could be more acute for researchers and practitioners based at institutions in the Global South (emerging economies primarily in the tropics and Southern Hemisphere) than in the Global North (advanced economies primarily in the Northern Hemisphere, with the exception of Australia and New Zealand; Appendix 1.1). Given LAI's diverse range of applications, it has the potential to be a powerful tool for marine conservation. However, the aforementioned barriers could severely limit the widespread, equitable use of LAI.

We addressed the following questions: How has LAI been used to date, and by whom? Is there alignment between LAI applications and conservation practitioner priorities? What barriers currently limit LAI applications? And, finally, what steps can current LAI users take to increase the accessibility of this technology for those in the conservation community? To answer these questions, we used tropical and subtropical shallow coral reefs as a case study to examine the trends in LAI literature and evaluate the perspectives of potential and current LAI users. We reviewed 151 coral reef LAI studies published from 2010 to 2021 and complemented our literature review with a 25-question online survey, which was completed by 135 coral reef

scientists and conservation practitioners. We also conducted 30-min videoconference interviews (hereafter semistructured interviews) with 45 survey participants who volunteered to be contacted to further discuss their survey responses (survey responses and interview details in Appendices 1.1 and 1.2). The survey and semistructured interviews were conducted under the oversight of the UC San Diego Institutional Review Board (project 801952).

Coral reefs are an ideal case study for answering questions regarding the use and accessibility of conservation technology because LAI is being adopted relatively rapidly to study them (Burns et al. 2015; Figueira et al. 2015; Edwards et al. 2017; Young et al. 2017; Sandin et al. 2020; Couch et al. 2021) and because coral reefs represent an ecosystem in urgent need of conservation (Carpenter et al. 2008; Hughes et al. 2018). Although our findings are most directly applicable to the coral reef science and conservation fields, our recommendations for how to increase LAI accessibility are likely to be broadly applicable across the fields of marine science and conservation.

2. Current applications of large-area imagery

Potential applications of LAI in coral reef science have been described (Calders et al. 2020; Bongaerts et al. 2021; Ferrari et al. 2021; Rossi et al. 2021); here, we reviewed the coral reef LAI literature to identify common research themes, gaps where additional use of LAI could have greater impact, and alignment between existing research and conservation priorities.

We found that LAI has been gaining popularity in the coral reef field; >66% of all studies in our literature review were published since 2018 (Figure 1.2A). Furthermore, a majority of survey respondents in nearly every demographic group (sector, Global North vs. South, self-described scientist or conservation practitioner, and previous LAI experience) reported that they

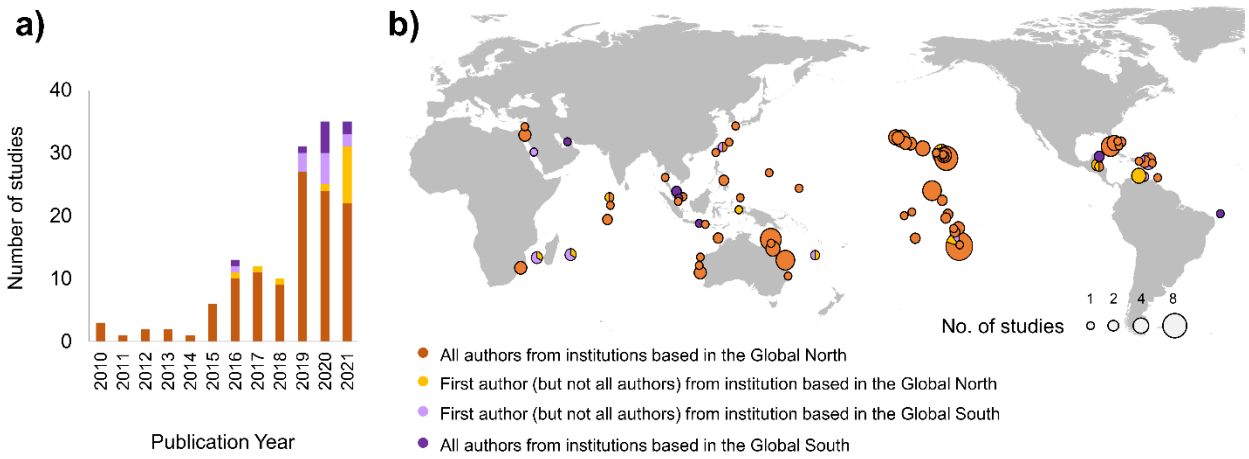

Figure 1.2: Coral reef studies that used large-area imagery (LAI) by A) publication year and B) location of study sites. Studies were categorized based on the location of the research institutions that the study authors hailed from at the time of publication. Studies that spanned multiple locations have multiple points on the map.

were likely or very likely to use this technology in the future, even though only 40% of survey respondents had experience with LAI (Appendix 1.2). Together, these results suggest LAI is rapidly becoming an industry standard for coral reef researchers, though this transition is likely still in the early stages.

Although use of LAI has been increasing, application of this technology remains concentrated on a few key topic areas (Figure 1.3A) including method development (i.e., validating the technology's precision and accuracy, 60% of studies), measuring habitat 3D structure (34% of studies), documenting change over time (24% of studies), and quantifying benthic community composition (20% of studies). Given the advantages of LAI (e.g., the ability to track change with precisely aligned models, the ability to quantify 3D structure), the popularity of these research topics is hardly surprising. However, we found that other research topics that are seemingly well suited for study with LAI are relatively underexplored, such as quantifying coral demographic rates (6% of studies) or tracking the fate of coral restoration projects (6% of studies).

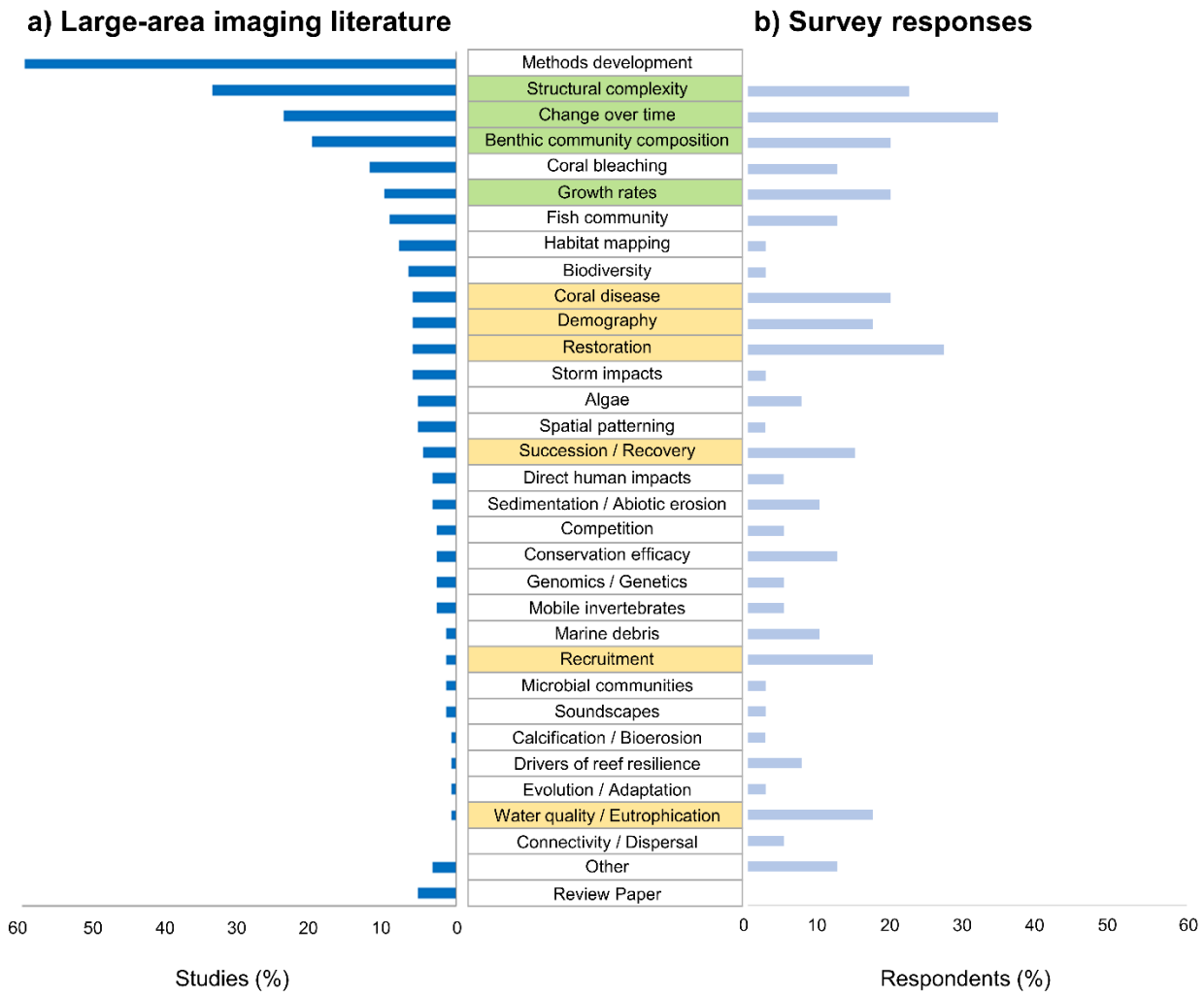

Figure 1.3: Comparison of A) the topics covered by coral reef studies published from 2010 to 2021 in which large-area imaging (LAI) was used (n = 151) and B) research interests of surveyed conservation practitioners (n = 41) (shading, 10 topic areas most frequently identified as priorities for research by conservation practitioners; green, topic covered in >10 published LAI studies; yellow, topics currently understudied using LAI). Most studies were assigned to multiple topic areas.

Our survey of coral reef scientists and conservation practitioners revealed a considerable disconnect between the research interests of survey respondents in the conservation sector and existing coral reef LAI literature (Figure 1.3B). Understudied research topics that emerged as priorities for conservation respondents included coral disease, coral demography, coral restoration, succession and recovery dynamics, coral recruitment, and water quality. Some of

these topics are not well suited for study with LAI alone (e.g., water quality), but could be investigated in novel ways if LAI were used in concert with other forms of data (e.g., fine-scale temperature, nutrient, or turbidity measurements). Use of LAI to study these and other conservation topics could help fill knowledge gaps and produce data with direct relevance to resource managers and conservation practitioners. Furthermore, survey respondents chose "visualizing and communicating reef condition" as the second most important application of LAI (Appendix 1.2), suggesting that future work should capitalize on the communications potential of LAI visuals (Figure 1.1C).

One potential explanation for the gap between conservation practitioner interests and existing LAI literature is a lack of equitable access to LAI technology. Through our online survey and semistructured interviews, we found that respondents working in conservation, the nonprofit sector, or at institutions in the Global South were more likely to face barriers to using LAI (Appendix 1.2). This accessibility gap was reflected in the geographic representation of LAI study authors. Only 6% of studies in our literature review were published by authors based solely at Global South institutions, whereas 78% of studies were published by authors based solely at Global North institutions (Figure 1.2BC). This discrepancy exists despite the fact that Global South countries contain a majority of coral reef area globally (UNEP-WCMC et al. 2021). Furthermore, among coral reef LAI studies conducted in Global South countries, 59% did not include any researchers from the country where the data were collected. This exceeds the rate of parachute science (i.e., research conducted by individuals from a country other than the country of the study site without investment in or collaboration with local scientists and community members) in the broader coral reef literature (40% [Stefanoudis et al. 2021]), suggesting that parachute science has been more prevalent in coral reef research in which LAI is used than in

coral reef research writ large. This is likely due to challenges related to the accessibility of LAI technology and reveals the extent to which LAI remains out of reach for a large swath of coral reef researchers globally. Unless concerted efforts are taken to make LAI more accessible, researchers in the Global South are likely to be excluded, perpetuating parachute science and research that is out of step with the needs of conservation practitioners as use of LAI becomes mainstream.

3. Barriers to adoption

To transform LAI from a niche methodology into an accessible and impactful form of conservation technology, barriers to LAI adoption need to be identified and removed. Our survey results showed that funding, equipment, training, and staff capacity are perceived as major barriers to LAI adoption. Conversely, opposition from funders or community groups, a lack of potential applications, and a lack of interest in LAI were less commonly perceived as barriers (Appendix 1.2). Across all demographic groups, adequate funding was ranked as the largest barrier to LAI adoption, although it was perceived to be a greater barrier by respondents who self-identified as part of the conservation community (Appendix 1.2).

3.1 Barriers faced by potential LAI users

Through our semistructured interviews, we found that individuals and organizations faced a distinct set of barriers at each stage of LAI adoption (Figure 1.4). Respondents who had yet to start using LAI but were planning to use the technology in the near future commonly cited challenges with securing adequate funding and articulating specific goals for their LAI research program. They tended to lack information about how the technology worked or how to collect imagery in the field. and they expressed a desire for training resources to close these knowledge

gaps. Those in this initial scoping phase frequently identified the cost of camera equipment as a barrier but were less likely to mention other impending costs, such as the price of computers, software, or salaries for staff dedicated to constructing 3D models and collecting ecological data from the resulting LAI data products. Instead, these costs were more often cited as barriers by respondents who had already begun to implement LAI.

3.2 Barriers faced by novice LAI users

Novice LAI users (respondents who had recently begun using LAI and were among the only researchers at their institution using LAI) identified the cost of software licenses as a major obstacle, particularly those from small nonprofit organizations that lacked access to discounted licensing options available to academic organizations. Staff capacity to conduct LAI field work was also cited as a major barrier, as was adequate training in software and data extraction methods. In particular, a lack of established and efficient data collection pipelines was cited as a barrier for data extraction, especially for those without access to training resources. This barrier was compounded by the time lag between image collection, point cloud reconstruction, and data extraction and analyses, especially for respondents who lacked access to high-speed computing or internet bandwidth for sharing large data sets with partners. Due to this time lag, which could last for months to years, respondents cited difficulty with using LAI for rapid surveys or disturbance event response, compared to *in situ* survey data that are ready for analyses when divers exit the water (Couch et al. 2021; Urbina-Barreto et al. 2021).

3.3 Barriers faced by experienced LAI users

Experienced LAI users (those from organizations with well-established LAI research programs) identified a distinct set of challenges related to scaling up data collection (Figure 1.4).

These barriers included adequate storage to back up image and 3D model data sets, staff capacity to collect ecological data from LAI products, and the ability to maintain funding for long-term or large-scale monitoring efforts. The previously mentioned time lag of model construction and data processing tended to compound as organizations scaled up LAI efforts, suggesting that this particular barrier to adoption could increase, rather than decrease, as organizations continue using LAI.

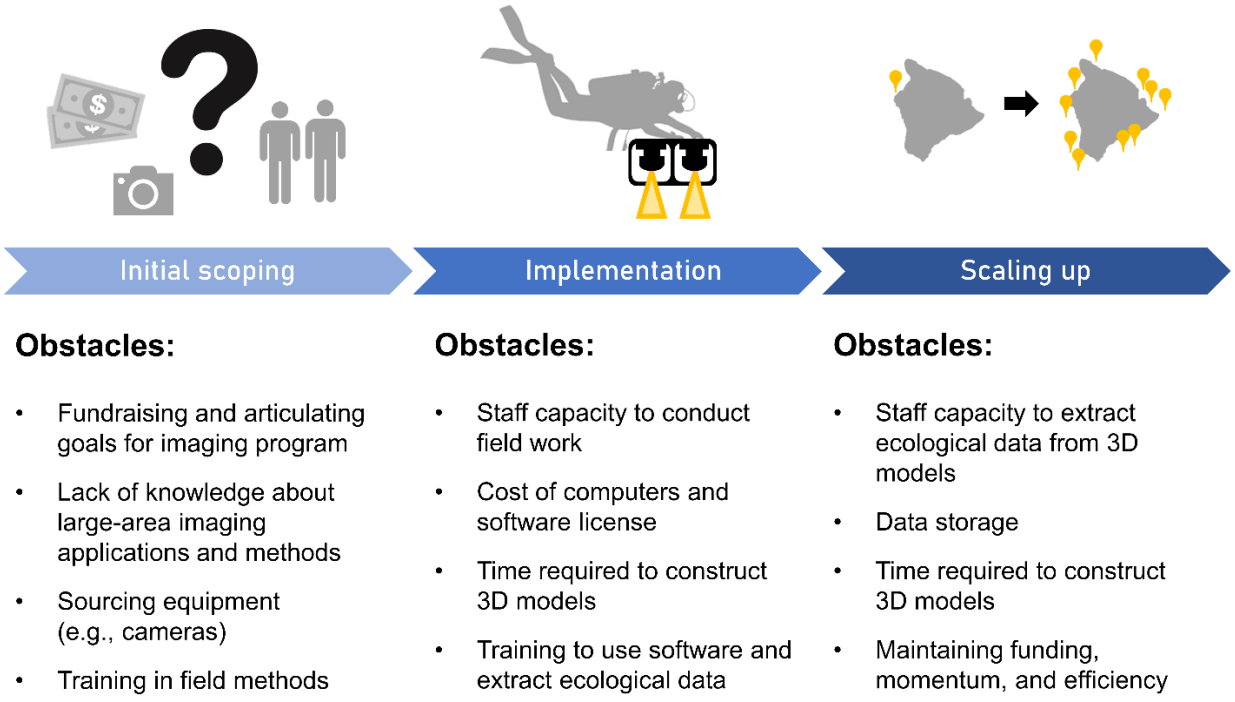

Figure 1.4: Most common barriers to adopting large-area imaging faced by coral reef researchers and conservation practitioners, derived from semistructured interviews with 45 survey respondents. Barriers to adoption differ among phases of technology adoption.

3.4 Ethical considerations

The barriers to LAI adoption we documented are broadly similar to those facing other conservation technologies (Lahoz-Monfort et al. 2019; Speaker et al. 2021), from emerging technologies, such as AUVs and eDNA, to more established technology such as GIS. We assert that having a comprehensive understanding of potential barriers at the outset of LAI adoption

will help new users account for resource and staffing needs to better navigate said barriers. However, we acknowledge that some organizations will never be able to bear the cost of adopting LAI, and others may only be able to afford a streamlined version that relies on low-cost equipment (e.g., GoPros instead of DSLR cameras) or freeware that might not meet data quality standards. This imbalance in resources and capacity raises equity and social justice concerns that need to be addressed by the marine science community as LAI becomes an industry standard. Scientists at well-resourced organizations should consider where they can fit into this sequence of barriers to help alleviate obstacles and facilitate onboarding of this technology.

4. Recommendations to increase the accessibility of LAI

Although there are a number of logistical, monetary, and technical challenges that currently limit the accessibility of LAI, these challenges are by no means insurmountable. We recommend actions that current LAI users (or their institutions) can take to increase LAI accessibility for new users and those in the conservation community. These recommendations were developed based on feedback solicited in our semistructured interviews and can be broadly categorized as investments either in training and capacity building or in research and development (Table 1.1).

Develop and fund workshops and trainings: Interviewees commonly expressed the desire for more LAI training workshops, extension courses, or video tutorials, with modules focused on each step of the LAI process, the technology's potential applications, and associated costs. Institutions that currently use LAI at scale should dedicate a portion of their budgets to providing LAI trainings and workshops. These workshops will be most useful if they are tailored to multiple audiences to reflect the different uses of LAI, if they are updated periodically to

reflect advances in both LAI software and hardware, and if they include funding for trainees to purchase their own LAI equipment.

Create partnerships for image storage, processing, and analysis: Partnerships with government agencies, big nongovernmental organizations (NGOs), or universities can increase the capacity of small organizations or individual researchers. These partnerships would allow new LAI users to outsource the computational or time intensive steps of LAI (i.e., image matching and point cloud generation) and provide access to LAI expertise and equipment. One example of such a platform is GeoNadir (https://geonadir.com/), a website for organizing, processing, and storing drone imagery.

Build a community of LAI users and create a LAI knowledge hub: Once initial partnerships have been formed to support new LAI users, steps should be taken to formalize those partnerships and expand collaboration across sectors. One avenue for this collaboration would be a LAI knowledge hub, which would serve as a forum for users to interact with a broad community of practitioners. This hub could also provide trainings, process and store image and 3D model data, and host workshops with practitioners to codevelop software tools and pipelines for analyzing 3D data sets.

Recognize the diversity of user goals: Every organization has different goals for LAI; some intend to use it primarily as a visualization tool, others focus on extracting ecological data, and still others seek to document environmental impacts (e.g., for litigation purposes). Creative users will come up with new, unforeseen uses. These users will have different training, equipment, and staffing needs. Early adopters of LAI who provide training to their peers should recognize that LAI is a tool with diverse applications and that there are technological and social

barriers to adopting LAI. Thus, it will be important to design software and research pipelines that accommodate potential users from a range of backgrounds and varied applications.

Publish research pipelines: Researchers should continue to publish open-access analytical pipelines, standard operating procedures, and supplementary methods as LAI technology progresses. These pipelines should be thorough and easy to follow and should cover a range of data types, from traditional metrics (e.g., percent cover, linear rugosity) to more advanced LAI metrics (e.g., volumetric change, survivorship, etc.). Users should be encouraged to recognize the common features of these pipelines rather than considering them as competing, mutually exclusive standards.

Develop standardized methods: Multiple different LAI pipelines exist (Gutierrez-Heredia et al. 2016; Raoult et al. 2016; Suka et al. 2019; Bayley & Mogg 2020; Lange & Perry 2020; Rodriguez et al. 2021). An effort to collate these pipelines and develop overarching guidance of LAI best practices would make the technology more accessible for new users. Furthermore, developing a standard set of metrics to quantify the accuracy and precision of LAI products would help new and existing LAI users, peer reviewers, and the broader research community interpret findings from LAI-based research.

Improve LAI software: Developing open-access software that is fast and user friendly will be critical if LAI is to become a viable option for practitioners in the Global South. TagLab (Pavoni et al. 2021b) was suggested by interviewees as a model of accessible LAI freeware. While freeware is being developed, universities should explore partnerships with small NGOs and community groups to facilitate access to LAI software and computing power.

Develop machine learning tools to efficiently collect data from LAI products: Extracting information from LAI products can be time-consuming, but researchers have made

considerable strides in developing machine learning approaches to expedite this process (Parsons et al. 2018; Pavoni et al. 2021b; Yuval et al. 2021; Runyan et al. 2022). Collecting additional training data and innovating machine learning methods are important contributions that the academic community can make to improve the accessibility of LAI to conservation practitioners because it would reduce the time lag associated with extracting usable ecological data.

Conduct conservation-relevant research using LAI: More work is needed to bridge the gap between the metrics and approaches used in academia and those that are relevant to conservation practitioners. This includes collecting and calibrating LAI data that can serve as a direct analogue to *in situ* metrics that conservation practitioners have used for decades so that long-term monitoring data sets can be compatible with LAI (Palma et al. 2017; Couch et al. 2021). Furthermore, researchers should seek to fill gaps in the LAI-based literature enumerated here (Figure 1.3) because those gaps were identified as priorities by conservation practitioners. Studies that use LAI to evaluate the efficacy of marine management (Bayley et al. 2019b; Palma et al. 2019) or test different conservation interventions (Voss et al. 2019) will help demonstrate the potential of this technology for conservation. Visuals of LAI should also be utilized to convey scientific findings, restoration progress, and conservation needs to decision makers and involve members of the public (van den Bergh et al. 2021).

5. Conclusions

If properly used, LAI has the potential to be an impactful form of conservation technology. The ability to archive visual ecological baselines, track change over time, develop novel metrics, and scale up ecosystem monitoring will be invaluable for resource managers as marine ecosystems continue to change rapidly. Researchers at well-resourced institutions have served as the pioneers of LAI method development and application. These same researchers now

have an ethical responsibility to make LAI more accessible by facilitating the transfer of technology from the ivory tower to the hands of conservation practitioners. Academic researchers in particular have an opportunity as educators to train their colleagues outside academia. This includes developing training materials, hosting workshops, fostering partnerships for data processing and analyses, establishing clear communications with partners, publishing clear pipelines and standardized methods, working with developers to improve software related to all stages of the LAI pipeline, and conducting LAI-based research that is relevant to conservation practitioners. These steps, among others, will help maximize the positive impact of LAI for conservation. More broadly, similar actions can be taken to improve the accessibility of other technologies with relevance to conservation.

Table 1.1: Recommended investments in training, capacity building, and research and development for increasing the accessibility of large-area imaging (LAI) technology for the coral reef conservation community based on semistructured interviews with 45 survey participants.

Type of investment	Recommendation
Training and capacity building	Develop and fund workshops and trainings
	Create partnerships for photo storage, processing, and analysis
	Build a community of LAI users and create a LAI knowledge hub
	Recognize the diversity of user goals
Research and development	Publish LAI research pipelines
	Develop standardized LAI methods
	Develop machine learning tools to efficiently collect data from LAI products
	Improve software accessibility, speed, and usability
	Conduct conservation-relevant research using LAI

6. Acknowledgements

Chapter 1, in full, is a reprint of the material as it appears in Conservation Biology. McCarthy, Orion S.; Contractor, Kanisha; Figueira, William F; Gleason, Arthur C. R.; Viehman, T. Shay; Edwards, Clinton B; Sandin, Stuart A. 2023. The dissertation author was the primary investigator and author of this paper.

We acknowledge everyone who took or helped distribute the coral reef scientist and conservation practitioner survey and thank especially the 45 respondents who took the time to discuss their survey responses in depth with us. Their interviews were instrumental to development of the recommendations proposed here. We also thank the UC San Diego Institutional Review Board and the team at ResearchRabbit for their responsiveness as we navigated their search engine. O.M. was supported by the NSF Graduate Research Fellowship Program. A.G. was supported by the Pew Fellows Program in Marine Conservation at The Pew Charitable Trusts. Finally, while we provide recommendations for making large-area imagery more accessible to a global audience, we acknowledge that the authors of this study are all based at Global North institutions. It is our hope that future work on this topic can continue to address the barriers scientists and conservation practitioners face in the Global South.

Chapter 2 – Identifying the drivers of structural complexity on Hawaiian coral reefs

Orion S. McCarthy, Jennifer E. Smith, Vid Petrovic, and Stuart A. Sandin

Abstract

Habitat structural complexity is created by biotic and abiotic processes that operate over a range of scales. This can be seen clearly on coral reefs, where corals and reef geomorphology create structure from mm to km scales. Here, we quantified the relative contribution of biotic and abiotic structures to habitat complexity using 'Structure from Motion', a technology that allows accurate 3D models of environments to be reconstructed from overlapping photographs. We calculated the linear fractal dimension of these models using a virtual analogue of a profile gauge. By adjusting the spacing between profile gauge rods, we partitioned structural complexity into a series of scale intervals. We identified scales that were most indicative of coral cover (0.5-16 cm) and reef geomorphology (16-256 cm). We found that reefs in the Main Hawaiian Islands have more complexity at finer scales than reefs in the Northwest Hawaiian Islands, which we attribute to the latitudinal gradient in coral cover along the archipelago. At coarser scales, islands at each end of the archipelago have sites with high structural complexity, with less complexity in the center of the archipelago. These differences are consistent with geologic factors shaping island uplift, subsidence, and reef formation. In addition, we found that different coral genera and morphologies display unique patterns of fractal dimension, with branching Porites corals creating the greatest amount of habitat structure at nearly all scales. This study demonstrates how multi-scale approaches can be used to identify the processes responsible for reef structural complexity and changes in structure over time.

1. Introduction

In many ecosystems, there is a strong relationship between species diversity and the structural complexity of the associated habitat (Henderson & Robertson 1999; Graham 2004; Ishii et al. 2004; Tews et al. 2004; Graham & Nash 2013), and coral reefs are no exception. Among the most biodiverse ecosystems on the planet (Knowlton et al. 2010), coral reefs are an amalgamation of abiotic and biotic structures shaped by the growth and accretion of scleractinian corals (Grigg 1998; Perry & Alvarez-Filip 2019), hydrodynamic forces (Dollar 1982; Donovan et al. 2018; Levenstein et al. 2022), and island evolution (Clague 1996; Kench & Mann 2017). Numerous studies have demonstrated a relationship between reef structure and coral cover and morphology (Alvarez-Filip et al. 2011a; Graham & Nash 2013; Darling et al. 2017). The substrate of a coral reef forms a patchwork of holes, crevices, overhangs, and other refugia of various sizes, which in turn serves as habitat for fish and invertebrates across a range of scales (Friedlander & Parrish 1998; Wilson et al. 2007; González-Rivero et al. 2017).

Structural complexity can be defined as the diversity and arrangement of habitat structure in both the vertical and horizontal direction (Tokeshi & Arakaki 2012). On coral reefs, structural complexity has been found to be a predictor of herbivory (Vergés et al. 2011; Santano et al. 2021; but see Oakley-Cogan et al. 2020), reef fish assemblage variation (Harborne et al. 2012; González-Rivero et al. 2017; Ferrari et al. 2018), and reef resilience and recovery potential (Graham et al. 2015; Burns et al. 2016). Furthermore, changes in structural complexity due to climate-driven losses in coral cover are expected to negatively impact coral reef biodiversity in the coming decades (Bozec et al. 2015). Thus, measuring structural complexity can serve as a proxy for other aspects of reef condition, including habitat quality and benthic community

composition, while repeated measurements can enable scientists, reef managers, and conservation practitioners to track changes in reef condition over time.

Given the ecological importance of structural complexity on coral reefs, scientists have invested considerable time and energy to develop and refine methods for quantifying the 3D structure of these habitats. Linear rugosity, the ratio of the contour distance across a surface to the linear horizontal distance that contour traverses, has historically been the most commonly used metric to quantify structural complexity (Graham & Nash 2013; Young et al. 2017). Efforts to measure linear rugosity *in situ* date back to the 1970s with the advent of the chain-and-tape approach (Risk 1972). Linear rugosity can also be measured *in situ* using a profile gauge, an instrument that consists of a series of parallel rods in a linear frame. When placed on the substrate from above, the rods slide independently to rest on the shallowest object beneath, approximating the contour of the substrate along a line (McCormick 1994; Vermeij et al. 2007). The spacing between profile gauge rods determines the resolution of the linear rugosity measurement, and thus a profile gauge provides a scale-dependent measure of linear rugosity. Although widely used, methods for measuring linear rugosity *in situ* are time-consuming, prone to user error, potentially damaging to the habitat, and impractical for measuring large areas of the benthos across multiple scales (Storlazzi et al. 2016; Bayley et al. 2019a).

Recently, there has been growing interest in using 3D modeling to quantify the structural complexity of coral reefs (D'Urban Jackson et al. 2020; Ferrari et al. 2021; Lepczyk et al. 2021). These studies, made possible by rapid advances in computing power and data storage, use 'Structure from Motion' (SfM) to reconstruct underwater environments using the overlap between photographs (Westoby et al. 2012; Burns et al. 2015). As a type of photogrammetry, SfM relies on parallax, the apparent displacement of an object when viewed from multiple

different directions, to reconstruct 3D scenes from 2D data (Anderson et al. 2019). SfM allows researchers to conduct semi-automated 'virtual field work' from these digital representations of nature. This technique has the potential to transform the speed and scale at which scientists measure structural complexity (Couch et al. 2021), while improving our ability to make repeatable measurements and track change through time (Yuval et al. 2021). Already, SfM has been used to quantify coral growth rates (Ferrari et al. 2017; Sandin et al. 2020; Kodera et al. 2020), changes in structural complexity following disturbance events (Burns et al. 2016; Ferrari et al. 2016), spatial heterogeneity in complexity (Leon et al. 2015), the influence of coral colony morphology on complexity (Burns et al. 2015; Figueira et al. 2015), and the relationship between fish abundance and structural complexity (González-Rivero et al. 2017; Ferrari et al. 2018).

One of the most promising applications of SfM is the ability to measure structural complexity across a range of scales. The substrate of a coral reef comprises structures that span several orders of magnitude in size, and these structures influence the biology and ecology of reef organisms (Hatcher et al. 1987; Nash et al. 2014; Levenstein et al. 2022). For instance, the way in which organisms interact with the structure of the reef depends on their body size. This phenomenon, termed the textural discontinuity hypothesis, was first noted by Holling to describe the size distribution of birds and mammals in relation to habitat structure (Holling 1992) and has since been shown to apply to coral reef fish assemblages as well (Hixon & Beets 1993; Nash et al. 2013). Thus, it is important to consider how structural complexity varies across a range of scales in order to draw ecological inferences about reef fish assemblages (Luckhurst & Luckhurst 1978; Nash et al. 2014; Fukunaga et al. 2020b; Urbina-Barreto et al. 2022), mobile invertebrates (Vytopil & Willis 2001; Lee 2006) and reef-scale hydrodynamics, from boundary

layer characteristics (Levenstein et al. 2022) to wave setup (Franklin et al. 2013; Monismith et al. 2013).

Prior to the widespread use of SfM, several studies used *in situ* methods to quantify structural complexity across multiple scales. Chains with links of various sizes have been used to examine the scale dependence of linear rugosity (Knudby & LeDrew 2007), and wheels of varying diameters have been used to quantify the length of reef contours at different scales (Nash et al. 2013; Richardson et al. 2017). SfM enables researchers to efficiently measure reef structure

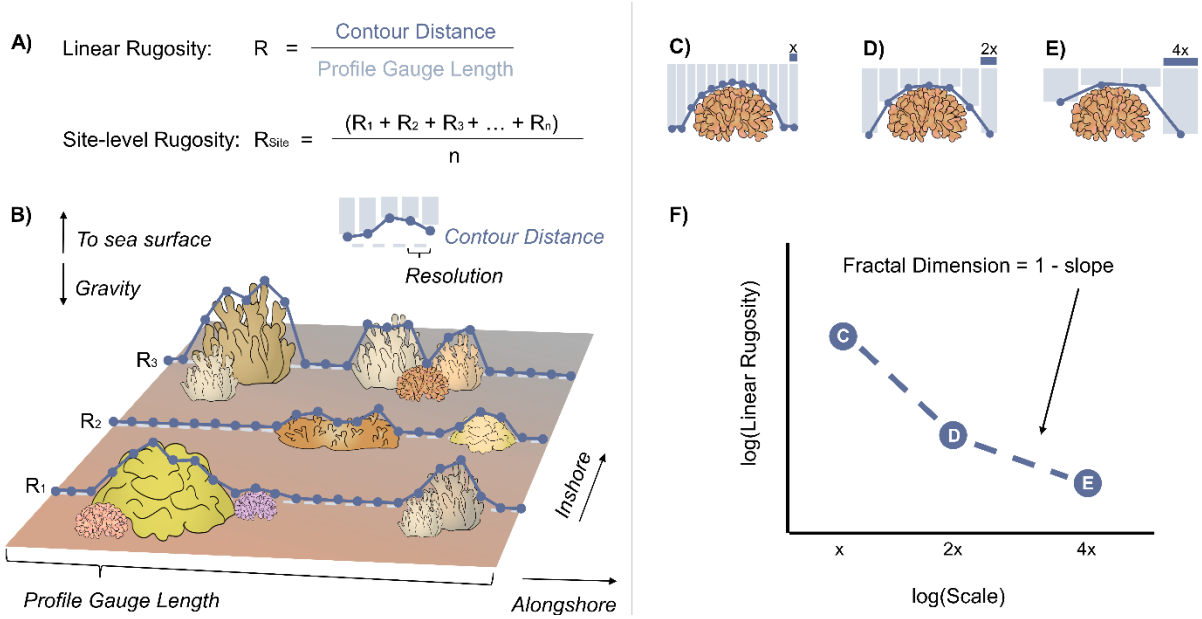

Figure 2.1: Linear rugosity A) is the ratio of the contour distance across a surface to the linear horizontal distance that contour traverses and B) can be measured using a profile gauge, a tool that consists of a series of parallel rods in a linear frame. When placed on the substrate, the rods slide independently to rest on the shallowest object beneath, approximating the contour of the substrate along a line. The virtual profile gauge tool was designed as an analogue to a real profile gauge and uses a series of virtual cylindrical rods to measure the vertical height of the point cloud along virtual transects. Users can select the number of rods per transect as well as the length, number, and orientation of the transects with respect to the point cloud. C–F) Linear rugosity is a function of the resolution of the measurement instrument (i.e. the profile gauge). The rate of change in rugosity between 2 levels of resolution (C to D or D to E) can be used to calculate fractal dimension. Fractal dimension is not constant for objects that are not true fractals and can change between different scale intervals. F) is adapted from Nash et al. (2013).

at high resolution over a large extent of habitat with minimal effort in the field. Importantly, researchers can use these data to calculate structural metrics at different scales (Bryson et al. 2017; Fukunaga et al. 2020a), eliminating the need to identify a single measurement scale *in situ*.

While linear rugosity is the most widely used metric of coral reef structural complexity (Graham & Nash 2013), fractal dimension is arguably a more relevant metric because it accounts for the scale dependence of reef structure (Fukunaga et al. 2020a). Fractal dimension is a measure of an object's ability to fill Euclidean space and describes the complexity of a shape (Mandelbrot 1983; Sugihara & May 1990; Halley et al. 2004). In the context of linear structural complexity, fractal dimension represents the rate at which the apparent length of the reef contour increases as the resolution of measurement becomes finer, and can be calculated using measurements of linear rugosity made at different levels of resolution (Nash et al. 2013). In ecological terms, fractal dimension is related to the amount of space along the reef contour that is available to organisms of a certain size class and may change depending on the scale of measurement and characteristics of the underlying substrate (Sugihara & May 1990; Tokeshi & Arakaki 2012). For example, if the contour of a coral colony is measured at both 1 and 10 cm resolution, the difference between the lengths of those contours can be attributed to structural features of the colony that are between 1 and 10 cm in size (Figure 2.1). In this sense, fractal dimension can be used to partition complexity by scale, quantify the abundance of structures (and thus habitat availability) within a given size range, and contextualize the gain or loss of structural complexity over time.

Few studies have utilized multi-scale patterns of structural complexity to gain insights into coral reef ecology, geology, and natural history. While some studies have used fractal dimension to study coral reef structural complexity across multiple scales (Bradbury et al. 1984;

Nash et al. 2013; Young et al. 2017; Fukunaga et al. 2020a), these studies were either limited in their geographic scope or calculated a single value of fractal dimension across a large range of scales. Specifically, this study addresses the following questions: 1) how does fractal dimension of the reef substrate change across scales, 2) do biotic and abiotic reef structures exhibit different patterns of fractal dimension across scales, and 3) do different coral genera and growth forms exhibit distinct site- and patch-scale patterns of fractal dimension?

Here, we use the term biotic structure to refer to structure created by living or recently living benthic organisms and the term abiotic structure to refer to reef geomorphology created by either geologic or biogenic processes over longer timescales (i.e., spur and groove formations, boulder fields, etc.). We demonstrate that our approach can be used to identify the scale(s) where reef structure is most complex, which allows us to determine the relative importance of biotic and abiotic processes in creating habitat. This, in turn, can inform decisions about what scales are most relevant for monitoring changes in coral reef structural complexity over time. To our knowledge, this study represents one of the first archipelago-scale efforts to partition coral reef structural complexity into different scale intervals using fractal dimension and SfM.

2. Methods

2.1 Study Design

This analysis of biotic and abiotic drivers of structural complexity is based on data from coral reefs in the Main Hawaiian Islands (MHI) and Northwest Hawaiian Islands (NWHI). The Hawaiian archipelago is an ideal location for this study because it spans a gradient of latitude (from 18.9−28.4°N) and geologic age (from 0.4 million yr [Hawai'i] to 29.8 million yr [Kure Atoll]; Clague 1996), with older, high-latitude reefs in the northwest and younger, low-latitude

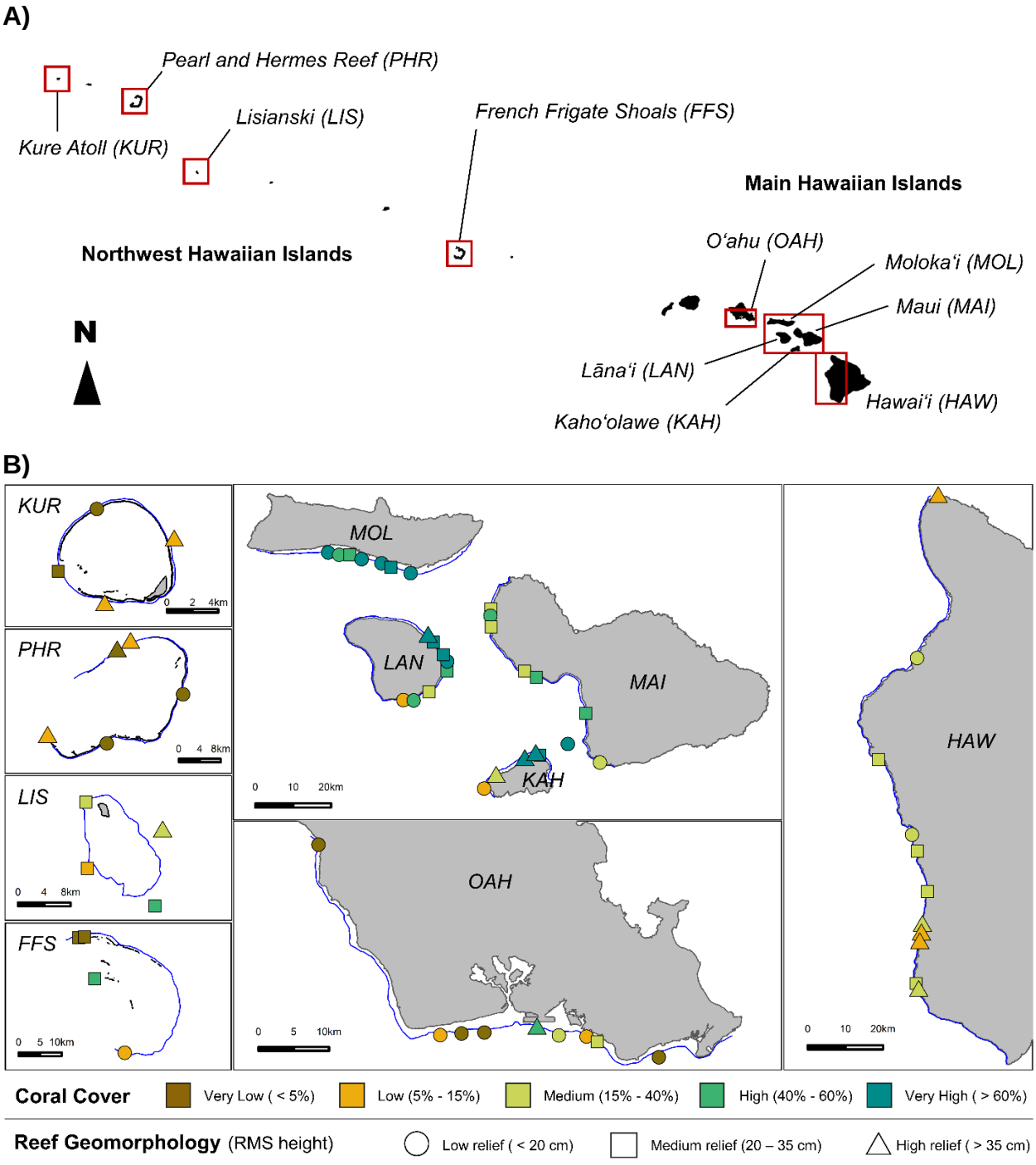

Figure 2.2: A) The Hawaiian archipelago, showing the 10 islands surveyed in this study. Red boxes indicate inset maps, which show the location of all study sites (n = 65). B) Sites are symbolized by coral cover (color) and root mean square (RMS) height (shape). Blue lines represent the 10 m isobath around each island (leeward side only for the Main Hawaiian Islands)

reefs in the southeast. Millions of years of weathering, erosion, and subsidence have shaped the geomorphology of older islands and atolls, which can be reasonably expected to have different nearshore topography than younger islands. Similarly, coral cover varies throughout the archipelago as a function of latitude: coral cover and coral growth decrease as latitude increases (Vroom & Braun 2010; Jouffray et al. 2015), reaching a threshold north of Kure Atoll, beyond which the rate of coral growth drops below the rate of reef subsidence (Grigg 1982). Baseline surveys in the archipelago have demonstrated the effects of both geology and latitude on Hawaiian benthic communities and fish assemblages (Rooney et al. 2008; Friedlander et al. 2009; Vroom & Braun 2010; Jouffray et al. 2015). Thus, the Hawaiian archipelago represents a unique opportunity to explore the effects of biology and geomorphology on coral reef structural complexity.

We surveyed 65 forereef sites spanning 6 of the MHI (Hawai'i, Maui, Kaho'olawe, Lāna'i, Moloka'i, and O'ahu) and 4 atolls in the NWHI (French Frigate Shoals, Lisianski, Pearl and Hermes, and Kure; Figure 2.2). Sites were surveyed between July 2016 and August 2017 as part of 5 separate research expeditions. The distance between sites varied by island, but the median distance between neighboring sites was 4.83 km, with the closest sites located 1.11 km apart. Sites had a mean (±SD) depth of 11.3 ± 2.7 m (range: 4.5−17.7 m) and were located on the leeward side of islands in the MHI to control for the effect of wave energy on coral assemblages. We did not restrict sampling to leeward coastlines for the NWHI since past studies have found forereef zonation patterns in the NWHI to be complex and variable between atolls (Vroom et al. 2005; Schopmeyer et al. 2011), suggesting that leeward vs. windward exposure may not be the primary driver of benthic community composition in the NWHI, as it is in the MHI. The number of sites per island was standardized by the amount of nearshore habitat, using the length

of an island's leeward 10 m isobath as a proxy (or total 10 m isobath for the NWHI). The number of sites per island ranged from 11 (Hawai'i) to 4 (Kure, Lisianski, and French Frigate Shoals; Figure S2.1).

2.2 Field Procedures

We used SfM to construct a 3D model of each forereef site from underwater photographs. The field procedures for establishing and photographing sites using an SfM workflow have been previously documented (Sandin et al. 2020) and are only briefly described here. At each site, a team of divers placed 6 calibration tiles to delineate the boundaries of a 10 × 10 m site (3 tiles per inshore site boundary; Figure S2.2). Divers recorded the depth of each tile and placed four 50 cm scale bars within the site's boundaries. Following site setup, one diver swam approximately 1.5 m above the benthos carrying a custom-built camera rig. At the majority of sites, the camera rig was equipped with 2 D7000 SLR Nikon cameras (18 and 55 mm lenses) in Ikelite underwater housings. Sites from 2 expeditions were photographed using a different camera setup (35 mm lens DSLR Nikon and a GoPro 11). To account for differences between these camera setups, we excluded sites (n = 4) where low-quality GoPro imagery led to errors in model reconstruction (i.e., model warping, erroneous 'floating' points). Cameras were programmed to take a photograph every 1 s, recording approximately 5000 images per site. The diver carrying the camera rig swam slowly in a gridded pattern to ensure maximal overlap between successive images and swam several meters beyond the edge of the 10 × 10 m site to ensure full coverage and minimize edge distortion.

2.3 Model construction and data collection

Photographs from each site were used to generate a dense point cloud reconstruction of the coral reef benthos using the commercially available software *Metashape* (Agisoft). While other SfM studies commonly convert these point clouds into 'mesh' reconstructions of the benthos, mesh outputs require interpolation which can introduce structural error, especially in high-relief areas. Since SfM cannot reconstruct regions of the reef where overlap between photos is limited, the resulting point cloud is in actuality a 2.5D representation of the reef surface with empty space in areas with limited photo coverage (e.g. overhangs, the interstitial space of a branching coral colony). To best account for this error and avoid interpolation, we opted to measure linear rugosity directly from the point cloud itself, since the point cloud represents the most geometrically accurate reconstruction of the substrate. We used linear rugosity, a one-dimensional measurement of structural complexity, because linear rugosity calculations require no interpolation, are easily interpretable and computationally transparent, and are comparable with *in situ* approaches such as a profile gauge. Furthermore, these factors make it transparent to interpret cross-scale patterns of rugosity, which is the crux of this study.

We analyzed the point cloud directly using the custom-built software *Viscore* (Petrovic et al. 2014). Once the point cloud for each site was constructed, we used Viscore to perform all further post-processing and analysis. As a precursor to any analysis, we oriented each point cloud with respect to the sea surface using *in situ* depth measurements and adjusted the scale using the 50 cm scale bars as a reference. After scaling and orienting the point cloud, we used the virtual point intercept tool (VPI) to analyze benthic community composition and the virtual profile gauge tool (VPG) to measure structural complexity. Both VPI and VPG are designed as virtual analogues of traditional *in situ* survey methods (random point intercept method and a profile

gauge, respectively). The mechanics of these Viscore tools are described in detail elsewhere (Fox et al. 2019 for VPI; Figures S2.3–S2.5 in the Appendix 2 for VPG) and are described in limited detail here.

We used VPI to assess benthic composition within each 10 × 10 m site following a stratified random sampling design. We chose these dimensions to match the footprint of our rugosity measurements and because this scale has been shown to be sufficient to capture benthic patchiness and taxonomic heterogeneity on coral reefs (Palma et al. 2017). For this study, we divided each site into a 32 × 32 cell grid and used VPI to identify a single random point from within each grid cell, resulting in approximately 10 points/m^2 (Dumas et al. 2009; Figure S2.6). A single researcher with training in Hawaiian benthic taxonomy identified the substrate under each random point by referencing the raw imagery used to generate the point cloud. We identified points to the finest taxonomic resolution possible, typically either to genus or species level, and then grouped these IDs into one of 6 functional categories: turf algae, macroalgae, crustose coralline algae, sand, coral, or other. The 'other' category included cryptic encrusting organisms not considered to contribute meaningfully to structural complexity on Hawaiian reefs (primarily zoanthids, sponges, and tunicates), and only once exceeded 1% of the total benthic cover. For points landing on coral, we recorded the growth form of the colony as well (branching, encrusting, massive, plating, or corymbose).

We used VPG to measure the structural complexity of each site. To mimic a profile gauge (McCormick 1994), VPG drops virtual rods orthogonally from the plane describing the sea surface onto the point cloud below (Figure 2.1). Each rod records the depth of the first (i.e., shallowest) point encountered in the point cloud at the given 2D coordinate. Virtual rods are arranged continuously along a transect, and the spacing between the center of each rod is

equivalent to the resolution of the profile gauge. The contour distance along each profile gauge is simply the sum of the Euclidean distances between adjacent rod termini. We calculated the linear rugosity for each profile gauge by dividing the contour distance by the length of the profile gauge. To minimize the impact of substrate slope on rugosity, we measured reef contours in the alongshore rather than inshore direction (Figure S2.5).

We measured reef structure using 100 virtual profile gauges per site, each with a resolution of 0.5 cm. Profile gauges were 10.24 m long to enable data subsetting by a base 2 geometric series (to simulate 10 different resolutions of measurement, from 0.5−256 cm) and were spaced 10.24 cm apart. These settings were chosen to assess the structural complexity of benthic communities across a range of scales: 10.24 m profile gauges are long enough to intersect numerous coral colonies or other structural features, and the minimum resolution of 0.5 cm is detailed enough to capture intra-colony detail while approaching the resolution limits of the point cloud. Sub-setting profile gauges via a base 2 geometric series from 0.5−256 cm created equivalent scale intervals on the log−log plot of linear rugosity vs. resolution, which simplified calculations of fractal dimension (Nash et al. 2013). The choice of 100 transects per site reflected a tradeoff between exhaustive sampling and computational efficiency. For each site, we averaged the linear rugosity of all 100 profile gauges to obtain a single site-level value of linear rugosity at each level of resolution. We did not quantify site-level variance of linear rugosity due to spatial autocorrelation of neighboring profile gauges. Any gaps in the point cloud or missing depth values were excluded from linear rugosity calculations (Figure S2.4).

We also measured the structural complexity of the most common coral morphotypes (branching *Montipora* spp., encrusting *Montipora* spp., branching *Porites* spp., massive *Porites* spp., and encrusting *Porites* spp.) and non-living substrate (dead coral skeletons and sand/rubble)

across a range of scales. Using a subset of our 65 models, we identified patches of reef with uniform benthic composition and measured the rugosity of each patch using a 3 m long virtual profile gauge.

2.4 Fractal dimension

We used linear rugosity measurements from 10 different levels of resolution to calculate fractal dimension *(D)* of the substrate, using $D = 1 - S$, where S is the slope between each successive rugosity value on a log−log plot of linear rugosity vs. profile gauge resolution (Figure 2.1; Sugihara & May 1990; Nash et al. 2013). Values of D range from 1−2; $D = 1$ for Euclidean shapes, where contour length is constant regardless of scale, and $D = 2$ for shapes where the apparent contour length increases toward infinity when measured at finer and finer levels of resolution. While other studies have calculated a single value of D between one fine and one coarse resolution (Fukunaga et al. 2020a), we calculated 9 values of D, one for each scale interval. This approach allowed us to partition structural complexity by scale and frame reef structure in the context of its ecological function (i.e., habitat provisioning for organisms of certain size classes; Nash et al. 2013). Before using this approach to assess the fractal dimension of our SfM point clouds, we tested it using simulated data. We simulated reef profiles with small-, intermediate-, and large-scale reef features of known size, and found that values of D peaked in scale intervals that corresponded to the size of simulated reef structures (Figure S2.7).

2.5 Statistical analysis

To identify the scales at which corals and reef geomorphology contribute to overall reef structure throughout the Hawaiian archipelago, we constructed generalized additive models (GAMs) to test the relationship between fractal dimension and 3 explanatory variables (coral

cover, root mean square [RMS] height, and latitude) at each scale interval. We used RMS height, a metric that has been used to quantify topography in terrestrial settings (Shepard et al. 2001), as a proxy for reef geomorphology. To calculate RMS height, we calculated the distance between each profile gauge rod terminus and the plane of best fit through the model and then calculated the standard deviation of these distances for each site. To test if RMS height was an adequate proxy for reef geomorphology, we visually assessed the geomorphology of our models and assigned each site a score between 0 (low relief) and 5 (high relief) following the methods of Wilson et al. (2007). We found a strong correlation between these visual assessments of geomorphology and RMS height ($r = 0.865$), which supports our use of RMS height as a proxy for reef geomorphology. We also tested for relationships between RMS height, coral cover, and latitude, and found no strong correlations between these explanatory variables.

We chose to use GAMs because fractal dimension exhibited a non-linear relationship with our explanatory variables (coral cover, RMS height, and latitude) at certain scale intervals and based on the assumption that these variables were additive in terms of predicting our response variable. We used a Gaussian error distribution and untransformed data. Smoothing terms were selected through generalized cross-validation, and diagnostic tests indicated that a basis dimension of $k = 9$ was appropriate for model fit for coral cover and RMS height, while $k = 5$ was appropriate for latitude. One site with extreme RMS height (Site PHR 52) had high leverage (Cook's distance >> 1), so we excluded it from this analysis.

To investigate the effect of coral morphotype on fractal dimension, we categorized sites based on their most abundant coral genus and morphology, which resulted in the following levels: branching *Montipora* reefs (n = 6), encrusting *Montipora* reefs (n = 12), branching *Porites* reefs (n = 13), massive *Porites* reefs (n = 8), and encrusting *Porites* reefs (n = 2). We

excluded sites with less than 15% coral cover from this analysis based on natural breaks in our data and the assumption that corals contribute only marginally to overall reef structure below that percent cover threshold. We also excluded encrusting *Porites* sites given the limited sample size (n = 2).

We treated the categorical variable of coral morphotype as a fixed effect and tested for differences in fractal dimension between levels using an ANOVA. We performed a 1-way ANOVA at each scale interval using generalized least squares to explicitly account for heterogeneity of variance between factor levels. Other ANOVA assumptions were met: the data were normally distributed in almost all instances, and sites were separated by >1 km and could thus be considered independent (i.e., sites were not close enough to overlap the same reef structural features). To account for multiple comparisons, we used a reduced alpha value (α = 0.01) to consider both GAM and ANOVA results significant and performed Tukey's test of multiple comparisons to identify differences between levels for each ANOVA fixed effect. Analyses were conducted using the 'mgcv', 'nlme', 'multcomp', and 'rstatix' packages in R v.4.0.5 (Hothorn et al. 2008; Wood 2011; Pinheiro et al. 2018; Kassambra 2019; R Core Team 2022).

3. Results

Site-level fractal dimension varied depending on the scale interval considered but ranged between 1.289 and 1.001 across all sites and scales. Overall, fractal dimension was highest at the 2−4 cm scale interval (mean ± 1 SD: $D_{2\text{-}4}$ = 1.145 ± 0.064) and lowest at the 128−256 cm scale interval ($D_{128\text{-}256}$ = 1.017 ± 0.015).

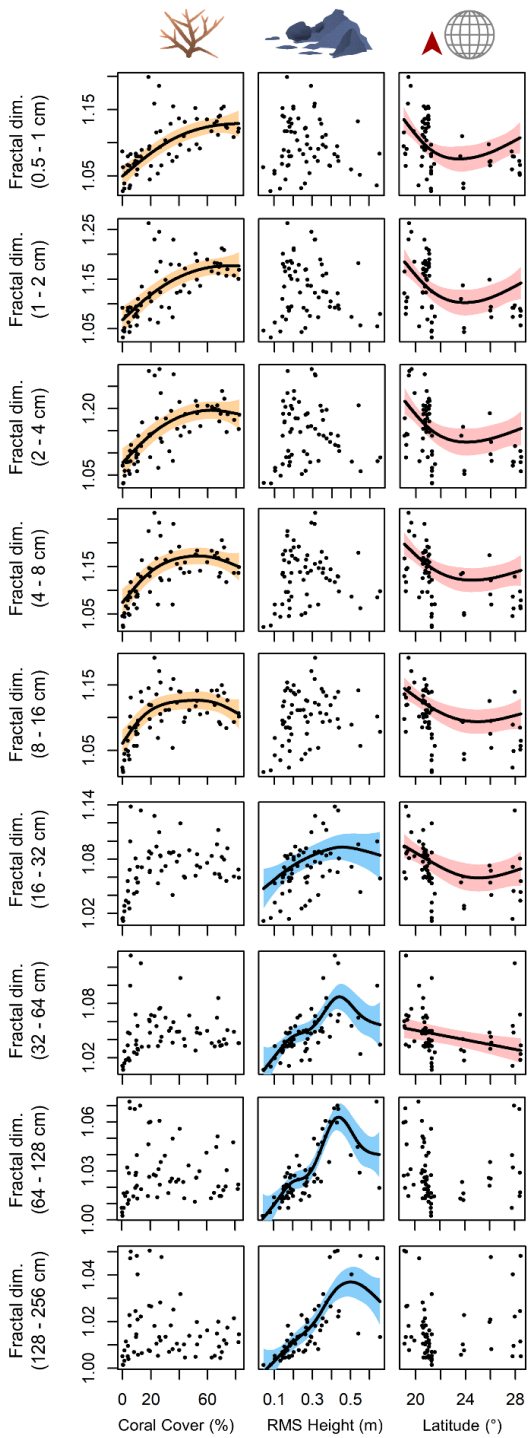

Figure 2.3: Partial effect of coral cover, root mean square (RMS) height, and latitude on fractal dimension, shown for each scale interval. Shading indicates significant relationships at $\alpha = 0.01$ (yellow: coral cover; blue: RMS height; red: latitude) and 95% confidence intervals. Fractal dimension was significantly related to coral cover at scales finer than 16 cm and significantly related to RMS height (a proxy for reef geomorphology) at scales coarser than 16 cm. Full results are shown in Table S2.2.

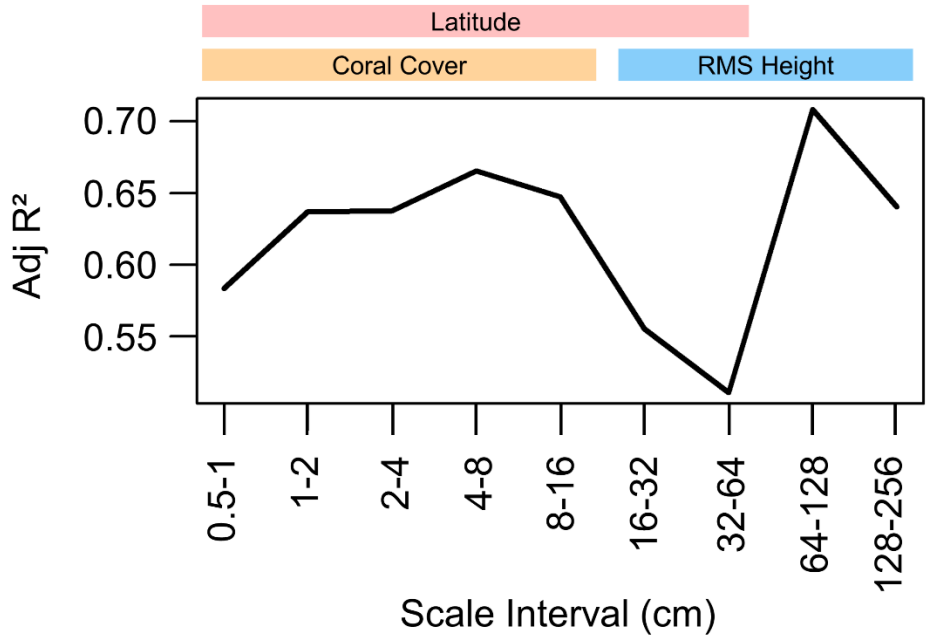

Figure 2.4: Adjusted R^2 value at each scale interval shown for our generalized additive model, which incorporates coral cover, root mean square (RMS) height, and latitude as explanatory variables for fractal dimension. Colors denote the scale intervals over which each explanatory variable was significant (at $\alpha = 0.01$). The decline in adjusted R2 from 16 to 64 cm indicates that neither coral cover nor RMS height is a strong predictor of reef structure at intermediate scales and that a transition zone between biotic and abiotic reef structure exists in this scale range.

3.1 Coral cover and fractal dimension

We found a significant relationship between total coral cover and fractal dimension at all scales finer than 16 cm (Figure 2.3). At these scales, adjusted R^2 values ranged from 0.584 (0.5−1 cm scale) to 0.666 (4−8 cm scale; Figure 2.4). At the finest scale intervals (0.5−4 cm), fractal dimension increased monotonically with coral cover, while at coarser scales (4−16 cm) fractal dimension was highest at reefs with intermediate coral cover and lower at reefs with very high or very low coral cover. For example, at the 8−16 cm scale interval, the fractal dimension for reefs with >70% coral cover had comparable fractal dimension to reefs with 20% coral cover (Figure 2.3).

When considering only sites with >20% coral cover, fractal dimension did not exhibit a significant relationship with coral cover at any scale. However, differences between sites became apparent when the identity of specific corals was considered rather than total percent coral cover. Using 3 m long profile gauges to measure reef structure at the patch scale, we found different patterns of fractal dimension between genera (*Porites* and *Montipora*) and growth forms (branching, encrusting, and massive; Figure 2.5A). Branching corals in particular displayed higher fractal dimension across scales than massive or encrusting corals. We found that skeletons of dead corals also created reef structure; patch-scale measurements of coral skeletons produced values of fractal dimension comparable to those of encrusting corals. Surveys of coral rubble and sand patches produced the lowest values of fractal dimension of all benthic categories considered.

Analysis of reef structure at the site-scale mirrored patch-scale results, with significant differences in fractal dimension emerging for different coral morphotypes at 7 of 9 scale intervals (Figure 2.5B, Table S2.1). Reefs where branching *Porites* was most abundant were most structurally complex overall and had significantly higher fractal dimension than all other types of reefs at 3 scale intervals (1−2, 2−4, and 4−8 cm). Conversely, branching *Montipora* reefs had moderate fractal dimension at small scale intervals but the lowest fractal dimension of all reef types at scale intervals larger than 4 cm. Reefs characterized by encrusting *Montipora* had similar fractal dimension to branching *Montipora* reefs at small scales but were more similar to branching *Porites* reefs at larger scale intervals. Finally, reefs characterized by massive *Porites* had the lowest fractal dimension of all reef types at scales finer than 4 cm, but increasingly high fractal dimension relative to other reefs at larger scale intervals. While patterns of fractal dimension varied across scales, the maximum value for all reef types was observed in

the 2−4 cm scale range *($D_{2\text{-}4}$* = 1.240 ± 0.037 for branching *Porites*, $D_{2\text{-}4}$ = 1.170 ± 0.017 for branching *Montipora*, $D_{2\text{-}4}$ = 1.192 ± 0.030 for encrusting *Montipora*, and $D_{2\text{-}4}$ = 1.146 ± 0.039 for massive *Porites)*. Average coral cover differed between reef types as well: reefs dominated by branching *Montipora* had the highest average coral cover (75.7 ± 6.3%), followed by encrusting *Montipora* reefs (56.6 ± 14.1%), branching *Porites* reefs (38.9 ± 15.1%), and massive *Porites* reefs (26.1 ± 8.4%).

3.2 RMS height and fractal dimension

We found a significant relationship between RMS height and fractal dimension at all scale intervals coarser than 16 cm (Figure 2.3). At these scales, adjusted R^2 values peaked at the 64−128 cm scale interval (R^2 = 0.708). At the coarsest scale intervals, fractal dimension increased with increasing RMS height until reaching a threshold of 40−50 cm RMS height, above which fractal dimension either leveled off or began to decrease.

3.3 Latitudinal trends

Coral cover and RMS height varied between sites and displayed regional patterns (Figure 2.2). Average coral cover was highest in the Maui Nui region (Moloka'i: 65.6 ± 7.6%; Lāna'i: 57.6 ± 25.1%; Kaho'olawe: 48.1 ± 30.5%; Maui: 40.8 ± 13.6%) and lowest in the westernmost atolls of the NWHI (Kure: 6.4 ± 3.8%; Pearl and Hermes: 5.7 ± 5.8%). Other islands had intermediate levels of coral cover (Hawai'i: 17.9 ± 7.7%; O'ahu: 13.7 ± 15.4%; French Frigate Shoals: 15.1 ± 19.2%; Lisianski: 31.5 ± 17.4%). Conversely, islands at both ends of the archipelago had sites with the largest RMS height (Hawai'i: 36.67 ± 16.74 cm; Kaho'olawe: 34.55 ± 13.93 cm; Lisianski: 31.62 ± 5.85 cm; Pearl and Hermes: 46.50 ± 34.99 cm; Kure: 36.27 ± 16.38 cm), while islands in the middle of the archipelago had sites with the lowest RMS height

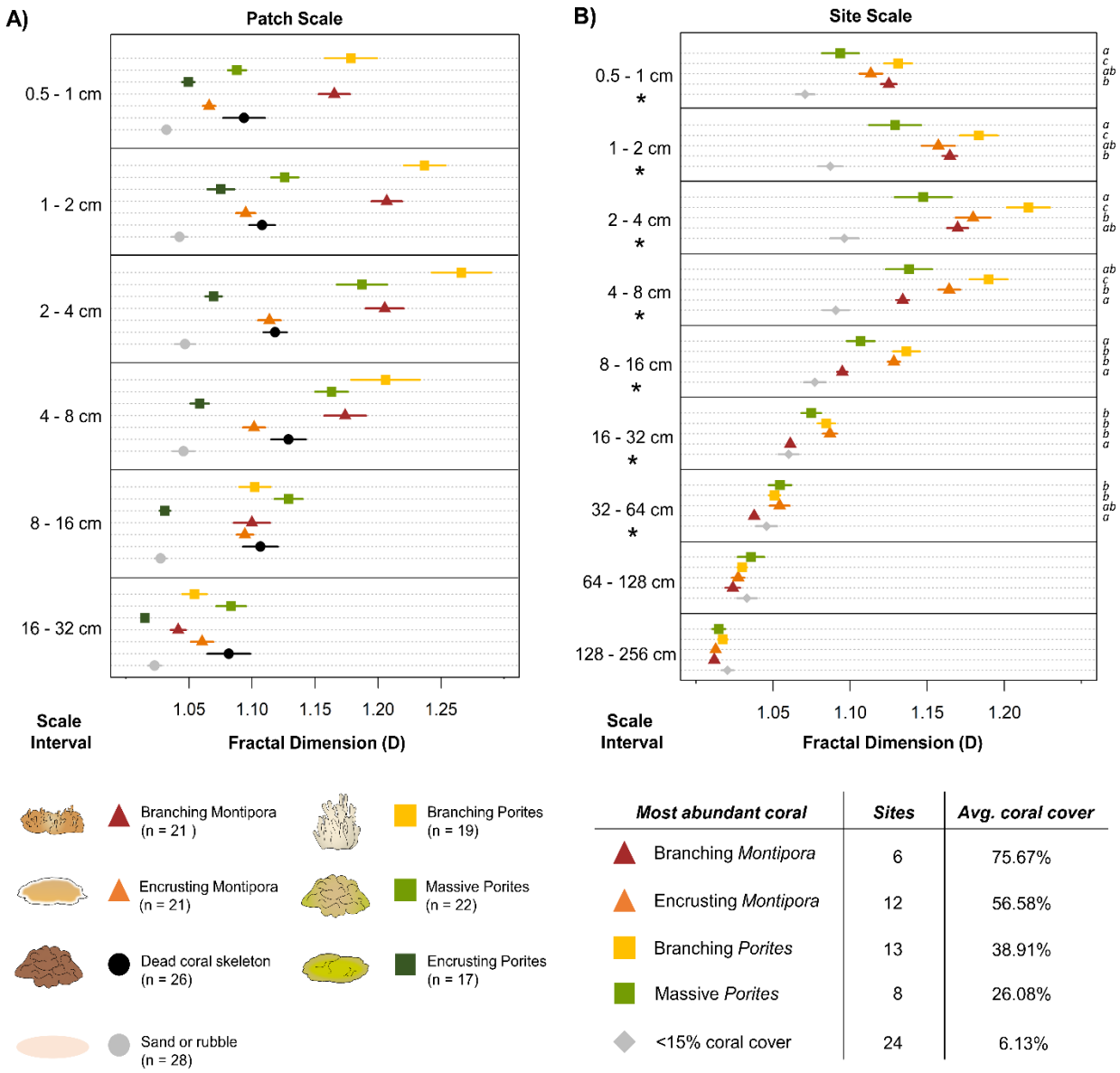

Figure 2.5: The fractal dimension of A) different coral morphotypes, surveyed at the patch scale across 6 different scale intervals and B) sites, based on the most abundant coral morphotype at each site. Sites with >15% total coral cover were classified into one of 4 reef types: branching *Montipora* reefs, encrusting *Montipora* reefs, branching *Porites* reefs, and massive *Porites* reefs. The average percent cover for each reef type is also shown. We tested for differences between reef types at each scale interval using a 1-way ANOVA with generalized least squares. Results were considered significant if $p < 0.01$. Differences between reef types at each scale interval are signified using lowercase letters, which were determined using Tukey's post hoc test of multiple comparisons. Error bars in both panels represent ±SE.

(Maui: 23.24 ± 6.62 cm; Lāna'i: 24.12 ± 7.54 cm; Moloka'i: 19.35 ± 6.89 cm; O'ahu: 15.55 ± 9.75 cm; French Frigate Shoals: 23.02 ± 6.06 cm).

Fractal dimension also varied throughout the island chain and was significantly related to latitude at most scale intervals (0.5−64 cm). At these scales, low-latitude reefs from Hawai'i and the Maui Nui region generally had the highest fractal dimension values, with the lowest values at reefs from O'ahu and intermediate values in the NWHI (Figure 2.3). Latitude was a significant predictor of fractal dimension at all scales at which coral cover was significant and 2 of the 4 scale intervals where RMS height was significant (16−32 and 32−64 cm).

4. Discussion

Studying the fractal dimension of reef contours across a range of scales can help to contextualize the role of biotic and abiotic processes in creating structure on reefs. Notably, we found a significant relationship between coral cover and fractal dimension at scales finer than 16 cm, which demonstrates that biotic processes primarily create reef structure at fine scales. Conversely, we found a significant relationship between fractal dimension and RMS height, our proxy for reef geomorphology, only at scales greater than 16 cm, suggesting that abiotic processes are primarily responsible for creating reef structure at larger scales. Across all sites, fractal dimension was highest at the 2−4 cm scale interval, and reefs overall had higher fractal dimension at small scales than larger scales. Additionally, we found that increases in coral cover do not necessarily correspond to increases in fractal dimension. For instance, at the 4−8 and 8−16 cm scale intervals, reefs with intermediate (30−60%) coral cover had the highest fractal dimension.

Our results demonstrate that the influence of biotic and abiotic processes on reef structural complexity can be detected across distinct and finite ranges of scales. In the Hawaiian

archipelago, the relative influence of biotic and abiotic processes on reef structure appears to transition around the 16 cm scale (Figure 2.4). Previous studies have identified abrupt shifts in cross-scale patterns of reef fractal dimension at a similar range of scales: between 16 and 32 cm in the Seychelles (Nash et al. 2013) and between 10 and 20 cm in the Great Barrier Reef (Bradbury et al. 1984). These similarities suggest that a transition zone between biotic and abiotic structure may be a widespread characteristic of coral reefs at this range of scales, although the precise boundaries of this transition zone will likely shift in response to coral colony size structure and community composition. In the context of the textural discontinuity hypothesis, this suggests that small- and large-bodied reef organisms may be interacting with different structural features in their habitat, features that are created by distinct processes and change in response to distinct environmental forcings.

Researchers should be cognizant of this transition zone. Measurements with a resolution of centimeters will be more ecologically relevant for studies focused on biotic structure than measurements with a resolution of decimeters or meters, which may not be able to detect fine-scale structural changes. While other researchers have used remote sensing data with meter resolution to characterize reef structure over large spatial extents in the MHI (Asner et al. 2021), our results suggest that measurements with such coarse resolution will lack the sensitivity needed to characterize many changes in biotic reef structure over time. High-resolution data collected over spatial extents of 100s of m^2, such as the SfM models used here, provide the resolution needed to track finescale changes in reef structure over ecologically relevant areas. Integrating these data with LIDAR or satellite-based remote sensing (Swetnam et al. 2018; Deng et al. 2019; Slocum et al. 2020) could enable researchers to answer additional questions across an even broader range of scales (i.e., entire coastlines to islands). However, when used in isolation, these

coarser-scale remote sensing approaches appear to be insufficient for characterizing biotic structural change on reefs.

It is important to note that using fractal dimension to quantify coral reef complexity does not mean that coral reefs are fractal structures (Halley et al. 2004). For an object to be considered fractal, it must exhibit self-similarity and scale invariance, meaning that any part of the object must resemble the entire object and that patterns reoccur across scales (Mandelbrot 1983; Purkis et al. 2006). By this definition, coral reefs are not fractals: reefs are composed of a diversity of biotic and abiotic structures that are not self-similar (i.e., a corallite does not necessarily resemble a coral colony). Additionally, our results demonstrate that rugosity does not exhibit a power law relationship with measurement resolution across all scale intervals (Figure 2.5), which violates the condition of scale invariance for fractals. Instead, the departure from a true power law relationship that we observed in this study indicates that more structural complexity exists at certain scale intervals than others. However, while objects in nature are rarely if ever truly fractal, they may exhibit fractal properties across a finite range of scales (Halley et al. 2004; Purkis et al. 2006).

We utilized a fractal approach to identify the relative contribution of coral cover and geomorphology to overall reef structure across a latitudinal gradient in the Hawaiian archipelago. With the exception of O'ahu, the MHI had greater fractal dimension than the NWHI at scales associated with coral cover (<16 cm). This is consistent with our benthic cover analysis, which showed that Moloka'i, Lāna'i, Maui, and Kaho'olawe had the highest levels of coral cover in the island chain, while atolls in the NWHI had low or intermediate coral cover. Despite having some of the most pristine reefs in the world, the NWHI are characterized by relatively low coral cover (Friedlander et al. 2009; Vroom & Braun 2010), due in part to their northerly location. Corals on

high-latitude reefs, such as the NWHI, face greater competition with macroalgae and more extreme temperature fluctuations, factors that reduce coral growth rates, accretion, and reproductive capacity (Kleypas et al. 1999; Abdo et al. 2012). However, it is important to note that other studies have found coral cover in the NWHI to be patchy, with concentrated areas of up to 80% coral cover in some locations and higher cover in lagoons than forereef habitats (Vroom & Braun 2010). Given that our surveys were confined to the forereef of 4 atolls, our results may not paint a complete picture of coral-driven complexity on NWHI reefs.

The non-linear relationship between fractal dimension and latitude may be the result of anthropogenic impact (i.e., low coral cover and low fractal dimension on reefs around human population centers in O'ahu) and the geologic history of the island chain. As recently as 20,000 years ago, the islands of Moloka'i, Lāna'i, Kaho'olawe, and Maui were connected as a single island known as Maui Nui (Price & Elliott-Fisk 2004; Field et al. 2019). As a result, the channels separating these islands are shallow and the reefs are geologically young, which may explain why many of our sites from the Maui Nui region had relatively low RMS height. The placement of these islands also shields their coastlines from wave energy (Field et al. 2019), allowing dense monocultures of *Porites compressa* and *Montipora capitata* to form in sheltered and relatively flat nearshore environments. This contrasts sharply with the island of Hawai'i, which has steep nearshore topography and is still actively volcanizing (Clague & Dalrymple 1987). This geologic history was evident in several of our sites from the southwest coast, which had large boulders, steep topography, and high fractal dimension at large scales. Although several sites in the NWHI also displayed steep underlying topography, the geomorphology of these reefs differs from that of younger islands. The underlying volcanic rock forming the NWHI has long since subsided and is now capped by limestone from millions of years of reef growth to form atolls (Rooney et al.

2008). Any extreme topography at these atolls is a result of erosion or growth of the reef itself rather than the geomorphology of the original island. Baseline studies in the region have noted that islands at the northwest end of the archipelago have more pronounced spur and groove geomorphology (Friedlander et al. 2009), which could be a result of greater exposure to wave energy (Rooney et al. 2008). So, while reefs at both ends of the archipelago have more extreme RMS height, the drivers shaping reef geomorphology are likely different.

In addition to detecting differences in reef structure across a latitudinal gradient, we also detected differences in coral-driven structure at the scale of monospecific patches and entire 100 m^2 sites. Our finding that branching *Porites* creates the most structure of the selected coral morphotypes is consistent with other studies (Richardson et al. 2017; Burns et al. 2019) and suggests that branching *Porites* represents a keystone structure-forming taxon on Hawaiian reefs. Patch- and site-scale results were largely consistent with the exception of encrusting *Montipora*, which had lower fractal dimension at the patch scale than the site scale. One explanation for this observation is that reefs dominated by encrusting *Montipora* tended to have higher percent cover of *Porites*, while reefs dominated by branching *Montipora* had almost no *Porites* cover. This suggests that communities with a greater diversity of coral genera and growth forms may provide greater amounts of structure than monospecific reefs, even if coral cover on monospecific reefs is high. Indeed, percent cover of live corals was twice as high on branching *Montipora* reefs than on branching *Porites* reefs, yet branching *Porites* reefs had higher fractal dimension at nearly all scales. By examining the fractal dimension of different coral communities, we were able to detect differences in structure that were not apparent when comparing reefs based on their total amount of coral cover alone. Taken together, these results support the findings of past studies that have found that structural complexity is not merely a function of coral cover (Alvarez-Filip

et al. 2011a; Richardson et al. 2017; González-Barrios & Álvarez-Filip 2018; Burns et al. 2019); the habitat a reef creates is dependent on the genera and growth form of its corals.

The ability to detect growth form and genus-specific patterns of fractal dimension is important because benthic communities are dynamic and shift in response to both anthropogenic and biophysical drivers (Gove et al. 2013; Jouffray et al. 2015, 2019). Donovan et al. (2018) demonstrated the existence of multiple reef regimes in the MHI and found that reefs may switch between regimes over time. Similarly, Rodgers et al. (2015) documented a change in the relative abundance of coral species in the MHI between 1999 and 2012 (encrusting *Montipora* spp. increased in abundance while *P. compressa*, the primary form of branching *Porites* in Hawai'i, decreased). It is possible that community composition in the MHI has shifted further since 2012, especially given that a severe bleaching event occurred in the archipelago from 2014−2015 (Couch et al. 2017; Chung et al. 2019). As ocean temperatures continue to warm, climate change is expected to impact benthic communities on coral reefs (Hoegh-Guldberg et al. 2007; Hughes et al. 2018; Eakin et al. 2019), which may in turn impact structural complexity due to a loss of total coral cover or a shift in the dominance of certain coral species (Burns et al. 2016; Ferrari et al. 2016; Wilson et al. 2019). Given our findings that coral skeletons contribute to overall reef structure, we expect that the scale and magnitude of structural change following bleaching events (where coral tissue is lost but coral skeletons remain for several years; Couch et al. 2017) would differ from disturbances such as storms (where the underlying coral skeleton may be destroyed; Burns et al. 2016). Because bleaching, storms, and shifts in community composition may impact reef structure and habitat availability in different ways, it will be important to employ multi-scale methods to contextualize these changes over time using a variety of remote sensing approaches. Furthermore, since biotic structures are likely more vulnerable to climatic disturbance than

abiotic structures and create structure at smaller scales, our results reaffirm the need for fine-scale structural complexity measurements to assess the resilience of biotic reef structure across space and time.

5. Conclusions

Our findings demonstrate that multi-scale analyses of structural complexity can provide much needed context about the degree to which biotic and abiotic processes contribute to structural complexity on coral reefs. By using fractal dimension to partition reef structure into a series of scale intervals, we were able to estimate the role of corals and reef geomorphology in creating reef structure across a latitudinal gradient in the Hawaiian archipelago. Interpreting these findings in the context of the textural discontinuity hypothesis, our results can serve as a proxy for habitat availability for reef organisms of different size classes. However, while several studies have shown that the relationship between fish assemblages and reef structure is dependent on body size (Friedlander & Parrish 1998; Harborne et al. 2012; Nash et al. 2013; Agudo-Adriani et al. 2019), further research using fractal methods is needed to test whether the textural discontinuity hypothesis holds true for reef fish assemblages across a wide range of oceanographic conditions, human impacts, and geographies.

Furthermore, our study highlights the limitations of structural complexity studies conducted at a single scale. These approaches paint a singular picture of reef structure that is relevant to only one size class of reef organisms. When time or resources prevent research programs from using multiple scales of measurement, care should be taken to choose the appropriate scale for the ecological question at hand. However, with technological advances made possible by SfM, it is increasingly practical to conduct multi-scale studies of numerous ecological phenomena, including structural complexity. This study highlights how SfM can be

harnessed to expand the utility of existing metrics, such as linear rugosity and fractal dimension, to allow us to learn something new that would not be feasible using conventional field approaches. SfM will allow researchers to innovate and learn more from coral reefs than was ever possible before, with direct applications to reef ecology and conservation.

6. Acknowledgements

Chapter 2, in full, is a reprint of the material as it appears in Marine Ecology Progress Series. McCarthy, Orion S.; Smith, Jennifer E.; Petrovic, Vid; Sandin, Stuart A. 2022. The dissertation author was the primary investigator and author of this paper.

We thank Lindsay Bonito, Zach Caldwell, Samantha Clements, Eric Conklin, Clinton Edwards, Emily Kelly, Christian McDonald, Nicole Pedersen, Chris Sullivan, Melissa Torres, Darla White, and Brian Zgliczynski for their help with data collection in the field. We also thank NOAA, the Hawai'i Division of Aquatic Resources, The Nature Conservancy – Hawai'i, and the Center for Marine Biodiversity and Conservation for field and logistical support, as well as the staff of all research vessels involved including the Aloha Kai, Alyce C, and Hi'ialikai. Special thanks to Nicole Pedersen for her help with 3D model construction and data storage, and to Adi Khen for creating the coral artwork used in Figures 2.1 and 2.5. Brice Semmens and Greg Rouse also provided valuable input during the early stages of project conception. We also thank the 2 anonymous reviewers whose feedback helped improve this study. This work was made possible by the efforts of the 100 Island Challenge, which has been supported by various organizations including the Scripps Family Foundation and the Moore Family Foundation. In addition, this work was also supported by the Bohn Family Foundation and Orion’s NSF Graduate Research Program Fellowship.

Chapter 3 – Fine-scale variation in community composition shapes ecosystem response to disturbance

Orion S. McCarthy, Emily L. A. Kelly, Anela K. Akiona, Samantha M. Clements, Tatiana Martinez, Nicole E. Pedersen, Cole Peralto, Katharine Ricke, Sarah L. Romero, Itana F. Silva, Mitchell H. Smelser, Kristy Wong Stone, Russell T. Sparks, and Jennifer E. Smith

Abstract

High variability in community composition at scales of meters to kilometers is common on tropical coral reefs. These ecosystems are characterized by frequent disturbance events, which can create a patchwork of successional stages within the same reef tract. The successional stage of a given community will impact its future stability, recovery potential, and trajectory over time. Thus, this fine-scale heterogeneity is of interest to natural resource managers. Using large-area imagery, we tracked benthic community dynamics across 36 leeward forereefs on four neighboring islands in the Maui Nui region of the Hawaiian Islands. Individual reefs exhibited complex temporal dynamics, but the region overall showed remarkable stability over a six-year period (2017 – 2023) despite impacts from high surf events, a marine heatwave, and unprecedented shifts in human behavior due to the COVID-19 pandemic – all against a backdrop of chronic anthropogenic stress. We document high spatial variation in benthic community composition that was only partially explained by island and environmental regime. Through hierarchical clustering, we identify three distinct community types across the region that could represent different successional stages of reef development. Reefs belonging to the same community type exhibited similar rates of change in coral cover and structural complexity over time, more so than reefs located on the same island. Importantly, reefs with low coral cover and

more *Porites* were most likely to see coral cover increase over time, while reefs with high coral cover and more *Montipora* were more likely to experience coral decline. Our findings highlight the influence of life-history and successional stage on community trajectories. Accounting for these factors, not simply overall coral cover, is essential for designing effective management interventions. Large-area imagery timeseries should be leveraged to inform site-specific management that accounts for a community's unique composition and history of disturbance.

1. Introduction

The question of how biological communities vary in space and time, and what mechanisms are responsible for such variation, is increasingly relevant for natural resource managers, who are tasked with maintaining ecosystem stability in an era of heightened anthropogenic impact. Management is more effective when resource managers understand the primary drivers of community variation within their jurisdiction (Pullin & Knight 2003; Wedding et al. 2018). Once locally-relevant drivers of community variation have been identified, managers can design targeted conservation interventions that reduce ecosystem degradation and promote recovery (Sugihara et al. 2012; Anthony et al. 2015; Donovan et al. 2023b; Gove et al. 2023).

To integrate a community ecology perspective in conservation decision making, resource managers often rely on data from long-term monitoring programs. These observational data provide important context about community variation, stability, and trajectory over time (Hughes & Connell 1999; Lindenmayer & Likens 2009; Moritz et al. 2021; Rodgers et al. 2021). However, applying monitoring data to identify causal drivers of community variation can be deceptively challenging, due in part to uncertainties related to scale (Hatcher et al. 1987; Menge

& Olson 1990; Levin 1992; Murdoch & Aronson 1999). How far in space and time can observations about ecosystem condition be extrapolated? Are neighboring sites replicates of the same community or different communities? Do observed patterns represent baseline conditions, recovery from disturbance, or transient dynamics (Hock et al. 2023)?

The answers to these questions will depend in part on the spatial and temporal scales encompassed by the monitoring program. Depending on the scale of observation, community dynamics may appear to be driven by environmental factors or appear decoupled, instead reflecting biotic feedbacks that manifest as regular pattern formation and spatial autocorrelation (Rietkerk & van de Koppel 2008; Legendre et al. 2014; Ford et al. 2020). Both of these observations can be true concurrently, since ecological systems are structured by both biotic and abiotic processes that operate at different spatial and temporal scales (Hatcher et al. 1987; Krummel et al. 1987; Kotliar & Wiens 1990; Holling 1992; Levin 1992). For example, the distribution of organisms in a habitat may be driven simultaneously by competition over the scale of meters and by climatic variation over the scale of hundreds of kilometers (Best et al. 2007; Ritchie et al. 2009; Meier et al. 2011; Barott et al. 2012). Similarly, community recovery following a disturbance will depend the scale of the disturbance in both magnitude and duration, but also the heterogeneity of disturbance impacts and the spatial distribution and composition of the surviving community (Connell 1997; Turner et al. 1998; Haire & McGarigal 2009; Dietzel et al. 2021). This is especially true for benthic communities on coral reefs, which exhibit high spatial and temporal variation due to their location in dynamic nearshore environments (Hughes & Connell 1999; Friedlander et al. 2003; Gouezo et al. 2019).

Succession on coral reefs is constantly reset by disturbance events, which foster diversity in both space and time (Grigg 1983; Gouezo et al. 2019; Jouval et al. 2020). According to the

intermediate disturbance hypothesis, frequent and moderate strength disturbance events prevent competitive exclusion and allow diverse communities of organisms to coexist (Connell 1978; Dollar 1982; Grigg 1983; Rogers 1993; Mouillot et al. 2013). In addition to promoting species diversity, patchy disturbance impacts can also produce high landscape heterogeneity, even within the same reef tract. For example, exposed coastlines will bear the brunt of wave damage from incoming storms (Dietzel et al. 2021), as will shallower sites (Dollar 1982), compared to more sheltered locations mere meters to kilometers away. Sediment deposition onto corals may be concentrated at stream outflows (Jokiel et al. 2014; Minton et al. 2022) or on reefs with higher densities of macroalgae (Stamski & Field 2006). Water flow and turbidity moderate coral bleaching and mortality during marine heatwaves at the scale of 100s of meters to kilometers (Carlson et al. 2022; Morais et al. 2023; Yadav et al. 2023). Furthermore, the differential susceptibility of a given taxon to disturbance can lead to meter-scale patchiness of disturbance impacts (Maragos & Grigg 1974; Burns et al. 2016; Jouval et al. 2020), producing a complex post-disturbance community that represents a patchwork of successional stages (Hughes & Connell 1999; Gouezo et al. 2019).

Identifying the successional stage of a community can provide useful context for natural resource managers (Gouezo et al. 2021). Different successional stages essentially represent different community types, or reef regimes, each characterized by its own cast of species and rates of competition, recruitment, habitat structural complexity, and herbivory (Rogers 1993; Connell 1997; Dudgeon et al. 2010). Temporal trends and recovery potential will also differ among reef regimes (Dudgeon et al. 2010; Donovan et al. 2018; Crisp et al. 2022; Cresswell et al. 2023). For example, coral growth in recently disturbed low-density communities will mostly be controlled by environmental conditions, whereas interspecific competition will play a larger

role on later-stage successional communities with higher coral densities (Rogers 1993; Mouillot et al. 2013). Thus, reef regimes will likely respond differently to acute and chronic anthropogenic impacts as well as conservation interventions (Jouffray et al. 2019).

Studies that seek to identify and map different coral reef regimes have mostly spanned large gradients in environmental variables across regional or archipelagic scales (Jouffray et al. 2015, 2019; Smith et al. 2016; Donovan et al. 2018). This large-scale perspective is particularly useful for identifying differences in community composition that are driven by strong environmental gradients, such as community variation between leeward and windward coastlines (Storlazzi et al. 2005; Williams et al. 2013; Donovan et al. 2018). Large-scale studies are also useful for identifying locations where human impacts have decoupled expected bio-physical relationships (Sandin et al. 2008; Williams et al. 2015; Smith et al. 2016). However, fewer studies have sought to identify distinct reef regimes across small (intra-island) spatial gradients with limited oceanographic variability (but see DeVantier et al. 1998), even though intra-island scale studies are more consistent with the jurisdictional purview of most natural resource management agencies (Sandin et al. 2022). Spatial variation in community composition can be substantial among reefs on the same island (kilometer scale; Murdoch & Aronson 1999; Friedlander et al. 2003; Ford et al. 2020; Sandin et al. 2022) or even within the same reef (meter scale; Hughes et al. 1999; Ross et al. 2012; Edwards et al. 2017). Heterogeneity of reef regimes at these scales could indicate the need for a fine-grained, site-specific approach to management.

Failing to account for sources of community variation at scales relevant to management can reduce management efficacy (Kotliar & Wiens 1990; Pullin & Knight 2003; Rogers et al. 2015). However, it can be difficult to design an appropriate monitoring program without prior knowledge of the processes driving community variation, and the scales over which those

processes operate (Hatcher et al. 1987; Wiens 1989; Gouezo et al. 2021). Conservation technology that allows resource managers to study community structure at multiple scales simultaneously can help. One such technology is large-area imagery, also known as Structure from Motion photogrammetry. Large-area imagery surveys can reconstruct 3D models of benthic environments covering 100s of square meters with millimeter scale resolution (Edwards et al. 2023). When these data are collected repeatedly at fixed sites, the added temporal dimension creates new opportunities for multi-scale studies of community variation in space and time (McCarthy et al. 2023).

Here, we utilize a timeseries of 3D coral reef models from the Maui Nui region of the Hawaiian Islands to 1) describe spatial and temporal variation in benthic community composition; 2) determine if reefs with similar community composition display similar successional trajectories; and 3) identify the drivers of change in coral cover and structural complexity. The spatial scale of this study corresponds to the management jurisdiction of the Maui office of the Hawai'i Division of Aquatic Resources, and complements statewide long-term monitoring conducted via the Hawai'i Coral Reef Assessment and Monitoring Program (CRAMP; Brown et al. 2008; Rodgers et al. 2015; Sparks et al. 2015).

2. Methods

2.1 Study design

The Hawaiian islands of Maui, Kaho'olawe, Lāna'i, and Moloka'i were connected as recently as 21,000 – 12,000 years ago, forming a single island called Maui Nui (Grigg et al. 2002; Price & Elliott-Fisk 2004; Field et al. 2019). Today, these neighboring islands are separated by a series of shallow (< 300m) channels that are largely protected from open ocean swell (Storlazzi et al. 2005). Due in part to reduced wave exposure, reef tracts in the region have

higher coral cover than elsewhere in the Hawaiian Islands (Field et al. 2019). However, each island is also exposed to a unique combination of anthropogenic impacts. Maui is home to > 140,000 residents and hosts > 2 million tourists per year (Hawai'i Tourism Authority 2023), and as a result Maui's reefs are exposed to higher levels of nutrient pollution, fishing, sediment runoff and other chronic stressors (Brown 2004; Smith et al. 2005; Dailer et al. 2010; Vermeij et al. 2010; Maynard et al. 2019; Weng et al. 2023). Moloka'i and Lāna'i host smaller communities (< 10,000 people), while Kaho'olawe is uninhabited. Access to Kaho'olawe, including for fishing, is restricted due to the presence of unexploded ordinances (Cox & Jokiel 1995). Although these islands have a smaller human population than Maui, they suffer from chronic sedimentation due to overgrazing by invasive ungulates (Cox & Jokiel 1995; Stamski & Field 2006; Jokiel et al. 2014; Minton et al. 2022), and in the case of Kaho'olawe, severe degradation from decades of munitions testing by the US military (Cox & Jokiel 1995). Compared to elsewhere in the Main Hawaiian Islands, reefs on Lāna'i and Kaho'olawe are generally understudied due to their relative inaccessibility (Cox & Jokiel 1995; Field et al. 2019; Minton et al. 2022).

We surveyed 36 fixed long-term monitoring sites in the Maui Nui region (Figure S3.1). Surveys were completed as part of the 100 Island Challenge, a broader effort to document global patterns of coral reef condition and change over time (Naughton et al. 2015; Sandin et al. 2020). Sites were not placed randomly, and were confined to known reef tracts. In keeping with the sampling design of the 100 Island Challenge, we identified eight to twelve sites per island, focusing on hardbottom forereef habitat with leeward exposure at approximately 10m depth. In practice, the depths of our sites ranged from 3.4 to 11.3m (mean depth = 9.0m) to capture several important reef tracts in Maui Nui that are primarily found at depths shallower than 10m (i.e.,

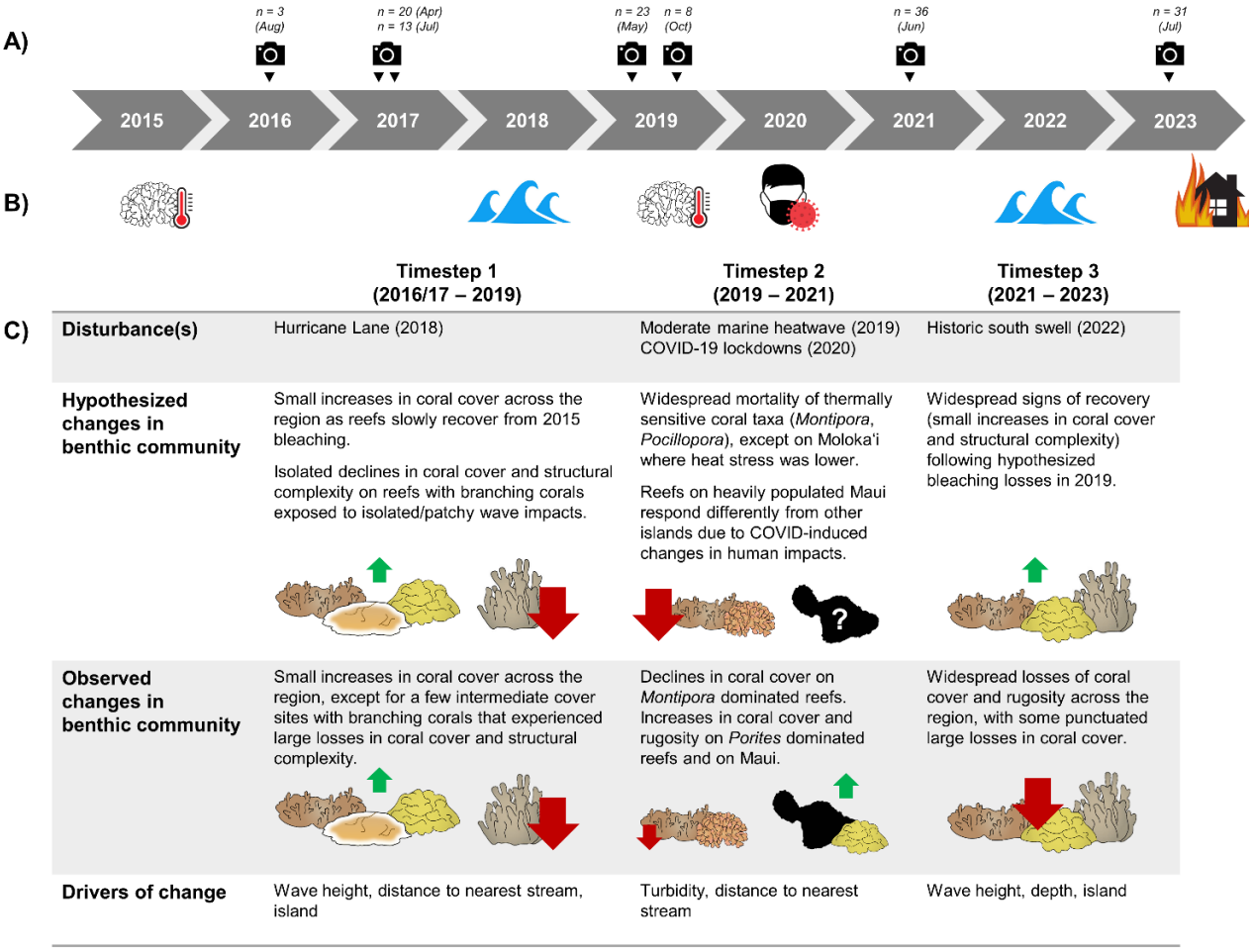

Figure 3.1: A) A timeline of survey effort, with cameras representing field expeditions. The number of sites surveyed in each expedition is also noted. B) Notable disturbance events in Maui Nui from 2015 to 2023. C) Hypothesized patterns of coral cover and rugosity change in each timestep are compared with observed patterns of change. Observations were consistent with expectations for timestep 1, partially consistent for timestep 2, and not consistent for timestep 3. Factors that best explained change in both coral cover and rugosity are shown in the bottom row. Vector graphics represent the following coral taxa, from left to right: *Montipora capitata*, *Montipora patula*, *Porites lobata*, *Porites compressa*, and *Pocillopora*.

West Maui). Several sites on Maui and Moloka'i are positioned close to or overlap with fixed long-term CRAMP transects maintained by the state of Hawai'i (Figure S3.2).

We completed our first survey between July 2016 and July 2017, and resurveyed sites in 2019, 2021, and 2023 (Figure 3.1A). Most sites were surveyed four times (n = 30), while a minority were surveyed only three times (n = 2) or twice (n = 4). Between 2016 and 2023,

several moderate disturbance events impacted reefs in the region (Figure 3.1B). Marine heatwaves caused widespread coral bleaching before (2015) and during (2019) our timeseries (McCarthy et al. *in prep.a*; Couch et al. 2017; Winston et al. 2022; Yadav et al. 2023). Hurricane Lane narrowly missed Maui Nui in 2018 but still generated large swell, while a historic south swell impacted the region in 2022 (Nugent et al. 2020; Osher 2022). Finally, changes in human behavior due to the COVID-19 pandemic (i.e., lockdowns, temporary cessation of tourism) altered anthropogenic impacts on Maui Nui's reefs in 2020 (Weng et al. 2023). It is worth noting that the devastating 2023 wildfires on Maui occurred just after our 2023 surveys. Nearshore impacts from wildfire debris or runoff are currently unclear and are not covered in this study.

2.2 Large-area imagery surveys

We surveyed fixed long-term monitoring sites using large-area imagery, also known as Structure from Motion photogrammetry. This technology relies on parallax, the apparent displacement of an object when viewed from multiple directions, to generate composite 2D or 3D models of benthic environments from overlapping imagery (Edwards et al. 2023). Large-area imaging has been used extensively to study coral reefs (McCarthy et al. 2023; Remmers et al. 2023), including to quantify habitat structural complexity (Burns et al. 2016; Ferrari et al. 2017; McCarthy et al. 2022), benthic community composition (McNamara et al. 2019; Palma et al. 2019; Fukunaga et al. 2022), and the spatial patterning of benthic organisms (Edwards et al. 2017; Price et al. 2021). Importantly, contiguous swaths of reef (hundreds of m^2) can be precisely relocated and imaged over multiple years. These timeseries allow researchers to track changes in structural complexity and successional patterns of entire benthic communities at high spatial and taxonomic resolution (Ferrari et al. 2016; Magel et al. 2019; Sandin et al. 2020).

Our large-area imaging surveys followed the methods of Edwards et al. 2017. A diver recorded the GPS coordinates of a stainless-steel stake or eyebolt embedded in the reef, which served as a permanent reference for site relocation. Following the first survey, divers also used a "roadmap" (a top-down view of the 3D model printed on underwater paper) to ensure that site boundaries aligned with previous years. The boundaries of each 10 x 10 m site were marked with six calibration tiles and four reference floats to aid in diver navigation. During the survey, one diver measured the depth of each calibration tile and placed four 0.5m long scale bars within the site boundaries. The other diver swam 1.5m over the benthos with a custom camera rig, following a gridded pattern to produce high overlap between photos. The custom camera rig contained two Nikon DSLR cameras (D7000, except for in the 2023 surveys which used D780) within Ikelite underwater housings. One camera was equipped with a wide-angle lens (18mm for D7000, 24mm for D780), while the other was equipped with a telephoto lens (55mm for D7000, 60mm for D780). Both cameras used an automatic one-second interval timer, which resulted in roughly 5,000 photos per site. On each pass, the camera diver swam several meters beyond the edge of the core 10 x 10 m site, creating a buffer zone of additional imagery. Each survey took approximately 50 minutes to one hour to complete.

After each field expedition, we generated a dense-point cloud reconstruction (3D model) of each site using *Agisoft Metashape* (St. Petersburg, Russia) following the procedures described in Cook et al. 2023. Imagery from both cameras was aligned, but only imagery from the wide-angle camera was used to generate 3D models. The telephoto images, which had higher resolution but a smaller spatial footprint than wide-angle images, were used as a reference for species ID (see section 2.3). Once 3D models were generated, we loaded them into *Viscore*, a custom software designed for 3D data visualization and ecological analysis (Petrovic et al. 2014;

Cook et al. 2023). Using Viscore, we entered depth and scale metadata and aligned 3D models of the same site collected in different years. This co-registration of models allowed us to analyze the same $100m^2$ benthic community across multiple points in time.

2.3 Ecological data extraction

We used our aligned timeseries of 3D models to quantify three metrics of benthic community composition: 1) percent cover of benthic taxa, 2) landscape heterogeneity, and 3) structural complexity (see below for details). All data were collected within a fixed 10 x 10 m plot for each site, with the exception of one site (Kaho'olawe 6), where incomplete image overlap resulted in poor reconstruction of one region of the 3D model from 2019. To account for these gaps, we positioned a 12 x 5 m plot in the fully reconstructed region of the 3D model, and used this fixed plot to collect ecological data for all years at this site.

For assessments of percent cover, we identified benthic taxa to the finest possible taxonomic resolution using Viscore's Virtual Point Intercept tool. This tool mimics *in situ* point intercept sampling by placing a user-defined number of stratified random points within a single quadrat in the 3D reef model (Fox et al. 2019). Users then access the raw images that underpin the 3D model to evaluate benthic cover at each stratified random point. This approach is superior to traditional photoquadrats because users can access several images (typically >20) to get multiple views of the point of interest, reducing error associated with blurry or occluded imagery. All points were identified by a single coral reef ecologist (OM), and these IDs were grouped into 15 categories chosen to reflect the dominant benthic taxa and functional groups in Hawai'i (Figure S3.3A).

To quantify landscape heterogeneity, we used a Voronoi tessellation to interpolate benthic point intercept data for each site. Other studies have used Voronoi tessellation to study

spatial patterning and landscape heterogeneity in forests (Mercier & Baujard 1997; Passolt et al. 2013) and cities (Miao et al. 2016). Here we used the Voronoi tessellation to calculate the proportion of Voronoi polygon boundaries that represent unlike adjacencies (where two different taxa border each other; Figure S3.4). Landscapes with a higher proportion of unlike adjacencies are less aggregated and have finer spatial grain, smaller patches, and more opportunities for interspecific interactions (Cushman et al. 2008; Wang et al. 2014). We used a density of 25 points/m^2 (2,500 points per site) to identify benthic taxa and calculate landscape heterogeneity. Previous work has found this density of points to be 1) sensitive enough to reliably detect benthic taxa with >1% cover, 2) ecologically relevant for analyzing landscape heterogeneity based on the typical size of coral colonies and algal patches, and 3) not excessively time consuming to collect (McCarthy et al. 2022; Figure S3.5).

We quantified structural complexity using two measures of linear rugosity as well as fractal dimension. These measures were derived from depth measurements collected using Viscore's Virtual Profile Gauge tool (McCarthy et al. 2022). This tool uses virtual rods to measure the height of the substrate along virtual transects, and the spacing between each rod determines the measurement resolution. The terminus of each rod can be connected to form a reef contour, and linear rugosity is calculated by dividing the length of this contour by the horizontal length of the transect. A perfectly flat surface has a linear rugosity of 1, with higher rugosity values corresponding to more structurally complex surfaces. Transects were oriented in the alongshore direction and spaced every 10cm within the same 10 x 10 m plot used to assess benthic cover. A single site-level rugosity value was obtained by averaging the linear rugosity of each transect. We measured linear rugosity at two resolutions (1cm and 50cm) and calculated fractal dimension (D) following Nash et al. 2013:

$$D = \frac{\log\left(R_{50cm} - R_{1cm}\right)}{\log\left(50cm - 1cm\right)}$$

These metrics of structural complexity have been found to correspond to different structural elements within benthic communities (Fukunaga et al. 2020a). Fine-scale linear rugosity (1cm resolution) is indicative of coral-generated structure, while coarse-scale linear rugosity (50cm resolution) is indicative of structure created by reef geomorphology (McCarthy et al. 2022). Fractal dimension describes the rate of change in rugosity between these two different scales (Nash et al. 2013).

2.4 Statistical analysis

To analyze spatial and temporal trends in benthic community composition, we first calculated the Bray-Curtis dissimilarity among all sites in all years. Our multivariate data consisted of 1) percent cover of 15 benthic classes, 2) landscape heterogeneity (the proportion of unlike adjacencies), and 3) structural complexity metrics (linear rugosity collected at 1cm and 50cm resolution, and fractal dimension). For comparability with percent cover data, we standardized landscape heterogeneity and structural complexity metrics to range from 0 to 1. We used non-metric multidimensional scaling (NMDS) to visualize benthic community composition in multidimensional space using the vegan package (Oksanen et al. 2022). Next, we performed a permutational multivariate analysis of variance (PERMANOVA) to identify significant drivers of benthic community variation. These drivers included island (fixed effect; Kaho'olawe, Lāna'i, Maui, and Moloka'i), depth (m), wave power (max monthly mean, kW/m), sea surface temperature (standard deviation, °C), chlorophyll-a (mean, mg/m^3), surface irradiance (mean, $mol\ m^{-2}\ d^{-1}$), sediment export (tons/ha/yr), and effluent ($gal/kg^2/day$) (Figure S3.6, Table S3.1). Environmental variables represent long-term average conditions for our sites and were sourced from the Ocean Tipping Points project (Whittier & El-kadi 2014; Falinski 2016; Li et al. 2016;

Wedding et al. 2018). None of the environmental variables had a correlation coefficient more extreme than 0.54 (Figure S3.7A). We used the LDM package (Hu & Satten 2023) to perform a repeated measures PERMANOVA to account for the non-independence of resampling fixed sites.

To identify groups of sites with similar benthic community composition, we performed a hierarchical cluster analysis using the complete linkage method within the hclust function in R (R Core Team 2023). Our observations from the field led us to believe that three ecologically distinct community types exist, which was supported by the hierarchical clustering dendrogram (Figure S3.8A). To explore the robustness of our results to clustering method, we also implemented clustering using Ward's method (Figure S3.8B). While a few sites changed position, the same three ecological groupings were achieved regardless of the clustering method employed. We considered clusters to represent distinct benthic communities, and tested the hypothesis that reefs of the same community type would respond similarly to disturbance events regardless of their location within Maui Nui. We used mixed-effects linear models to test whether the fixed factor of community type or island better described the following response variables: 1) change in coral cover, and 2) change in linear rugosity (1cm resolution) in each timestep. We calculated each response variable as the monthly rate of change between each survey for each site. We included site as a random effect in our models and modeled variance using the varIdent function to account for heteroskedasticity (Pinheiro et al. 2018). We used Tukey's honest significance test to identify significant pairwise differences using the emmeans package (Lenth et al. 2023), and used AIC to select the best model for both coral cover and rugosity change.

Lastly, we used multiple regression with generalized additive models (GAMs) to identify which environmental variable(s) best explained patterns of change in coral cover and rugosity for each timestep. We hypothesized that wave damage, bleaching related mortality, and sedimentation stress could have driven coral mortality during our timeseries (Figure 3.1C) and constructed a GAM to explore each hypothesis (Table S3.3). Unlike our PERMANOVA, which utilized long-term environmental averages, we obtained site-level data for each timestep (2016/17–2019, 2019–2021, and 2021–2023) for thermal stress (max degree heating weeks (°C/weeks); NOAA Coral Reef Watch 2020), wave height (90^{th} percentile (m); Cheung 2021), and turbidity (mean of quarterly max (FNU); Dogliotti et al. 2015; Li et al. 2022). Turbidity data were not available for our first timestep, so for each site we also quantified the distance to the nearest stream as a proxy for sedimentation (Hawai'i Statewide GIS Program 2016), which we log transformed to reduce the influence of outliers. We also quantified maximum thermal stress at each site in 2015 to test the hypothesis that bleaching impacts pre-dating our monitoring were responsible for coral cover and rugosity change from 2017–2019. For our second and third timestep, we tested the hypothesis that change in coral cover and rugosity in the preceding timestep would explain subsequent patterns of benthic change (via recovery dynamics, succession, or chronic degradation). Finally, we also incorporated island and community type to account the effect of local environmental factors and benthic community composition. To avoid issues related to multicollinearity, we didn't include environmental predictors with a correlation coefficient > 0.5 (Figure S3.7B-D), dropping the predictor believed to be less causally related to benthic community change. We used the package mgcv to implement our GAMs in R (Wood 2011). We initially limited the basis dimension to k = 5, and decreased k if model results

appeared to overfit the data. We selected the best models for coral cover and rugosity in each time step using AIC.

3. Results

3.1 Spatial patterns of benthic community composition

Across the entire timeseries, coral cover ranged from 18.36% (Kaho'olawe 6 in 2019) to 87.97% (Lāna'i 8 in 2019), with some sites dominated by *Montipora* and others by *Porites* (Figure S3.1). As of 2023, coral cover was highest on Moloka'i (62.75% ± 1.92%; mean ± SE), followed by Lāna'i (58.26% ± 5.25%), Kaho'olawe (52.36% ± 8.05%) and Maui (40.82% ± 4.20%) (Figure 3.2A,3.2C). Fine-scale linear rugosity ranged from 1.45 to 2.22 (Figure 3.2B,3.2D). In 2023, fine-scale linear rugosity was higher on Maui (1.80 ± 0.08) and Kaho'olawe (1.79 ± 0.07) and lower on Moloka'i (1.69 ± 0.03) and Lāna'i (1.68 ± 0.04).

We were able to identify three distinct benthic communities via hierarchical clustering (Figure 3.3). The first community had the lowest coral cover (35.09% ± 3.20%) and was characterized by large amounts of limestone framework covered in turf algae (53.52% ± 2.50%), low landscape heterogeneity, and moderate structural complexity. The most common coral in these communities were massive *Porites lobata* (15.23% ± 6.32% of total benthic cover). Less abundant benthic taxa (i.e., *Leptastrea*, *Psammocora*, sponges, zoanthids, etc.) were also more common on these reefs compared to other reefs in the region, albeit still rare. The second community had intermediate coral cover (55.74% ± 3.24%), high landscape heterogeneity, and high structural complexity. These communities hosted a diverse assemblage of corals and algae, with relatively high cover of branching *Porites compressa* (11.45% ± 1.76%), encrusting *Pavona* (1.24% ± 0.37%), crustose coralline algae (CCA) (9.19% ± 2.37%), and fleshy macroalgae (2.49% ± 0.87%). Finally, the third community had the highest coral cover (67.82% ± 2.61%),

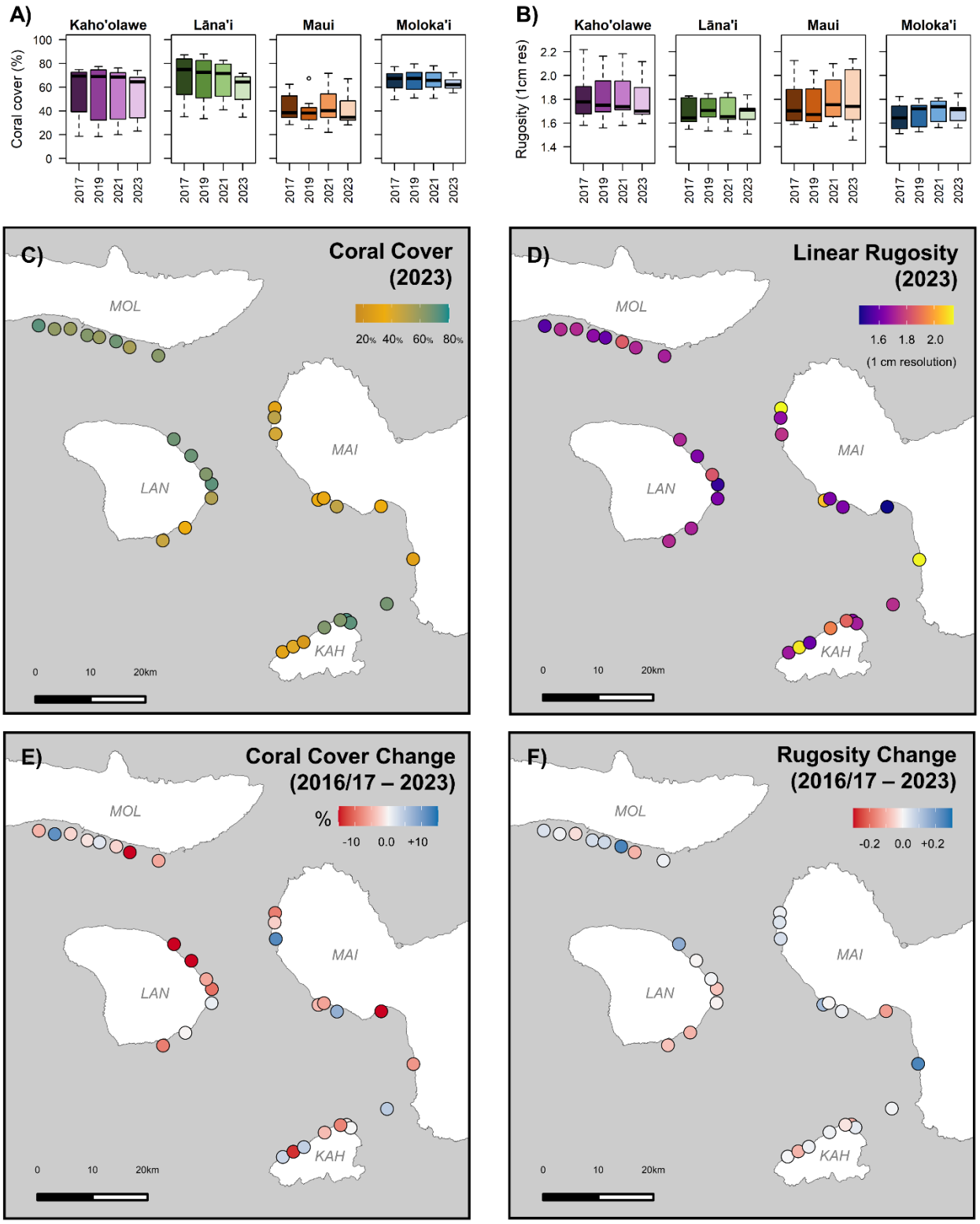

Figure 3.2: Boxplots show A) percent coral cover and B) fine-scale linear rugosity (1cm resolution) for each island in each year. Maps provide a snapshot of C) coral cover and D) rugosity in Maui Nui in 2023, and show net change in E) coral cover and F) rugosity over the full timeseries.

scant open space, low landscape heterogeneity and low structural complexity. These communities had high percent cover of encrusting, plating, and quasi-branching *Montipora capitata* (48.62% ± 2.07%) and encrusting *Montipora patula* (13.00% ± 4.17%). All summary statistics reported above for these benthic communities are from 2023, but are representative of other years in our timeseries.

Diverse intermediate cover reefs were widespread throughout the region, but the other two benthic communities tended to be concentrated on particular islands (Figure 3.4A). Low coral cover *Porites* reefs were found most commonly on Maui, followed by Kaho'olawe, while high coral cover *Montipora* reefs were found primarily on Moloka'i and Lāna'i. The average coral cover of each island reflects the spatial distribution of these community types. In addition, sites within 5km of each other exhibited significant autocorrelation in community composition (Figure S3.9). We found that spatial variation in community composition was largely unexplained by long-term environmental conditions. Our PERMANOVA indicated that variation in benthic community composition was best explained by island ($p < 0.001$, $R^2 = 0.227$). While irradiance was also significantly related to community composition ($p = 0.012$), the amount of variation it explained was small ($R^2 = 0.082$). None of the other environmental drivers displayed a significant relationship with benthic community composition (Table S3.1). In total, our seven environmental variables only explained 22.45% of benthic community variation, roughly the same amount explained by island. In other words, 54.83% of variation in benthic community composition was unexplained by island or the environmental variables analyzed here.

3.2 Temporal patterns of benthic community composition

Compared to patterns of spatial variation, we observed less temporal variation on Maui Nui’s reefs. Surveys of the same site from different years were tightly clustered in

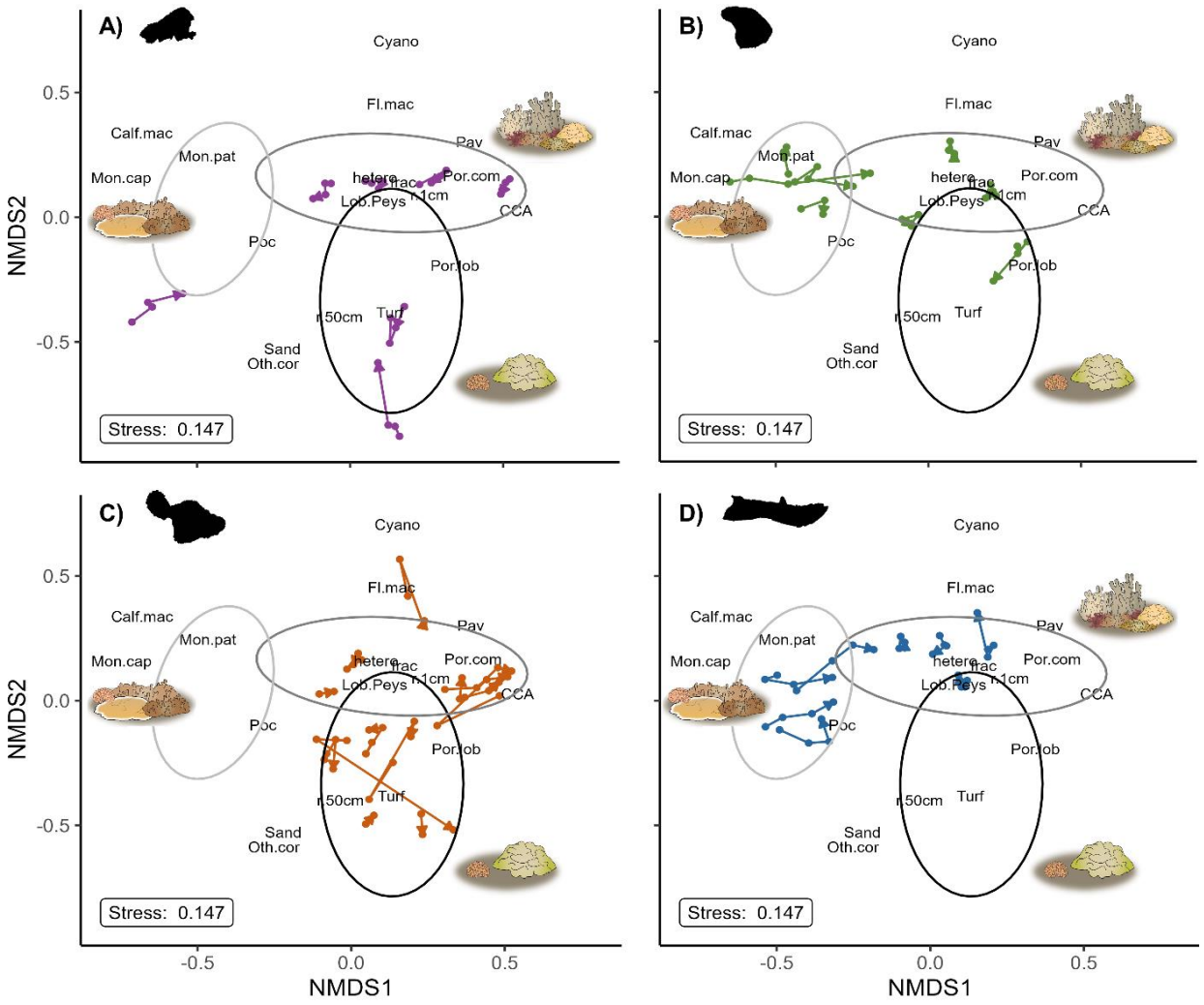

Figure 3.3: Non-metric Multidimensional Scaling (NMDS) ordination of benthic community composition illustrates successional trajectories for reefs on A) Kaho'olawe, B) Lāna'i, C) Maui, and D) Moloka'i. Ellipses denote community types identified through hierarchical clustering (light gray = high coral cover *Montipora* dominated reefs; dark gray = diverse intermediate coral cover reefs; black = low coral cover *Porites* dominated reefs). Text indicates benthic variables used in the ordination, including percent cover of various benthic taxa, structural complexity (r.1 = rugosity at 1cm resolution; r.50 = rugosity at 50cm resolution; frac = fractal dimension), and landscape heterogeneity (hetero).

multidimensional space (Figure 3.3, Figure S3.10), indicating that temporal variation within sites was smaller than spatial variation among sites. Furthermore, CRAMP sites located close to our large-area imagery fixed sites (n = 6) show evidence of temporal stability dating back to the early 2000s (Figure S3.2). Comparing the successional trajectories of sites among community types, we found community composition to be the most stable on diverse intermediate cover reefs. The

successional trajectories of these sites tended to be short, compact, and non-linear. Conversely, high cover *Montipora* sites showed more evidence of directional change over time, with most exhibiting a reduction in *Montipora* dominance (Figure 3.3, Figure S3.1). This community type experienced the largest loss in coral cover over the timeseries (-6.34% ± 2.62% in terms of absolute benthic cover; Figure 3.4B), yet these reefs simultaneously experienced an increase in structural complexity (+0.07 ± 0.04; linear rugosity at 1cm resolution; Figure 3.4C). The successional trajectories for low cover *Porites* sites were variable, with some sites exhibiting stasis and others undergoing notable change over time (Figure 3.3, Figure S3.1).

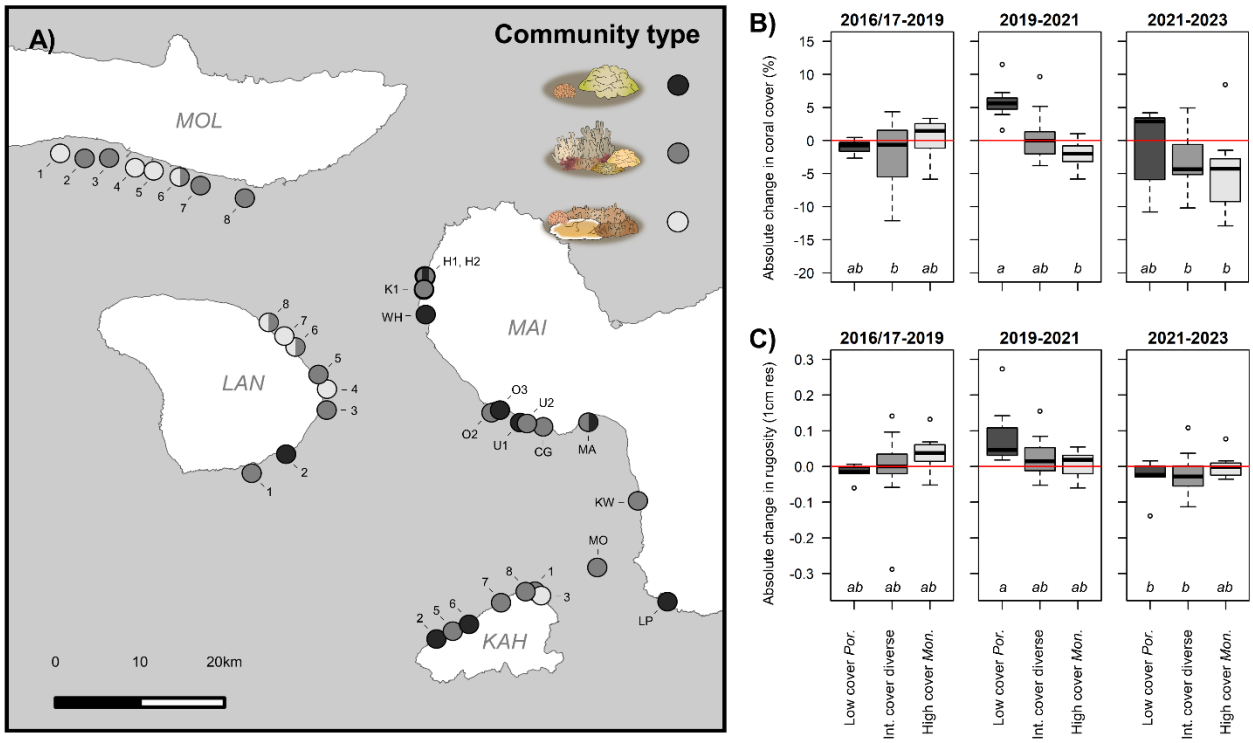

Figure 3.4: A) The distribution of benthic community types across Maui Nui. Community types were as follows: low coral cover *Porites* dominated reefs (black), diverse intermediate coral cover reefs (dark gray), and high coral cover *Montipora* dominated reefs (light gray). Points with multiple colors denote sites that shifted from one community type to another over the course of our timeseries. Only one site (Honokowai 1; H1) switched community types twice. Site abbreviations correspond to site names in Figure S3.1 and Figure S3.10. Change in B) coral cover and C) fine-scale linear rugosity are shown for each timestep by community type. Letters denote significant differences between groups.

Mean coral cover for the region was 55.75% ± 3.14% at the start of our timeseries in 2017 and 53.02% ± 2.87% at the end of our timeseries at 2023. This apparent stasis masks notable site-specific instances of change (Figure 3.2E-F, Figure S3.1). For example, some sites showed sustained increases in coral cover, such as Wahikuli (Maui) where coral cover increased from 31.11% to 43.19% over the timeseries. We also saw examples of shifts in algal composition, including shifts toward CCA dominance (Keawakapu, Maui) and periodic fleshy algae blooms (Kahekili, Maui, and several sites on Moloka'i). Overall, the largest temporal shift in community composition at any of our sites occurred at Mā'alaea, a shallow site on Maui that experienced large reductions in coral cover due to wave damage in 2022. Coral cover at this site declined from 62.42% to 34.63% from 2021 to 2023, and the site transitioned from a diverse community with intermediate coral cover to a *Porites* dominated reef with low coral cover and abundant turf algae. In total, five of our sites (14%) transitioned from one community type to another at some point in our six-year timeseries (Figure 3.4A). Three of these sites transitioned from *Montipora* dominance to more diverse, intermediate coral cover communities (Moloka'i 6, Lāna'i 6, and Lāna'i 8), while one site transitioned from intermediate cover to *Porites* dominance and then back to intermediate cover (Honokowai, Maui). Still, most sites remained within the same community type for the duration of the timeseries.

Our mixed-effects linear models revealed that rates of change in coral cover and fine-scale rugosity were spatially and temporally variable. Our main effects (community type or island) were not significantly related to our response variables (change in coral cover or rugosity) in any of our models. However, we did observe a significant interaction between our main effect and timestep in each model (Table S3.2). This indicates that coral cover and rugosity were not changing consistently over time (e.g., coral cover was not consistently declining on one island

more than another). Rather, in each timestep reefs from different community types (or different islands) changed in distinct ways from one another. AIC indicated that community type was a better predictor of change in coral cover and rugosity than was island (Table S3.2).

During the first timestep (2016/17–2019), coral cover slightly decreased on diverse intermediate cover reefs (-1.93% ± 1.15%), with no differences observed among islands (Figure 3.4B). This decline was best described in our GAMs by a combination of wave height, distance to the nearest stream, and island (adj. $R^2 = 0.483$; Figure S3.11). We did not observe significant differences in rugosity change among community types or islands in this timestep.

During the second timestep (2019–2021), coral cover increased significantly on low cover *Porites* reefs (+5.85% ± 1.15%) and on Maui (+4.93% ± 1.71%), and decreased significantly on high cover *Montipora* reefs (-2.09% ± 0.75%) (Figure 3.4B). Rugosity also increased significantly on low cover *Porites* reefs (+0.08 ± 0.03) during this timestep. Coral cover and rugosity were more likely to decline on reefs with high turbidity that were proximate to streams (coral: adj. $R^2 = 0.794$; rugosity: adj. $R^2 = 0.736$; Figure S3.12). Furthermore, reefs that had experienced a decline in rugosity in the prior timestep (2016/17–2019) were more likely to see rugosity increase during the second timestep.

In the final timestep (2021–2023), coral cover decreased significantly on diverse intermediate cover reefs (-4.60% ± 1.52%), on high cover *Montipora* reefs (-4.68% ± 2.75%), and on Lāna'i (-6.21% ± 1.84%) (Figure 3.4B). Rugosity decreased significantly during the final timestep at low cover *Porites* reefs (-0.03 ± 0.02) and diverse intermediate cover reefs (-0.02 ± 0.01; Figure 3.4C). Declines in coral cover and rugosity during the final timestep were best explained by a combination of wave height, depth, and island (coral adj. $R^2 = 0.325$, rugosity adj. $R^2 = 0.492$; Figure S3.13). Over the full six-year timeseries, coral cover increased on low cover

Porites reefs (+4.89% ± 3.59%) and decreased on diverse intermediate cover reefs (-6.32% ± 2.32%) and high cover *Montipora* reefs (-8.81% ± 3.64%).

4. Discussion

We tracked benthic community dynamics across 36 leeward forereef sites on Maui, Kaho'olawe, Lāna'i, and Moloka'i, collectively referred to Maui Nui. This region of the Hawaiian Islands represents a noteworthy bright spot of coral persistence in the Anthropocene (Cinner et al. 2016). The average coral cover we document in Maui Nui (55.75% ± 3.14% in 2017) is substantially higher than elsewhere in Hawai'i (24.1% ± 0.89% in 2012; Rodgers et al. 2015), the broader Pacific (21.3% ± 3.3% in 2016; Moritz et al. 2018), or the Caribbean (15.9% in 2019; Allen et al. 2021). Even accounting for the location of our sites within known reef tracts and their leeward exposure, which is known to promote high coral cover (Dollar 1982; Storlazzi et al. 2005; Gove et al. 2013), the widespread occurrence of reefs with > 70% coral cover in Maui Nui is remarkable given the degree of local human impacts and recent bleaching events in the region (Cox & Jokiel 1995; Brown et al. 2008; Vermeij et al. 2008; Dailer et al. 2010; Wedding et al. 2018; Minton et al. 2022). Here we interpret spatial and temporal patterns of variation and identify implications for natural resources management.

4.1 Spatial patterns of benthic community composition

We observed remarkable spatial variability in community composition (Figure 3.3, Figure 3.4) despite the fact that 1) Hawaiian coral reef benthic communities generally have low diversity and are dominated by generalist taxa (Grigg 1983; Rooney et al. 2008), 2) our study encompassed a relatively small region, with our furthest sites located only 90 km apart, 3) the four islands of Maui Nui share a common geologic history (Fletcher et al. 2008; Faichney et al. 2011; Field et al. 2019), and 4) our study was confined to sheltered leeward coastlines that

experience similar oceanographic conditions (Shultz et al. 2004; Wedding et al. 2018; Figure S3.6, Table S3.1).

Of all the variables we considered, island explained the most variability in benthic community composition. The islands studied here are geologically similar, but each has a unique history of colonization, land use, human impact and environmental degradation (Cox & Jokiel 1995; Brown et al. 2008; Ross et al. 2010; Maynard et al. 2019; Minton et al. 2022). Thus, high variation in benthic community composition among islands and low variation within islands would suggest that localized regimes of human or land-based impacts are driving community variation. This would be consistent with other studies from Hawai'i that highlight the importance of land-based impacts such as sedimentation, wastewater pollution, and urban runoff on coral reef condition (Gove et al. 2023). It also aligns with traditional resources management in Hawai'i that aims to reduce local human impacts on coral reefs by managing these systems as watersheds known as ahupua'a, or “ridge to reef” management (Delevaux et al. 2018; Winter et al. 2020). On Maui in particular, localized impacts such as overfishing (Williams et al. 2016; Donovan et al. 2023b), sediment runoff (Wedding et al. 2018), elevated nutrients (Dailer et al. 2010), invasive algae blooms (Smith et al. 2002), and wastewater pollution (Winston et al. 2022) have been identified as chronic drivers of reef degradation (Rodgers et al. 2015; Sparks et al. 2015). These factors are almost certainly responsible for the lower coral cover we observed on Maui, given the lack of geologic and oceanographic differences between Maui and neighboring islands. However, while the effect of island was significant, the amount of variation it explained was minor (22.72%).

Similarly, the seven environmental drivers we considered collectively explained only 22.45% of the variation in benthic community structure (Table S3.1). This is due in part to our

study design, where we controlled for wave exposure and depth over a small geographic area. Other studies have also found high residual variation after accounting for hypothesized drivers of benthic community composition on coral reefs (Murdoch & Aronson 1999; Gove et al. 2013; Sandin et al. 2022). In certain instances, the poor predictive power of environmental drivers has been attributed to anthropogenic disruption of key reef processes (e.g., overfishing reducing herbivory), which can diminish or disrupt expected relationships between benthic communities and oceanographic forcings (Williams et al. 2015, 2019; Donovan et al. 2023b). However, controlling for island, our proxy for local human impacts, should account for this decoupling. Instead, we found considerable spatial variation in benthic community composition that was not driven by oceanographic drivers or island (54.83% of variation).

The fine-scale variation in community composition that we observe could be driven by biotic processes that we did not quantify such as recruitment, corallivory, herbivory, or competition. These processes have been shown to produce scale-dependent feedbacks that lead to regular pattern formation in ecosystems (Rietkerk & van de Koppel 2008). For example, the density of reproductive adults has been shown to impact both recruit dispersal (Field et al. 2019; Pedersen et al. 2019) and survival (Marhaver et al. 2017), thereby influencing the spatial aggregation of conspecifics in subsequent generations (Pedersen et al. 2019; Sandin et al. 2022). Aggregations of corallivores, most notably crown of thorns starfish (*Acanthaster plancii*), can also contribute to the patchiness of benthic landscapes through spatially concentrated coral predation (Houk et al. 2014; Carlot et al. 2020). *A. plancii* have been found to target certain coral taxa, such as *Montipora* and *Pocillopora* (Sparks et al. 2015; Keesing 2021), and at low to moderate densities, this selective feeding can contribute to landscape heterogeneity and promote diversity by preventing the dominance of competitive taxa (Colgan 1987; DAR 2006; Sparks et

al. 2015). Similarly, the behavior and dispersal abilities of important reef herbivores (e.g., urchins, parrotfish, surgeonfish, etc.) have been found to differentially impact the composition of algal communities from the scale of centimeters to kilometers (Sandin & McNamara 2012; Edwards et al. 2013; Brandl & Bellwood 2016; Streit et al. 2019). This in turn shapes the competitive dynamics between corals and algae, which constantly compete for limited benthic space (Smith et al. 2010; Barott et al. 2012; George et al. 2021). The arrangement and morphology of sessile competitors can shape the outcome of competition (Rogers 1993; Brito-Millán et al. 2019b; George et al. 2021) and lead to spatial self-organization of taxa at larger scales (Rietkerk & van de Koppel 2008).

In addition to the biotic processes noted above, environmental conditions interact with species morphology and life-history traits to create spatial gradients in community structure (Wiens 1989; Murdoch & Aronson 1999; Storlazzi et al. 2005; Ferrari et al. 2016; Sandin et al. 2022). On Hawaiian coral reefs, taxa with higher skeletal densities such as *P. lobata* and *Pocillopora* tend to dominate habitats with more wave exposure, while reefs that are sheltered from wave energy tend to support higher cover of fast growing yet delicate plating and branching corals such as *M. capitata* and *P. compressa* (Dollar 1982; Fletcher et al. 2008; Rodgers et al. 2015; Donovan et al. 2018). When herbivory is viewed as a type of disturbance, a similar pattern of relative dominance can be seen in algae: on herbivore-dominated reefs, less palatable algae such as CCA dominate, whereas fleshy algae and turf dominate in reefs with less herbivory (Smith et al. 2001; Kelly et al. 2017). Intermediate disturbance resets competitive dynamics and promotes the persistence of multiple taxa. Without periodic disturbance, competitive coral or algal taxa will outcompete their slower growing neighbors to dominate the benthos (Rogers 1993; Smith et al. 2010; Darling et al. 2012; Kayal et al. 2015), theoretically proceeding to a

successional endpoint or “climax community” (Maragos & Grigg 1974; Turner et al. 1998; Gouezo et al. 2019).

Climax communities are rare on coral reefs because disturbances tend to occur too frequently to allow one species to sustain dominance (Grigg 1983; Hughes & Connell 1999; Gouezo et al. 2019). Yet the exceptionally high cover and dominance of *Montipora* on reefs in south Moloka'i and northeast Lāna'i (Figure 3.3, Figure 3.4) implies that these reef tracts historically have had low exposure to severe disturbances, otherwise coral cover would not be able to reach such extremes. For example, an assessment of bleaching mortality following a severe marine heatwave in 2015 documented low coral mortality in south Moloka'i and northeast Lāna'i, compared to moderate mortality in West Maui (Rosinski et al. 2017). Frequent spikes in turbidity are common on south Moloka'i and northeast Lāna'i (Jokiel et al. 2014; Minton et al. 2022), and if such turbidity coincided with heat stress, this could have reduced bleaching severity in 2015 (Carlson et al. 2022). Over longer timescales, a highly turbid nearshore environment could help to explain the dominance of *M. capitata* on these reefs, given this taxon’s demonstrated tolerance for sedimentation stress (Padilla-Gamiño et al. 2014). Whether or not south Moloka'i and northeast Lāna'i’s reefs qualify as climax communities, it is worth noting they may not represent a “resilient” or “optimal” ecosystem state. *Montipora* dominance has resulted in more homogenous reefscapes with fewer opportunities for interspecific interactions. Structural complexity was also lower on these reefs due to the dominance of encrusting growth forms, which provide less habitat for reef fish of different size classes (Friedlander et al. 2003; Richardson et al. 2017; McCarthy et al. 2022). A lack of functional redundancy and habitat diversity could leave these communities vulnerable to degradation, especially since the most

abundant taxa on these reefs are among the most susceptible to bleaching (Jokiel & Brown 2004; McLachlan et al. 2021; Winston et al. 2022) and predation by *A. plancii* (Sparks et al. 2015).

4.2 Temporal patterns of benthic community composition

Complex patterns of coral cover and rugosity change over our timeseries (Figure 3.2E-F) suggest that biotic and environmental factors may be interacting in unpredictable ways to shape successional trajectories. Other studies in Hawai'i have documented stability in average coral cover at island scales but high variation in reef trajectories within islands (Rodgers et al. 2015; Sparks et al. 2015; Minton et al. 2020; Gove et al. 2023). This fine-scale variation supports the notion that a single reef tract is in fact a patchwork of successional stages created by the localized impacts from both acute and chronic disturbance events (Turner et al. 1998; Murdoch & Aronson 1999; Ross et al. 2012; Dietzel et al. 2021; Moritz et al. 2021). Here, we suggest that community composition can serve as a useful indicator of successional stage and future reef trajectory. Indeed, we found that community type was a better predictor of coral cover and rugosity change than was island, which supports the notion that biotic processes are important drivers of benthic community variation within Maui Nui.

The three community types we identify here each responded differently to disturbance events over our timeseries. Intermediate coral cover reefs exhibited the least temporal variation, which could indicate a stabilizing effect of species diversity, high interspecific competition, and frequent moderate disturbance, which prevent any one taxon from gaining dominance (Connell 1978; Rogers 1993; Mouillot et al. 2013). In contrast, high cover *Montipora* reefs exhibited the strongest signs of directional succession, with several shifting away from *Montipora* dominance toward a more diverse coral community in response to multiple disturbance events (Figure 3.3, Figure S3.1). It is more feasible for these reefs to experience large declines in coral cover

compared to large increases, since the high density of *Montipora* and limited free space asymptotically limit further *Montipora* growth on these reefs (Rogers 1993; Gouezo et al. 2019; George et al. 2021). A high density of conspecifics has also been shown to promote transmission of coral disease, which could also limit coral growth (Aeby et al. 2011). Furthermore, it is possible that a historically low-disturbance regime enabled the persistence of sensitive haplotypes within these climax communities, and a loss of sensitive haplotypes during multiple disturbances from 2017 to 2023 caused coral cover to decline (Burgess et al. 2021).

While coral cover on *Montipora* dominated reefs declined, coral cover increased on low cover, *Porites* dominated reefs. According to our PERMANOVA results, *Porites* dominated reefs were characterized by slightly higher levels of sedimentation and nutrient effluent (Figure S3.10), and were more commonly found on the island of Maui (Figure 3.4). Thus, it seems likely that these communities have been shaped by chronic human impacts that favor the survival of stress-tolerant corals (Ross et al. 2010, 2012; Darling et al. 2012; Maynard et al. 2019). It is worth noting that *Montipora* on these low-cover reefs actually remained stable over our timeseries, whereas *Montipora* declined on intermediate and high coral cover reefs (Figure S3.14). This supports the notion that human-impacted reefs are dominated by stress-tolerant *individuals*, not just stress-tolerant taxa, a pattern that has been documented elsewhere (Parkinson et al. 2015; Caruso et al. 2021; Smith et al. 2022a). Still, *P. lobata* was primarily responsible for the surprising increase in coral cover we observed on these reefs through the 2019 bleaching event and COVID-19 pandemic (Figure 3.4B, Figure S3.12). This increase could be due to coral acclimatization and selection for thermal tolerance following exposure to heat stress in 2015 (McCarthy et al. *in prep.a*), which would better position these communities to persist through future thermal stress as well. The increase in coral cover we observed on these

reefs, especially as higher coral cover communities experienced decline, supports the view that degradation can indirectly contribute to community stability and persistence by favoring the dominance of stress-tolerant organisms (Côté & Darling 2010).

Isolating the impact of bleaching on coral cover trajectories is difficult because heat stress was closely followed by the COVID-19 pandemic in 2020. COVID travel restrictions had marked effects on tourism on Maui in particular (Weng et al. 2023). Reduced tourism altered the behavior of reef fish at Molokini (offshore of Maui; Weng et al. 2023) and could have also translated into lower wastewater volume around Maui, temporarily reducing a source of chronic stress and allowing corals to invest more energy toward growth rather than maintenance (Darling et al. 2012; Kayal et al. 2015; Gove et al. 2023). Yet, economic hardship and reduced oversight triggered by COVID-lockdowns could have led to increased fishing pressure within marine protected areas, as has been documented elsewhere (Coll 2020; Phua et al. 2021; King et al. 2022). These impacts would be expected to degrade ecosystem function in the long term. Thus, the impacts of COVID-19 on marine conservation are likely multifaceted (Coll 2020), and it is currently unclear whether COVID-19 represented a net positive or negative for Maui Nui's reefs.

Despite experiencing multiple notable disturbances, including a marine heatwave and COVID-19, changes in coral cover and rugosity were best explained by wave and sedimentation impacts that occurred during our timeseries (Figures S3.7-S3.9). Sedimentation is a chronic stressor on nearshore environments across Maui Nui (Cox & Jokiel 1995; Brown et al. 2008; Maynard et al. 2019; Minton et al. 2022). Sedimentation can reduce coral growth and recruitment and can occur either as the result of runoff or from resuspension of previously deposited sediment (Jokiel et al. 2014). Thus, storms represent a frequent source of disturbance for nearshore benthic communities, both via wave action (which can cause coral breakage and

sediment resuspension; Storlazzi et al. 2005; Minton et al. 2022) and precipitation (which produces runoff that deposits new terrigenous sediment; Stamski & Field 2006). Other studies have found that chronic stressors better explain coral resistance and recovery over time than acute stressors, both in Hawai'i (Ross et al. 2010; Rodgers et al. 2015; Gove et al. 2023) and elsewhere (Connell 1997; Cresswell et al. 2023). Chronic stressors elevate already high levels of background mortality driven by intense competition among benthic organisms (Hughes & Connell 1999; Ross et al. 2010). This relationship between chronic stress and ecosystem function supports the notion that reef condition can be improved through land-based management actions that seek to reduce localized sources of chronic stress, specifically sedimentation and wastewater runoff (Anthony et al. 2015; Cinner et al. 2018; Obura et al. 2019; Gove et al. 2023).

5. Conclusions

By resurveying fixed sites with large-area imagery, we were able to track fine-scale spatial and temporal changes in benthic community composition with high confidence (Figure S3.5). This approach enabled us to characterize multiple aspects of ecosystem condition over time, including community composition, habitat structural complexity, and the spatial arrangement and interactions of benthic organisms. These data complement existing long-term monitoring data from the state of Hawai'i (Brown et al. 2008; Sparks et al. 2015) and reveal remarkably high coral cover and temporal stability on Maui Nui's leeward reefs (Figure S3.2). Still, the considerable spatial variation we document here serves as an important reminder that no two reefs are the same. Management approaches that account for this spatial heterogeneity will be able to target locally-relevant drivers of reef decline (Rogers et al. 2015). As an example, targeted fisheries regulations in Kahekili (West Maui) have helped increase herbivory to counteract the localized impact of elevated anthropogenic nutrients (Smith et al. 2005; Ross et al.

2012; Williams et al. 2016; Brown 2019). Similarly targeted management should be deployed to address emerging threats, such as the 2023 West Maui wildfires, which are likely to have patchy impacts on nearshore habitats via runoff of ash, debris, and toxic compounds (Wall et al. 2023). Long-term monitoring programs, which enable managers to incorporate information about local disturbance history and successional trajectories, are foundational to such management (Hughes & Connell 1999; Rodgers et al. 2015; Smith et al. 2016; Crisp et al. 2022). Maintaining capacity for spatially and taxonomically detailed long-term monitoring is of critical importance in this current era of increased global change.

6. Acknowledgements

Chapter 3, in part, is currently being prepared for submission for publication of the material. McCarthy, Orion S.; Kelly, Emily L. A.; Akiona, Anela K.; Clements, Samantha M.; Martinez, Tatiana; Pedersen, Nicole E.; Peralto, Cole; Ricke, Katharine; Romero, Sarah L.; Silva, Itana F.; Smelser, Mitchell H.; Stone, Kristy W.; Sparks, Russell T; Smith, Jennifer E. The dissertation author was the primary researcher and author of this material.

We would like to thank all of the divers who helped collect large-area imagery, including Lindsay Bonito, Clinton Edwards, Travis Matteson, Yui Takeshita, and Or Ben-Zvi, and the 100 Island Challenge for providing logistical support and field equipment. Field work was also supported by the NOAA Coral Reef Ecosystem Division 2016 HARAMP cruise and Hi'ialakai crew, Ultimate Whale Watch, Maui Divers, Dive Maui, Lee James, Amy and Craig Venema, Toni and Peter Colombo, Will and Meghan Dailer, Darla White, and George and Donna Brown. Clinton Edwards, Morgan Winston, and Yi-Juan Hu provided helpful feedback and technical support that improved our analysis. Adi Khen graciously designed custom coral graphics for our figures. Special thanks to Nicole Pedersen for support with 3D model construction, data

management, and Viscore training, and to Elise Gonzales and Conor Elliott for hours spent assisting with species ID. This work was conducted under a Special Activities Permit (SAP: MA 17-53) from the Department of Land and Natural Resources Office of Conservation and Coastal Lands, and a Right of Entry Permit from the Kaho'olawe Island Reserve Commission (Scripps 3D Reef Mapping, April 2017). Special thanks to Samuel Lemmo, Dean Tokeshi, and Michael Naho'opi'i for their assistance with the permitting process. Finally, we would like to thank our funding sources, including the National Science Foundation (GRFP), the 100 Island Challenge, the Bohn Family, Ferguson Family, the Scripps Family Foundation, and other generous donors.

Chapter 4 – Corals that survive repeated thermal stress show signs of selection and acclimatization

Orion S. McCarthy, Morgan Winston, and Jennifer E. Smith

Abstract

Climate change is transforming coral reefs by increasing the frequency and intensity of marine heatwaves, often leading to coral bleaching and mortality. Coral communities have demonstrated modest increases in thermal tolerance following repeated exposure to moderate heat stress, but it is unclear whether these shifts represent acclimatization of individual colonies or mortality of thermally susceptible individuals. For corals that survive repeated bleaching events, it is important to understand how past bleaching responses impact future growth potential. Here, we track the bleaching responses of 1,832 corals in leeward Maui through multiple marine heatwaves and document patterns of coral growth and survivorship over a seven-year period. While we find limited evidence of acclimatization at population scales, we document reduced bleaching over time in specific individuals, primarily in the stress-tolerant taxa *Porites lobata*, suggesting potential acclimatization. For corals that survived both bleaching events, we find no relationship between bleaching response and coral growth in three of four taxa studied. This decoupling between bleaching and growth suggests that coral survivorship is a better indicator of future growth than is a coral's bleaching history. Corals that have survived recent and repeated exposure to thermal stress have a demonstrated capacity for resilience, and should be considered good candidates as outplants for coral restoration. Survivorship followed a latitudinal thermal stress gradient, but because this gradient was small, it is likely that local

environmental factors also drove differences in coral performance among sites. Efforts to reduce human impacts at low performing sites would likely improve coral survivorship in the future.

1. Introduction

Coral reefs are among the most vulnerable ecosystems on Earth to the impacts of anthropogenic climate change (Doney et al. 2012; Hoegh-Guldberg et al. 2017; Hughes et al. 2018). Climate change has increased the severity and frequency of marine heatwaves (Oliver et al. 2018; Bindoff et al. 2019; IPCC 2021), which disrupt the growth and survival of Scleractinian corals, the key foundation organisms on shallow water coral reefs throughout the tropics (Richardson et al. 2020). Marine heatwaves have already begun to reshape coral communities globally by reducing coral cover (Hughes et al. 2017; Couch et al. 2017; Eakin et al. 2019; Sully et al. 2019; van Woesik et al. 2022) and inducing shifts in benthic community composition toward more stress-tolerant coral taxa (Moritz et al. 2018; McClanahan et al. 2020), sponges and soft corals (Norström et al. 2009), and fleshy seaweeds (Ostrander et al. 2000; Arif et al. 2022; Tebbett et al. 2023). Without concerted action to address climate change, projections for the future of coral reefs are dire (van Hooidonk et al. 2016; Hoegh-Guldberg et al. 2017; Sully et al. 2022). Still, Scleractinian corals have persisted through major environmental changes since the Triassic (Pandolfi et al. 2011). More recently, certain coral populations have demonstrated capacity to persist in marginal environments or through intense environmental disturbances (Camp et al. 2018). These corals are a source of hope for coral researchers, conservation practitioners, and the general public, a sign that a future with functional coral reefs is still a possibility.

Disturbance events transform communities by inducing physiological stress that reduces the growth, survivorship, competitive ability, or fecundity of certain organisms (Sousa 1984; Bramanti et al. 2015; Battisti et al. 2016; Morais et al. 2021). For corals, stress can manifest as bleaching due to the breakdown of symbiosis between corals and their dinoflagellate symbionts in the family *Symbiodiniaceae* (van Woesik et al. 2022). Without their symbionts, corals lack their primary source of nutrition (Grottoli et al. 2006; Anthony et al. 2009). While mortality is not an inevitable outcome of coral bleaching (Fox et al. 2019, 2021; Page et al. 2023), prolonged bleaching can result in partial or complete mortality of coral colonies.. A variety of environmental stressors can cause coral bleaching, but bleaching is most commonly studied in relation to marine heatwaves (Sully et al. 2019; Khen et al. 2023). In this context, bleaching onset is determined primarily by the intensity and duration of heat stress that corals experience (Middlebrook et al. 2010; Marzonie et al. 2023). Recent studies that document an increase in the magnitude of heat stress required to induce coral bleaching and mortality (Sully et al. 2019; González-Barrios et al. 2023; Lachs et al. 2023a) suggest that corals may possess the ability to acclimatize to heat stress over time.

Acclimatization refers to the process of phenotypic change that occurs within the lifespan of a single individual to cope with environmental stress (Coles et al. 2018). In corals, acclimatization to heat stress can occur through a variety of mechanisms, including morphological plasticity (Zawada et al. 2019; Million et al. 2022; Khen et al. 2023), epigenetic modifications (Rodríguez-Casariego et al. 2020), and symbiont shuffling (Baker et al. 2004; Claar et al. 2020; Leinbach et al. 2023). Signs of acclimatization have been documented in coral populations in Australia (Maynard et al. 2008; DeCarlo et al. 2019), Hawai'i (Barnhill et al. 2020; Yadav et al. 2023), Kenya (McClanahan 2017), Malaysia (Szereday & Amri 2021), Palau

(Lachs et al. 2023a), the Persian Gulf (Smith et al. 2022a), and the Red Sea (Mantanona & DeCarlo 2023). However, the cumulative stress of repeated bleaching is non negligible, and can reduce coral physiological performance over time (Grottoli et al. 2014; Roper et al. 2023) rather than induce acclimatization. Furthermore, when thermal stress is severe, bleaching-induced mortality can result in a population bottleneck that reduces opportunities for acclimatization to occur (Dietzel et al. 2021; Burn et al. 2023). Even following sequential heatwaves of moderate intensity, signs of acclimatization may not be evident at ecologically relevant scales (Winston et al. *in prep*).

At a global scale, there is evidence that coral bleaching thresholds have increased by 1°C since 1980 (Shlesinger & van Woesik 2023), with less severe bleaching observed on reefs that have previously been exposed to thermal stress (Sully et al. 2019; González-Barrios et al. 2023). While this increase in thermal tolerance could be due to widespread coral acclimatization, it could also be driven by other factors. Environmental conditions during a marine heatwave, such as high primary productivity, cloud cover, and turbidity, can act synergistically to reduce coral bleaching and mortality (Anthony et al. 2007; Carilli et al. 2012; Carlson et al. 2022; van Woesik et al. 2022). Furthermore, the appearance of acclimatization could actually be the result of shifts in coral community composition toward thermally tolerant species due to bleaching-related mortality of vulnerable taxa (Hughes et al. 2018; Moritz et al. 2018; McClanahan et al. 2020; Fox et al. 2021) rather than improvements in the thermal tolerance of individual corals. As climate change intensifies, it is important that we understand whether changes in reef-scale thermal tolerance are driven by coral acclimatization or taxonomic turnover.

Tracking the fate of individual corals through multiple marine heatwaves is one mechanism to better understand the drivers and prevalence of coral acclimatization to heat stress

(Matsuda et al. 2020; Sandin et al. 2020; Edmunds & Riegl 2020; Morais et al. 2021). Many observational studies of coral bleaching use population-scale metrics to quantify bleaching trends (i.e., percent of colonies bleached; Khen et al. 2023) rather than track the fate of individual coral colonies (but see Bourne et al. 2008; Montano et al. 2010; Claar et al. 2020; Morais et al. 2021). Fate tracking can be hindered by the challenge of relocating and precisely delineating the boundaries of coral colonies *in situ*. This is particularly difficult for species where partial mortality causes colonies to split (fission) and regrow (fusion) over time (Furby et al. 2017; Brito-Millán et al. 2019a). This challenge can be ameliorated by large-area imaging technology (a.k.a. photogrammetry or Structure from Motion), which allows researchers to reconstruct 3D models of the reef benthos that can be used to precisely locate and track coral colonies through time (Edwards et al. 2023; McCarthy et al. 2023). Large-area imagery has been used to quantify growth and mortality in demographically complex corals that display high rates of fusion and fission (Sandin et al. 2020; Rodriguez et al. 2021). However, large-area imaging is a relatively recent technology in the coral reef field, which limits the temporal scope of most studies. Furthermore, large-area imagery timeseries would need to document sequential marine heatwaves in order to be useful for studying coral acclimatization, which can be a tall order.

Few studies have been conducted that 1) document the impact of sequential bleaching events on coral populations, 2) track individual coral colonies through time using large-area imaging, and 3) quantify patterns of coral bleaching, growth, and mortality in taxa with fission and fusion dynamics (but see Fukunaga et al. 2022). Here we track the fate of individual corals in leeward Maui to quantify the impact of successive bleaching events on coral growth and survivorship. Specifically, we sought to answer the following questions: 1) do individual corals, as well as coral populations, show evidence of acclimatization, 2) do corals that experience less

bleaching grow more than corals that severely bleach and recover; and 3) do different coral populations show similar responses to sequential heat stress in terms of bleaching, growth, and survivorship? This research holds particular relevance for coral restoration, given ongoing efforts to identify, cultivate, and outplant thermally-tolerant coral genets as a form of climate-smart restoration (Van Oppen et al. 2015). If shifts in thermal tolerance in acclimatized corals are long lasting, or if certain locations or populations emerge as bastions of resilience, these corals could serve as parent colonies for restoration efforts (Caruso et al. 2021; Million et al. 2022).

2. Methods

2.1 Study sites

We surveyed populations of four coral taxa (*Montipora capitata*, *Montipora patula*, *Pocillopora* spp., and *Porites lobata*) at six sites in leeward Maui: Kahekili, Wahikuli, Olowalu, Ukumehame, Keawakapu, and Molokini. Our timeseries at these sites consists of five surveys (August 2014, November 2015, July 2017, October 2019, and June 2021), two of which coincide with documented bleaching events (2015 and 2019; Figure S4.1). These sites all represent hardbottom tropical coral reef habitat and range from 30.7% to 82.1% coral cover, 4.5 m to 10 m depth, and 41 m to 487 m from shore (Table S4.1). The focal coral taxa studied here all represent common and important reef building species on Hawaiian coral reefs (Brown 2004; Rodgers et al. 2015; Sparks et al. 2015).

The Hawaiian Islands have historically had a low incidence of bleaching compared to other coral reef ecoregions (Rodgers et al. 2017), but the archipelago was impacted by marine heatwaves in 2014, 2015, and 2019 that caused widespread coral bleaching (Rodgers et al. 2017; Couch et al. 2017; Wall et al. 2021; Winston et al. 2022). While the spatial footprint and intensity of the 2015 and 2019 bleaching events varied throughout the Hawaiian archipelago

(Figure S4.1A-B), heat stress was similar in 2015 and 2019 for leeward Maui (mean increase of 0.42 degree heating weeks (DHW) from 2015 to 2019 across sites, Figure S4.2, Table S4.1). This makes Maui an ideal natural experiment to identify signs of coral acclimatization, since we would expect similar levels of bleaching in 2015 and 2019 in response to similar heat stress.

2.2 Data collection

We used large-area imaging (photogrammetry) to capture a 3D snapshot of coral reef condition at our six sites in leeward Maui in 2014, 2015, 2017, 2019, and 2021. Large-area imaging is the process of generating a composite visual reconstruction (i.e., 3D model, orthoprojection, DEM, etc.) via the overlap of many component images (McCarthy et al. 2023). Large-area imaging has been used with increased frequency to archive coral reef structure and condition, and provides a basis for *in silico* field work to answer a variety of ecological questions (D'Urban Jackson et al. 2020; Bongaerts et al. 2021; Ferrari et al. 2021; McCarthy et al. 2023). Details of our large-area imaging workflow are available elsewhere (Edwards et al. 2023) and will be described in minimal detail here.

At each fixed site, divers entered the water with two D7000 SLR Nikon cameras in Ikelite underwater housings that were attached to a custom frame. One camera had a focal length of 18mm to capture a wider view of the reef and ensure appropriate overlap between pictures, while the other camera had a focal length of 55mm to capture higher resolution imagery to aid in species identification. Divers marked the boundaries of each 10 x 10 m long-term monitoring plot with six calibration tiles, and placed four 0.5 m long scale bars within the plot. One diver was tasked with placing the calibration tiles and recording the depth of each tile, while the other diver placed the scale bars and then swam 1.5 m over the reef in a gridded pattern with the camera rig. The camera interval timer on each camera was set to take a picture every second,

resulting in approximately 5,000 pictures per site over the course of a 50 to 60 min dive. The camera diver imaged a core area of 10x10 m, and swam several meters beyond the calibration tiles to ensure that a buffer region (> 1 m wide) around the core area was also imaged.

Once imagery was collected, we used the software Agisoft Metashape (St. Petersburg, Russia) to build a dense point cloud, which we refer to here as a 3D model. After building the 3D models in Metashape, we loaded them into the custom software Viscore (Petrovic et al. 2014) for postprocessing. These postprocessing steps included 1) scaling the 3D model using the 0.5 m scale bars, 2) entering depth measurements collected at each calibration tile so that the 3D model could be oriented with respect to the sea surface, 3) manually aligning 3D models of the same site collected in different years, and 4) exporting a high-resolution top-down view of the model known as an orthoprojection. Each 12 x 12 m orthoprojection had a resolution of 1 mm/pixel. We used these orthoprojections rather than the 3D models for all subsequent data collection.

2.3 Coral tracing

Researchers from both Scripps Institution of Oceanography (SIO) and Arizona State University (ASU) used the orthoprojections to delineate patches of live coral tissue. Researchers all followed the same SOP to trace coral colonies (Rodrguez et al. 2021) but used different software to do so (TagLab for SIO, ArcGIS Pro for ASU). In both instances, coral patches were traced onto the orthoprojection, and these tracings were exported as shapefiles to allow the data to be interoperable with TagLab and ArcGIS Pro. We found no effect of software on traced planar area (Figure S4.3). Furthermore, all shapefiles of traced coral patches used in this project were QCed and edited by a single annotator (OM) in TagLab to control for any potential effect of tracing software. We used the high-resolution imagery that underlies the 3D model (a.k.a. raw images) as a reference to assist with tracing and species ID. For this study, we chose to identify

Pocillopora to the genus level because morphology is not a good indicator of species ID for *Pocillopora* in Hawai'i (Johnston et al. 2018), whereas the three other taxa could be confidently identified to species. For *P. lobata*, we focused on massive and submassive growth forms to avoid confusion with the related branching coral *Porites compressa*.

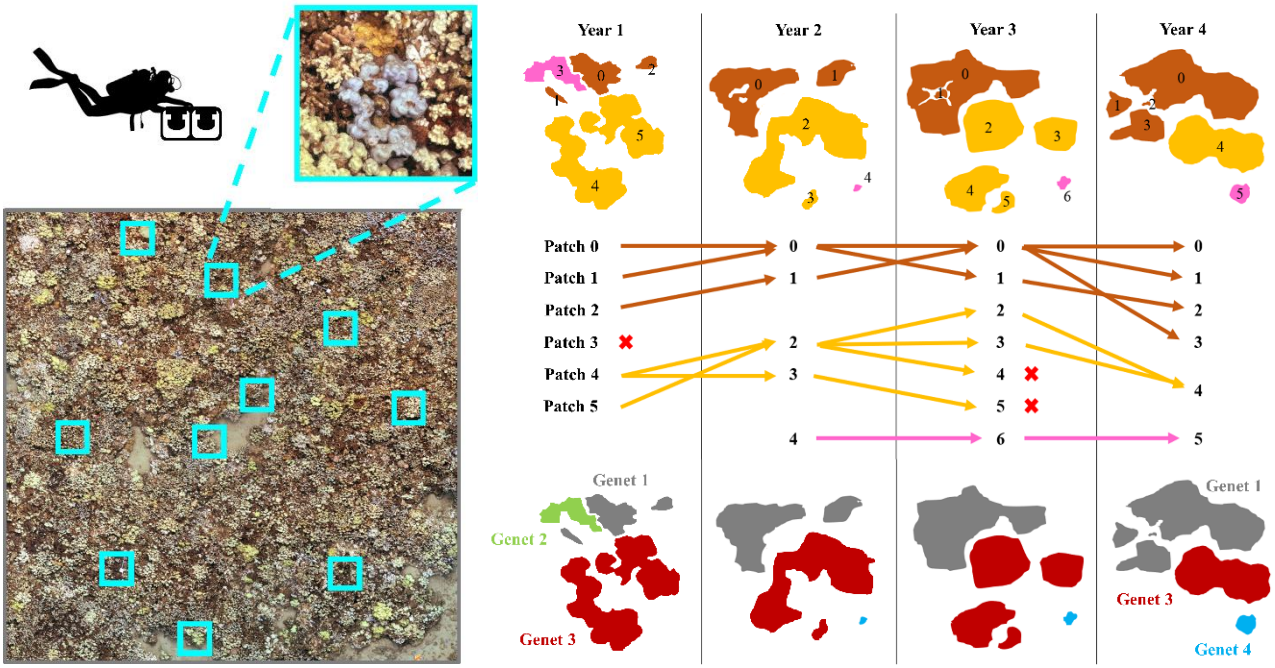

Figure 4.1: An example orthoprojection shows the location of randomly placed 0.5 m^2 quadrats (turquoise). For each quadrat, an annotator traced patches of live coral tissue > 5 cm in diameter. Patches were linked temporally to form a network of patches that were interconnected by fission (splitting via partial mortality) and fusion (growing together into a single patch). Annotators traced patches of live tissue < 5 cm in diameter and patches that fell outside of the quadrat if these patches were connected via fusion or fission to a genet within a quadrat. An example quadrat with traced patches is illustrated here, with fission and fusion represented by arrows. Patches are color coded by species (above) and genet (below) and numbered sequentially in each year. Each linked network of patches is considered to be its own genet and assigned a unique ID number that is consistent across the timeseries. In this example, only genets 1 and 3 survived the full timeseries, while genet 2 experienced complete mortality between years 1 and 2. Genet 4 recruited to the reef between years 1 and 2, and as such wouldn't be included in this study, since our analysis focused on the cohort of coral genets that were alive at the start of the timeseries (genets 1, 2, and 3 in this example).

After corals were traced, we used TagLab to "match" patches of live tissue that represented the same individual through time. This created a network of temporally linked coral

patches (Figure 4.1). This enabled us to more accurately identify individual genets of corals such as *Porites* and *Montipora*, which readily exhibit fusion and fission over time due to partial morality (Ross 2015; Sandin et al. 2020; Morais et al. 2021; Rodriguez et al. 2021). Hereafter we use "patch" to denote a single contiguous region of live coral tissue in one timepoint, and "genet" to denote a network of patches interconnected through time (Figure 4.1). While we cannot definitively say that linked corals represent a single genetic individual (since we did no genetic testing), the precise tracking capabilities afforded by overlapping orthoprojections and associated raw images enable us to identify individual genets with a reasonable degree of confidence. We performed all subsequent analyses at the genet level, and considered a genet to have survived the full timeseries if at least one patch of that genet existed in both 2014 (our first sampling year) and 2021 (our final sampling year). For each genet, we calculated the total planar area (cm^2) in each timestep by summing the planar area of individual associated patches.

To achieve an appropriate sample size of *M. capitata*, *M. patula*, and *P. lobata*, we traced corals within 10 randomly placed non-overlapping 0.5 m^2 quadrats within the orthoprojection (Figure 4.1). Following Rodriguez et al. (2021), we identified and traced all coral patches with a diameter > 5cm whose centroid fell within the boundaries of a quadrat. To account for fission and fusion dynamics, we also traced patches outside of a quadrat or < 5cm in diameter if they were temporally linked to a genet inside a quadrat. At sites where < 40 genets were traced in our first timestep, we placed additional quadrats (up to 25 total) and continued tracing taxa until we reached 40 genets or until 25 quadrats had been placed. For *Pocillopora*, which was less abundant than other taxa, we identified and traced all patches within each 12 x 12 m orthoprojection. To ensure a balanced design for statistical analyses, we randomly selected 100

P. lobata genets for n = 2 sites where > 100 genets had been traced. The total number of coral genets traced per site, year, and taxa is shown in Table S4.2.

2.4 Bleaching

We assessed the extent and severity of bleaching for every patch of coral tissue > 1cm^2 in each year of our timeseries. First, we visually estimated bleaching extent as the percent of a patch's area (0-100%) with some degree of paling unrelated to coral growth or disease. Focusing on this bleached tissue only, we then scored bleaching severity (from 0 to 3) based on the overall degree of paling observed (0 for < 5% of pigmentation lost; 1 for 5 – 50%, 2 for 50 – 95%, and 3 for > 95%; Rodriguez et al. 2021). When estimating both bleaching extent and severity, we used Viscore's Virtual Point Intercept interface (Fox et al. 2019) to reference the original imagery. This allowed us to view multiple angles of each coral patch to assess bleaching, enabling us to account for changes in tissue color due to lighting or image quality.

Once we assessed bleaching extent and severity for all patches in all years, we calculated genet-level bleaching extent and severity in each timepoint by summing bleaching extent and severity across patches, weighted by patch area. Then, we incorporated both bleaching extent and severity into a single bleaching metric for each genet in each timepoint (Figure 4.2). According to this metric, genets fell into one of five categories: no bleaching or very minor paling, minor bleaching, moderate bleaching, severe bleaching, or extreme bleaching. If a genet changed by more than one step between 2015 and 2019, the genet was considered to have an increased or decreased bleaching response over time (e.g., a genet that was moderately bleached in 2015 and extremely bleached in 2019 had an "increased bleaching response", while a genet that exhibited severe bleaching in 2015 and minor bleaching in 2019 had a "decreased bleaching response").

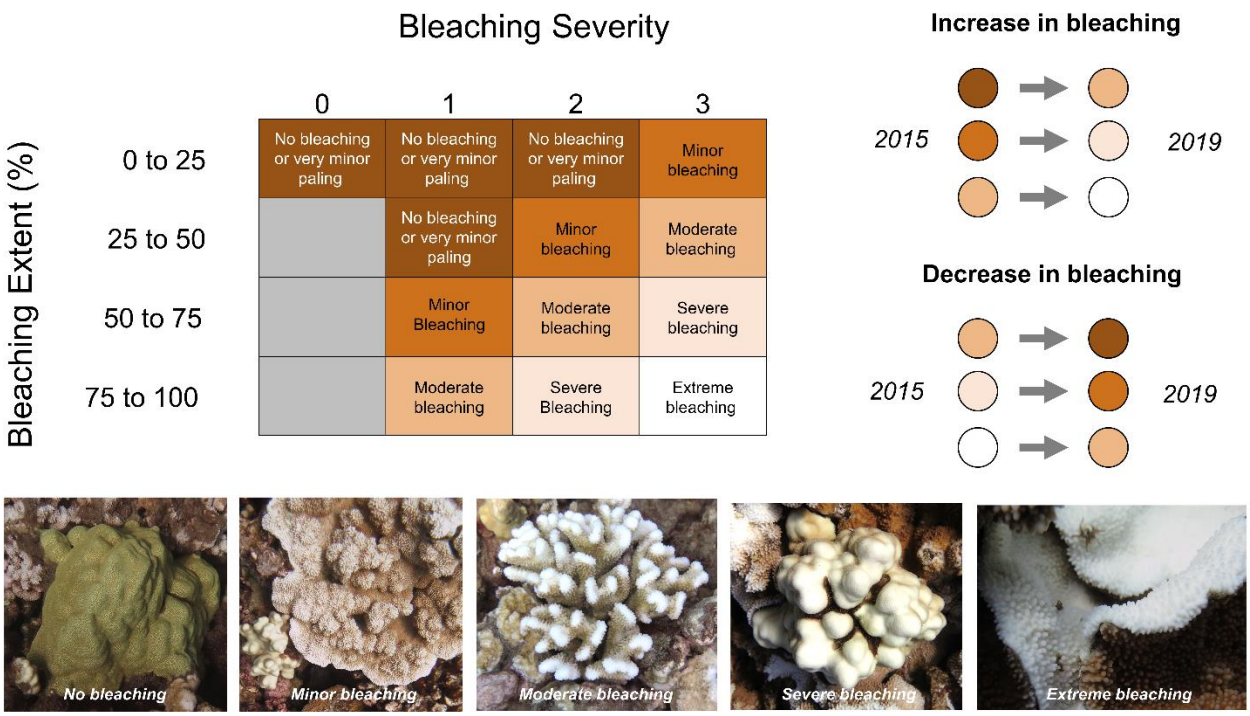

Figure 4.2: All patches of live coral tissue > 1cm^2 were assigned a bleaching score based on their bleaching extent and severity. Each genet was assigned the most common bleaching score across all of its patches (weighted by patch area). The five bleaching scores were 1) no bleaching or very minor paling, 2) minor bleaching, 3) moderate bleaching, 4) severe bleaching, and 5) extreme bleaching. Representative pictures of each bleaching score are shown below. Genets were considered to have shown an increase or decrease in bleaching over time if they changed by two or more bleaching scores from 2015 to 2019.

We considered genets that changed one bleaching step or less between 2015 and 2019 to have a stable bleaching response over time. Among these stable genets, those that exhibited moderate bleaching or higher were considered to have "high bleaching susceptibility", and all other genets were considered to be "thermally tolerant". These bleaching responses (thermally tolerant, decreased bleaching response, increased bleaching response, and high bleaching susceptibility) were used as fixed factors to compare genets over time.

2.5 Statistical analysis

To test for signs of acclimatization among surviving genets in each population (corals of the same taxa within a given site), we employed a bootstrapping approach using only genets that

were present in both bleaching events. We calculated the difference between each genet's bleaching score in 2015 and 2019, which produced an integer response variable ranging from -4 to 4, where 0 indicated no change in bleaching, -4 indicated extreme bleaching in 2015 and no bleaching in 2019, and 4 indicated no bleaching in 2015 and extreme bleaching in 2019. Then, we generated a null distribution of the median change in bleaching scores for each coral population via 100,000 resamples. P values were calculated as the proportion of all resamples where the population's median change in bleaching score was ≥ 0, and we used $\alpha = 0.05$ as our threshold of significance. We did not test for acclimatization in two populations of *Pocillopora* spp. which had a low sample size of surviving genets (< 10 genets).

To test if coral populations at each site exhibited different bleaching responses, we created a contingency table of surviving genets based on their bleaching responses over time. We performed Fisher's exact test to test the null hypothesis that there was no relationship between site and bleaching response. We performed this test for all permutations of sites for each taxon and calculated adjusted p values using the Bonferroni correction for multiple comparisons. We assigned post hoc letters at a significance level of $\alpha = 0.05$ to indicate significant differences in bleaching response between coral populations at different sites. We also pooled data by site and performed the same test to identify significant differences in bleaching response among coral taxa. Separately, we pooled observations across sites and ran a logistic regression of bleaching probability vs. genet size in 2015 and 2019 to quantify the relationship between bleaching and genet size. For this analysis, we coded bleaching as a binary variable (0 for genets with no signs of bleaching or just minor bleaching, and 1 for genets with moderate, severe, or extreme bleaching) in order to perform the logistic regression.

To test if acclimatized and thermally tolerant genets exhibited higher growth over the timeseries than other corals, we performed an ANCOVA for each coral taxon, focusing on surviving genets only. We used bleaching response (thermally tolerant, decreasing bleaching susceptibility, increasing bleaching susceptibility, and high bleaching susceptibility) as a fixed effect, only retaining levels with a sample size ≥ 10 for analysis. Our continuous predictor variable was genet planar area at the start of the timeseries, and our response variable was genet planar area at the end of the timeseries. Genet planar area was natural log transformed for normality, and model assumptions were visually assessed using residual plots and quantitatively using Shapiro tests for normality and Cochran tests for homogeneity of variance. We performed a separate ANCOVA using site as a fixed effect to test for significant differences in coral growth among sites for each taxon. All models used a significance level of $\alpha = 0.05$.

Finally, to test for differences in coral survivorship among sites, we performed a logistic regression using all traced genets (not just survivors) for each taxon. We used site as a fixed effect, log transformed planar area of genets in 2014 as our predictor variable, and coded genet survivorship as a binary response variable (0 = genet did not survive until 2021, 1 = genet survived from 2014 to 2021). There were significant interactions between multiple sites, so to facilitate interpretation we conducted pairwise comparisons between sites that didn't interact. We calculated adjusted p values using the Bonferroni correction for multiple comparisons at a significance level of $\alpha = 0.05$. To test for differences in coral survivorship among taxa, we also pooled genets by site and ran a logistic regression of survivorship vs. initial genet size. We completed statistical analyses using the 'dplyr', 'emmeans', 'multcomp', 'coin', and 'rstatix' packages in R v. 4.0.5 (Searle et al. 1980; Hothorn et al. 2006, 2008; Kassambra 2019; R Core Team 2023; Wickham et al. 2023).

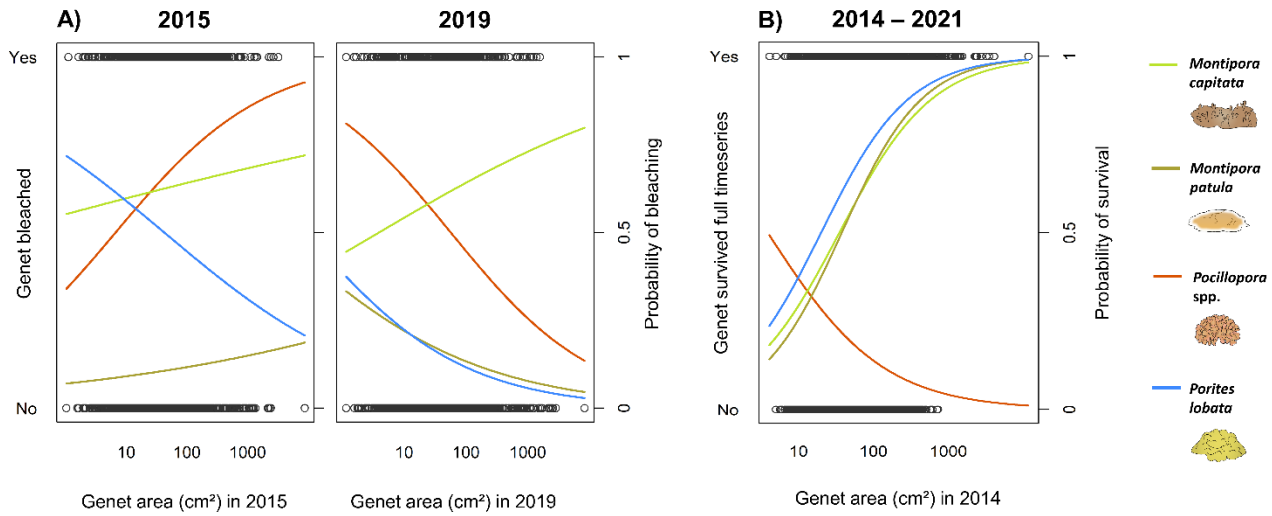

Figure 4.3: A) The probability of bleaching as a function of genet planar area in both 2015 and 2019, shown for each taxon. Bleaching was converted into a binary variable for this analysis (1 for genets with moderate, severe, or extreme bleaching, 0 for genets with minor or no bleaching). B) The probability that a genet survived to the end of the timeseries (2021) is shown as a function of its planar area at the start of the timeseries (2014). Planar area was a significant predictor of survivorship for all taxa ($p < 0.001$ for all taxa), and was positively related to survivorship for *Montipora* and *Porites*, but negatively related to survivorship in *Pocillopora*.

3. Results

In total, we tracked the fate of 1,832 coral genets across six sites from 2014 to 2021. *Pocillopora* exhibited exceptionally low survivorship: 15.7% of *Pocillopora* genets survived from 2014 to 2021 compared to 54.4% of *M. capitata* genets, 51.3% of *M. patula* genets, and 63.2% of *P. lobata* genets. Bleaching prevalence was high for *Pocillopora* and *M. capitata* during both bleaching events: 70.0% of *Pocillopora* and 62.0% of *M. capitata* genets that survived to 2015 experienced moderate, severe, or extreme bleaching in the first bleaching event, while 50.4% of *Pocillopora* and 60.3% of *M. capitata* genets that survived until 2019 experienced moderate, severe, or extreme bleaching in the second bleaching event (Figure S4.4). This contrasts with *M. patula*, which experienced low bleaching during both bleaching events (10.6% in 2015, 16.8% in 2019), and *P. lobata*, which experienced high bleaching in 2015 (51.0%) but low bleaching in 2019 (16.0%; Figure S4.4). We also observed an inconsistent

relationship between genet size and the probability of bleaching across taxa and bleaching events (Figure 4.3). In 2015, the probability of bleaching increased with genet size for *Pocillopora* ($p < 0.001$) but decreased with genet size for *P. lobata* ($p < 0.001$), and exhibited no significant relationship with size for either species of *Montipora* (*M. capitata* $p = 0.348$; *M. patula* $p = 0.364$). In 2019, bleaching probability increased with genet size for *M. capitata* ($p = 0.047$) but decreased with genet size for the other taxa (*M. patula* $p = 0.027$; *Pocillopora* $p = 0.021$; *P. lobata* $p = 0.002$).

3.1 Evidence of acclimatization

Patterns of acclimatization over the course of this study differed among coral taxa. We found no evidence of acclimatization at the population level for either species of *Montipora* (Figure 4.4A-B), with more variability in bleaching over time for *M. capitata* compared to *M. patula*. Genets of *M. capitata* were more likely to experience an increase or decrease in bleaching from 2015 and 2019, while a majority of *M. patula* genets consistently exhibited the same bleaching response (no bleaching) over time. Conversely, we did find evidence for acclimatization in specific *Pocillopora* and *P. lobata* populations (Figure 4.4C-D): *Pocillopora* from Kahekili and Olowalu exhibited less severe bleaching in 2019 compared to 2015 ($p < 0.001$ and $p = 0.042$, respectively). *Pocillopora* that survived until 2019 from Ukumehame demonstrated increasing bleaching susceptibility over time, although our sample size is small for that population. *Pocillopora* at Molokini and Wahikuli were excluded from the analysis, since the vast majority of genets at those sites perished after the first bleaching event in 2015. For *P. lobata*, we found significant evidence of population-scale acclimatization at Keawakapu ($p = 0.023$) and Molokini ($p = 0.010$). Across all sites, *P. lobata* genets were most likely to exhibit signs of acclimatization, ranging from 18.0% of all *P. lobata* genets at Wahikuli to 39.1% of all

P. lobata genets at Olowalu. It was more common, however, for *P. lobata* genets to exhibit the same bleaching severity in both years (often no bleaching), particularly at Kahekili, Wahikuli, and Ukumehame.

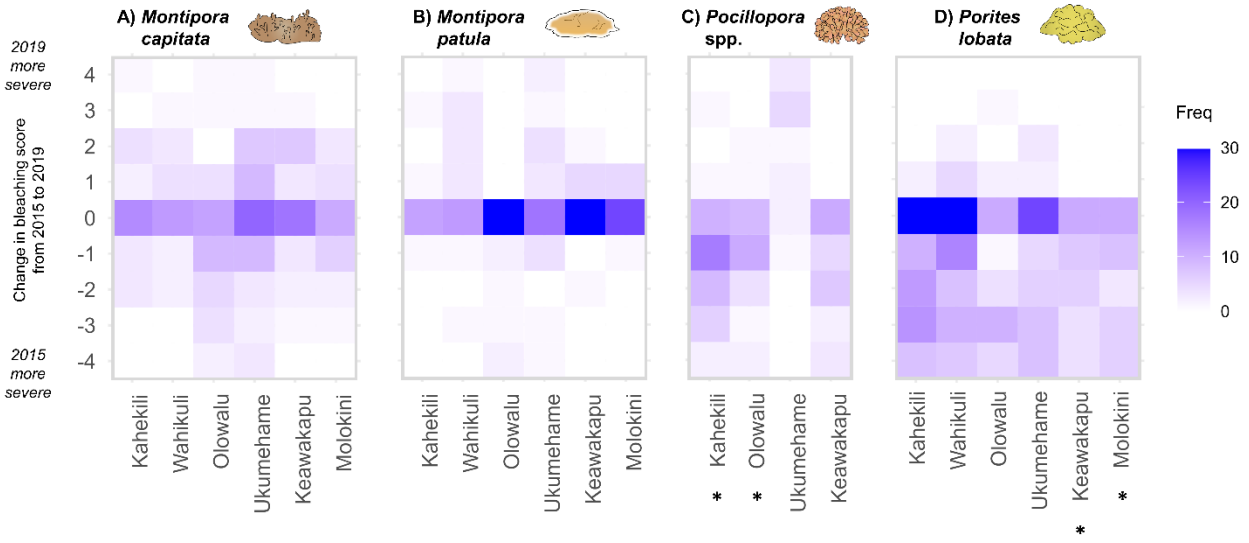

Figure 4.4: A heatmap illustrating how genet bleaching scores changed between 2015 and 2019, shown across taxa and sites. For each genet that survived through 2019, we calculated the difference in bleaching score between 2015 and 2019. Negative values indicate more severe bleaching in 2015, positive values indicate more severe bleaching in 2019, and 0 indicates no change in bleaching. We observed significant decreases in bleaching over time for *Pocillopora* populations at Kahekili ($p < 0.001$) and Olowalu ($p = 0.042$), and for *Porites lobata* populations at Keawakapu ($p = 0.023$) and Molokini ($p = 0.010$).

3.2 Population bleaching response

We tracked genets based on their response to thermal stress in 2015 and 2019, and found that the bleaching response of genets strongly differed among species ($p < 0.001$). In general, *M. capitata* had the largest proportion of genets that bleached in both 2015 and 2019 (highly susceptible to bleaching), *M. patula* had the largest proportion of thermally tolerant genets, and *P. lobata* had the largest proportion of genets that exhibited signs of acclimatization (Figure 4.5). However, we observed site-level variation in these trends, with some populations exhibiting

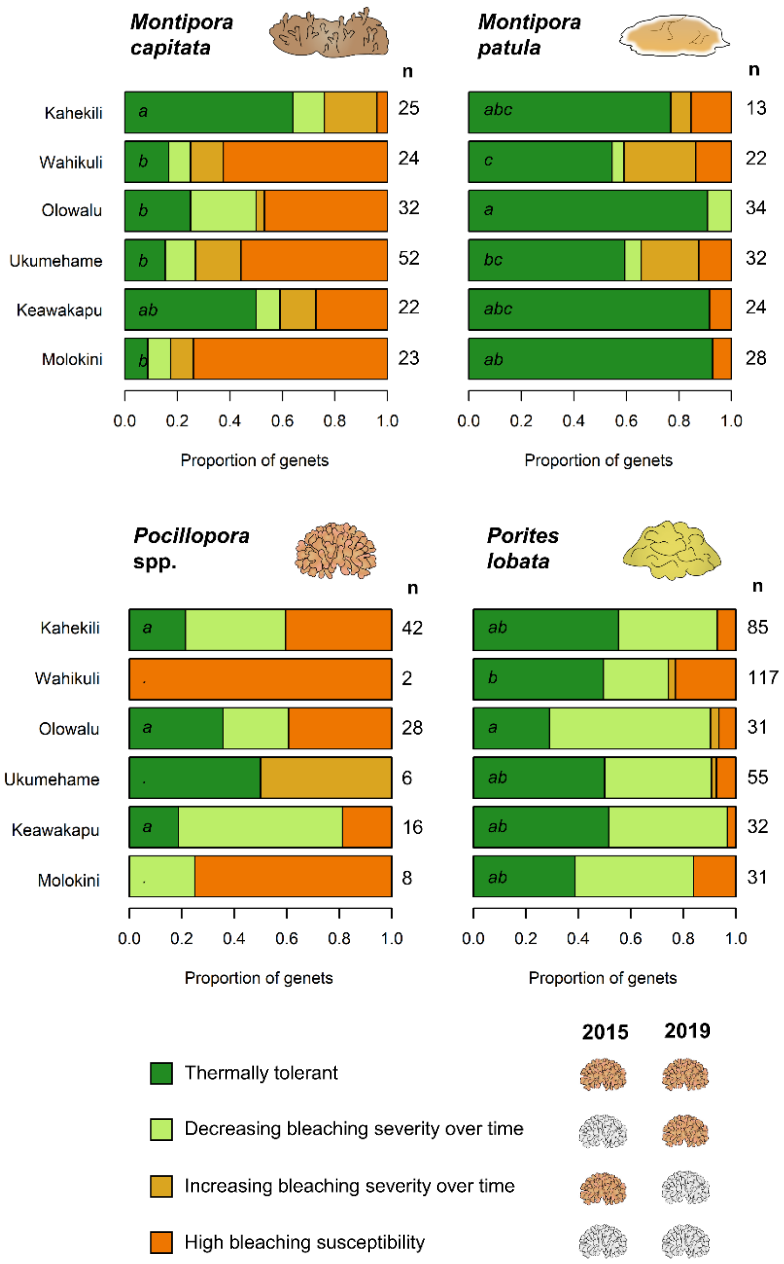

Figure 4.5: Surviving genets at each site shown by their response to heat stress in 2015 and 2019. Dark green indicates genets that didn't bleach in either event, light green indicates genets that bleached more in 2015 than 2019, yellow indicates genets that bleached more in 2019 than 2015, and orange indicates genets that bleached in both events. Letters denote significant differences between populations in terms of their bleaching response. The number of surviving genets in each population is shown to the right of each plot.

higher proportions of thermally tolerant and acclimatized genets than others. Most strikingly, the bleaching response of *M. capitata* genets at Kahekili was significantly different from all other sites except for Keawakapu, driven by a higher proportion of thermally tolerant individuals (Figure 4.5). We also observed a larger proportion of *P. lobata* genets that were highly susceptible to bleaching at Wahikuli, whereas at Olowalu more genets exhibited signs of acclimatization. We also found significantly more *M. patula* genets with increasing bleaching susceptibility at Wahikuli and Ukumehame compared to Olowalu (Figure 4.5). We did not observe any significant differences in bleaching response among *Pocillopora* populations, although our analysis was limited to genets from Kahekili, Olowalu, and Keawakapu due to the small sample size of surviving genets at our other three sites (Figure 4.5).

3.3 Growth

For genets of *M. capitata* and *Pocillopora* that survived the full timeseries, we found no evidence that genet growth or shrinkage was a function of a genet's bleaching response over time ($p = 0.052$ and $p = 0.073$ respectively). In other words, genets of these taxa that bleached repeatedly and survived were just as likely to grow or shrink as genets that didn't bleach and survived (Figure 4.6A). We chose not to conduct an ANCOVA for *M. patula* since genets exhibited minimal variation in bleaching response (78% of genets didn't bleach in either event), although we observed no obvious relationship between bleaching response and growth or shrinkage for this species (Figure 4.6A). Interpreting the results for *P. lobata* was more complex due to the presence of a significant interaction between initial genet size in 2014 and final genet size in 2021 ($p_{site} = 0.004$, $p_{interaction} = 0.003$). Small *P. lobata* genets (< 100 cm^2 in 2014) that survived the full timeseries didn't exhibit a relationship between bleaching history and genet growth or shrinkage. However, larger genets (> 100 cm^2 in 2014) that experienced repeated

bleaching were more likely to experience partial mortality and genet shrinkage compared to thermally tolerant individuals, which exhibited a nearly 1:1 relationship between planar area in 2014 and 2021. Thus, bleaching history appears to have more of an impact on the growth trajectory of surviving genets in *P. lobata* compared to the other taxa studied here.

While bleaching history didn't impact coral growth for three of the four taxa studied here, we observed site-level differences in growth for all focal taxa (Figure 4.6B). In particular, corals from Keawakapu exhibited the most partial mortality and shrinkage over the course of the timeseries. *M. patula* genets from Keawakapu had significantly lower growth than *M. patula* genets from all other sites except Ukumehame ($p < 0.001$), while *Pocillopora* genets from Keawakapu had significantly lower growth than *Pocillopora* from Olowalu ($p = 0.015$). For *P. lobata*, we found that genets at Molokini had significantly lower growth than *P. lobata* all other sites except for Keawakapu ($p = 0.003$). A significant interaction between initial and final genet size complicated interpretation for *M. capitata* ($p_{site} = 0.002$, $p_{interaction} = 0.021$). Smaller *M. capitata* genets from Molokini (< 100 cm^2 in 2014) appear to have grown more than genets from other sites, but this difference disappears for larger genets. Instead, for larger *M. capitata* genets (> 100 cm^2 in 2014), Keawakapu appears to have significantly lower growth rates. The slope between genet size in 2014 and 2021 is similar for *M. capitata* populations from Molokini, Ukumehame, Olowalu, and Keawakapu, and indicates positive growth over time for small genets and shrinkage over time for large genets. Final size is a more consistent function of initial genet size for *M. capitata* at Kahekili and Wahikuli, although for both sites there is evidence of shrinkage over time rather than growth.

3.4 Survivorship

We found a significant relationship between survivorship from 2014 to 2021 and initial genet planar area for all taxa ($p < 0.001$). *M. capitata, M. patula,* and *P. lobata* exhibited a strong positive relationship between 2014 planar area and probability of genet survival through 2021, with no significant differences in survivorship among those three taxa. Conversely, *Pocillopora* genets exhibited a strong negative relationship between 2014 planar area and survivorship. The probability of survivorship was considerably lower for *Pocillopora* than for the other taxa. For example, a *Pocillopora* genet with a planar area of 100 cm^2 in 2014 would be expected to survive until 2021 just 13.8% of the time, whereas a similarly sized genet of *M. capitata, M. patula,* and *P. lobata* in 2014 would respectively have a 67.6%, 68.8%, and 76.7% probability of survivorship until 2023. The vast majority of *Pocillopora* mortality occurred between 2015 and 2017, likely due to the 2015 bleaching event, while mortality for the other three taxa was more evenly distributed across the timeseries (Figure S4.5).

As with coral growth, we observed site-level differences in genet survivorship from 2014 to 2021. For many sites, interactions between genet size and survivorship reduced interpretability of results. However, we were generally able to identify sites with the highest and lowest survivorship through pairwise comparisons of sites that did not exhibit significant interactions (Figure 4.6C; Table S4.3). Ukumehame stood out for high survivorship of *M. capitata*, *M. patula*, and *P. lobata*, Kahekili exhibited high survivorship of both *Pocillopora* and *P. lobata*, and Wahikuli exhibited high survivorship of *P. lobata*. Conversely, Keawakapu had low survivorship of *M. capitata*, *M. patula*, and *P. lobata*, and Molokini had low survivorship of *M. capitata*, *Pocillopora*, and *P. lobata*. Olowalu had low survivorship of *M. capitata* compared to other sites, while Ukumehame and Wahikuli both had low survivorship of *Pocillopora*.

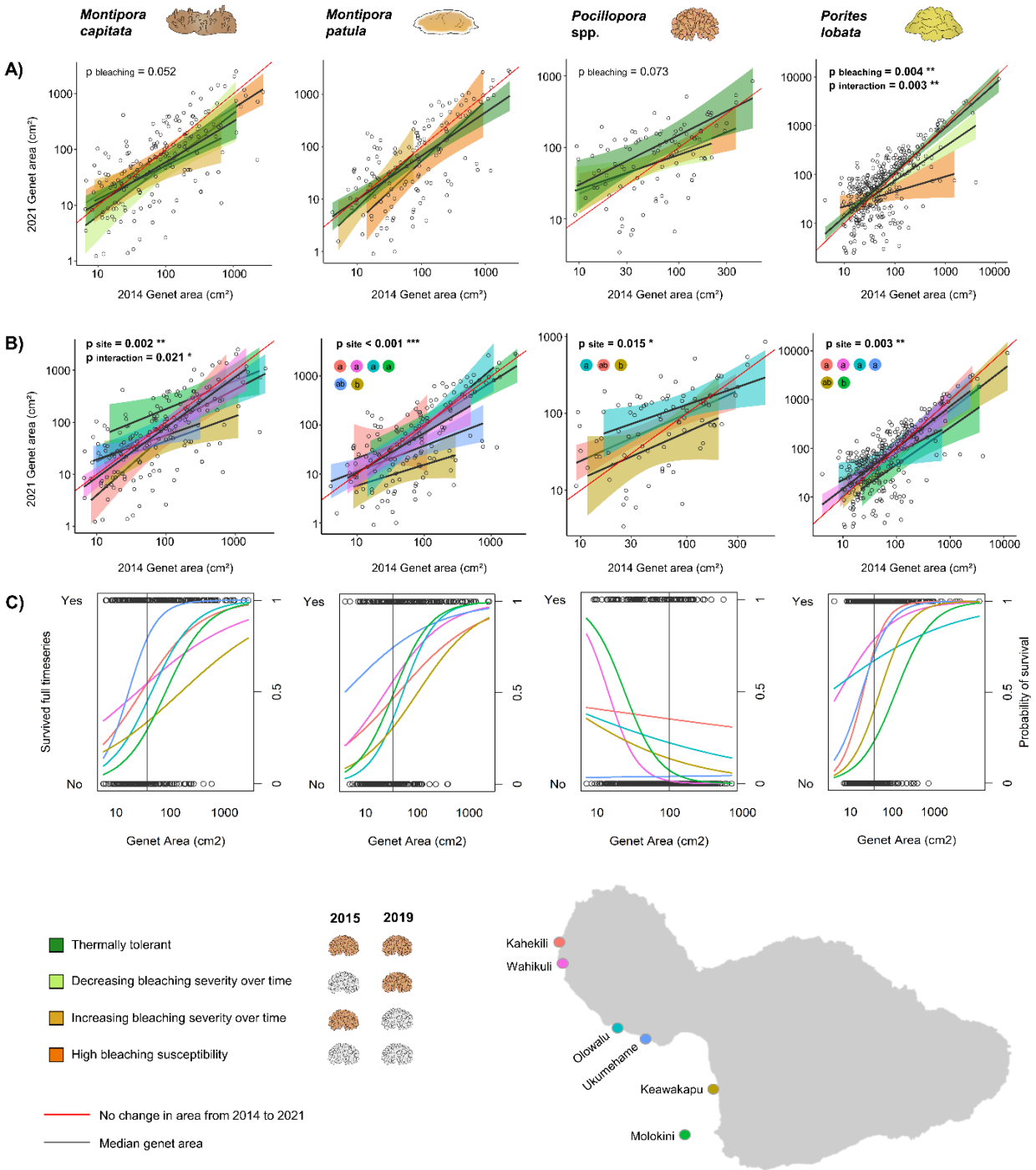

Figure 4.6: A-B) Log-scale plots show patterns of growth and shrinkage in genets that survived the full timeseries as a function of A) genet bleaching history and B) site. Genets that fall on the red diagonal line experienced no change in planar area between 2014 and 2021, those above it experienced growth, and those below it experienced shrinkage. C) For each taxon, site-level patterns of survivorship are shown as a function of genet planar area in 2014. The vertical gray line in each plot represents the median planar area of that taxon in 2014. The key in the bottom left corresponds to bleaching histories in A. Sites on the map denote color coding in B-C. Color-coded post-hoc letters in B show significant differences between sites.

4. Discussion

We tracked the fate of hundreds of corals through sequential marine heatwaves of moderate intensity. By comparing the bleaching response of individuals through time, we sought to document evidence of acclimatization at organismal and population levels. Taken in concert with growth and survivorship data, we were able to test whether past bleaching responses influenced growth in corals that survived the full timeseries. Finally, variation in coral bleaching, growth, and survivorship among six sites in leeward Maui reflects the unique environmental history that each of these reefs faces. Interactions between environmental and anthropogenic factors likely contribute to site-level variation in coral performance over time.

4.1 Acclimatization

We were able to quantify the prevalence of acclimatization for both individual corals as well as entire populations. We did not find evidence of widespread acclimatization on reefs in leeward Maui, in keeping with other studies in the region (Winston et al. *in prep*), although a few populations did exhibit significant reductions in bleaching severity and extent over time, most notably *Pocillopora* at Kahekili.

While signs of acclimatization at the population level were limited, individual genets (primarily *P. lobata*) did exhibit decreased bleaching severity and extent over time. Massive *Porites* employs a stress tolerant life-history strategy (Darling et al. 2012; Kayal et al. 2015; Sandin et al. 2020; Morais et al. 2021) and has a demonstrated ability to acclimatize to repeated heat stress (Carilli et al. 2012; DeCarlo et al. 2019; McLachlan et al. 2022). Massive *Porites* are generally among the most thermally tolerant corals on Indo-Pacific reefs (McClanahan et al. 2020; Khen et al. 2023), although thermal tolerance relative to other taxa has been shown to decline under severe thermal stress (Burn et al. 2023). The heat tolerance of *Porites* contrasts

with that of faster growing coral taxa such as *Acropora* and *Pocillopora*, which have been consistently found to be among the least resistant to thermal stress (McClanahan et al. 2020; Wall et al. 2021; Speare et al. 2022; Burn et al. 2023; Yadav et al. 2023). These taxa tend to experience more mortality but have demonstrated the capacity to rapidly recolonize reef communities after heat stress abates (Moritz et al. 2018; Morais et al. 2021; Page et al. 2023). However, severe mortality events can hamper recovery by eliminating sources of recruits (Dietzel et al. 2021). This could be a factor at play in Maui, where *Pocillopora* abundance has remained consistently low following widespread bleaching and mortality in 2015.

Compared to *Porites*, evidence for acclimatization in *Montipora* and *Pocillopora* is more mixed. Coles et al. (2018) found that *M. capitata* and *Pocillopora damicornis* from Kāne'ohe Bay took longer to bleach and showed higher survivorship when experimentally reared at 31°C in 2017 compared to in 1970. Association with thermally-tolerant symbionts has also been found to increase bleaching resistance in *M. capitata* (Innis et al. 2018; de Souza et al. 2021; Drury et al. 2022) and *Pocillopora* (Palacio-Castro et al. 2023), although studies have found mixed evidence for symbiont shuffling as a mechanism to achieve long-term acclimatization in *M. capitata* (de Souza et al. 2021; Harris et al. 2022). Rather, it appears that high phenotypic variation in pigmentation exists for *M. capitata*, with both pale and highly pigmented variants observed on reefs even in the absence of heat stress (Figure S4.4; Matsuda et al. 2020). While studies have observed a relationship between pigmentation and performance under heat stress in *Montipora* in Hawai'i (Sparks et al. 2015; Innis et al. 2018), there is little evidence that more pigmented variants are being selected for and becoming more dominant over time. Indeed, we found considerable phenotypic variation in *M. capitata* bleaching, including shifts in the pigmentation of individual genets over time (both darkening and paling) during both bleaching

and non-bleaching years (Figure S4.4). Yet we observed no reductions in *M. capitata* bleaching at the population level over our timeseries. These results likely reflect *M. capitata*'s ability to use heterotrophy to supplement nutritional deficits in the absence of symbionts (Grottoli et al. 2006; McLachlan et al. 2022), which could reduce the need for *M. capitata* to undergo acclimatization through some other mechanism. While *Pocillopora* survivors showed patterns of reduced bleaching consistent with acclimatization at certain sites, we are unable to ascribe a mechanism for those shifts. Symbiont shuffling could play a role, but site-specific changes in anthropogenic or environmental impact from 2015 to 2019 could as well.

Compared to extreme heatwaves that cause widespread mortality, moderate thermal stress would be expected to produce more variable bleaching responses among individual corals and promote natural selection for thermal tolerance (Pandolfi et al. 2011; Fox et al. 2019; Burn et al. 2023; Marzonie et al. 2023). Both the 2015 and 2019 heat stress events were moderate in severity and duration in Hawai'i compared to elsewhere in the Pacific (Hughes et al. 2017; Eakin et al. 2019; Fox et al. 2019), just barely surpassing the 8 DHW threshold where coral mortality is be expected. The considerable mortality we observed from 2014 to 2021 indicates that certain individuals were being selected against, whereas survivors showed a lack of cumulative stress from bleaching, as evidenced by the absence of any relationship between growth rate and bleaching history. Selection for thermal tolerance has been observed on reefs elsewhere (Hughes et al. 2018; Moritz et al. 2018; McClanahan et al. 2020; González-Barrios et al. 2023), resulting in notable shifts in coral community composition toward stress-tolerant species. Admittedly, it is also possible that the timing of our 2019 survey influenced our results. We collected imagery just before peak heat stress was reached in October 2019, so it is possible that bleaching could have continued to worsen for several weeks after our imagery was collected. That being said, our

results are consistent with other analyses that have found less severe bleaching in 2019 compared to 2015 in Hawai'i (Asner et al. 2022; Winston et al. 2022), so it is unlikely that the timing of our surveys alone can explain the results we observe here.

4.2 Growth

While the bleaching responses we observed are consistent with known taxonomic patterns of thermal tolerance in Hawaiian corals (Brown 2004; Sparks et al. 2015; McLachlan et al. 2022; Winston et al. 2022; Yadav et al. 2023), we found a striking disconnect between bleaching and growth over the course of our timeseries. With the exception of large *Porites*, genets that repeatedly bleached and survived did not demonstrate slower growth or more partial mortality than thermally tolerant or acclimatized genets over the course of our timeseries. This decoupling between bleaching and growth is not surprising given inconsistent findings in the literature. While heat stress was found to negatively impact growth in *M. capitata* and *Pocillopora* in Kāne'ohe Bay (Coles et al. 2018; Huffmyer et al. 2023), stress bands in *Porites* skeletons from the Red Sea suggest an upregulation of calcification following bleaching (Mantanona & DeCarlo 2023) and exposure to moderate heat stress has been shown to increase skeletal growth in *Pocillopora* (Lachs et al. 2023b; Roper et al. 2023) and *Acropora* (Walker et al. 2023).

The lack of relationship between bleaching and coral growth that we observe could be the result of complex physiological trade-offs between maintenance and growth. For instance, *Pocillopora* colonies that were experimentally acclimated to 31°C prioritized lipid accumulation and tissue growth over skeletal extension (Roik et al. 2023). More generally, studies have found that energetic costs associated with hosting the heat-tolerant symbiont *Durusdinium* can result in trade-offs for the coral host including reduced growth and fecundity (Jones & Berkelmans 2010;

Harris et al. 2022). However, other studies of heat stressed corals fail to document trade-offs between thermal tolerance and growth at ecological scales (Rivera et al. 2022; Lachs et al. 2023b). Given this mixed evidence, even among studies of the same species, it seems likely that trade-offs between heat tolerance and growth are site specific and dependent on local environmental conditions and exposure history (Rivera et al. 2022).

Another explanation for the decoupling we observe between bleaching responses and coral growth could be the complexity of fusion and fission dynamics in our focal taxa. Partial mortality can cause a coral genet to split into multiple independent fragments, or ramets, which can either regrow and fuse back into a single genet, or continue living as functionally separate individuals. These individual ramets each experience their own trajectory of growth, shrinkage, and mortality based on interspecific interactions and hyper-localized environmental conditions (Hughes & Jackson 1980; Furby et al. 2017; Brito-Millán et al. 2019a; Hernández-Landa et al. 2020). These processes make it more complicated to identify and track the fate of "individuals" and can result in complex growth trajectories across an entire genet. Partial mortality, fusion, and fission are especially apparent in encrusting and massive corals like *M. capitata*, *M. patula*, and *P. lobata* (Ross 2015; Matsuda et al. 2020), and can help these individuals avoid whole-colony mortality following environmental stress (Ross et al. 2010) even if most tissue is lost. For example, partial mortality may be concentrated on the top of coral colonies following exposure to higher irradiance during a bleaching event (Sparks et al. 2015). However, these corals can persist via regrowth of tissue that survived bleaching in shaded or cryptic regions of the colony (Matsuda et al. 2020). Due to these complexities, most studies tracking coral growth and survivorship focus on taxa with identifiable, discrete colonies that display little fission or fusion, such as *Pocillopora* (Kodera et al. 2020; Kopecky et al. 2023). Our results demonstrate that such

approaches may be inadequate for describing demographic and recovery dynamics in locations like Hawai'i, where fusion and fission predominate.

4.3 Survivorship

While we observed decoupling between bleaching and growth on Maui's reefs, we observed more congruence between bleaching and survivorship as a function of genet size. Our observation that smaller genets of *P. lobata* and *M. patula* were more likely to bleach and less likely to survive the full duration of our timeseries is consistent with literature on size-based survivorship in corals. Small coral colonies have a greater surface area to volume ratio and less energy reserves, which make them more vulnerable to whole-colony mortality, whereas injury in larger corals is more likely to lead to partial mortality (Bak & Meesters 1998; Furby et al. 2017; Kodera et al. 2020). The influence of coral size on bleaching is less straightforward. Some studies have found small colonies to be more susceptible to bleaching (Winston et al. *in prep*; Johnston et al. 2020), while others have found large colonies to be more susceptible (Brandt 2009; Burn et al. 2023), and still others document no relationship between bleaching and colony size (Ortiz et al. 2009; Rodgers et al. 2017). Interestingly, while we observed divergent bleaching responses for *M. capitata* and *M. patula*, both in severity and as a function of size, these species displayed nearly identical patterns of survivorship. This supports other studies in Hawai'i that have found a disconnect between bleaching and survivorship in *M. capitata* (Matsuda et al. 2020; Yadav et al. 2023) and likely reflects taxonomic and life-history similarities between *Montipora* species.

In *Pocillopora*, size-dependent patterns of bleaching and survivorship reversed over time, with more bleaching and mortality in larger genets in 2015, followed by more bleaching and mortality in smaller genets in 2019 (Figure S4.6). While we would expect to see the highest

mortality in smaller size classes in *Pocillopora* (Sandin et al. 2020; Kodera et al. 2020), higher mortality in large *Pocillopora* colonies in response to bleaching has been observed before (Speare et al. 2022; Kopecky et al. 2023). In Moorea, the coexistence of multiple cryptic species of *Pocillopora* led to the appearance of a positive relationship between colony size and mortality after a bleaching event (Burgess et al. 2021). However, through genetic testing, researchers revealed that the largest *Pocillopora* colonies all belonged to a single haplotype with high bleaching susceptibility, and found no relationship between colony size and mortality within this haplotype. Thus, the shift in size-dependent mortality we observe from 2015 to 2019 could represent the loss of cryptic *Pocillopora* diversity in Maui. But because morphology is not a good indicator of species identification in Hawaiian *Pocillopora*, we would need genetic testing to confirm that species diversity is a driver of survivorship. Still, if the loss of cryptic species diversity is indeed responsible for the survivorship trends we observe here, it suggests that bleaching events are driving a shift in coral community composition in Maui toward taxa with higher thermal tolerance.

4.4 Variation among sites

The severity of thermal stress was remarkably consistent across study sites in leeward Maui and between bleaching events, although local scale variability undoubtably exists that is not captured in satellite data at the 5km grid scale (Grimaldi et al. 2023). That being said, we would expect similar levels of bleaching and mortality across sites and through time based on the satellite DHW data available, with slightly lower levels of mortality expected in northern sites compared to southern sites (Table S4.1) assuming a static threshold of 8 DHW for mortality (Pandolfi et al. 2011; Kayanne 2017; Couch et al. 2017). Importantly, despite their shared thermal history, these sites each experience a unique combination of local environmental and

Table 4.1: A summary of the best and worst performing coral populations with respect to their bleaching response over time, growth rates, and probability of survivorship. Coral populations with significantly higher proportions of thermally tolerant or acclimatized genets, significantly higher rates of growth, and significantly higher probabilities of survivorship are categorized here as "best performing sites". Kahekili and Olowalu has the most evidence of resilient coral populations, while Molokini and Keawakapu has the least.

	Taxa	Bleaching	Growth	Survivorship
Best performing sites	*Montipora capitata*	Kahekili	Molokini (small genets)	Ukumehame
	Montipora patula	Olowalu	Kahekili Wahikuli Molokini Olowalu	Ukumehame
	Pocillopora spp.	Kahekili Olowalu Keawakapu	Olowalu	Kahekili
	Porites lobata	Olowalu	Kahekili Wahikuli Olowalu Ukumehame	Kahekili Ukumehame Wahikuli
Worst performing sites	*Montipora capitata*	Olowalu Ukumehame Wahikuli Molokini	Keawakapu (large genets)	Olowalu Molokini Keawakapu
	Montipora patula	Ukumehame Wahikuli	Keawakapu	Keawakapu
	Pocillopora spp.	Not enough survivorship to assess bleaching responses at Wahikuli, Ukumehame, and Molokini	Keawakapu	Ukumehame Molokini Wahikuli
	Porites lobata	Wahikuli	Molokini	Keawakapu Molokini

anthropogenic impacts that could also explain divergent patterns of coral bleaching, growth, and recovery across populations (Brown 2004, 2019; Dailer et al. 2010; Ross 2015). Indeed, chronic stressors such as urban runoff, sedimentation, coral disease, overfishing of herbivores and algal overgrowth have been shown to be more important contributors to coral tissue loss in Maui than acute pulse events (Ross et al. 2010, Ross et al. 2012).

In our study, coral populations at Kahekili and Olowalu showed the greatest resilience to thermal stress, while populations at Keawakapu and Molokini showed the least resilience (Table

4.1). Corals at Kahekili in particular showed higher rates of thermal tolerance (*M. capitata*) and acclimatization (*Pocillopora*) than conspecifics elsewhere, even compared to populations just 3 km away at Wahikuli that experienced near identical heat stress. Kahekili has a complex history of management and anthropogenic impacts. Situated just offshore of the Lahaina Wastewater Reclamation Facility, Kahekili's reefs have been subject to elevated concentrations of nitrogen from wastewater effluent that seeps out of nearby injection wells (Smith et al. 2005; Dailer et al. 2010). Elevated nutrients at Kahekili have contributed to occasional mass algal blooms that overgrow corals (Smith et al. 2005; Ross et al. 2012; Brown 2019). A cycle of algal blooms prompted the state Division of Aquatic Resources to establish the Kahekili Herbivore Fisheries Management Area in 2009 (Williams et al. 2016). Efficacy of these protections has fluctuated over time, but there is evidence that protecting herbivorous fish has kept macroalgae coverage low and increased coverage of crustose coralline algae (Williams et al. 2016), which is a less effective coral competitor (Smith et al. 2001) and promotes coral recruitment (Vermeij 2005).

A combination of fisheries management and elevated nutrients could explain the improved bleaching response we observed at Kahekili. Moderate nutrient enrichment has been shown to delay the onset of bleaching (Han et al. 2022) and reduce bleaching-associated mortality by improving the photosynthetic efficiency of symbionts (Fox et al. 2021) or by enhancing water column chlorophyll-a, which in turn can reduce irradiance and support coral heterotrophy (Keighan et al. 2023). However, it is important to note that the interactive effects of nutrient enrichment and macroalgae have been found to be especially harmful for corals during and immediately after bleaching events (Donovan et al. 2020, 2021), since nutrients enhance the growth and competitive ability of macroalgae (Smith et al. 2001). This suggests that control of

macroalgae through fisheries management is fundamental to the bleaching resistance that we document here.

It is possible that repeated algal blooms over multiple decades could have already selected for stress-tolerant corals at Kahekili, enhancing community resistance to disturbance (Côté & Darling 2010; Winston et al. 2022). This pattern has been observed elsewhere in Hawai'i (Barnhill & Bahr 2019). The reverse of this phenomenon could explain the poor performance of corals at Molokini, a highly protected site located offshore of Maui within the Molokini Shoal Marine Life Conservation District. Aside from high levels of tourism (Weng et al. 2023), Molokini has fewer local human impacts than other sites in Maui. It is possible that the protection and remoteness of Molokini allowed more sensitive coral genets to persist until 2015, which would explain the lower survivorship compared to more heavily impacted sites such as Kahekili. However, we also document low survivorship at Keawakapu, a site with a similar suite of anthropogenic impacts to Kahekili (Vermeij et al. 2008; Dailer et al. 2010), albeit without fisheries management. The small number of sites considered here, combined with each site's multifaceted and unique history, complicate any assumptions of causality. While the exact sources of variation in coral performance are uncertain, it's clear that that local anthropogenic impacts are interacting with bleaching history and species composition to shape the trajectory of each site's benthic community over time.

4.5 Implications for coral restoration

For coral restoration to be effective, outplanted corals must be able to persist through future climate-related disturbance events (Bostrom-Einarsson et al. 2020; Hein et al. 2020; Ferrari et al. 2021). To this end, restoration practitioners have sought to propagate thermally tolerant phenotypes or genotypes (Van Oppen et al. 2015; Caruso et al. 2021) in hopes that these

outplants prove more resilient over time. Here, we show that thermally tolerant genets do not always outperform their bleached conspecifics, whether due to trade-offs associated with thermal tolerance, complex fusion and fission growth pathways, or the confounding effects of local environmental factors. For example, we found that sites with a higher proportion of tolerant individuals were not necessarily sites with the highest survivorship (Table 4.1). *Montipora* at Ukumehame that survived the full timeseries were among the most bleaching susceptible, but had the highest survivorship compared to other sites. Conversely, surviving genets at Keawakapu and Molokini did not exhibit high rates of bleaching, but did show lower growth (*Porites* at Molokini; *Pocillopora* and *Montipora* at Keawakapu).

This disconnect holds important implications for coral restoration efforts, both in Hawai'i and elsewhere. Our findings demonstrate how sequential bleaching events shape coral communities, weeding out susceptible individuals and leaving behind a population with the demonstrated ability to survive thermal stress. These survivors now constitute the bulk of Maui's reef communities and could act as a source population for coral restoration efforts. Based on our results, restoration practitioners in Maui looking to obtain parent colonies for restoration projects should feel comfortable selecting any colony of *M. capitata, M. patula,* or *P. lobata,* provided that the colony is big enough to have reasonably recruited to the reef prior to 2015 and looks healthy (i.e., is not slowly declining as a result of past heat stress or other impacts). Our results do not support targeting specific phenotypes of *Montipora* or *Porites* based on perceived thermal resistance, since we observed growth and survivorship across a spectrum of phenotypes. The best available indicator of survivorship under future thermal stress is survivorship through past thermal stress events, which can be assumed for large colonies present on Maui's reefs today.

The one exception to this conclusion is *Pocillopora*. Given the low thermal tolerance and low survivorship we observed here, any restoration projects focused on *Pocillopora* should seek to identify and raise thermally tolerant strains or individuals, as they would have the best potential to survive future heat stress. However, based on survivorship rates observed here, it is likely that even thermally tolerant outplants of *Pocillopora* would have lower survivorship than outplants of more stress-tolerant taxa, such as *Porites*. Ultimately, the decision of which taxa to select for coral restoration depends on the ecological and social goals of the project (Bostrom-Einarsson et al. 2020; Hein et al. 2020). For instance, *Pocillopora* restoration could be used as a mechanism to boost recruitment or diversity on reefs where *Pocillopora* abundance has remained depressed following repeat bleaching. If the goal of restoration is simply to increase coral cover and persistence through future heat stress, *Porites* and *Montipora* are more advisable options.

5. Conclusions

Over seven years and two bleaching events of similar magnitude, coral populations in Maui demonstrated hallmarks of selection and resilience. While we did not find widespread support for reef-scale acclimatization, we did find evidence of possible acclimatization for individual genets, primarily in the massive coral *P. lobata*. We also document selection against thermally susceptible individuals, with implications for the overall diversity and future thermal tolerance of Maui's reefs. One important implication of selection is that bleaching and growth were largely decoupled for corals that survived repeated exposure to heat stress in Maui. The resilience of these survivors will no doubt be tested by future heatwaves. In the meantime, it will be important to the track colony-level patterns of bleaching, growth, and survivorship for multiple taxa (including those with fusion and fission dynamics) at broad ecological scales to understand geographic trends in coral acclimatization and selection. These efforts should harness

advances in large-area imaging and coral genetics to identify the underlying mechanisms responsible for acclimatization and the impact of selection on coral populations. This knowledge in turn can be used to improve projections of reef persistence under climate change, and inform decisions related to coral restoration.

6. Acknowledgements

Chapter 4, in part, has been submitted for publication of the material as it may appear in PLoS ONE, McCarthy, Orion S.; Winston, Morgan; Smith, Jennifer E., 2024. The dissertation author was the primary researcher and author of this paper.

We would like to thank the divers who helped conduct the large-area imagery surveys, including Anela Akiona, Donna Brown, Samantha Clements, Emily Kelly, Susan Kram, Travis Matteson, Melissa Torres, and Darla White. Special thanks to Emily Kelly for establishing this large-area imagery timeseries back in 2014. Field work would not have been possible without the support of local partners in Maui, including Ultimate Whale Watch, Dive Maui, Maui Divers, Lee James, Peter and Toni Colombo, Craig and Amy Venema, Don McLeish, Will and Megan Dailer, and George and Donna Brown. We would also like to thank undergraduate research volunteers Solomon Chang, Andre Lai, Veronika Pearson, Varun Sachin Shirhatti, and Victoria Vasquez for their tireless work assisting with tracing coral patches. We also thank Tom Oliver, Courtney Couch, and Mary Donovan, who provided input on project conception and initial results, and Adi Khen for designing the coral graphics used in our figures. Funding was provided to OM by the National Science Foundation, and to JES by the Scripps Family Foundation, the Bohn Family, and other generous donors.

Chapter 5 – Evaluating the predictive capacity of coral reef resilience assessments

Orion S. McCarthy, Eric Conklin, Katharine Ricke, Russell T. Sparks, and Jennifer E. Smith

Abstract

To maximize conservation impact in the 21st century, natural resource managers must consider local conservation efforts in the context of global climate change. One approach, termed resilience-based management, seeks to prioritize management of "resilient" locations where vulnerability to climate change is projected to be low. Resilience assessments, which use ecologic and anthropogenic indicators to predict future ecosystem resilience across a management jurisdiction, are used to prioritize resilient locations for site-specific management interventions, thereby promoting the persistence of locations with the best shot at surviving climate change. While resilience assessments have been widely applied to inform management, particularly for coral reefs, their precision and accuracy have rarely been validated. We used a timeseries of coral reef 3D models to 1) conduct resilience assessments at the same fixed sites in multiple years, and 2) track multi-scale metrics of resistance and recovery from a bleaching event over a decade. This allowed us to compare resilience predictions across assessments (precision) and test whether resilience predictions aligned with observed patterns of resistance and recovery (accuracy). We found that resilience assessments of coral reefs are capable of generating consistent resilience predictions over time, but that those predictions were not correlated with observed resistance or recovery dynamics. Our results reinforce the need to model resistance and recovery as distinct processes (rather than a single metric of "resilience") and to reevaluate the functional linkage between ecologic indicators and both resistance and

recovery. Where possible, practitioners should validate the accuracy of resilience assessment predictions with long-term monitoring. Functional indicators of resistance and recovery should be used to inform site-specific management interventions in concert with feedback from local stakeholders and communities.

1. Introduction

Coral reefs are ecologically and economically important ecosystems that face threats at multiple scales. On a global scale, climate change is expected to reduce the abundance and diversity of reef building corals via recurrent marine heat waves, ocean acidification and deoxygenation, stronger storms, and sea level rise (Hoegh-Guldberg et al. 2007; Anthony 2016; Hughes et al. 2017, 2020; van Woesik et al. 2022). Indeed, coral reefs have already been severely impacted by climate change in many parts of the tropics (Hughes et al. 2018; Eakin et al. 2019; Sully et al. 2019), and ocean temperatures have already risen by 0.9°C globally (van Hooidonk et al. 2016). On a local level, reefs are also impacted by natural and anthropogenic stressors including overfishing, coastal development, nutrient pollution, sedimentation, tourism, and outbreaks of coral disease and crown of thorns starfish (Donovan et al. 2021; Good & Bahr 2021; Andrello et al. 2022).

From a conservation perspective, it is imperative to address both local and global stressors to ensure continued coral reef functioning in the 21st century (Darling et al. 2019). Specifically, international action is required to reduce greenhouse gas emissions and prevent worst-case scenarios for coral reefs globally (van Hooidonk et al. 2016; IPCC 2021). However, natural resource managers have limited recourse for mitigating the threats posed by climate change (Anthony et al. 2015; Maynard et al. 2015) and typically focus on mitigating local threats to reefs in their jurisdiction, such as by imposing fishing regulations, establishing marine

protected areas, or reducing urban runoff (Topor et al. 2019; Donovan et al. 2021, 2023b; Gouezo et al. 2021; McLeod et al. 2021; Gove et al. 2023).

Due to limited financial and political resources, it is often impractical to reduce local impacts everywhere. Thus, resource managers typically prioritize specific locations for targeted conservation (Wilson & Law 2016). One widely-used approach for prioritizing coral reef conservation is resilience-based management, which seeks to ensure reef persistence by identifying "resilient" reefs and prioritizing their conservation with site-specific management interventions (Gibbs & West 2019; McLeod et al. 2021). In this context, reefs are considered "resilient" if they are better able to resist and recover from disturbance without shifting to a less desirable (non-coral dominated) state (Holling 1973; McClanahan et al. 2012). Locations with high resilience and low exposure to disturbance are considered to have lower vulnerability to climate change (Lam et al. 2020; Shockley 2023). Under resilience-based management, ecologic and anthropogenic indicators are used to predict reef vulnerability (a process known as a "resilience assessment"), and locations with low relative vulnerability are prioritized for management. Resilience-based management seeks to reduce local stressors so that resilient reefs are better positioned to endure global stressors (Harris et al. 2017; Lam et al. 2020).

The concept of resilience-based management was first proposed for coral reefs more than two decades ago (West & Salm 2003) and began to be operationalized via resilience assessments in the early 2010s (Obura & Grimsditch 2009; Maynard et al. 2010; McClanahan et al. 2012). Coral reef resilience assessments have since been conducted in more than 40 countries and territories (McLeod et al. 2021), spanning the Indian Ocean (Macharia et al. 2016; Manikandan et al. 2017; Cowburn et al. 2018), Coral Triangle (Maynard et al. 2012; Harris et al. 2017; Minsaris et al. 2019; Vo et al. 2019), Pacific (Knudby et al. 2013; Maynard et al. 2015, 2019;

Oliver et al. 2020; Bang et al. 2021), and Caribbean (Grimsditch et al. 2011; Ladd & Collado-Vides 2013; Maynard et al. 2014, 2017b). These assessments have been largely successful at informing site-specific management actions, due in part to the active participation of non-governmental organizations and government agencies (McLeod et al. 2021).

Despite the growing popularity of resilience-based management, a number of uncertainties exist about the efficacy of this approach. Most resilience assessments are conducted at a single point in time (Maynard et al. 2015; McLeod et al. 2021), and few studies exist that test the accuracy of resilience assessment predictions following major stress events (but see Minton et al. 2020; Bang et al. 2021). Furthermore, the relative importance of different resilience indicators (the variables used to calculate resilience), as well as their functional relationship to resilience, is not fully understood (McClanahan et al. 2012; Gibbs & West 2019; Minton et al. 2020; Bang et al. 2021). As a result, it is unclear how sensitive resilience assessments are to the choice of indicators or to their weighting, the methods used to assess indicators, or the year in which the assessment is conducted. These questions need to be resolved so that the effectiveness of this widely used conservation approach can be validated.

A rigorous evaluation of resilience assessment predictive capacity of is overdue. In this study, we used a decade-long timeseries of large-area imagery (3D coral reef models) to conduct multiple sequential resilience assessments of fixed sites in leeward Maui. We compared resilience predictions made with large-area imagery to resilience predictions made by Maynard et al. 2019, which used *in situ* surveys to conduct a resilience assessment at the same sites in Maui in 2018. This study represents the first time large-area imagery has been used to conduct a resilience assessment (McCarthy et al. 2023). Importantly, our large-area imagery timeseries also allowed us to quantify multi-scale metrics of benthic community resistance to and recovery from

a major bleaching event, which occurred one year after our timeseries began (our large-area imagery timeseries spans 2014 to 2023, and bleaching occurred in 2015; Sparks et al. 2015; Rosinski et al. 2017; Chung et al. 2019). This study design allowed us to answer the following questions: 1) are site-level predictions of resilience robust to differences in methodology and survey year; and 2) do resilience assessments accurately predict resistance and recovery? If resilience predictions vary considerably from year to year or between methods, or if they do not reflect observed patterns of resistance and recovery, their value as a spatial planning and conservation decision making tool would be diminished.

2. Methods

2.1 *In situ* 2018 resilience assessment

In March 2018, researchers from the Nature Conservancy and Hawai'i Division of Aquatic Resources surveyed seven indicators of reef resilience (Table 5.1) at 31 shallow (3-7m) and 20 deep (8-13m) sites in leeward Maui (hereafter referred to as the *in situ* survey). *In situ* survey methods are described in detail in Maynard et al. 2019. Briefly, divers assessed coral cover, coral diversity, and the ratio of calcifying to fleshy benthic cover (reef builder ratio) using 20 randomly selected 0.8 x 0.6 m photoquadrats collected along three 25m transects. They also conducted visual surveys of coral health and juvenile coral density within twelve 0.25m^2 quadrats, assessed linear rugosity using a 10m brass chain, and estimated the length and biomass of herbivorous fish within three 25 x 5m belt transects. The seven unweighted resilience indicators were normalized and used to calculate each site's relative resilience. The final result was a ranking of sites based on their predicted resilience, which informed the development of site-specific management recommendations (Maynard et al. 2019).

Table 5.1: A description of the ecological metrics used to conduct the 2018 resilience assessment in leeward Maui, adapted from Maynard et al. 2019. For this study, we omitted herbivorous fish biomass because that data was not captured in the large-area imagery timeseries.

Metric	Description	Functional linkage to resilience	Years surveyed
Coral cover	Percent of the benthos (%) occupied by living corals.	Corals provide many of a reef's ecosystem services, such habitat provisioning and wave attenuation. Higher coral cover is generally seen as an indicator of reef health.	2014 – 2023 (annually)
Reef builder ratio	Ratio of the percent cover of corals and calcifying algae to the percent cover of fleshy algae and other sessile invertebrates.	Corals and calcifying algae cement the reef together and provide settlement substrate for coral recruits. Reef builder ratio represents the balance between these calcifying organisms and non-calcifiers.	2014 – 2023 (annually)
Coral diversity	Simpsons diversity index for coral community (unitless, ranges from 0 to 1).	A more diverse assemblage of corals has higher functional redundancy and can provide more habitat niches for different reef organisms.	2014 – 2023 (annually)
Coral health	Percent (%) of colonies surveyed with signs of disease, bleaching, or algal overgrowth (inverted in this study to get % of healthy colonies)	Indicators of compromised coral health, such as disease, bleaching, and algal overgrowth, are signs that corals are facing chronic stress.	2014, 2015, 2017, 2019, 2021
Juvenile coral density	Density (#/m²) of colonies under 5cm in diameter (in this study, *Pocillopora* that were not detected in an earlier year).	Coral recruits represent a demographic influx of new individuals into the population. Coral recruitment is a mechanism for coral recovery after disturbance.	2014, 2015, 2017, 2019, 2021
Linear rugosity	Ratio of the distance traversed by the reef's contour to the distance traversed by a straight line. (unitless, lower bounded by 1).	Linear rugosity is a metric of 3D structural complexity. Habitats with more structural complexity can support a more diverse assemblage of fish and invertebrates.	2014 – 2023 (annually)
Herbivorous fish	The biomass (g/m²) of all herbivorous fish, calculated from fish lengths estimated by divers along belt transects.	Herbivorous fish eat algae that can overgrow and outcompete corals. Grazing by these fish help to preserve a balance between corals and algae on the reef.	NA

2.2 Large-area imagery timeseries

Researchers from the Scripps Institution of Oceanography began using large-area imagery to monitor coral reefs in leeward Maui in 2014, and have surveyed the same fixed 10 x 10 m sites annually, with the exception of 2020. Sites were surveyed twice in 2015, once in July (pre-bleaching) and once in November, coinciding with the peak of a major bleaching event (Sparks et al. 2015; Rosinski et al. 2017; Chung et al. 2019). Six large-area imagery sites are located closely to or directly overlap with sites used in the *in situ* 2018 resilience assessment

(Kahekili, Wahikuli, Olowalu, Ukumehame, Keawakapu, and Molokini; Figure 5.1A; Table S5.1): Those hardbottom forereef sites are the focus of this study and range between 4.5 and 10m depth.

To conduct large-area imagery surveys, divers relocated fixed monitoring sites with the aid of GPS coordinates, permanent stainless-steel stakes or eye-bolts, and a 2D photomosaic "site map" printed on underwater paper. Once the site was located, divers placed six calibration tiles and four floats to mark the edges of the fixed 10 x 10 m site, and placed four 0.5m scale bars within the site. One diver measured the depth of each calibration tile and, prior to 2016, the distance among calibration tiles in lieu of placing scale bars. The other diver swam approximately 1.5m above the substrate in a gridded pattern holding a custom rig equipped with two Nikon D7000 SLR cameras (except in 2023, where Nikon D780 SLRs were used) in Ikelite underwater housings. One camera was equipped with a wide-angle lens (18mm for 2014-2022, 24mm for 2023) and the other was equipped with a telephoto lens (55mm for 2014-2022, 60mm for 2023). Focal lengths were adjusted in 2023 to ensure that the spatial footprint of each photo was consistent between the D7000 and D780 cameras. Each camera was set with a 1 second interval timer, producing approximately 5,000 total photos per site. The camera diver swam several meters beyond the 10 x 10 m site boundary to ensure a buffer zone of imagery was collected.

Once imagery was collected, researchers used the software *Agisoft Metashape* (St. Petersburg, Russia) to align the 5,000 underwater images (hereafter referred to as raw images) and build a dense point cloud reconstruction of the benthos (hereafter referred to as the 3D model). Once the 3D model was constructed, researchers loaded it into *Viscore*, a custom data visualization and ecological analysis software developed at UC San Diego (Petrovic et al. 2014).

Using Viscore, researchers entered depth and scaling metadata collected in the field, color corrected imagery, and manually aligned 3D models of the same site collected in different years. These aligned timeseries of 3D models form the basis of ecological analysis conducted in this study.

2.3 Assessing resilience indicators using large-area imagery

For each site in each timepoint, we used our large-area imagery timeseries to assess six of the seven resilience indicators used by Maynard et al. 2019. Large-area imagery, also known as photogrammetry, has been shown to be reliable source of ecological data on coral cover, health, and demography, as well as 3D structural metrics, with accuracy comparable to or exceeding that of *in situ* surveys (Bryson et al. 2017; Burns et al. 2020; Couch et al. 2021; Urbina-Barreto et al. 2021). However, because large-area imagery only reconstructs static features of the benthos, we were not able to assess herbivorous fish biomass using our timeseries. To achieve consistency across datasets, we omitted herbivorous fish biomass as a resilience indicator and re-calculated resilience scores from Maynard et al. 2019 using the remaining six indicators: percent coral cover, reef builder ratio, coral diversity, juvenile coral density, coral health, and linear rugosity (Table 5.1).

We calculated the percent cover of benthic taxa using Viscore's virtual point intercept tool (VPI; Fox et al. 2019), which places a user-defined number of stratified random points (here 2,500) within a quadrat (here 10 x 10 m) in the coral reef 3D model. The user has access to the raw imagery that underlies the 3D model, which allows each VPI point to be viewed from multiple angles before a taxonomic ID is assigned. A single researcher with experience in Hawaiian benthic taxonomy (OM) identified the benthos under each VPI point to the lowest possible taxonomic resolution, and taxa were later assigned to one of 15 functional groups (seven

coral groups, six algal groups, one group of "other" sessile invertebrates (i.e., tunicates, sponges, or zoanthids), or sand; Figure S5.4). We used percent cover data to calculate three of our resilience indicators: percent coral cover, coral diversity (Simpsons diversity), and reef builder ratio (ratio of the percent cover of corals and calcifying algae to the percent cover of fleshy algae and other sessile invertebrates).

For juvenile coral surveys, we counted all *Pocillopora* colonies < 5cm in diameter within a 12 x 12 m plot, only including corals that had not been detected in a previous timestep. We chose not to include *Montipora* and *Porites* due to the difficulty of distinguishing true juveniles from partial mortality of larger colonies via benthic imagery. *Montipora* and *Porites* commonly undergo fission and fusion, which can make it difficult to distinguish colony boundaries after years of partial mortality and regrowth (McCarthy et al. *in prep.a*). *Pocillopora* have a more discrete shape, less partial mortality, and easily identifiable juveniles. While the 2018 *in situ* survey included juvenile *Montipora* and *Porites*, *in situ* coral recruit surveys are capable of achieving higher resolution than solely image-based approaches (Edmunds et al. 1998; Burgess et al. 2010). Focusing solely on *Pocillopora* in the large-area imagery surveys allowed us to have confidence in our image-based assessments of juvenile coral density.

To assess coral health, we surveyed corals for signs of severe bleaching, algal overgrowth, and coral disease. Corals that exhibited one or more of these conditions were considered to have compromised health. We surveyed each coral visually using the raw images that underly the 3D model. Our ability to access to multiple images of any given coral allowed us to account for apparent signs of compromised health (i.e., discoloration) that were an artifact of poor image quality or overexposure. We assessed the health of individual corals in four taxa (*Montipora capitata*, *Montipora patula*, *Pocillopora* spp., and *Porites lobata*) that we also

tracked for colony-scale analyses of resistance and recovery (see section 2.5.2). We calculated the prevalence of compromised health for each taxon and then calculated a single rate of compromised health for each site, weighting the four taxa equally. Maynard et al. 2019 used the percent of colonies with signs of compromised health as an indicator in their *in situ* 2018 resilience assessment and then inverted the normalized value so that high values would denote high resilience. Here, we simply used the percent of colonies without signs of compromised health as our resilience indicator, as has been done elsewhere (Gibbs & West 2019), and recalculated values from Maynard et al. 2019 accordingly.

Finally, we assessed linear rugosity using Viscore's virtual profile gauge tool (McCarthy et al. 2022), which measures the depth of the reef contour at a fixed interval (here every 1cm) along a series of linear transects (here 10m long). We calculated linear rugosity as the distance traversed by each reef contour divided by the linear distance traversed by each transect. For linear rugosity, a value of 1 corresponds to a completely flat surface, with increasing large values denoting increasingly rough surfaces with greater structural complexity (Risk 1972). We measured linear rugosity in the alongshore direction using 99 transects, each spaced 10cm apart, to cover the same spatial footprint as the $100m^2$ quadrat used to assess percent cover.

2.4 Predicting site resilience based on resilience indicators

We predicted site-level resilience based on six indicators (Table 5.1) following the approach of Maynard et al. 2019, which is consistent with other resilience assessments (Maynard et al. 2015; Harris et al. 2017; Gibbs & West 2019; Minton et al. 2020). We predicted resilience separately for each year where data was available for all indicators: five years of large-area imagery data (2014, 2015, 2017, 2019, and 2021), and one year of *in situ* data (2018). For each year, we normalized each resilience indicator by dividing by its maximum value. Following this

approach, the “best performing” site for a given indicator would have a normalized value of 1, and normalized values of lower performing sites would represent a decimal percentage relative to the best performing site. We calculated the unweighted average of the six normalized indicators to generate a resilience score for each site. Finally, we normalized resilience scores to calculate each site’s relative resilience, where the site predicted to be most resilient had a value of 1. To examine the temporal variability of resilience predictions and the relative influence of different resilience indicators, we performed a canonical analysis of principal coordinates (CAP; Anderson & Willis 2003) using the Euclidean distance matrix of normalized resilience indicators for all sites in all years (Maynard et al. 2015, 2019; Figure 5.2).

2.5 Quantifying observed patterns of resistance and recovery

To validate the predictive accuracy of our resilience assessments, we quantified resistance and recovery over our timeseries with respect to the 2015 bleaching event (Table 5.2). We used both community- and colony-scale data to quantify resistance and recovery, as has been done elsewhere (Minton et al. 2020). Tracking benthic dynamics within fixed $100m^2$ sites enabled us to quantify patterns of succession over a decade and account for the influence of both corals and algae on change in community structure. Tracking the fate of individual corals representing four key reef-building taxa allowed us to track changes in population demographics across our six sites. This multi-scale approach allowed us to account for important processes underlying resistance and recovery that may only be evident at a given range of scales (Hatcher et al. 1987; Mumby et al. 2014a; Donovan et al. 2023a). For example, a shift from fleshy to calcifying algae dominance would indicate important shifts in nutrient input or herbivory (Littler, Mark M., Littler 1984; Smith et al. 2010) and would be more readily detected at the community scale. Conversely, a pulse in coral recruitment would indicate population fecundity and future

coral growth, and would be more readily detected at the colony scale (Bramanti et al. 2015; Brito-Millán et al. 2019a; Edmunds & Riegl 2020). Importantly, all of our metrics of resistance and recovery (at both scales) were integrated over time, which contrasts to the indicators used in the resilience assessment (Table 5.1), which were measured at a single point in time.

Table 5.2: Metrics used to quantify patterns of resistance and recovery observed in response to a major bleaching event (2015). Multiple metrics were used to capture resistance and recovery dynamics observed at different scales (community scale and colony scale). Patterns of bleaching susceptibility, coral growth, and coral survivorship are sourced from McCarthy et al. *in prep.a.* (denoted by *).

	Scale	Metric	Description	Timeframe
Resistance	Community	Similarity	**Similarity of pre- and post-bleaching benthic community** (high similarity = high resistance)	2015 – 2016
	Community	Coral cover	**Percent of pre-bleaching coral cover lost 1 yr post-bleaching** (low coral cover loss = high resistance)	2015 – 2016
	Colony	Size frequency distribution	**Shift in colony size frequency distribution following bleaching** (no shift toward smaller colonies = high resistance)	2014 – 2017
	Colony*	Bleaching susceptibility	**Proportion of colonies that exhibited signs of thermal tolerance or acclimatization between 2015 and 2019 bleaching events** (more thermally tolerant or acclimatized colonies = high resistance)	2014 – 2021
	Colony*	Coral survivorship	**Probability of colony survival as a function of initial colony size** (high survivorship = high resistance)	2014 – 2021
Recovery	Community	Similarity	**Annual rate of change in similarity between pre- and post-bleaching communities** (increasing similarity to pre-bleaching comm. over time = high recovery)	2016 – 2023
	Community	Coral cover	**Percent of pre-bleaching coral cover regained annually** (increasing coral cover over time = high recovery)	2016 – 2023
	Colony	Size frequency distribution	**Shift in colony size frequency distribution 2 to 6 yrs post-bleaching** (shift toward pre-bleaching distribution = high recovery)	2017 – 2021
	Colony*	Coral growth	**Change in colony area over 7 yrs** (more coral growth = high recovery)	2014 – 2021

2.5.1 Community-scale indicators of resistance and recovery

Following the approach of McCarthy et al. *in prep.b*, we quantified benthic community composition using multivariate data collected from 3D coral reef models. Multivariate data consisted of percent cover of benthic taxa (7 coral taxa, 6 algal functional groups, sand, and other sessile invertebrates; Figure S5.4), structural complexity (linear rugosity at 1cm and 50 cm resolution and fractal dimension), and landscape heterogeneity (proportion of unlike adjacencies, derived from percent cover data). Using this multivariate data for our six focal sites across ten years of sampling, we calculated the Bray-Curtis dissimilarity matrix and used non-metric multidimensional scaling (NMDS) to visualize successional trajectories for each site (Figure S5.5). We included benthic community data from 30 other sites in Maui Nui (surveyed in 2021) in our NMDS so that successional trajectories could be interpreted within a broader regional context.

To quantify community-scale patterns of resistance and recovery for each site (Table 5.2), we calculated the similarity in community composition between the last pre-bleaching survey (July 2015) and each post-bleaching survey (November 2016 through July 2023). Similarity is the inverse of dissimilarity, which we calculated using the Bray-Curtis index via the vegan package in R (Oksanen et al. 2022). We quantified resistance as the similarity between the last pre-bleaching survey (July 2015) and the first post-bleaching survey (November 2016), with high similarity indicating high resistance to bleaching impacts (Donohue et al. 2016; Lemoine 2021). To quantify recovery, we calculated the slope of the best fit line through similarity values from 2016 to 2023, where a positive slope indicated that community composition became more similar to the pre-disturbance community over time (Graham et al. 2015). We also quantified resistance and recovery for each site based on changes in coral cover over time, since percent

coral cover is a widely used metric of coral reef health with direct relevance to resource managers (McClanahan et al. 2012; Ford et al. 2018). Here we quantified resistance as the percent of pre-bleaching coral cover that had been lost one-year post-bleaching. For recovery, we calculated the annual rate of coral cover change from 2016 to 2023, and interpreted a positive slope as an indicator of coral recovery (Lam et al. 2017; Cresswell et al. 2023; Gove et al. 2023). Finally, to account for minor differences in thermal exposure among sites (McCarthy et al. *in prep.a*), we standardized rates of resistance and recovery by the maximum degree heating weeks each site experienced in 2015.

2.5.2 Colony-scale indicators of resistance and recovery

For our colony scale analysis, we quantified the size-frequency distribution of four coral taxa (*M. capitata, M. patula, Pocillopora* spp., and *P. lobata*) to track demographic shifts in coral populations in response to the 2015 bleaching event. To do this, we traced the boundaries of corals using 2D orthoprojections of 3D coral reef models following the approach of Rodriguez et al. 2021. We used the freeware semantic segmentation platform TagLab (Pavoni et al. 2021b) to trace coral boundaries and link corals through time that represented the same individual. Since corals can split into multiple independent ramets via partial mortality (fission), which can later regrow back into a single colony (fusion), we considered all patches of live coral tissue linked in time via fission and fusion to represent a single "genet" and calculated size frequency distributions for coral genets, rather than coral patches, as has been done elsewhere (Winston et al. *in prep*; Sandin et al. 2020; Rodriguez et al. 2021).

To achieve an appropriate sample size of genets, we traced corals within 10 randomly placed 0.5m^2 quadrats. We increased the number of quadrats for less abundant taxa until we reached a minimum sample size of 40 genets or had placed 25 quadrats. We traced all genets that

had at least one patch of live coral tissue > 5 cm diameter with a centroid inside a quadrat. If a genet was traced in one year, we searched for it in other years and traced all associated patches, even if they were smaller than our 5cm diameter cutoff or located outside of a quadrat. We summed the planar area of interconnected patches to calculate the planar area (cm^2) of each genet in each year, and then log transformed the planar area to generate a size frequency distribution of coral genets for each taxa at each site (Bak & Meesters 1998; Rodriguez et al. 2021). We used 2-sample Kolmogorov-Smirnov (K-S) tests to identify significant shifts in size frequency distributions between 2014 – 2017 and 2017 – 2021 for each taxon at each site. We interpreted a significant decline in coral size-frequency from 2014 – 2017 as evidence of partial mortality and low resistance to bleaching, and considered a significant increase in coral size frequency from 2017 – 2021 as evidence of recovery (Table 5.2). In addition to size frequency distributions, we utilized rates of bleaching susceptibility, survivorship, and growth documented by McCarthy et al. *in prep.a* at these same sites. We considered sites with higher proportions of thermally tolerant or acclimatized corals and sites with significantly higher survivorship to have higher resistance, and sites with significantly higher growth rates to have higher recovery (Table 5.2).

2.5.3 Ranking sites based on community- and colony-scale patterns of resistance and recovery

We compiled our disparate community and colony scale metrics into a composite ranking of resistance (Figure 5.1B) and recovery (Figure 5.1C). For each metric, we assigned the best performing sites a value of 1 and the worst performing sites a value of -1. For community scale metrics, we considered sites > 1 standard deviation from the mean (for resistance) or from 0 (for recovery) to be best (+1 SD) or worst (-1 SD) performing. For colony scale metrics, we considered sites with significantly higher rates of thermal tolerance, survivorship, growth, or a

significant size frequency shift back toward their pre-disturbance distribution to be best performing, and those with significantly higher rates of bleaching, mortality, shrinkage, or a significant size frequency shift away from their pre-disturbance distribution to be worst performing. Sites that did not qualify as best or worst performing for a given metric were coded as 0. Once all metrics were coded as -1, 0, or 1, we calculated the mean value of resistance and recovery for each site, weighting of community and colony scale metrics so that each scale accounted for 50% of the final resistance and recovery ranking. Finally, we regressed site resistance and recovery rankings by predicted resilience rankings for each year that a resilience assessment was conducted (Figure S5.2) to evaluate the predictive accuracy of resilience assessments for our six sites in leeward Maui.

3. Results and Discussion

To be effective, resilience assessments need to be both precise and accurate: relative resilience rankings must be consistent so that the same locations are prioritized regardless of the sampling methodology used or year surveyed, and resilience rankings must accurately predict ecosystem resistance and recovery potential. Our ability to conduct multiple resilience assessments and extract multi-scale metrics of resistance and recovery from a large-area imagery timeseries allowed us to quantify the precision and accuracy of the resilience assessment methodology. Overall, we found that resilience assessments are capable of producing precise rankings of relative resilience, but that these rankings did not accurately predict observed resistance and recovery for our sites in leeward Maui.

3.1 High precision of resilience assessment predictions

While the relative resilience of our sites exhibited minor fluctuations through time, certain sites were consistently predicted to have high (Molokini) or low (Wahikuli) relative

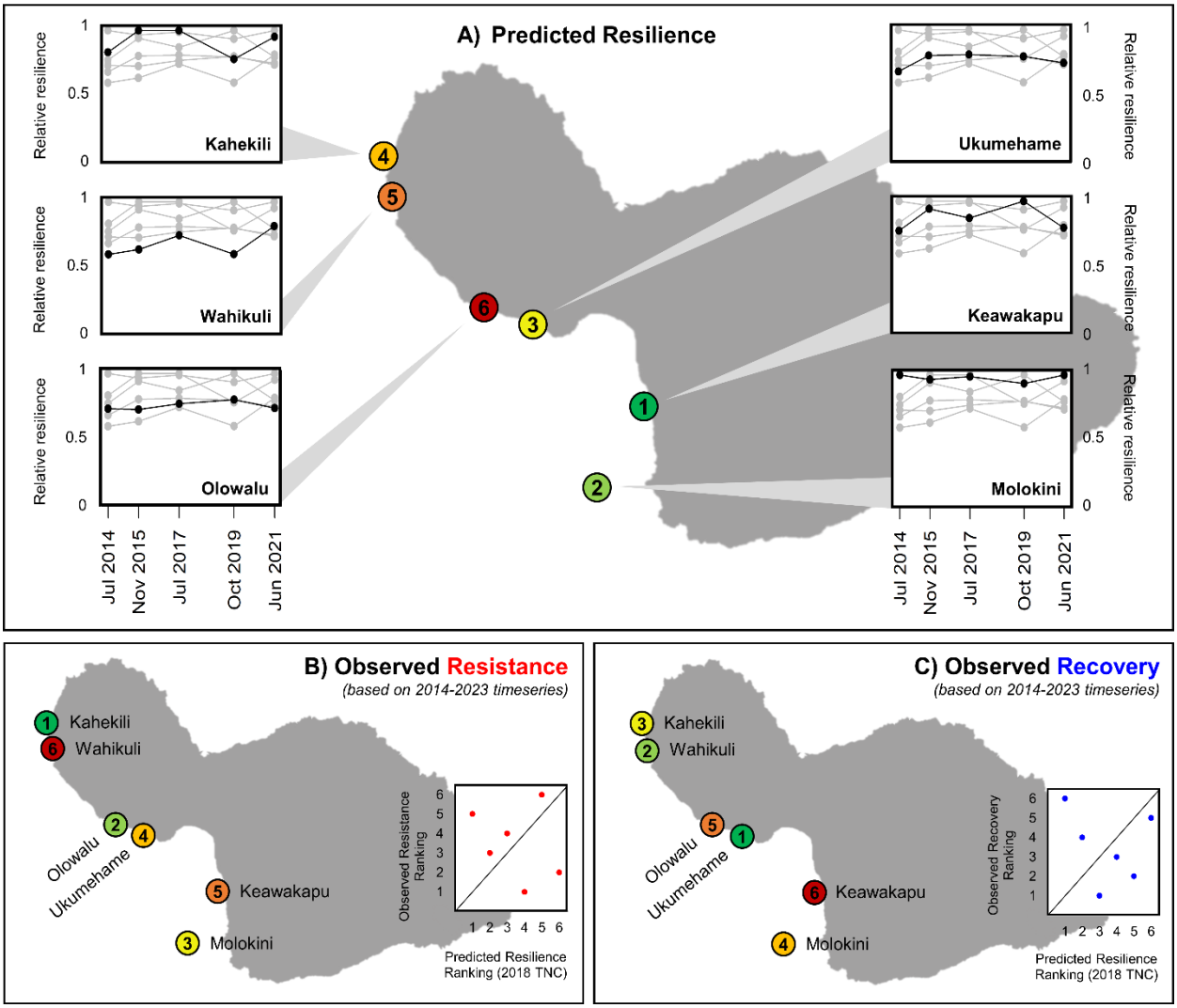

Figure 5.1: A) A map of the six resilience assessment sites in leeward Maui. Sites are symbolized by their relative resilience, as predicted by Maynard et al. 2019 (1 = highest resilience relative to other sites, 6 = lowest resilience). Inset plots in A) show the relative resilience of each site over time as predicted using large-area imagery collected in 2014, 2015, 2017, 2019, and 2021. The predicted resilience of each site fluctuated over time, although certain sites were consistently predicted to have high resilience (Molokini) or low resilience (Wahikuli). Predicted resilience (A) contrasted with observed patterns of B) resistance and C) recovery over the duration of the timeseries (2014-2023). Resistance and recovery were quantified in response to the 2015 bleaching event (see Table 2). Inset plots in B) and C) show the relationship between predicted resilience (from the *in situ* 2018 assessment) and observed resistance and recovery. Site-level trends in resistance and recovery are shown in detail in Figures 3 and 4.

resilience (Figure 5.1A). Kahekili and Keawakapu were also predicted to have high relative resilience, but exhibited more fluctuation in their resilience scores over time than Molokini, whereas Olowalu and Ukumehame were predicted to have moderate to low resilience but typically performed better than Wahikuli. The minor fluctuations we observe are consistent with other sensitivity analyses of resilience assessments, which have found that applying different weighting schemes to resilience indicators disproportionately impacts the rank order of mid-tier sites, whereas high or low resilience sites are predicted more consistently (Gibbs & West 2019; Minton et al. 2020). The precision of resilience rankings over time is not entirely unexpected for Maui, given that benthic community composition in Maui Nui has been shown to be temporally stable since at least 2017 (McCarthy et al. *in prep.b*). Indeed, the successional trajectories of our sites did not overlap and occupy unique regions of multidimensional space (Figure S5.5), which suggests that spatial variability in community composition is greater than temporal variability at the scale of our study. We might expect to see decreased temporal precision in resilience scores in less stable reef systems, or if resilience was quantified at a different scale (Donovan et al. 2023a).

Our CAP analysis (Figure 5.2) revealed that sites were consistently associated with particular resilience indicators regardless of survey year or methodology (*in situ* vs. large-area imaging). This was especially true for Molokini, which was characterized by high coral cover and calcifying cover relative to other sites, and Keawakapu, which was characterized by high rugosity and coral diversity relative to other sites. Importantly, not all indicators contributed to resilience scores equally. Juvenile coral density and reef builder ratio had the greatest variability among sites, meaning those indicators disproportionately influenced resilience scores, whereas rugosity, coral health, and coral diversity had the lowest variability among sites (Figure S5.1).

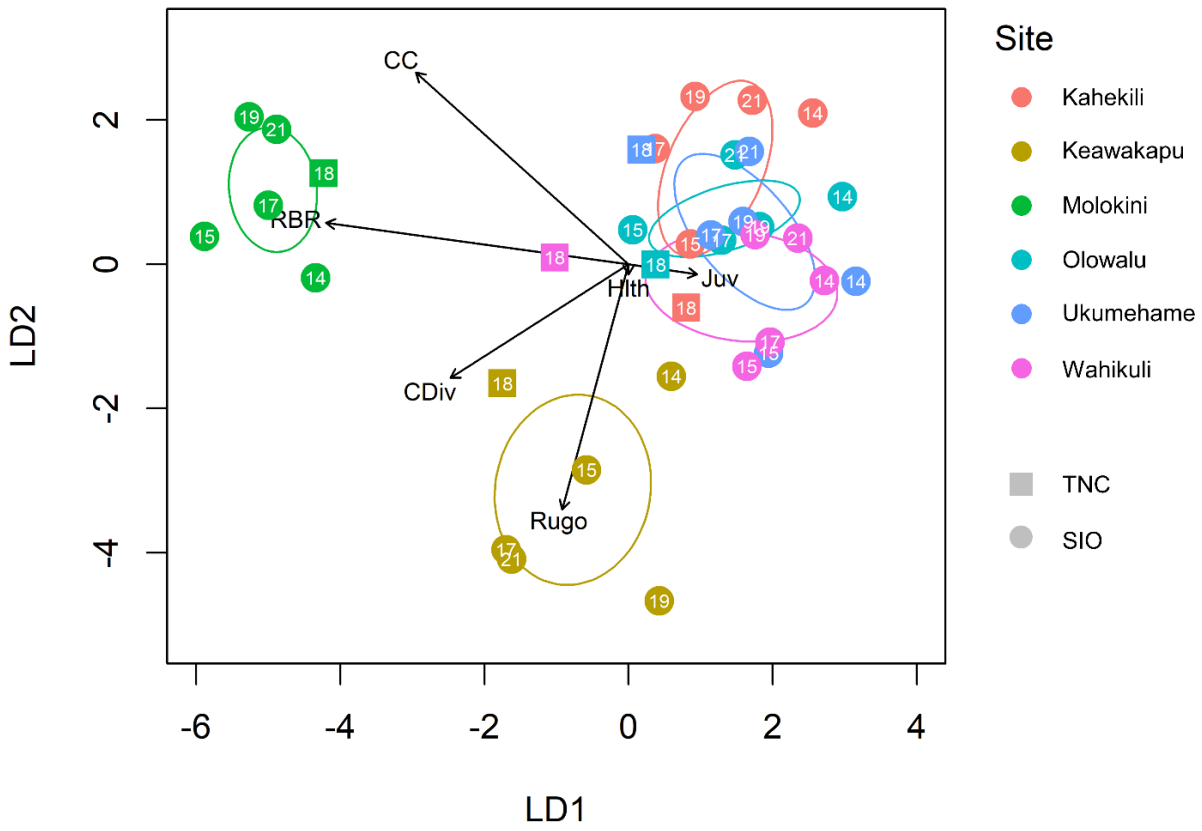

Figure 5.2: Canonical Analysis of Principal Coordinates (CAP) ordination showing the relative contribution of the six resilience indicators (arrows) to resilience scores. Sites are color-coded, and the number inside each point corresponds to the year of the survey. Ellipses show the standard deviation of resilience scores for each site. Point shape indicates the organization that conducted the resilience assessment (square for *in situ* surveys conducted by the Nature Conservancy, circle for large-area imagery surveys conducted by the Scripps Institution of Oceanography). Resilience indicator abbreviations are as follows: CC = coral cover, RBR = reef builder ratio, CDiv = coral diversity, Hlth = coral health, Juv = juvenile coral density, Rugo = linear rugosity.

Variability in juvenile coral density was driven by exceptionally low densities at certain sites, including a complete lack of juveniles detected in 2021 at four of the six sites. While this was due in part to our ability to detect only *Pocillopora* juveniles, other assessments of juvenile corals in Hawai'i, including the *in situ* 2018 assessment at these same sites, have found high spatial variability in juvenile coral density despite looking across multiple taxa (Figure S5.1; Maynard et al. 2019; Minton et al. 2020; Couch et al. 2023). Counterintuitively, Kahekili had the highest juvenile coral density in four of the six years surveyed, despite a high abundance of

fleshy macroalgae and cyanobacteria, which hinder coral recruitment (Vermeij 2005; Kuffner et al. 2006; Barott et al. 2012; Smith et al. 2022b). *Pocillopora* at Kahekili have been previously shown to have more bleaching resistance and higher survivorship compared to elsewhere in Maui (Figure 5.4E; McCarthy et al. *in prep.a*), so it's possible that self-seeding by this population could drive the relatively robust recruitment observed here.

3.2 Low accuracy of resilience assessment predictions

We found little correlation between predicted resilience and observed patterns of resistance or recovery for our sites in leeward Maui (Figure 5.1BC, Figure S5.2). The biggest deviation from expectations was Keawakapu, which was predicted to be the most resilient site by the *in situ* assessment. Over our timeseries, this site demonstrated the second lowest resistance and lowest recovery of all sites, driven by partial mortality and low survivorship across the four coral taxa studied (Figure 5.4). Coral cover at Keawakapu dropped from a pre-bleaching high of 55.08% to 37.83% one-year post-bleaching and has continued to decline, reaching 28.23% in 2023 (Figure 5.3B). This represents the largest decline in coral cover across our sites. Furthermore, this site appears to be undergoing a shift in community composition away from *Montipora* toward crustose coralline algae (Figure S5.4, Figure S5.5). The cause of this shift is unclear, although we observed similar declines in *Montipora* at other monitoring sites in leeward Maui not included in this study. At these other sites, anecdotal reports of coral predation by *Acanthaster* spp. (crown of thorns starfish; COTS) have been invoked to explain *Montipora* declines, since COTS have been documented to prefer feeding on *Montipora* over *Porites* (Sparks et al. 2015). However, we did not observe any COTS at Keawakapu during our surveys. We did observe high densities of urchins, and herbivory by urchins could explain the dominance of crustose coralline algae at this site (Lewis & Smith 2019). Boring by urchins, combined with

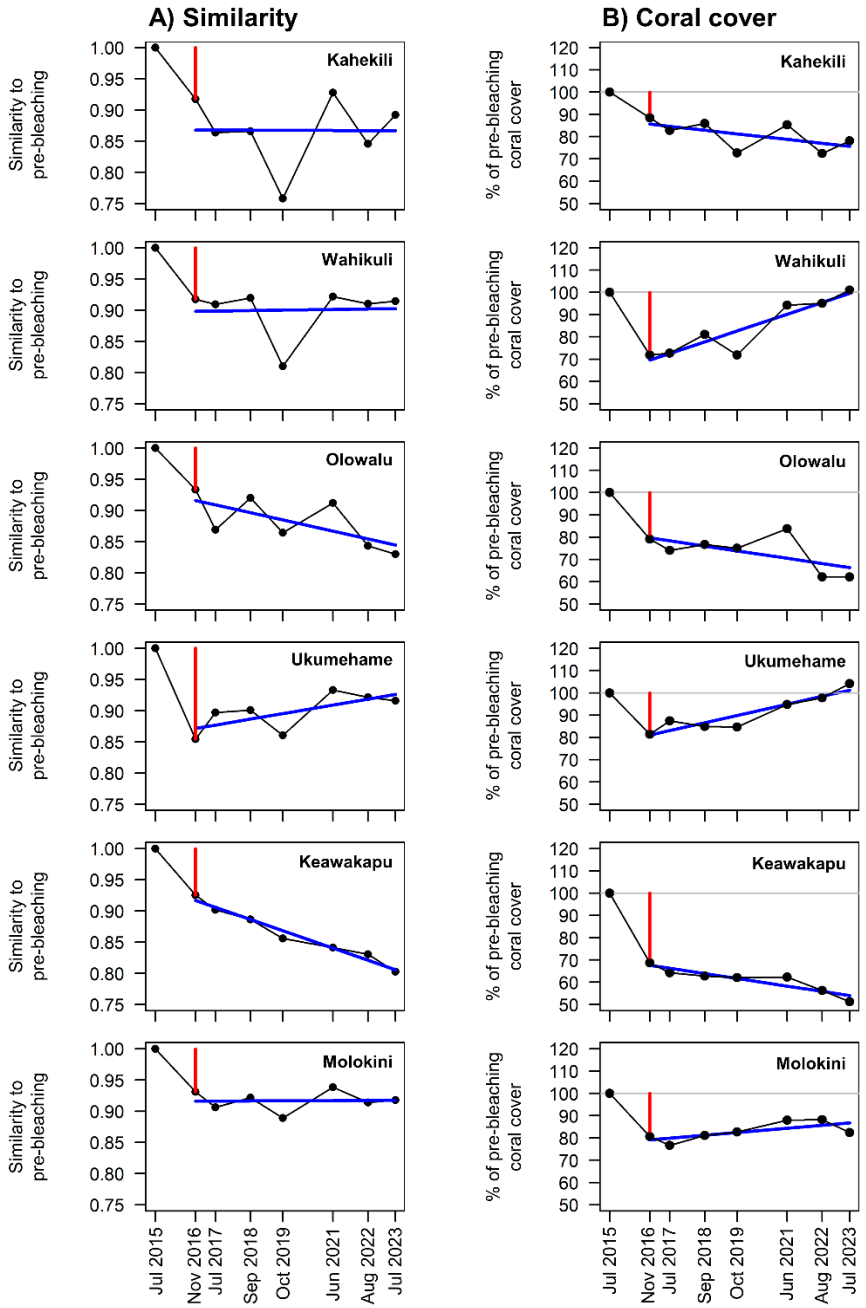

Figure 5.3: Community-scale resistance (red) and recovery (blue) from the 2015 bleaching event for six sites in leeward Maui. Graphs show A) the similarity between the pre-bleaching benthic community and the benthic community in subsequent years, and B) coral cover as the percent of pre-bleaching cover in July 2015. Resistance to disturbance, denoted by the red vertical line, is quantified as A) the similarity between the pre-bleaching (July 2015) and post-bleaching (November 2016) community, and B) the change in coral cover from July 2015 to November 2016. Low similarity and large declines in coral cover indicate that a site has low resistance. Recovery from disturbance, denoted by the blue line of best fit, is quantified as the annual rate of change in A) similarity and B) coral cover. A positive slope indicates that a site is regaining coral cover and returning toward its initial community composition, while a negative slope indicates continued decline.

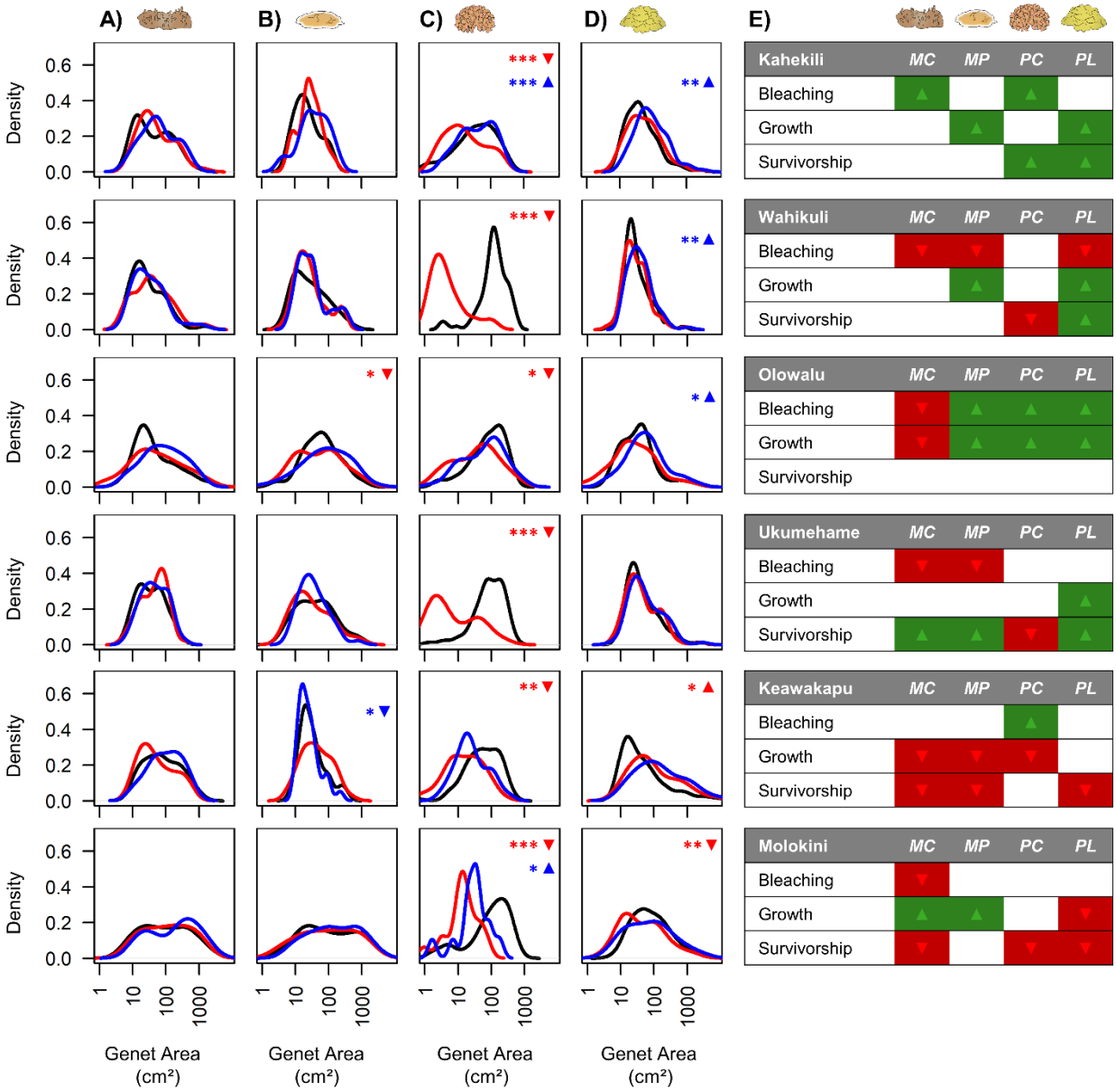

Figure 5.4: Colony-scale resistance and recovery from the 2015 bleaching event for six sites in leeward Maui. For each site, coral size frequency distributions are shown for A) *Montipora capitata*, B) *Montipora patula*, C) *Pocillopora* spp., and D) *Porites lobata* in 2014 (black, pre-bleaching), 2017 (red, 2 years post-bleaching), and 2021 (blue, 6 years post-bleaching). Asterisks denote significant change in a population's size frequency distribution from 2014 to 2017 (red) or 2017 to 2021 (blue), while arrows indicate the direction of the change (see Table S2 for p values). Size frequency distributions for *Pocillopora* in 2021 are omitted for Ukumehame and Wahikuli due to a small sample size (n < 10). E) Patterns of bleaching susceptibility, growth, and survivorship are shown for each taxon at each site, adapted from McCarthy et al. *in prep.a*. Green indicates sites with significantly higher rates of thermal tolerance/acclimatization, growth, or survivorship compared to other sites, while red indicates sites with significantly lower rates, and blank cells indicate no significant difference. Abbreviations correspond to the taxa in A-D: MC = *M. capitata*, MP = *M. patula*, PC = *Pocillopora*, and PL = *P. lobata*.

anthropogenic nutrient pollution, could also contribute to bioerosion of the reef, which could explain the slow and persistent decline in coral cover we observed (Vermeij et al. 2010; Prouty et al. 2017). However, despite tracking multiple metrics of resistance and recovery at high spatial resolution, we are unable to definitively identify a mechanism for the coral decline observed at Keawakapu.

In contrast to Keawakapu, some sites were predicted to have low resilience but showed strong recovery potential. While Wahikuli showed low resistance to bleaching and experienced a sizeable decline in coral cover from 2015 (42.78%) to 2016 (30.77%), coral cover rebounded and even exceeded pre-bleaching cover by 2023 (43.19%; Figure 5.3B). Ukumehame also showed strong recovery, with an overall increase in coral cover over our timeseries (43.72% in 2014 to 48.39% in 2023). Recovery at Wahikuli was driven by growth and survivorship of *P. lobata*, while high survivorship of both *Montipora* and *Porites* drove recovery at Ukumehame (Figure 5.4). Both Ukumehame and Wahikuli share similar community composition (Figure S5.4) and resilience indicator scores (Figure 5.2), and are dominated by the stress-tolerant coral *P. lobata*. Other reefs dominated by *P. lobata* in the broader Maui Nui region have also shown recovery potential in recent years, more so than sites dominated by *Porites compressa* or *M. capitata* (McCarthy et al. *in prep.b*). Taken together, this suggests that abundance of *P. lobata* might be a useful indicator of recovery potential for reefs in Maui.

Benthic communities at Kahekili and Olowalu showed higher resistance to bleaching than predicted, driven by a high proportion of thermally tolerant and acclimatized corals. At Kahekili, resistance was further supported by high coral survivorship. This resistance is notable because Kahekili has struggled with periodic algae blooms and elevated anthropogenic wastewater input for decades (Smith et al. 2005; Dailer et al. 2010), which have been

documented to negatively impact Kahekili's corals (Ross et al. 2012). In response to these stressors, the state created the Kahekili Herbivorous Fisheries Management Area in 2009 to promote herbivory and control algae growth (Williams et al. 2016). This management could help explain the resistance we observe. Still, even with management to support herbivorous fish, Kahekili still has higher abundance of macroalgae and cyanobacteria than elsewhere in Maui (Brown 2019), factors that have been shown to be negatively associated with resistance and recovery (Done 1992; Kuffner et al. 2006; Hughes et al. 2007; Donovan et al. 2021).

3.3 What is driving the disconnect between resilience assessment predictions and observed patterns of resistance and recovery?

This is not the first study to document a resilience assessment with low predictive accuracy. A retrospective analysis of a resilience assessment from west Hawai'i island found no correlation between resilience predictions and reef resistance (quantified as change in coral abundance from 2015 to 2016, as well as bleaching prevalence) or recovery (quantified as change in coral abundance from 2016 to 2019) (Minton et al. 2020). Using multiple metrics of resistance and recovery (Table 5.2), our results corroborate those of Minton et al. 2020 and highlight the limitations of the resilience assessment methodology. Here we discuss three potential explanations for the lack of concordance between resilience predictions and observed patterns of resistance and recovery: 1) resistance and recovery need to be modeled separately, 2) different or additional resilience indicators need to be used, and 3) our current resilience indicators need to be interpreted differently.

To the first point, an ecosystem's capacity to resist and recover from disturbance are controlled by fundamentally different processes (West & Salm 2003; Côté & Darling 2010; Donohue et al. 2013; Hodgson et al. 2015). For example, stress-tolerant taxa within a community are often better positioned to survive disturbance events, while community recovery may be

driven primarily by faster growing or more fecund taxa (Turner et al. 1998; Darling et al. 2013; Pulsford et al. 2014). This disconnect was apparent for our sites in leeward Maui, as site rankings of resistance and recovery were not correlated ($r = -0.143$). Choosing indicators that are functionally linked to either resistance or recovery could help improve future resilience assessments (McClanahan et al. 2012). While some studies have taken this approach, it is still common practice to combine separate resistance and recovery indicators to generate a single resilience score (Nunes et al. 2022; Moritsch & Foley 2023). We argue that collapsing resistance and recovery into a single metric of resilience reduces assessment interpretability and utility for informing management. Modeling resistance and recovery separately could help to differentiate sites like Olowalu (high resistance, low recovery) and Wahikuli (low resistance, high recovery), which likely require different management interventions.

Second, it is possible that different indicators would have produced more accurate resilience predictions. It is worth noting that there is robust empirical support for the resilience indicators used here (Obura & Grimsditch 2009; McClanahan et al. 2012; Maynard et al. 2017a), which have been applied widely in other resilience assessments (Knudby et al. 2013; Maynard et al. 2015, 2017b; Harris et al. 2017; Minsaris et al. 2019; Minton et al. 2020). Furthermore, Maynard et al. 2019 customized their selection of resilience indicators to reflect local context, eschewing commonly used indicators (i.e., macroalgae abundance, thermal variability) because they displayed little meaningful variation across their sites in leeward Maui. Still, even the empirically supported indicators used here poorly predicted both resistance and recovery. While coral cover and coral health were moderately correlated with resistance, no other indicators were positively related to resistance or recovery (Figure S5.3). Other indicators not measured here, such as herbivorous fish biomass, coral predation scars, or the abundance of thermally tolerant

corals, could have been better predictors. In general, indicators associated with reef function, such as recruitment or herbivory, have been shown to better predict community response to both disturbance and management than indicators without a functional connection (Mouillot et al. 2013; Ford et al. 2018). However, others have cautioned against including too many indicators in resilience assessments, following the assumption that reef resilience is controlled by a small number of influential processes (McClanahan et al. 2012) and that including extraneous indicators dampens the signal of meaningful ones (Maynard et al. 2010; Bang et al. 2021). The relationship between indicators also needs to be considered. Including multiple indicators of the same reef process will bias resilience predictions toward that process. In that vein, others have argued against including anthropogenic stressors (i.e., sedimentation, nutrient input) as indicators, since the impact of these stressors should be already reflected by ecologic indicators (Bang et al. 2021).

Finally, the poor predictive accuracy of our resilience assessment could stem from our interpretation of the resilience indicators used here. Assigning a value judgement to indicators, where high normalized values denote low vulnerability to disturbance, assumes a unidirectional relationship between reef processes and resilience that may be overly simplistic (Mumby et al. 2014b; Anthony et al. 2015; Ford et al. 2018; Lam et al. 2020). Shifts in species composition and competitive dynamics caused by chronic degradation can decouple expected relationships between environmental drivers and reef performance (Williams et al. 2015). In some instances, human-impacted reefs have been shown to be more stable (McCarthy et al. *in prep.b*; Gross & Edmunds 2015) or exhibit faster recovery following disturbance (Cresswell et al. 2023; Gove et al. 2023) than more pristine reefs. The reasons for this disconnect are multifaceted, and can be attributed partially to the effect of disturbance on benthic competition (Mouillot et al. 2013;

George et al. 2021), selection for stress-tolerant individuals (Darling et al. 2013; Camp et al. 2018), and complex or antagonistic interactions between sequential disturbances (i.e., a bleaching event followed by a COTS outbreak). In this study, we found a moderate negative correlation between recovery and several resilience indicators (rugosity, coral health, and reef builder ratio; Figure S5.3), which suggests that sites exhibiting signs of degradation are actually showing greater recovery capacity than more pristine sites. Stress tolerant corals like *P. lobata* may have a competitive advantage at sites with high human impact, and may be better able to persist and recover following bleaching (Darling et al. 2012; Kayal et al. 2015). This notion of increased resilience with increasing degradation has been proposed previously for coral reefs (Côté & Darling 2010) and other ecosystems (Grman et al. 2010). We do not suggest that more degraded communities are preferable to pristine ones. While degraded communities might exhibit more stability, the chronic removal of sensitive taxa represents a loss of functional diversity that can diminish provisioning of ecosystem services (Villéger et al. 2010; Alvarez-Filip et al. 2011b; González-Barrios et al. 2023). Rather, we suggest that degraded communities exhibit potential for resilience and should not be overlooked in a management context (Donohue et al. 2016).

3.4 Management implications

Resilience-based management aims to 1) identify "resilient" reefs with low vulnerability to climate change so that more resilient locations can be prioritized for management; and 2) inform site-specific management interventions to ensure the persistence of priority reefs (Gibbs & West 2019; McLeod et al. 2019, 2021). In regards to the first aim, we find that the resilience assessment methodology, when used in isolation, is unlikely to be effective at prioritizing sites for conservation, given the low predictive accuracy of this and other resilience assessments

(Minton et al. 2020). In circumstances where resilience assessments are planned (or have already been applied) to prioritize management, we strongly recommend that practitioners continue monitoring functional indicators of resistance and recovery to validate the accuracy of resilience predictions.

In regards to the second aim, we maintain that resilience assessments have immense potential to support site-specific management, particularly by identifying the ecological mechanisms responsible for resistance and recovery. For instance, a reef experiencing protracted coral decline (such as Keawakapu) could be suffering from suppressed herbivory, elevated nutrients, or outbreaks of coral predators, each of which would prompt a different management response (fisheries regulations, land-based pollution remediation, and predator removal, respectively). Functional indicators of resistance and recovery can help managers identify the right interventions for a given site (National Academies of Sciences 2019; Winter et al. 2020) and distinguish between manageable vs. unmanageable stressors (Anthony et al. 2015; Harris et al. 2017). Resilience assessments have been used extensively in this regard. A global analysis of coral reef resilience assessments found that more than half resulted in management actions (McLeod et al. 2021), including marine spatial planning (Knudby et al. 2013; Ladd & Collado-Vides 2013; Cowburn et al. 2018), fisheries management (Grimsditch et al. 2011; Maynard et al. 2012), and restoration (Maynard et al. 2014). When ecological indicators are combined with social indicators, resilience assessments can be used to manage reefs as interconnected socio-ecological systems (Weeks & Jupiter 2013; Oliver et al. 2020).

To reconcile the two aims of resilience assessments, we suggest that managers rely on input from local communities to identify priority locations for management. Once priority locations for management have been identified, managers should work with communities to

customize management interventions based on site-level indicators of resistance and recovery. Such an approach would more equitable and defensible than an approach based on ecological indicators alone (Thiault et al. 2019; Winter et al. 2020; González-Espinosa et al. 2023). Such an approach will require more engagement of local stakeholders at multiple points in the management process, a step that has been recommended previously as an avenue for improving resilience-based management (Maynard et al. 2015; McLeod et al. 2021).

3.5 Limitations and future directions

This study represents the first time large-area imagery has been applied to conduct a resilience assessment, and is one of the only studies to evaluate resilience assessment precision across multiple years and methodologies (but see Minton et al. 2020; Bang et al. 2021). Still, it is worth considering several limitations to the results presented here. First, we were only able to consider the resilience of a small number of sites (n = 6) due to limited spatial overlap between our large-area imagery timeseries and the *in situ* 2018 resilience assessment. Still, even with this limited sample size, the amount of effort required to quantify resilience indicators and resistance and recovery metrics was considerable. Our analysis required us to assign taxonomic IDs to >148,000 stratified random points, delineate and assess the health of >15,000 patches of live coral tissue, and visually survey >4,000m^2 of substrate for juvenile corals. AI-assisted image analysis and coral colony segmentation are active areas of research with the potential to speed ecological data extraction from large-area imagery in the near future (Yuval et al. 2021; Pavoni et al. 2021a; Rossi et al. 2021; van den Bergh et al. 2021; Runyan et al. 2022). This automation, combined with longer timeseries, should enable researchers to collect time-integrated metrics of reef resistance and recovery (i.e., coral growth, survivorship, size frequency distributions, etc.) across larger scales.

Another limitation was our inability to obtain fish survey data for our sites. Herbivory regulates the competitive dynamics between corals and algae (Smith et al. 2001; Kelly et al. 2017) and is hypothesized to be one of the most important drivers of reef resilience (McClanahan et al. 2012; Maynard et al. 2015; Ford et al. 2018; Chung et al. 2019; Donovan et al. 2023b). While we could have used large-area imagery to quantify the density of other important herbivores, namely urchins, the functional role of herbivorous fish and urchins are not necessarily analogous, and herbivory by reef fish and urchins have been shown to impact benthic community composition in divergent ways (Vermeij et al. 2010; Sandin & McNamara 2012; Donovan et al. 2021). To avoid conflating the functional role of different herbivores, we chose to omit herbivore biomass as a resilience indicator in our assessments. We recalculated resilience rankings from Maynard et al. 2019 without herbivore biomass, and found that they were qualitatively similar for our six sites. Thus, it is unlikely that our failure to include fish biomass explains the low predictive accuracy of resilience assessments for our sites in leeward Maui. Still, we advocate that future resilience assessments include indicators of herbivory if at all possible.

A final consideration is whether the scale of our study is sufficient to observe recovery dynamics (Minton et al. 2020; Donovan et al. 2023a; Hock et al. 2023). Based on recovery rates observed elsewhere in the Pacific, annual monitoring over nearly a decade should be sufficient to resolve initial trajectories of community recovery (or lack thereof) in response to bleaching (Gouezo et al. 2019; Moritz et al. 2021; Cresswell et al. 2023). However, transient dynamics in community composition can play out over decades, hindering the recovery of otherwise resilient reefs (Hock et al. 2023). In addition, it is unlikely that a reef will be equally resilient to all forms of disturbance, and the order and timing of sequential disturbances can dramatically shift a reef's

trajectory. Thus, only additional monitoring can confirm whether the recovery trends we observed will continue. Similarly, other resilience assessments have found high levels of spatial variability in resilience scores (Maynard et al. 2010, 2015; Gibbs & West 2019), and it is likely that our six sites do not capture the full variability of reef resilience in leeward Maui. We encourage readers to refer to related research on benthic community successional dynamics across the Maui Nui region (McCarthy et al. *in prep.b*) to contextualize the results presented here.

4. Conclusions

Using a large-area imagery timeseries, we found that resilience assessments are capable of producing consistent predictions of site resilience over time. However, these predictions did not accurately reflect trends in resistance and recovery for our sites in leeward Maui, diminishing their value as a marine spatial planning tool. However, indicators of resistance and recovery still have value for informing site-specific management at reefs deemed to be important by local communities. Care should be taken to select indicators that are appropriate for a given context and thought to be functionally related to reef processes (McClanahan et al. 2012; Ford et al. 2018; Lam et al. 2020).

Critically, our results highlight the importance of modelling resistance and recovery separately, as they represent different processes and may exhibit opposing trends (Donohue et al. 2013; Hodgson et al. 2015). Accordingly, more research is needed to develop process-based indicators of reef function (Ford et al. 2018; Gouezo et al. 2021; McLeod et al. 2021; Hock et al. 2023) and determine whether these functions are related to resistance or to recovery (Graham et al. 2011; McLeod et al. 2019). Long-term monitoring using large-area imaging will be a critical tool in this regard, as it will enable novel metrics to be quantified across multiple scales in space

and time (McCarthy et al. 2023). Process-based metrics that provide insights into coral demography, such as size frequency distributions, growth rates, and survivorship, may prove particularly useful for identifying mechanistic drivers of coral resistance and recovery (McClanahan et al. 2012; Edmunds & Riegl 2020; Rodriguez et al. 2021). Finally, concepts underpinning resilience-based management should be re-examined, namely the assumption that more pristine sites are less vulnerable to disturbance (Côté & Darling 2010). Such research will prove invaluable for informing coral reef management in our current era of rapid climate change.

5. Acknowledgements

Chapter 5, in part, is currently being prepared for submission for publication of the material. McCarthy, Orion S.; Conklin, Eric; Ricke, Katharine; Sparks, Russell T.; Smith, Jennifer E. The dissertation author was the primary researcher and author of this material.

We would like to thank the Nature Conservancy and Division of Aquatic Resources (DAR) for their active participation in this study and for their willingness to revisit the predictions of their 2018 resilience assessment. We are grateful to the divers who conducted field work with the Nature Conservancy (Jamie Caldwell, Zach Caldwell, Megan Donahue, Kim Fuller, Austin Greene, Julia Rose, Anita Tsang, and Bert Weeks) and Scripps Institution of Oceanography (Anela Akiona, Corinne Amir, Donna Brown, Samantha Clements, Ku'ulei Gunderson, Emily Kelly, Susan Kram, Travis Matteson, Sarah Romero, Anna Rothstein, Caroline Sabharwal, Michell Smelser, Yui Takeshita, Melissa Torres, Darla White, and Or Ben Zvi). The 100 Island Challenge provided equipment for large-area imagery surveys, and Nicole Pedersen supported 3D model construction and data curation. Special thanks to Emily Kelly for having the foresight to initiate our large-area imaging timeseries back in 2014, and to Adi Khen for designing custom coral artwork for our figures. Field work logistics were supported by DAR,

Exact Game Fishing Inc., Kristina Jenkins, Alana Yurkanin, Ultimate Whale Watch, Dive Maui, Maui Divers, Lee James, Peter and Toni Colombo, Craig and Amy Venema, Don McLeish, Will and Meghan Dailer, and George and Donna Brown. The Nature Conservancy's 2018 report was improved via contributions from DAR, the West Maui Ridge to Reef Initiative, the Maui Nui Marine Resource Council, and the Maui Coral Recovery Team, and was funded through the NOAA Coral Reef Conservation Program, SymbioSeas and the Harold K.L. Castle Foundation. Scripps Institution of Oceanography field work was funded with support from a UC San Diego Global Policy School fellowship, an NSF Graduate Research Fellowship Program award, and contributions from the Bohn Family, the Ferguson Family, Michael Joo, and the Scripps Family Foundation.

REFERENCES

Abdo DA, Bellchambers LM, Evans SN. 2012. Turning up the heat: increasing temperature and coral bleaching at high latitude coral reefs of the Houtman Abrolhos Islands. PLOS ONE **7**.

Aeby GS, Williams GJ, Franklin EC, Kenyon J, Cox EF, Coles S, Work TM. 2011. Patterns of coral disease across the Hawaiian Archipelago: Relating disease to environment. PLoS ONE **6**.

Agudo-Adriani EA, Cappelletto J, Cavada-Blanco F, Cróquer A. 2019. Structural complexity and benthic cover explain reef-scale variability of fish assemblages in Los Roques National Park, Venezuela. Frontiers in Marine Science **6**:1–12. Frontiers Media S.A.

Allan BM, Nimmo DG, Ierodiaconou D, VanDerWal J, Koh LP, Ritchie EG. 2018. Futurecasting ecological research: The rise of technoecology. Ecosphere. DOI: 10.1002/ecs2.2163.

Allen ME, Bervoets T, Doyle E, Edwards PET, Hawkridge J, Maréchal J, McField M, Sandrine P, Pena M, Souter D, Towle EK. 2021. Chapter 12: Status and trends of coral reefs in the Caribbean region.

Alvarez-Filip L, Côté IM, Gill JA, Watkinson AR, Dulvy NK. 2011a. Region-wide temporal and spatial variation in Caribbean reef architecture: Is coral cover the whole story? Global Change Biology **17**:2470–2477.

Alvarez-Filip L, Dulvy NK, Côté IM, Watkinson AR, Gill JA. 2011b. Coral identity underpins architectural complexity on Caribbean reefs. Ecological Applications **21**:2223–2231.

Anderson K, Westoby MJ, James MR. 2019. Low-budget topographic surveying comes of age: Structure from motion photogrammetry in geography and the geosciences: Progress in Physical Geography **43**:163–173. SAGE Publications Ltd.

Anderson MJ, Willis TJ. 2003. Canonical analysis of principal coordinates: A useful method of constrained ordination for ecology. Ecology **84**:511–525.

Andrello M, Darling ES, Wenger A, Suárez-Castro AF, Gelfand S, Ahmadia GN. 2022. A global map of human pressures on tropical coral reefs. Conservation Letters **15**:1–12.

Anthony KRN. 2016. Coral Reefs under Climate Change and Ocean Acidification: Challenges and Opportunities for Management and Policy. Annual Review of Environment and Resources **41**:59–81.

Anthony KRN, Connolly SR, Hoegh-Guldberg O. 2007. Bleaching, energetics, and coral mortality risk: Effects of temperature, light, and sediment regime. Limnology and Oceanography **52**:716–726.

Anthony KRN, Hoogenboom MO, Maynard JA, Grottoli AG, Middlebrook R. 2009. Energetics approach to predicting mortality risk from environmental stress: A case study of coral

bleaching. Functional Ecology **23**:539–550.

Anthony KRN, Marshall PA, Abdulla A, Beeden R, Bergh C, Black R, Eakin CM, Game ET, Gooch M, Graham NAJ, Green A, Heron SF, van Hooidonk R, Knowland C, Mangubhai S, Marshall N, Maynard JA, Mcginnity P, Mcleod E, Mumby PJ, Nyström M, Obura D, Oliver J, Possingham HP, Pressey RL, Rowlands GP, Tamelander J, Wachenfeld D, Wear S. 2015. Operationalizing resilience for adaptive coral reef management under global environmental change. Global Change Biology **21**:48–61. Blackwell Publishing Ltd.

Arif S, Graham NAJ, Wilson SK, MacNeil MA. 2022. Causal drivers of climate-mediated coral reef regime shifts. Ecosphere **13**:e3956.

Asner GP, Vaughn NR, Foo SA, Heckler J, Martin RE. 2021. Abiotic and Human Drivers of Reef Habitat Complexity Throughout the Main Hawaiian Islands. Frontiers in Marine Science **8**.

Asner GP, Vaughn NR, Martin RE, Foo SA, Heckler J, Neilson BJ, Gove JM. 2022. Mapped coral mortality and refugia in an archipelago-scale marine heat wave. Proceedings of the National Academy of Sciences of the United States of America **119**:1–6.

Bak RPM, Meesters EH. 1998. Coral population structure: The hidden information of colony size-frequency distributions. Marine Ecology Progress Series **162**:301–306. Inter-Research.

Baker AC, Starger CJ, McClanahan TR, Glynn PW. 2004. Corals' adaptive response to climate change. Nature **430**:741–741.

Bang AHY, Kuo CY, Wen CKC, Cherh KL, Ho MJ, Cheng NY, Chen YC, Chen CA. 2021. Quantifying Coral Reef Resilience to Climate Change and Human Development: An Evaluation of Multiple Empirical Frameworks. Frontiers in Marine Science **7**. Frontiers Media S.A.

Barnhill KA, Bahr KD. 2019. Coral resilience at Malauka'a fringing reef, Kāne'ohe Bay, O'ahu after 18 years. Journal of Marine Science and Engineering **7**.

Barnhill KA, Jogee N, Brown C, McGowan A, Rodgers K, Bryceson I, Bahr K. 2020. Acclimatization drives differences in reef-building coral calcification rates. Diversity **12**:1–14.

Barott KL, Williams GJ, Vermeij MJA, Harris J, Smith JE, Rohwer FL, Sandin SA. 2012. Natural history of coral-algae competition across a gradient of human activity in the Line Islands. Marine Ecology Progress Series **460**:1–12.

Battisti C, Poeta G, Fanelli G. 2016. Classification criteria for disturbance events. Page Environmental Science and Engineering (Subseries: Environmental Science).

Bayley DTI, Mogg AOM. 2020. A protocol for the large-scale analysis of reefs using Structure from Motion photogrammetry. Methods in Ecology and Evolution. DOI: 10.1111/2041-210x.13476.

Bayley DTII, Mogg AOMM, Koldewey HJ, Purvis A. 2019a. Capturing complexity: field-testing the use of "structure from motion" derived virtual models to replicate standard measures of reef physical structure. PeerJ **7:e6540**. PeerJ Inc.

Bayley DTII, Mogg AOMM, Purvis A, Koldewey HJ. 2019b. Evaluating the efficacy of small-scale marine protected areas for preserving reef health: A case study applying emerging monitoring technology. Aquatic Conservation-marine and Freshwater Ecosystems **29**:2026–2044. John Wiley and Sons Ltd.

Best AS, Johst K, Münkemüller T, Travis JMJ. 2007. Which species will succesfully track climate change? The influence of intraspecific competition and density dependent dispersal on range shifting dynamics. Oikos **116**:1531–1539.

Bindoff NL, Cheung WWL, Kairo JG, Arístegui J, Guinder VA, Hallberg R, Hilmi N, Jiao N, Karim MS, Levin L, O'Donoghue S, Purca Cuicapusa SR, Rinkevich B, Suga T, Tagliabue A, Williamson P. 2019. Chapter 5: Changing Ocean, Marine Ecosystems, and Dependent Communities.

Bongaerts P, Dubé CE, Dubé CE, Prata KE, Gijsbers JC, Achlatis M, Achlatis M, Hernandez-Agreda A. 2021. Reefscape Genomics: Leveraging Advances in 3D Imaging to Assess Fine-Scale Patterns of Genomic Variation on Coral Reefs. Frontiers in Marine Science **8**:1–18.

Bostrom-Einarsson L, Babcock RC, Bayraktarov E, Ceccarelli DM, Cook N, Ferse SCA, Hancock B, Harrison P, Hein M, Shaver E, Smith A, Suggett D, Stewart-Sinclair PJ, Vardi T, McLeod IM. 2020. Coral restoration – A systematic review of current methods, successes, failures and future directions. PLOS ONE **15**:e0226631.

Bourne D, Iida Y, Uthicke S, Smith-Keune C. 2008. Changes in coral-associated microbial communities during a bleaching event. International Society for Microbial Ecology Journal **2**:350–363.

Bozec YM, Alvarez-Filip L, Mumby PJ. 2015. The dynamics of architectural complexity on coral reefs under climate change. Global Change Biology **21**:223–235. Blackwell Publishing Ltd.

Bradbury R, Reichelt R, Green D. 1984. Fractals in ecology: methods and interpretation. Marine Ecology Progress Series **14**:295–296. Inter-Research Science Center.

Bramanti L, Iannelli M, Fan TY, Edmunds PJ. 2015. Using demographic models to project the effects of climate change on scleractinian corals: *Pocillopora damicornis* as a case study. Coral Reefs **34**:505–515. Springer Berlin Heidelberg.

Brandl SJ, Bellwood DR. 2016. Microtopographic refuges shape consumer-producer dynamics by mediating consumer functional diversity. Oecologia **182**:203–217. Springer.

Brandt ME. 2009. The effect of species and colony size on the bleaching response of reef-building corals in the Florida Keys during the 2005 mass bleaching event. Coral Reefs

28:911–924.

Brito-Millán M, Vermeij M, Alcantar E, Sandin S. 2019a. Coral reef assessments based on cover alone mask active dynamics of coral communities. Marine Ecology Progress Series **630**:55–68. Inter-Research Science Center.

Brito-Millán M, Werner BT, Sandin SA, McNamara DE. 2019b. Influence of aggregation on benthic coral reef spatio-temporal dynamics. Royal Society Open Science **6**. Royal Society Publishing.

Brown D. 2019. An ecological comparison of turf algae between two sites on West Maui that differ in anthropogenic impacts. University of Hawai'i.

Brown EK. 2004. Spatial and temporal differences observed on six reefs off west Maui. University of Hawai'i.

Brown EK, Jokiel PL, Rodgers KS, Smith WR, Roberts LM. 2008. The status of the reefs along south Moloka'i; five years of monitoring. Pages 51–58 The coral reef of south Moloka'i. Hawai'i: portrait of a sediment-threathened fringing reef.

Bryson M, Ferrari R, Figueira WF, Pizarro O, Madin J, Williams SB, Byrne M. 2017. Characterization of measurement errors using structure-from-motion and photogrammetry to measure marine habitat structural complexity. Ecology and Evolution **7**:5669–5681. John Wiley and Sons Ltd.

Burgess SC, Johnston EC, Wyatt ASJ, Leichter JJ, Edmunds PJ. 2021. Response diversity in corals: hidden differences in bleaching mortality among cryptic *Pocillopora* species. Ecology **102**:1–13.

Burgess SC, Osborne K, Sfiligoj B, Sweatman H. 2010. Can juvenile corals be surveyed effectively using digital photography?: Implications for rapid assessment techniques. Environmental Monitoring and Assessment **171**:345–351.

Burn D, Hoey AS, Matthews S, Harrison HB, Pratchett MS. 2023. Differential bleaching susceptibility among coral taxa and colony sizes, relative to bleaching severity across Australia's Great Barrier Reef and Coral Sea Marine Parks. Marine Pollution Bulletin **191**:114907. Elsevier Ltd.

Burns JHR, Delparte D, Gates RD, Takabayashi M. 2015. Integrating structure-from-motion photogrammetry with geospatial software as a novel technique for quantifying 3D ecological characteristics of coral reefs. PeerJ **3:e1077**:1–19. PeerJ Inc.

Burns JHR, Delparte D, Kapono L, Belt M, Gates RD, Takabayashi M. 2016. Assessing the impact of acute disturbances on the structure and composition of a coral community using innovative 3D reconstruction techniques. Methods in Oceanography **15**–**16**:49–59. Elsevier.

Burns JHR, Fukunaga A, Pascoe KH, Runyan A, Craig BK, Talbot J, Pugh A, Kosaki RK. 2019. 3D habitat complexity of coral reefs in the Northwestern Hawaiian Islands is driven by

coral assemblage structure. Pages 61–67 ISPRS Annals of the Photogrammetry, Remote Sensing and Spatial Information Sciences. Copernicus GmbH.

Burns JHR, Weyenberg G, Mandel T, Ferreira SB, Gotshalk D, Kinoshita CK, Marshall MJ, Del Moral NAV, Murphy SJ, Pascoe KH, Runyan A, Spengler AJ, Wells BD, Wilde DK, Pelayo R. 2020. A Comparison of the Diagnostic Accuracy of in-situ and Digital Image-Based Assessments of Coral Health and Disease. Frontiers in Marine Science **7**.

Calders K, Phinn SR, Ferrari R, Ferrari R, Leon JX, León J, Armston J, Asner GP, Disney M. 2020. 3D imaging insights into forests and coral reefs. Trends in Ecology and Evolution **35**:6–9. Elsevier Ltd.

Camp EF. 2022. Contingency planning for coral reefs in the Anthropocene; The potential of reef safe havens. Emerging Topics in Life Sciences **6**:107–124.

Camp EF, Schoepf V, Mumby PJ, Hardtke LA, Rodolfo-Metalpa R, Smith DJ, Suggett DJ. 2018. The future of coral reefs subject to rapid climate change: Lessons from natural extreme environments. Frontiers in Marine Science **5**:1–21.

Carilli J, Donner SD, Hartmann AC. 2012. Historical temperature variability affects coral response to heat stress. PLoS ONE **7**:1–9.

Carlot J, Rovère A, Casella E, Harris D, Grellet-Muñoz C, Chancerelle Y, Dormy E, Hedouin L, Parravicini V. 2020. Community composition predicts photogrammetry-based structural complexity on coral reefs. Coral Reefs **39**:967–975.

Carlson RR, Li J, Crowder LB, Asner GP. 2022. Large-scale effects of turbidity on coral bleaching in the Hawaiian islands. Frontiers in Marine Science **9**:1–15.

Carneiro IM, Sá JA, Chiroque-Solano PM, Cardoso FC, Castro GM, Salomon PS, Bastos AC, Moura RL. 2024. Precision and accuracy of common coral reef sampling protocols revisited with photogrammetry. Marine Environmental Research.

Carpenter KE, Abrar M, Aeby GS, Aeby G, Aronson RB, Banks S, Bruckner AW, Chiriboga A, Cortés J, Cortes JE, Delbeek JC, DeVantier L, Edgar GJ, Edwards AJ, Fenner D, Guzman HM, Hoeksema BW, Hodgson G, Johan O, Licuanan WY, Livingstone SR, Lovell ER, Moore JA, Obura D, Ochavillo D, Polidoro B, Precht WF, Quibilan MCC, Reboton C, Richards ZT, Rogers AD, Sanciangco JC, Sheppard A, Sheppard C, Smith JE, Stuart SN, Turak E, Veron J, Wallace CC, Weil E, Wood E. 2008. One-third of reef-building corals face elevated extinction risk from climate change and local impacts. Science. DOI: 10.1126/science.1159196.

Carrivick JL, Smith MW, Quincey DJ. 2016. Structure from motion in the geosciences. Wiley-Blackwell.

Caruso C, Hughes K, Drury C. 2021. Selecting Heat-Tolerant Corals for Proactive Reef Restoration. Frontiers in Marine Science **8**.

Cattaneo-Vietti R. 2021. The essential role of diving in marine biology. Bulletin of Environmental and Life Sciences **3**.

Cheung KF. 2021. WaveWatch III (WW3) Global Wave Model. July 2016 to July 2023. Distributed by the Pacific Islands Ocean Observing System (PacIOOS).

Chirayath V, Instrella R. 2019. Fluid lensing and machine learning for centimeter resolution airborne assessment of coral reefs in American Samoa. Remote Sensing of the Environment **235**.

Chung AE, Wedding LM, Meadows A, Moritsch MM, Donovan MK, Gove J, Hunter C. 2019. Prioritizing reef resilience through spatial planning following a mass coral bleaching event. Coral Reefs **38**:837–850. Springer Verlag.

Cinner JE, Huchery C, MacNeil MA, Graham NAJ, McClanahan TR, Maina J, Maire E, Kittinger JN, Hicks CC, Mora C, Allison EH, D'Agata S, Hoey A, Feary DA, Crowder L, Williams ID, Kulbicki M, Vigliola L, Wantiez L, Edgar G, Stuart-Smith RD, Sandin SA, Green AL, Hardt MJ, Beger M, Friedlander A, Campbell SJ, Holmes KE, Wilson SK, Brokovich E, Brooks AJ, Cruz-Motta JJ, Booth DJ, Chabanet P, Gough C, Tupper M, Ferse SCA, Sumaila UR, Mouillot D. 2016. Bright spots among the world's coral reefs. Nature **535**:416–419. Nature Publishing Group.

Cinner JE, Maire E, Huchery C, Aaron MacNeil M, Graham NAJ, Mora C, McClanahan TR, Barnes ML, Kittinger JN, Hicks CC, D'Agata S, Hoey AS, Gurney GG, Feary DA, Williams ID, Kulbicki M, Vigliola L, Wantiez L, Edgar GJ, Stuart-Smith RD, Sandin SA, Green A, Hardt MJ, Beger M, Friedlander AM, Wilson SK, Brokovich E, Brooks AJ, Cruz-Motta JJ, Booth DJ, Chabanet P, Gough C, Tupper M, Ferse SCA, Rashid Sumaila U, Pardede S, Mouillot D. 2018. Gravity of human impacts mediates coral reef conservation gains. Proceedings of the National Academy of Sciences of the United States of America **115**:E6116–E6125.

Claar DC, Starko S, Tietjen KL, Epstein HE, Cunning R, Cobb KM, Baker AC, Gates RD, Baum JK. 2020. Dynamic symbioses reveal pathways to coral survival through prolonged heatwaves. Nature Communications **11**:1–10. Springer US.

Clague DA. 1996. The growth and subsidence of the Hawaiian-Emperor volcanic chain. Pages 35–50 The origin and evolution of the Pacific Island biotas, New Guinea to eastern Polynesia: patterns and processes. SPB Academic Publishing.

Clague DA, Dalrymple GB. 1987. The Hawaiian-Emperor volcanic chain. Page Volcanism in Hawai'i.

Coles SL, Bahr KD, Rodgers KS, May SL, McGowan AE, Tsang A, Bumgarner J, Han JH. 2018. Evidence of acclimatization or adaptation in Hawaiian corals to higher ocean temperatures. PeerJ **2018**. PeerJ Inc.

Colgan MW. 1987. Coral reef recovery on Guam (Micronesia) after catastrophic predation by Acanthaster planci. Ecology **68**:1592–1605.

Coll M. 2020. Environmental effects of the COVID-19 pandemic from a (marine) ecological perspective. Ethics in Science and Environmental Politics **20**:42–55. Inter-Research Science Center.

Colwell RN. 1983. The manual of remote sensing2nd Editio. American Society for Photogrammetry.

Conley DD, Hollander ENR. 2021. A Non-destructive Method to Create a Time Series of Surface Area for Coral Using 3D Photogrammetry. Frontiers in Marine Science. DOI: 10.3389/fmars.2021.660846.

Connell JH. 1978. Diversity in tropical rain forests and coral reefs. Science **199**:1302–1309.

Connell JH. 1997. Disturbance and recovery of coral assemblages. Coral Reefs **16**:101–113.

Cook S, Rojano SG, Edwards CB, Bollinger MA, Pierce J, Viehman TS. 2023. Standard operating procedures for the use of large-area imaging in tropical shallow water coral reef monitoring, research, and restoration: Applications for Mission Iconic Reefs restoration in the Florida Keys National Marine Sanctuary. NOAA Technical Mem.

Costanza R, de Groot R, Sutton P, van der Ploeg S, Anderson SJ, Kubiszewski I, Farber S, Turner RK. 2014. Changes in the global value of ecosystem services. Global Environmental Change **26**:152–158.

Côté IM, Darling ES. 2010. Rethinking ecosystem resilience in the face of climate change. PLoS Biology **8**.

Couch CS, Burns JHR, Liu G, Steward K, Gutlay TN, Kenyon J, Eakin CM, Kosaki RK. 2017. Mass coral bleaching due to unprecedented marine heatwave in Papahānaumokuākea Marine National Monument (Northwestern Hawaiian Islands). PLoS ONE **12**. Public Library of Science.

Couch CS, Oliver TA, Dettloff K, Huntington BE, Tanaka KR, Vargas-Ángel B. 2023. Ecological and environmental predictors of juvenile coral density across the central and western Pacific. Frontiers in Marine Science **10**.

Couch CS, Oliver TA, Suka R, Lamirand M, Asbury M, Amir C, Vargas-Ángel B, Winston M, Huntington BE, Huntington B, Lichowski F, Halperin A, Gray AK, Garriques J, Samson J. 2021. Comparing Coral Colony Surveys From In-Water Observations and Structure-From-Motion Imagery Shows Low Methodological Bias. Frontiers in Marine Science.

Cowburn B, Samoilys MA, Obura D. 2018. The current status of coral reefs and their vulnerability to climate change and multiple human stresses in the Comoros Archipelago, Western Indian Ocean. Marine Pollution Bulletin **133**:956–969.

Cox EF, Jokiel PL. 1995. An Evaluation Of The Nearshore Coral Reef Resources Of Kahoolawe, Hawai'i.

Cresswell AK, Renton M, Langlois TJ, Thomson DP, Lynn J, Claudet J. 2023. Coral reef state influences resilience to acute climate-mediated disturbances. Global Ecology and Biogeography **00**:1–13.

Crisp SK, Tebbett SB, Bellwood DR. 2022. A critical evaluation of benthic phase shift studies on coral reefs. Marine Environmental Research **178**:105667. Elsevier Ltd.

Cushman SA, McGarigal K, Neel MC. 2008. Parsimony in landscape metrics: Strength, universality, and consistency. Ecological Indicators **8**:691–703.

D'Urban Jackson T, Williams GJ, Walker-Springett G, Davies AJ, Jackson TD, Williams GJ, Walker-Springett G, Davies AJ, Davies AJ. 2020. Three-dimensional digital mapping of ecosystems: a new era in spatial ecology. Proceedings of The Royal Society B: Biological Sciences **287**. Royal Society Publishing.

Dailer ML, Knox RS, Smith JE, Napier M, Smith CM. 2010. Using δ15N values in algal tissue to map locations and potential sources of anthropogenic nutrient inputs on the island of Maui, Hawai'i, USA. Marine Pollution Bulletin **60**:655–671.

DAR. 2006. Status of Maui's Coral Reefs.

Darling E, Mcclanahan T, Maina J, Gurney G, Graham N, Januchowski-Hartley F, Cinner J, Mora C, Hicks C, Maire E. 2019. Strategic conservation and management of coral reefs in the Anthropocene. Nature Ecology & Evolution **3**.

Darling ES, Alvarez-Filip L, Oliver TA, Mcclanahan TR, Côté IM. 2012. Evaluating life-history strategies of reef corals from species traits. Ecology Letters **15**:1378–1386.

Darling ES, Graham NAJ, Januchowski-Hartley FA, Nash KL, Pratchett MS, Wilson SK. 2017. Relationships between structural complexity, coral traits, and reef fish assemblages. Coral Reefs **36**:561–575. Springer Verlag.

Darling ES, McClanahan TR, Côté IM. 2013. Life histories predict coral community disassembly under multiple stressors. Global Change Biology **19**:1930–1940.

de Souza MR, Caruso C, Ruiz-Jones L, Drury C, Gates RD, Toonen RJ. 2021. Community composition of coral-associated Symbiodiniaceae is driven by fine-scale environmental gradients. Preprint (bioRxiv).

DeCarlo TM, Harrison HB, Gajdzik L, Alaguarda D, Rodolfo-Metalpa R, D'Olivo J, Liu G, Patalwala D, McCulloch MT. 2019. Acclimatization of massive reef-building corals to consecutive heatwaves. Proceedings of the Royal Society B: Biological Sciences **286**.

Delevaux JMS, Winter KB, Jupiter SD, Blaich-Vaughan M, Stamoulis KA, Bremer LL, Burnett K, Garrod P, Troller JL, Ticktin T. 2018. Linking land and sea through collaborative research to inform contemporary applications of traditional resource management in Hawai'i. Sustainability (Switzerland) **10**.

Deng F, Rodgers M, Xie S, Dixon TH, Charbonnier S, Gallant EA, Velez, Christian ML, Ordonez M, Malservisi R, Voss NK, Richardson JA. 2019. High-resolution DEM generation from spaceborne and terrestrial remote sensing data for improved volcano hazard assessment — A case study at Nevado del Ruiz, Colombia. Remote Sensing of the Environment **233**.

DeVantier LM, De'ath G, Done TJ, Turak E. 1998. Ecological assessment of a complex natural system: A case study from the Great Barrier Reef. Ecological Applications **8**:480–496.

Dietzel A, Connolly SR, Hughes TP, Bode M. 2021. The spatial footprint and patchiness of large-scale disturbances on coral reefs. Global Change Biology **27**:4825–4838.

Dixon AM, Forster PM, Beger M. 2021. Coral conservation requires ecological climate-change vulnerability assessments. Frontiers in Ecology and the Environment **19**:243–250.

Dogliotti AI, Ruddick KG, Nechad B, Doxaran D, Knaeps E. 2015. A single algorithm to retrieve turbidity from remotely-sensed data in all coastal and estuarine waters. Remote Sensing of Environment **156**:157–168.

Dollar SJ. 1982. Wave Stress and Coral Community Structure in Hawai'i. Coral Reefs **I**:71–81.

Done TJ. 1992. Phase shifts in coral reef communities and their ecological significance. Hydrobiologia **247**:121–132.

Doney SC, Ruckelshaus M, Emmett Duffy J, Barry JP, Chan F, English CA, Galindo HM, Grebmeier JM, Hollowed AB, Knowlton N, Polovina J, Rabalais NN, Sydeman WJ, Talley LD. 2012. Climate change impacts on marine ecosystems. Annual Review of Marine Science **4**:11–37.

Donohue I, Hillebrand H, Montoya JM, Petchey OL, Pimm SL, Fowler MS, Healy K, Jackson AL, Lurgi M, McClean D, O'Connor NE, O'Gorman EJ, Yang Q. 2016. Navigating the complexity of ecological stability. Ecology letters **19**:1172–1185.

Donohue I, Petchey OL, Montoya JM, Jackson AL, Mcnally L, Viana M, Healy K, Lurgi M, O'Connor NE, Emmerson MC. 2013. On the dimensionality of ecological stability. Ecology Letters **16**:421–429.

Donovan MK, Adam TC, Shantz AA, Speare KE, Munsterman KS, Rice MM, Schmitt RJ, Holbrook SJ, Burkepile DE. 2020. Nitrogen pollution interacts with heat stress to increase coral bleaching across the seascape. Proceedings of the National Academy of Sciences of the United States of America **117**:5351–5357.

Donovan MK, Alves C, Burns J, Drury C, Meier OW, Ritson-Williams R, Cunning R, Dunn RP, Goodbody-Gringley G, Henderson LM, Knapp ISS, Levy J, Logan CA, Mudge L, Sullivan C, Gates RD, Asner GP. 2023a. From polyps to pixels: understanding coral reef resilience to local and global change across scales. Landscape Ecology **38**:737–752. Springer Netherlands.

Donovan MK, Burkepile DE, Kratochwill C, Shlesinger T, Sully S, Oliver TA, Hodgson G, Freiwald J, van Woesik R. 2021. Local conditions magnify coral loss after marine heatwaves. Science **372**:977–980.

Donovan MK, Counsell CWW, Donahue MJ, Lecky J, Gajdzik L, Marcoux SD, Sparks R, Teague C, Donovan MK. 2023b. Evidence for managing herbivores for reef resilience. Proceedings of the Royal Society B **290**.

Donovan MK, Friedlander AM, Lecky J, Jouffray JB, Williams GJ, Wedding LM, Crowder LB, Erickson AL, Graham NAJ, Gove JM, Kappel C V., Karr K, Kittinger JN, Norström A V., Nyström M, Oleson KLL, Stamoulis KA, White C, Williams ID, Selkoe KA. 2018. Combining fish and benthic communities into multiple regimes reveals complex reef dynamics. Scientific Reports **8**. Nature Publishing Group.

Drury C, Bean NK, Harris CI, Hancock JR, Huckeba J, Martin CH, Roach TNF, Quinn RA, Gates RD. 2022. Intrapopulation adaptive variance supports thermal tolerance in a reef-building coral. Communications Biology **5**.

Dudgeon SR, Aronson RB, Bruno JF, Precht WF. 2010. Phase shifts and stable states on coral reefs. Marine Ecology Progress Series **413**:201–216.

Dumas P, Bertaud A, Peignon C, Léopold M, Pelletier D. 2009. A 'quick and clean' photographic method for the description of coral reef habitats. Journal of Experimental Marine Biology and Ecology **368**:161–168.

Eakin CM, Sweatman HPA, Brainard RE. 2019. The 2014–2017 global-scale coral bleaching event: insights and impacts. Coral Reefs **38**:539–545. Springer Verlag.

Edmunds PJ, Aronson RB, Swanson DW, Levitan DR, Precht WF. 1998. Photographic Versus Visual Census Techniques for the Quantification of Juvenile Corals. Bulletin of Marine Science **62**:937–946.

Edmunds PJ, Riegl B. 2020. Urgent need for coral demography in a world where corals are disappearing. Marine Ecology Progress Series **635**:233–242. Inter-Research.

Edwards CB, Eynaud Y, Williams GJ, Pedersen NE, Zgliczynski BJ, Gleason ACRR, Smith JE, Sandin SA. 2017. Large-area imaging reveals biologically driven non-random spatial patterns of corals at a remote reef. Coral Reefs **36**:1291–1305. Springer Verlag.

Edwards CB, Friedlander AM, Green AG, Hardt MJ, Sala E, Sweatman HP, Williams ID, Zgliczynski B, Sandin SA, Smith JE. 2013. Global assessment of the status of coral reef herbivorous fishes: Evidence for fishing effects. Proceedings of the Royal Society B: Biological Sciences **281**:7–11.

Edwards CB, Viehman TS, Battista T, Bollinger MA, Charendoff J, Cook S, Combs I, Couch CS, Ferrari R, Figueira WF, Gleason ACR, Gordon S, Greene W, Kuester F, McCarthy OS, Oliver TA, Pedersen NE, Petrovic V, Rojano S, Runyan H, Sandin SA, Zgliczynski BJ. 2023. Large-area imaging in tropical shallow water coral reef monitoring, research, and

restoration: A practical guide to survey planning, execution, and data extraction.

Faichney IDE, Webster JM, Clague DA, Braga JC, Renema W, Potts DC. 2011. The impact of the Mid-Pleistocene Transition on the composition of submerged reefs of the Maui Nui Complex, Hawai'i. Palaeogeography, Palaeoclimatology, Palaeoecology **299**:493–506. Elsevier B.V.

Falinski K. 2016. Predicting sediment export into tropical coastal ecosystems to support ridge to reef management. University of Hawai'i at Mānoa.

Ferrari R, Bryson M, Bridge T, Hustache J, Williams SB, Byrne M, Figueira W. 2016. Quantifying the response of structural complexity and community composition to environmental change in marine communities. Global Change Biology **22**:1965–1975. Blackwell Publishing Ltd.

Ferrari R, Figueira WF, Pratchett MS, Boube T, Adam A, Kobelkowsky-Vidrio T, Doo SS, Atwood TB, Byrne M. 2017. 3D photogrammetry quantifies growth and external erosion of individual coral colonies and skeletons. Scientific Reports **7**:1–9. Nature Publishing Group.

Ferrari R, Lachs L, Pygas DR, Humanes A, Sommer B, Figueira WF, Edwards AJ, Bythell JC, Guest JR. 2021. Photogrammetry as a tool to improve ecosystem restoration. Trends in Ecology and Evolution **36**:1093–1101.

Ferrari R, Malcolm HA, Byrne M, Friedman A, Williams SB, Schultz A, Jordan AR, Figueira WF. 2018. Habitat structural complexity metrics improve predictions of fish abundance and distribution. Ecography **41**:1077–1091. Blackwell Publishing Ltd.

Field ME, Storlazzi CD, Gibbs AE, D'antonio NL, Cochran SA. 2019. The Major Coral Reefs of Maui Nui, Hawai'i.

Figueira WF, Ferrari R, Weatherby E, Porter AG, Hawes S, Byrne M. 2015. Accuracy and Precision of Habitat Structural Complexity Metrics Derived from Underwater Photogrammetry. Remote Sensing **7**:16883–16900. MDPI AG.

Fletcher CH, Bochicchio C, Conger CL, Engels MS, Feirstein EJ, Frazer N, Glenn CR, Grigg RW, Grossman EE, Harney JN, Isoun E, Murray-Wallace C V, Rooney JJ, Rubin KH, Sherman CE, Vitousek S. 2008. Geology of Hawai'i Reefs. Pages 435–487 Coral Reefs of the USA.

Foo SA, Asner GP. 2019. Scaling up coral reef restoration using remote sensing technology. Frontiers in Marine Science **6**:1–8. Frontiers Media S.A.

Ford AK, Eich A, McAndrews RS, Mangubhai S, Nugues MM, Bejarano S, Moore BR, Rico C, Wild C, Ferse SCA. 2018. Evaluation of coral reef management effectiveness using conventional versus resilience-based metrics. Ecological Indicators **85**:308–317. Elsevier.

Ford H V, Gove JM, Davies AJ, Graham NAJ, Healey JR, Conklin EJ, Williams GJ. 2020. Spatial scaling properties of coral reef benthic communities:1–11.

Fox MD, Carter AL, Edwards CB, Takeshita Y, Johnson MD, Petrovic V, Amir CG, Sala E, Sandin SA, Smith JE. 2019. Limited coral mortality following acute thermal stress and widespread bleaching on Palmyra Atoll, central Pacific. Coral Reefs **38**:701–712. Springer Verlag.

Fox MD, Cohen AL, Rotjan RD, Mangubhai S, Sandin SA, Smith JE, Thorrold SR, Dissly L, Mollica NR, Obura D. 2021. Increasing Coral Reef Resilience Through Successive Marine Heatwaves. Geophysical Research Letters **48**:1–11.

Franklin G, Mariño-Tapia I, Torres-Freyermuth A. 2013. Effects of reef roughness on wave setup and surf zone currents. Journal of Coastal Research **65**:2005–2010.

Friedlander A, Keller K, Wedding L, Clarke A, Monaco M. 2009. A marine biogeographic assessment of the Northwestern Hawaiian Islands. Page NOAA Technical Memorandum NOS NCCOS 84. Prepared by NCCOS's Biogeography Branch in cooperation with the Office of National Marine Sanctuaries Papahanaumokuakea Marine National Monument. Silver Spring, MD. 363 pp.

Friedlander AM, Brown EK, Jokiel PL, Smith WR, Rodgers KS. 2003. Effects of habitat, wave exposure, and marine protected area status on coral reef fish assemblages in the Hawaiian archipelago.

Friedlander AM, Parrish JD. 1998. Habitat characteristics affecting fish assemblages on a Hawaiian coral reef. Journal of Experimental Marine Biology and Ecology **224**:1–30.

Fukunaga A, Burns JHR, Pascoe KH, Kosaki RK. 2020a. Associations between benthic cover and habitat complexity metrics obtained from 3D reconstruction of coral reefs at different resolutions. Remote Sensing **12**.

Fukunaga A, Burns JHR, Pascoe KH, Kosaki RK. 2022. A remote coral reef shows macroalgal succession following a mass bleaching event. Ecological Indicators **142**:109175. Elsevier Ltd.

Fukunaga A, Kosaki RK, Pascoe KH, Burns JHR. 2020b. Fish assemblage structure in the Northwestern Hawaiian Islands is associated with the architectural complexity of coral-reef habitats. Diversity **12**:1–19.

Furby KA, Smith JE, Sandin SA. 2017. *Porites superfusa* mortality and recovery from a bleaching event at Palmyra Atoll, USA. PeerJ **2017**.

George EE, Mullinix JA, Meng F, Bailey BA, Edwards C, Felts B, Haas AF, Hartmann AC, Mueller B, Roach TNF, Salamon P, Silveira C. 2021. Space-filling and benthic competition on coral reefs. PeerJ **9**:1–25.

Gibbs DA, West JM. 2019. Resilience assessment of Puerto Rico's coral reefs to inform reef management. PLoS ONE **14**:1–21.

Giglio VJ, Aued AW, Cordeiro CAMM, Eggertsen L, Ferrari DS, Pinheiro HT, Segal B,

Waechter LS, Bender MG. 2023. A Global Systematic Literature Review of Ecosystem Services in Reef Environments. Environmental Management. DOI: 10.1007/s00267-023-01912-y. Springer US.

Gleason ACR, Lirman D, Williams D, Gracias NR, Gintert BE, Madjidi H, Pamela Reid R, Boynton GC, Negahdaripour S, Miller M, Kramer P. 2007. Documenting hurricane impacts on coral reefs using two-dimensional video-mosaic technology. Marine Ecology **28**:254–258.

González-Barrios FJ, Álvarez-Filip L. 2018. A framework for measuring coral species-specific contribution to reef functioning in the Caribbean. Ecological Indicators **95**:877–886. Elsevier.

González-Barrios FJ, Estrada-Saldívar N, Pérez-Cervantes E, Secaira-Fajardo F, Álvarez-Filip L. 2023. Legacy effects of anthropogenic disturbances modulate dynamics in coral reefs. Global Change Biology **29**:3285–3303.

González-Espinosa PC, Bossier S, Singh GG, Cisneros-Montemayor AM. 2023. Integrating equity-focused planning into coral bleaching management. Ocean Sustainability **2**.

González-Rivero M, Harborne AR, Herrera-Reveles A, Bozec YM, Rogers A, Friedman A, Ganase A, Hoegh-Guldberg O. 2017. Linking fishes to multiple metrics of coral reef structural complexity using three-dimensional technology. Scientific Reports **7**:1–15. Nature Publishing Group.

Good AM, Bahr KD. 2021. The coral conservation crisis: interacting local and global stressors reduce reef resiliency and create challenges for conservation solutions. SN Applied Sciences **3**. Springer Nature.

Gouezo M, Fabricius KE, Harrison P, Golbuu Y, Doropoulos C. 2021. Optimizing coral reef recovery with context-specific management actions at prioritized reefs. Journal of Environmental Management **295**:1–15.

Gouezo M, Golbuu Y, Fabricius K, Olsudong D, Mereb G, Nestor V, Wolanski E, Harrison P, Doropoulos C. 2019. Drivers of recovery and reassembly of coral reef communities. Proceedings of the Royal Society B: Biological Sciences **286**.

Gove JM, Williams GJ, Lecky J, Brown E, Conklin E, Counsell C, Davis G, Donovan MK, Falinski K, Kramer L, Kozar K, Li N, Maynard JA, Mccutcheon A, Mckenna SA. 2023. Coral reefs benefit from reduced land – sea impacts under ocean warming. Nature:1–7. Springer US.

Gove JM, Williams GJ, McManus MA, Heron SF, Sandin SA, Vetter OJ, Foley DG. 2013. Quantifying climatological ranges and anomalies for Pacific coral reef ecosystems. PLoS ONE **8**.

Graham MH. 2004. Effects of local deforestation on the diversity and structure of southern California giant kelp forest food webs. Ecosystems **7**:341–357. Springer New York.

Graham NAJ, Jennings S, Macneil MA, Mouillot D, Wilson SK. 2015. Predicting climate-driven regime shifts versus rebound potential in coral reefs. Nature. DOI: 10.1038/nature14140. Nature Publishing Group.

Graham NAJ, Nash KL. 2013. The importance of structural complexity in coral reef ecosystems. Coral Reefs **32**:315–326.

Graham NAJ, Nash KL, Kool J. 2011. Coral reef dynamics in a changing world. Coral Reefs **30**:283–294.

Grigg RW. 1982. Darwin point: A threshold for atoll formation. Coral Reefs **1**:29–34.

Grigg RW. 1983. Community structure, succession and development of coral reefs in Hawai'i. Marine Ecology Progress Series **11**:1–14.

Grigg RW. 1998. Holocene coral reef accretion in Hawai'i: a function of wave exposure and sea level history. Coral Reefs **17**:263−272.

Grigg RW, Grossman EE, Earle SA, Gittings SR, Lott D, McDonough J. 2002. Drowned reefs and antecedent karst topography,Au'au Channel, S.E. Hawaiian Islands. Coral Reefs **21**:73–82.

Grimaldi CM, Lowe RJ, Benthuysen JA, Cuttler MVW, Green RH, Gilmour JP. 2023. Hydrodynamic and atmospheric drivers create distinct thermal environments within a coral reef atoll. Coral Reefs **42**:693–706. Springer Berlin Heidelberg.

Grimsditch GD, Arnold S, Bey H de, Brown JB, Engel S, Leon R de, Vermeij M. 2011. Coral reef resilience assessment of the Bonaire National Marine Park, Netherlands Antilles.

Grman E, Lau JA, Schoolmaster DR, Gross KL. 2010. Mechanisms contributing to stability in ecosystem function depend on the environmental context. Ecology Letters **13**:1400–1410.

Gross K, Edmunds PJ. 2015. Stability of Caribbean coral communities quantified by long-term monitoring and autoregression models. Ecology **96**:1812–1822.

Grottoli AG, Rodrigues LJ, Palardy JE. 2006. Heterotrophic plasticity and resilience in bleached corals. Nature **440**:1186–1189.

Grottoli AG, Warner ME, Levas SJ, Aschaffenburg MD, Schoepf V, McGinley M, Baumann J, Matsui Y. 2014. The cumulative impact of annual coral bleaching can turn some coral species winners into losers. Global Change Biology **20**:3823–3833.

Gutierrez-Heredia L, Benzoni F, Murphy E, Reynaud EG. 2016. End to End Digitisation and Analysis of Three-Dimensional Coral Models, from Communities to Corallites. PLOS ONE. DOI: 10.1371/journal.pone.0149641.

Haelewaters D, Hofmann T, Romero-Olivares A. 2021. Ten simple rules for Global North researchers to stop perpetuating helicopter research in the Global South. PLOS

Computational Biology **17**:e1009277.

Haire SL, McGarigal K. 2009. Changes in fire severity across gradients of climate, fire size, and topography: A landscape ecological perspective. Fire Ecology **5**:86–103.

Halley JM, Hartley S, Kallimanis AS, Kunin WE, Lennon JJ, Sgardelis SP. 2004. Uses and abuses of fractal methodology in ecology. Ecology Letters **7**:254–271.

Han JHJ, Stefanak MP, Rodgers KS. 2022. Low-level nutrient enrichment during thermal stress delays bleaching and ameliorates calcification in three Hawaiian reef coral species. PeerJ **10**.

Harborne AR, Mumby PJ, Ferrari R. 2012. The effectiveness of different meso-scale rugosity metrics for predicting intra-habitat variation in coral-reef fish assemblages. Environmental Biology of Fishes **94**:431–442.

Harris CI, Bean NK, Baker AC, Gates RD, Drury C. 2022. Stable symbiont communities persist in parents, gametes, and larvae of *Montipora capitata* across historical bleaching phenotypes.

Harris JL, Estradivari E, Fox HE, McCarthy OS, Ahmadia GN. 2017. Planning for the future: Incorporating global and local data to prioritize coral reef conservation. Aquatic Conservation: Marine and Freshwater Ecosystems **27**:65–77. John Wiley and Sons Ltd.

Hatcher BG, Imberger J, Smith S V. 1987. Scaling analysis of coral reef systems: an approach to problems of scale. Coral Reefs **5**:171–181.

Hawai'i Statewide GIS Program. 2016. Streams - Hawai'i. Distributed by the Pacific Islands Ocean Observing System (PacIOOS).

Hawai'i Tourism Authority. 2023. Maui County Overview.

Hein MY, Beeden R, Birtles A, Gardiner NM, Le Berre T, Levy J, Marshall N, Scott CM, Terry L, Willis BL. 2020. Coral restoration effectiveness: Multiregional snapshots of the long-term responses of coral assemblages to restoration. Diversity **12**:1–22.

Henderson PA, Robertson BA. 1999. On structural complexity and fish diversity in an Amazonian floodplain. Advances in Economic Botany:45–58.

Hernández-Landa RC, Barrera-Falcon E, Rioja-Nieto R. 2020. Size-frequency distribution of coral assemblages in insular shallow reefs of the Mexican Caribbean using underwater photogrammetry. PeerJ **2020**:1–30.

Hixon MA, Beets JP. 1993. Predation, prey refuges, and the structure of coral-reef fish assemblages. Ecological Monographs **63**:77–101.

Hock K, Hastings A, Doropoulos C, Babcock RC, Ortiz JC, Thompson A, Mumby PJ. 2023. Transient dynamics mask the resilience of coral reefs. Theoretical Ecology. DOI:

10.1007/s12080-023-00570-4. Springer Netherlands.

Hodgson D, McDonald J, Hosken DJ. 2015. What do you mean, “resilient”? Trends in Ecology and Evolution **30**:503–506.

Hoegh-Guldberg O, Mumby PJ, Hooten AJ, Steneck RS, Greenfield P, Gomez E, Harvell CD, Sale PF, Edwards AJ, Caldeira K, Knowlton N, Eakin CM, Iglesias-Prieto R, Muthiga N, Bradbury RH, Dubi A, Hatziolos ME. 2007. Coral reefs under rapid climate change and ocean acidification. Science **318**:1737–1742.

Hoegh-Guldberg O, Poloczanska ES, Skirving W, Dove S. 2017. Coral reef ecosystems under climate change and ocean acidification. Frontiers in Marine Science **4**.

Holling CS. 1973. Resilience and stability of ecological systems. Annual Review of Ecology and Systematics **4**:1–23.

Holling CS. 1992. Cross-scale morphology, geometry, and dynamics of ecosystems. Ecological Monographs **1**:447–502.

Hothorn T, Bretz F, Westfall P. 2008. multcomp: Simultaneous inference in general parametric models. Biometrical Journal **50**:346–363.

Hothorn T, Hornik K, Van De Wiel MA, Zeileis A. 2006. A lego system for conditional inference. American Statistician **60**:257–263.

Houk P, Benavente D, Iguel J, Johnson S, Okano R. 2014. Coral Reef Disturbance and Recovery Dynamics Differ across Gradients of Localized Stressors in the Mariana Islands. PLoS ONE **9**.

House JE, Brambilla V, Bidaut LM, Christie AP, Pizarro O, Madin JS, Dornelas M. 2018. Moving to 3D: Relationships between coral planar area, surface area and volume. PeerJ **2018**.

Hu Y-J, Satten GA. 2023. Testing hypotheses about the microbiome using the Linear Decomposition Model.

Huffmyer AS, Bean NK, Majerová E, Harris CI, Drury C. 2023. Variable intraspecific genetic diversity effects impact thermal tolerance in a reef-building coral. Coral Reefs **42**:119–129. Springer Berlin Heidelberg.

Hughes DJ, Alderdice R, Cooney C, Kuhl M, Pernice M, Voolstra CR, Suggett DJ. 2020. Coral reef survival under accelerating ocean deoxygenation. Nature Climate Change **10**:296–307.

Hughes TP, Baird AH, Dinsdale EA, Moltschaniwskyj N, Pratchett MS, Tanner JE, Willis BL. 1999. Patterns of recruitment and abundance of corals along the Great Barrier Reef. Nature **397**:59–63.

Hughes TP, Connell JH. 1999. Multiple stressors on coral reefs: A long-term perspective.

Limnology and Oceanography **44**:932–940.

Hughes TP, Jackson JBC. 1980. Do corals lie about their age? Some demographic consequences of partial mortality, fission, and fusion. Science **209**:713–715.

Hughes TP, Kerry JT, Álvarez-Noriega M, Álvarez-Romero JG, Anderson KD, Baird AH, Babcock RC, Beger M, Bellwood DR, Berkelmans R, Bridge TC, Butler IR, Byrne M, Cantin NE, Comeau S, Connolly SR, Cumming GS, Dalton SJ, Diaz-Pulido G, Eakin CM, Figueira WF, Gilmour JP, Harrison HB, Heron SF, Hoey AS, Hobbs JPA, Hoogenboom MO, Kennedy E V., Kuo CY, Lough JM, Lowe RJ, Liu G, McCulloch MT, Malcolm HA, McWilliam MJ, Pandolfi JM, Pears RJ, Pratchett MS, Schoepf V, Simpson T, Skirving WJ, Sommer B, Torda G, Wachenfeld DR, Willis BL, Wilson SK. 2017. Global warming and recurrent mass bleaching of corals. Nature **543**:373–377.

Hughes TP, Kerry JT, Baird AH, Connolly SR, Dietzel A, Eakin CM, Heron SF, Hoey AS, Hoogenboom MO, Liu G, McWilliam MJM, Pears RJ, Pratchett MS, Skirving WJ, Stella JS, Torda G. 2018. Global warming transforms coral reef assemblages. Nature **556**:492–496. Nature Publishing Group.

Hughes TP, Rodrigues MJ, Bellwood DR, Ceccarelli D, Hoegh-Guldberg O, McCook L, Moltschaniwskyj N, Pratchett MS, Steneck RS, Willis B. 2007. Phase Shifts, Herbivory, and the Resilience of Coral Reefs to Climate Change. Current Biology **17**:360–365.

Innis T, Cunning R, Ritson-Williams R, Wall CB, Gates RD. 2018. Coral color and depth drive symbiosis ecology of *Montipora capitata* in Kāneʻohe Bay, O'ahu, Hawai'i. Coral Reefs **37**:423–430. Springer Berlin Heidelberg.

IPCC. 2021. Climate Change 2021: The Physical Science Basis. Contribution of Working Group I to the Sixth Assessment Report of the Intergovernmental Panel on Climate Change. Cambridge University Press, Cambridge, United Kingdom and New York, NY, USA,.

Ishii HT, Tanabe S-I, Hiura T. 2004. Exploring the relationships among canopy structure, stand productivity, and biodiversity of temperate forest ecosystems. Forest Science **50**:342–355.

Jankowski MW, Gardiner NR, Jones GP. 2015. Depth and reef profile: effects on the distribution and abundance of coral reef fishes. Environmental Biology of Fishes **98**:1373–1386.

Johnston DW. 2019. Unoccupied Aircraft Systems in Marine Science and Conservation. Annual Review of Marine Science. DOI: 10.1146/annurev-marine-010318-095323.

Johnston EC, Counsell CWW, Sale TL, Burgess SC, Toonen RJ. 2020. The legacy of stress: Coral bleaching impacts reproduction years later. Functional Ecology **34**:2315–2325.

Johnston EC, Forsman ZH, Toonen RJ. 2018. A simple molecular technique for distinguishing species reveals frequent misidentification of Hawaiian corals in the genus *Pocillopora*.

Jokiel PL, Brown EK. 2004. Global warming, regional trends and inshore environmental conditions influence coral bleaching in Hawai'i. Global Change Biology **10**:1627–1641.

Jokiel PL, Rodgers KS, Storlazzi CD, Field ME, Lager C V, Lager D. 2014. Response of reef corals on a fringing reef flat to elevated suspended-sediment concentrations : Moloka'i , Hawai'i:1–16.

Jones A, Berkelmans R. 2010. Potential costs of acclimatization to a warmer climate: Growth of a reef coral with heat tolerant vs. sensitive symbiont types. PLoS ONE **5**.

Jouffray JB, Nyström M, Norström A V., Williams ID, Wedding LM, Kittinger JN, Williams GJ. 2015. Identifying multiple coral reef regimes and their drivers across the Hawaiian archipelago. Philosophical Transactions of the Royal Society B: Biological Sciences **370**:1–8. Royal Society of London.

Jouffray JB, Wedding LM, Norström A V., Donovan MK, Williams GJ, Crowder LB, Erickson AL, Friedlander AM, Graham NAJ, Gove JM, Kappel C V., Kittinger JN, Lecky J, Oleson KLL, Selkoe KA, White C, Williams ID, Nyström M. 2019. Parsing human and biophysical drivers of coral reef regimes. Proceedings of the Royal Society B: Biological Sciences **286**. Royal Society Publishing.

Jouval F, Bigot L, Bureau S, Quod JP, Penin L, Adjeroud M. 2020. Diversity, structure and demography of coral assemblages on underwater lava flows of different ages at Reunion Island and implications for ecological succession hypotheses. Scientific Reports **10**. Nature Research.

Kaplanis NJ, Edwards CB, Eynaud Y, Smith JE. 2020. Future sea-level rise drives rocky intertidal habitat loss and benthic community change. PeerJ. DOI: 10.7717/peerj.9186.

Kassambra A. 2019. rstatix: pipe-friendly framework for basic statistical tests. R package version 0.3.1.

Kayal M, Vercelloni J, Wand MP, Adjeroud M. 2015. Searching for the best bet in life-strategy: A quantitative approach to individual performance and population dynamics in reef-building corals. Ecological Complexity **23**:73–84. Elsevier B.V.

Kayanne H. 2017. Validation of degree heating weeks as a coral bleaching index in the northwestern Pacific. Coral Reefs **36**:63–70. Springer Berlin Heidelberg.

Keesing JK. 2021. Optimal Foraging Theory Explains Feeding Preferences in the Western Pacific Crown-of-Thorns Sea Star Acanthaster sp. The Biological Bulletin **241**:303–329.

Keighan R, van Woesik R, Yalon A, Nam J, Houk P. 2023. Moderate chlorophyll-a environments reduce coral bleaching during thermal stress in Yap, Micronesia. Scientific Reports **13**:1–9. Nature Publishing Group UK.

Kelly ELA, Eynaud Y, Williams ID, Sparks RT, Dailer ML, Sandin SA, Smith JE. 2017. A budget of algal production and consumption by herbivorous fish in an herbivore fisheries management area, Maui, Hawai'i. Ecosphere **8**. Ecological Society of America.

Kench PS, Mann T. 2017. Reef Island Evolution and Dynamics: Insights from the Indian and

Pacific Oceans and Perspectives for the Spermonde Archipelago. Frontiers in Marine Science **4**.

Khen A, Wall CB, Smith JE. 2023. Standardization of in situ coral bleaching measurements highlights the variability in responses across genera, morphologies, and regions. PeerJ **11**:1–26.

Kindlmann P, Burel F. 2008. Connectivity measures: A review. Landscape Ecology **23**:879–890. Springer Netherlands.

King C, Adhuri DS, Clifton J. 2022. Marine reserves and resilience in the era of COVID-19. Marine Policy **141**:105093. Elsevier Ltd.

Kleypas JA, McManus JW, Menez LAB. 1999. Environmental limits to coral reef development: Where do we draw the line? American Zoologist **39**:146–159.

Knowlton N, Brainard RE, Fisher R, Moews M, Plaisance L, Caley MJ. 2010. Coral Reef Biodiversity. Pages 65–77 in Alasdair D. McIntyre, editor. Life in the World's Oceans. Blackwell Publishing Ltd.

Knudby A, Jupiter SD, Roelfsema CM, Lyons MB, Phinn SR. 2013. Mapping Coral Reef Resilience Indicators Using Field and Remotely Sensed Data. Remote Sensing **5**:1311–1334.

Knudby A, LeDrew E. 2007. Measuring structural complexity on coral reefs. Pages 181–188 Proceedings of the American Academy of Underwater Sciences 26th Symposium. AAUS, Dauphin Island, A.L.

Kodera SM, Edwards CB, Petrovic V, Pedersen NE, Eynaud Y, Sandin SA. 2020. Quantifying life history demographics of the scleractinian coral genus *Pocillopora* at Palmyra Atoll. Coral Reefs **39**:1091–1105. Springer.

Kopecky KL, Pavoni G, Nocerino E, Brooks AJ, Corsini M, Menna F, Gallagher JP, Capra A, Castagnetti C, Rossi P, Gruen A, Neyer F, Muntoni A, Ponchio F, Cignoni P, Troyer M, Holbrook SJ, Schmitt RJ. 2023. Quantifying the Loss of Coral from a Bleaching Event Using Underwater Photogrammetry and AI-Assisted Image Segmentation. Remote Sensing **15**.

Kotliar NB, Wiens JA. 1990. Multiple scales of patchiness and patch structure: A hierarchical framework for the study of heterogeneity. Oikos **59**:253–260.

Krummel JR, Gardner RH, Sugihara G, O'Neill R V, Coleman PR. 1987. Landscape patterns in a disturbed environment. Oikos **48**:321–324.

Kuffner IB, Walters LJ, Becerro MA, Paul VJ, Ritson-Williams R, Beach KS. 2006. Inhibition of coral recruitment by macroalgae and cyanobacteria. Marine Ecology Progress Series **323**:107–117.

Lachs L, Donner SD, Mumby PJ, Bythell JC, Humanes A, East HK, Guest JR. 2023a. Emergent increase in coral thermal tolerance reduces mass bleaching under climate change. Nature Communications **14**. Springer US.

Lachs L, Humanes A, Pygas DR, Bythell JC, Mumby PJ, Ferrari R, Figueira WF, Beauchamp E, East HK, Edwards AJ, Golbuu Y, Martinez HM, Sommer B, van der Steeg E, Guest JR. 2023b. No apparent trade-offs associated with heat tolerance in a reef-building coral. Communications Biology **6**:1–10. Springer US.

Ladd MC, Collado-Vides L. 2013. Practical applications of monitoring results to improve managing for coral reef resilience: a case study in the Mexican Caribbean. Biodiversity Conservation **22**:1591–1608.

Lahoz-Monfort JJ, Chadès I, Davies A, Fegraus E, Game ET, Guillera-Arroita G, Harcourt RG, Indraswari K, McGowan J, Oliver JL, Refisch J, Rhodes JR, Roe P, Rogers AD, Ward A, Watson DM, Watson JEM, Wintle BA, Joppa L. 2019. A call for international leadership and coordination to realize the potential of conservation technology. BioScience. DOI: 10.1093/biosci/biz090.

Lam VYY, Doropoulos C, Bozec YM, Mumby PJ. 2020. Resilience Concepts and Their Application to Coral Reefs. Frontiers in Ecology and Evolution **8**:1–14.

Lam VYY, Doropoulos C, Mumby PJ. 2017. The influence of resilience-based management on coral reef monitoring: A systematic review. PLoS ONE **12**:1–15.

Lange ID, Perry CT. 2020. A quick, easy and non-invasive method to quantify coral growth rates using photogrammetry and 3D model comparisons. Methods in Ecology and Evolution. DOI: 10.1111/2041-210x.13388.

Lee SC. 2006. Habitat complexity and consumer-mediated positive feedbacks on a Caribbean coral reef. Oikos **112**:442–447.

Legendre P, Gauthier O, Centre-ville S. 2014. Statistical methods for temporal and space – time analysis of community composition data †.

Leinbach SE, Speare KE, Strader ME. 2023. Reef habitats structure symbiotic microalgal assemblages in corals and contribute to differential heat stress responses. Coral Reefs **42**:205–217. Springer Berlin Heidelberg.

Lemoine NP. 2021. Unifying ecosystem responses to disturbance into a single statistical framework. Oikos **130**:408–421.

Lenth R V, Bolker B, Buerkner P, Gine-Vasquez I, Herve M, Jung M, Love J, Miguez F, Riebl H, Singmann H. 2023. emmeans: Estimated Marginal Means, aka Least-Squares Means.

Leon JX, Roelfsema CM, Saunders MI, Phinn SR, León J, Roelfsema CM, Saunders MI, Phinn SR. 2015. Measuring coral reef terrain roughness using "Structure-from-Motion" close-range photogrammetry. Geomorphology **242**:21–28. Elsevier.

Lepczyk CA, Wedding LM, Asner GP, Pittman SJ, Goulden T, Linderman M, Gang J, Wright R. 2021. Advancing Landscape and Seascape Ecology from a 2D to a 3D Science. BioScience. DOI: 10.1093/biosci/biab001.

Levenstein MA, Gysbers DJ, Marhaver KL, Kattom S, Tichy L, Quinlan Z, Tholen HM, Kelly LW, Vermeij MJA, Wagoner Johnson AJ, Juarez G. 2022. Millimeter-scale topography facilitates coral larval settlement in wave-driven oscillatory flow. PLoS ONE **17**:1–19.

Levin SA. 1992. The problem of pattern and scale in ecology. Ecology **73**:1943–1967.

Lewis LS, Smith JE. 2019. Functional diversity among herbivorous sea urchins on a coral reef: Grazing rate, dietary preference, and metabolism. Marine Ecology Progress Series **625**:71–87.

Li J, Carlson RR, Knapp DE, Asner GP. 2022. Shallow coastal water turbidity monitoring using Planet Dove satellites. Remote Sensing in Ecology and Conservation **8**:521–535.

Li N, Cheung KF, Stopa JE, Hsiao F, Chen Y-L, Vega L, Cross P. 2016. Thirty-four years of Hawai'i wave hindcast from downscaling of climate forecast system reanalysis. Ocean Modelling **100**:78–95.

Lindenmayer DB, Likens GE. 2009. Adaptive monitoring: a new paradigm for long-term research and monitoring. Trends in Ecology and Evolution **24**:482–486.

Lirman D, Gracias N, Gintert B, Gleason ACR, Deangelo G, Dick M, Martinez E, Reid RP. 2010. Damage and recovery assessment of vessel grounding injuries on coral reef habitats by use of georeferenced landscape video mosaics. Limnology and Oceanography: Methods **8**:88–97.

Lirman D, Gracias NR, Gintert BE, Gleason ACR, Reid RP, Negahdaripour S, Kramer P. 2007. Development and application of a video-mosaic survey technology to document the status of coral reef communities. Environmental Monitoring and Assessment **125**:59–73.

Littler, Mark M., Littler DS. 1984. A relative dominance model for biotic reefs. Page Proceedings of the Joint Meeting of the Atlantic Reef Coggnitte Society of Reef Studies. Miami, Florida.

Liu G, Skirving WJ, Geiger EF, De La Cour JL, Marsh BL, Heron SF, Tirak K V., Strong AE, Eakin CM. 2017. NOAA Coral Reef Watch's 5km Satellite Coral Bleaching Heat Stress Monitoring Product Suite Version 3 and Four-Month Outlook Version 4. Reef Encounter **32**:39–45.

Luckhurst E, Luckhurst K. 1978. Analysis of the influence of substrate variables on coral reef fish communities. Marine Biology **49**:317–323.

Macharia D, Grimsditch GD, Abdulla A, Obura DO. 2016. Mapping Factors That Contribute to Coral Reef Resilience Using In situ and Satellite Data in East Africa. Pages 259–276 Estuaries: A Lifeline of Ecosystem Services in the Western Indian Ocean.

Magel JMT, Burns JHR, Gates RD, Baum JK. 2019. Effects of bleaching-associated mass coral mortality on reef structural complexity across a gradient of local disturbance. Scientific Reports **9**:1–12. Springer US.

Mandelbrot BB. 1983. The fractal geometry of nature. Freeman, San Francisco.

Manikandan B, Ravindran J, Vidya PJ, Shrinivasu S, Manimurali R, Paramasivam K. 2017. Resilience potential of an Indian Ocean reef: an assessment through coral recruitment pattern and survivability of juvenile corals to recurrent stress events. Environmental Science and Pollution Research International **24**:13614–13625.

Mantanona HC, DeCarlo TM. 2023. Coral growth persistence amidst bleaching events. Limnology And Oceanography Letters **8**:734–741.

Maragos JE, Grigg RW. 1974. Recolonization of hermatypic corals on submerged lawa flows in Hawai'i. Ecology **55**:387–395.

Marhaver KL, Verme MJA, Rohwer F, Sandin SA. 2017. Janzen-Connell effects in a broadcast-spawning Caribbean coral : distance-dependent survival of larvae and settlers Author (s): K . L . Marhaver , M . J . A . Vermeij , F . Rohwer and S . A . Sandin Published by : Wiley on behalf of the Ecological Socie **94**:146–160.

Martin CJM, Martin EA. 2002. An underwater photomosaic technique using Adobe Photoshop™. International Journal of Nautical Archaeology **31**:137–147.

Marzonie MR, Bay LK, Bourne DG, Hoey AS, Matthews S, Nielsen JJV, Harrison HB. 2023. The effects of marine heatwaves on acute heat tolerance in corals. Global Change Biology **29**:404–416.

Matsuda SB, Huffmyer AS, Lenz EA, Davidson JM, Hancock JR, Przybylowski A, Innis T, Gates RD, Barott KL. 2020. Coral Bleaching Susceptibility Is Predictive of Subsequent Mortality Within but Not Between Coral Species. Frontiers in Ecology and Evolution **8**:1–14.

Maynard J, Conklin E, Minton D, Williams GJ, Tracey D, Amimoto R, Lynch H, Carr R, Rose J, Sparks R, Fielding E, Sylva R, White D. 2019. Assessing the Resilience of Leeward Maui Reefs to Help Design a Resilient Managed Area Network. CRCP TM 33.

Maynard J, Marshall P, Parker B, Mcleod E, Ahmadia G, van Hooidonk R, Planes S, Williams G, Raymundo L, Beeden R, Tamelander J. 2017a. A Guide to Assessing Coral Reef Resilience For decision support.

Maynard JA, Anthony KRN, Marshall PA, Masiri I. 2008. Major bleaching events can lead to increased thermal tolerance in corals. Marine Biology **155**:173–182.

Maynard JA, Byrne J, Kerrigan K, Tracey D, Bohnsack K, Pagan F, Walczak J, Williams GJ. 2017b. Coral reef resilience to climate change in the Florida Reef Tract. Miami, FL.

Maynard JA, Lewis K, Brown J, Ahmadia GN. 2014. Assessing the relative resilience of the coral reefs of St. Croix, USVI.

Maynard JA, Marshall PA, Johnson JE, Harman S. 2010. Building resilience into practical conservation: Identifying local management responses to global climate change in the southern Great Barrier Reef. Coral Reefs **29**:381–391.

Maynard JA, McKagan S, Raymundo L, Johnson S, Ahmadia GN, Johnston L, Houk P, Williams GJ, Kendall M, Heron SF, van Hooidonk R, Mcleod E, Tracey D, Planes S. 2015. Assessing relative resilience potential of coral reefs to inform management. Biological Conservation **192**:109–119. Elsevier Ltd.

Maynard JA, Wilson J, Campbell S, Mangubhai S, Setiasih N, Sartin J, Ardiwijaya R, Obura D, Marshall P, Salm R, Heron S, Goldberg J. 2012. Assessing coral resilience and bleaching impacts in the Indonesian archipelago.

McCarthy OS, Contractor K, Figueira WF, Gleason ACR, Viehman TS, Edwards CB, Sandin SA. 2023. Closing the gap between existing large-area imaging research and marine conservation needs. Conservation Biology:1–11.

McCarthy OS, Kelly ELA, Akiona AK, Clements SM, Martinez T, Pedersen N, Peralto C, Ricke K, Romero SL, Silva IF, Smelser MH, Stone KW, Sparks RT, Smith JE. (*In Prep*). Fine-scale variation in community composition shapes response to disturbance in coral reefs.

McCarthy OS, Smith JE, Petrovic V, Sandin SA. 2022. Identifying the drivers of structural complexity on Hawaiian coral reefs. Marine Ecology Progress Series **702**:71–86. Inter-Research Science Center.

McCarthy OS, Winston M, Smith JE. (*In Prep*). Corals that survive repeated thermal stress show signs of selection and acclimatization.

McClanahan TR. 2017. Changes in coral sensitivity to thermal anomalies. Marine Ecology Progress Series **570**:71–85.

McClanahan TR, Darling ES, Maina JM, Muthiga NA, D'Agata S, Leblond J, Arthur R, Jupiter SD, Wilson SK, Mangubhai S, Ussi AM, Guillaume MMM, Humphries AT, Patankar V, Shedrawi G, Pagu J, Grimsditch G. 2020. Highly variable taxa-specific coral bleaching responses to thermal stresses. Marine Ecology Progress Series **648**:135–151.

McClanahan TR, Donner SD, Maynard JA, MacNeil MA, Graham NAJ, Maina J, Baker AC, Alemu I. JB, Beger M, Campbell SJ, Darling ES, Eakin CM, Heron SF, Jupiter SD, Lundquist CJ, McLeod E, Mumby PJ, Paddack MJ, Selig ER, van Woesik R. 2012, August 29. Prioritizing Key Resilience Indicators to Support Coral Reef Management in a Changing Climate.

McCormick MI. 1994. Comparison of field methods for measuring surface topography and their associations with a tropical reef fish assemblage. Marine Ecology Progress Series **112**:87–96.

Mcgarigal K, Cushman SA. 2002. Comparative evaluation of experimental approaches to the study of habitat fragmentation effects. Ecological Applications **12**:335–345.

McLachlan RH, Price JT, Munoz-Garcia A, Weisleder NL, Jury CP, Toonen RJ, Grottoli AG. 2021. Environmental gradients drive physiological variation in Hawaiian corals. Coral Reefs **40**:1505–1523.

McLachlan RH, Price JT, Muñoz-Garcia A, Weisleder NL, Levas SJ, Jury CP, Toonen RJ, Grottoli AG. 2022. Physiological acclimatization in Hawaiian corals following a 22-month shift in baseline seawater temperature and pH. Scientific Reports **12**.

McLeod E, Anthony KRN, Mumby PJ, Maynard J, Beeden R, Graham NAJ, Heron SF, Hoegh-Guldberg O, Jupiter S, MacGowan P, Mangubhai S, Marshall N, Marshall PA, McClanahan TR, Mcleod K, Nyström M, Obura D, Parker B, Possingham HP, Salm R V., Tamelander J. 2019. The future of resilience-based management in coral reef ecosystems. Journal of Environmental Management **233**:291–301. Elsevier.

McLeod E, Shaver EC, Beger M, Koss J, Grimsditch G. 2021. Using resilience assessments to inform the management and conservation of coral reef ecosystems. Journal of Environmental Management **277**:111384. Elsevier Ltd.

McNamara DE, Cortale N, Edwards C, Eynaud Y, Sandin SA. 2019. Insights into coral reef benthic dynamics from nonlinear spatial forecasting. Journal of the Royal Society Interface **16**.

Meier ES, Lischke H, Schmatz DR, Zimmermann NE. 2011. Climate, competition and connectivity affect future migration and ranges of European trees. Global Ecology and Biogeography **21**:164–178.

Menge BA, Olson AM. 1990. Role of scale and environmental factors in regulation of community structure. Trends in Ecology and Evolution **5**:52–57.

Mercier F, Baujard O. 1997. Voronoi diagrams to model forest dynamics in French Guiana. Page Second Annual Conference of GeoComputation.

Merlino S, Merlino S, Paterni M, Paterni M, Berton A, Massetti L, Massetti L, Massetti L. 2020. Unmanned Aerial Vehicles for Debris Survey in Coastal Areas: Long-Term Monitoring Programme to Study Spatial and Temporal Accumulation of the Dynamics of Beached Marine Litter. Remote Sensing. DOI: 10.3390/rs12081260.

Miao Z, Chen Y, Zeng X, Li J. 2016. Integrating spatial and attribute characteristics of extended voronoi diagrams in spatial patterning research: A case study of Wuhan City in China. ISPRS International Journal of Geo-Information **5**. MDPI AG.

Middlebrook R, Anthony KRN, Hoegh-Guldberg O, Dove S. 2010. Heating rate and symbiont productivity are key factors determining thermal stress in the reef-building coral *Acropora formosa*.

Miller S, Yadav S, Madin JS. 2021. The contribution of corals to reef structural complexity in Kāneʻohe Bay. Coral Reefs **40**:1679–1685. Springer Berlin Heidelberg.

Million WC, Ruggeri M, O'Donnell S, Bartels E, Conn T, Krediet CJ, Kenkel CD. 2022. Evidence for adaptive morphological plasticity in the Caribbean coral, *Acropora cervicornis*. Proceedings of the National Academy of Sciences **119**:1–10.

Minsaris LOA, Damar A, Imran Z, Madduppa H. 2019. The potential relative resilience of coral reefs in Wakatobi as a sustainable management foundation. Journal of Coastal Conservation **23**:995–1004.

Minton D, Conklin E, Carr R, Lynch H, Rose J, Caldwell Z, Most R. 2020. Evaluating Coral Reef Recovery Four Years Post-bleaching and Assessing the Effectiveness of Pre-bleaching Reef Resilience Rankings.

Minton D, Falinski K, Carr R, Lynch H, Rose J, Stark T, Wirt J, Conklin EJ. 2022. Coral Reef and Water Quality Surveys of the Keōmuku Reef Tract, Lānaʻi.

Monismith SG, Herdman LMM, Ahmerkamp S, Hench JL. 2013. Wave transformation and wave-driven flow across a steep coral reef. Journal of Physical Oceanography **43**:1356–1379.

Montano S, Seveso D, Galli P, Obura DO. 2010. Assessing coral bleaching and recovery with a colour reference card in Watamu Marine Park, Kenya. Hydrobiologia **655**:99–108.

Morais J, Morais RA, Tebbett SB, Pratchett MS, Bellwood DR. 2021. Dangerous demographics in post-bleach corals reveal boom-bust versus protracted declines. Scientific Reports **11**:1–7. Nature Publishing Group UK.

Morais J, Tebbett SB, Morais RA, Bellwood DR. 2023. Hot spots of bleaching in massive *Porites* coral colonies. Marine Environmental Research **193**:106276. Elsevier Ltd.

Moritsch MM, Foley M. 2023. Where are resilience-based management strategies appropriate for coral reefs? Mapping environmental conditions and trends in coral cover in Guam and American Samoa. Ciencias Marinas **49**:e3384.

Moritz C, Brandl SJ, Rouzé H, Vii J, Pérez-Rosales G, Bosserelle P, Chancerelle Y, Galzin R, Liao V, Siu G, Taiarui M, Nugues MM, Hédouin L. 2021. Long-term monitoring of benthic communities reveals spatial determinants of disturbance and recovery dynamics on coral reefs. Marine Ecology Progress Series **672**:141–152. Inter-Research Science Center.

Moritz C, Vii J, Lee Long W, Jerker T, Thomassin A, Planes S. 2018. Status and Trends of Coral Reefs of the Pacific.

Mouillot D, Graham NAJ, Villéger S, Mason NWH, Bellwood DR. 2013. A functional approach reveals community responses to disturbances. Trends in Ecology and Evolution **28**:167–177.

Mumby PJ, Chollett I, Bozec YM, Wolff NH. 2014a. Ecological resilience, robustness and vulnerability: how do these concepts benefit ecosystem management? Current Opinion in Environmental Sustainability **7**:22–27.

Mumby PJ, Wolff NH, Bozec YM, Chollett I, Halloran P. 2014b. Operationalizing the resilience of coral reefs in an era of climate change. Conservation Letters **7**:176–187. Wiley-Blackwell.

Murdoch TJT, Aronson RB. 1999. Scale-dependent spatial variability of coral assemblages along the Florida Reef Tract. Coral Reefs **18**:341–351. Springer-Verlag.

Nash KL, Allen CR, Angeler DG, Barichievy C, Eason T, Garmestani AS, Graham NAJ, Granholm D, Knutson M, Nelson RJ, Nystro¨m M, Nystro¨m N, Stow CA, Sundstrom SM. 2014. Discontinuities, cross-scale patterns, and the organization of ecosystems. Ecology **95**:654–667.

Nash KL, Graham NAJ, Wilson SK, Bellwood DR. 2013. Cross-scale habitat structure drives fish body size distributions on coral reefs. Ecosystems **16**:478–490.

National Academies of Sciences. 2019. A Research Review of Interventions to Increase the Persistence and Resilience of Coral Reefs. Washington DC.

Naughton P, Edwards C, Petrovic V, Kastner R, Kuester F, Sandin S. 2015. Scaling the annotation of subtidal marine habitats. 10th ACM International Conference on Underwater Networks and Systems, WUWNet 2015:0–4.

NOAA Coral Reef Watch. 2020. NOAA Coral Reef Watch Operational Daily Near-Real-Time Global 5-km Satellite Coral Bleaching Monitoring Products. Version 3.1. July 2014 to July 2023. Distributed by the Pacific Islands Ocean Observing System (PacIOOS).

Norström A V., Nyström M, Lokrantz J, Folke C. 2009. Alternative states on coral reefs: Beyond coral-macroalgal phase shifts. Marine Ecology Progress Series **376**:293–306.

Nugent AD, Longman RJ, Trauernicht C, Lucas MP, Diaz HF, Giambelluca TW. 2020. Fire and Rain: The Legacy of Hurricane Lane in Hawai'i. Bulleting of American Meteorological Society **101**:e954–e967.

Nunes VFC, Ferreira MTO, Ferreira Junior F, Amorim MBB, Sampaio CLS., Pinto TK. 2022. Do marine protected areas protect shallow coral reef systems? A resilience-based management approach in Tropical Southwestern Atlantic reefs. Journal of Coastal Conservation **26**.

Oakley-Cogan A, Tebbett SB, Bellwood DR. 2020. Habitat zonation on coral reefs: Structural complexity, nutritional resources and herbivorous fish distributions. PLoS ONE **15**:1–23.

Obura DO, Aeby G, Amornthammarong N, Appeltans W, Bax N, Bishop J, Brainard RE, Chan S, Fletcher P, Gordon TAC, Gramer L, Gudka M, Halas J, Hendee J, Hodgson G, Huang D, Jankulak M, Jones A, Kimura T, Levy J, Miloslavich P, Chou LM, Muller-Karger F, Osuka

K, Samoilys M, Simpson SD, Tun K, Wongbusarakum S. 2019. Coral reef monitoring, reef assessment technologies, and ecosystem-based management. Frontiers in Marine Science **6**:1–21.

Obura DO, Grimsditch G. 2009. Resilience Assessment of Coral Reefs: Rapid assessment protocol for coral reefs, focusing on coral bleaching and thermal stress.

Oksanen J, Simpson GL, Blanchet FG, Kindt R, Legendre P, Minchin PR, O'Hara RB, Solymos P, Stevens MHH, Szoecs E, Wagner H, Barbour M, Bedward M, Bolker B, Borcard D, Garvalho G, Chirico M, De Caceres M, Durand S, Evangelista HBA, FitzJohn R, Friendly M, Furneaux B, Hannigan G, Hill MO, Lahti L, McGlinn D, Ouellette M-H, Cunha ER, Smith T, Stier A, Ter Braak CJF, Weedon J. 2022. Community Ecology Package: Ordination, Diversity and Dissimilarities.

Olinger LK, Scott AR, McMurray SE, Pawlik JR. 2019. Growth estimates of Caribbean reef sponges on a shipwreck using 3D photogrammetry. Scientific Reports. DOI: 10.1038/s41598-019-54681-2.

Oliver ECJ, Donat MG, Burrows MT, Moore PJ, Smale DA, Alexander L V., Benthuysen JA, Feng M, Sen Gupta A, Hobday AJ, Holbrook NJ, Perkins-Kirkpatrick SE, Scannell HA, Straub SC, Wernberg T. 2018. Longer and more frequent marine heatwaves over the past century. Nature Communications **9**:1–12. Springer US.

Oliver TA, Hospital J, Brainard R. 2020. Spatial Prioritization under Resilience Based Management : Evaluating Trade-offs among Prioritization Strategies.

Ortiz JC, Gomez-Cabrera M del C, Hoegh-Guldberg O. 2009. Effect of colony size and surrounding substrate on corals experiencing a mild bleaching event on Heron Island reef flat (southern Great Barrier Reef, Australia). Coral Reefs **28**:999–1003.

Osher W. 2022. "Historic South Swell" dumps water on roadways, 18-24 foot surf expected. Maui Now.

Ostrander GK, Armstrong KM, Knobbe ET, Gerace D, Scully EP. 2000. Rapid transition in the structure of a coral reef community: The effects of coral bleaching and physical disturbance. Proceedings of the National Academy of Sciences of the United States of America **97**:5297–5302.

Padilla-Gamiño JL, Hédouin L, Waller RG, Smith D, Truong W, Gates RD. 2014. Sedimentation and the reproductive biology of the Hawaiian reef-building coral *Montipora capitata*. Biological Bulletin **226**:8–18.

Page CA, Giuliano C, Bay LK, Randall CJ. 2023. High survival following bleaching underscores the resilience of a frequently disturbed region of the Great Barrier Reef. Ecosphere **14**:1–22.

Palacio-Castro AM, Smith TB, Brandtneris V, Snyder GA, van Hooidonk R, Mate JL, Manzello D, Glynn PW, Fong P, Baker AC. 2023. Increased dominance of heat-tolerant symbionts creates resilient coral reefs in near-term ocean warming. Proceedings of the National

Academy of Sciences **120**:e2202388120.

Palma M, Casado MR, Pantaleo U, Cerrano C. 2017. High Resolution Orthomosaics of African Coral Reefs: A Tool for Wide-Scale Benthic Monitoring. Remote Sensing. DOI: 10.3390/rs9070705.

Palma MA, Magliozzi C, Casado MR, Pantaleo U, Fernandes JC, Coro G, Cerrano C, Leinster P, Fernandes JC, Coro G, Cerrano C, Leinster P. 2019. Quantifying coral reef composition of recreational diving sites: a structure from motion approach at seascape scale. Remote Sensing **11**. MDPI AG.

Pandolfi JM, Connolly SR, Marshall DJ, Cohen AL. 2011. Projecting coral reef futures under global warming and ocean acidification. Science **333**:418–422.

Parkinson JE, Banaszak AT, Altman NS, LaJeunesse TC, Baums IB. 2015. Intraspecific diversity among partners drives functional variation in coral symbioses. Scientific Reports **5**:1–12. Nature Publishing Group.

Parsons M, Bratanov D, Gaston KJ, Gonzalez F. 2018. UAVs, Hyperspectral Remote Sensing, and Machine Learning Revolutionizing Reef Monitoring. Sensors. DOI: 10.3390/s18072026.

Passolt G, Fix MJ, Toth SF. 2013. A Voronoi tessellation-based approach to generate hypothetical forest landscapes. Canadian Journal of Civil Engineering **40**:1–31.

Pavoni G, Corsini M, Pedersen N, Petrovic V, Cignoni P. 2021a. Challenges in the deep learning-based semantic segmentation of benthic communities from Ortho-images. Applied Geomatics **13**:131–146. Springer Science and Business Media Deutschland GmbH.

Pavoni G, Corsini M, Ponchio F, Muntoni A, Edwards CB, Pedersen NE, Sandin SA, Cignoni P. 2021b. TagLab: AI-assisted annotation for the fast and accurate semantic segmentation of coral reef orthoimages. Journal of Field Robotics. DOI: 10.1002/rob.22049.

Pedersen NE, Edwards CB, Eynaud Y, Gleason ACR, Smith JE, Sandin SA. 2019. The influence of habitat and adults on the spatial distribution of juvenile corals. Ecography **42**:1703–1713. Blackwell Publishing Ltd.

Perry CT, Alvarez-Filip L. 2019. Changing geo-ecological functions of coral reefs in the Anthropocene. Functional Ecology **33**:976–988.

Petrovic V, Vanoni DJ, Richter AM, Levy TE, Kuester F. 2014. Visualizing high definition three-dimensional and two dimensional data of cultural heritage sites. Mediterranean Archaeology and Archaeometry **14**:93–100.

Phua C, Andradi-Brown DA, Mangubhai S, Ahmadia GN, Mahajan SL, Larsen K, Friel S, Reichelt R, Hockings M, Gill D, Veverka L, Anderson R, Augustave LC, Awaludinnoer, Bervoets T, Brayne K, Djohani R, Kawaka J, Kyne F, Ndagala J, Oates J, Osuka K, Prvan M, Shah N, Vallarola F, Wenzel L, Widodo H, Wells S. 2021. Marine protected and

conserved areas in the time of COVID.

Piazza P, Piazza P, Cummings VJ, Guzzi A, Hawes I, Hawes I, Lohrer AM, Marini S, Marini S, Marriott PM, Menna F, Nocerino E, Nocerino E, Peirano A, Kim S, Schiaparelli S. 2019. Underwater photogrammetry in Antarctica: long-term observations in benthic ecosystems and legacy data rescue. Polar Biology. DOI: 10.1007/s00300-019-02480-w.

Pinheiro J, Bates D, DebRoy S, Sakar D, R Core Team. 2018. nlme: Linear and nonlinear mixed effects models. R package version 3.1-137.

Pittman S, Kneib R, Simenstad C. 2011. Practicing coastal seascape ecology. Marine Ecology Progress Series **427**.

Plaisance L, Caley MJ, Brainard RE, Knowlton N. 2011. The diversity of coral reefs: What are we missing? PLoS ONE **6**.

Powell B. 2010. Regional Ocean Modeling System (ROMS): Main Hawaiian Islands. April 15, 2015 to December 31, 2021. Distributed by the Pacific Islands Ocean Observing System (PacIOOS).

Price DM, Lim A, Callaway A, Eichhorn MP, Wheeler AJ, Lo Iacono C, Huvenne VAI. 2021. Fine-Scale Heterogeneity of a Cold-Water Coral Reef and Its Influence on the Distribution of Associated Taxa. Frontiers in Marine Science **8**. Frontiers Media S.A.

Price JP, Elliott-Fisk D. 2004. Topographic history of the Maui Nui complex, Hawai'i, and its implications for biogeography. Pacific Science **58**:27–45.

Prouty NG, Cohen A, Yates KK, Storlazzi CD, Swarzenski PW, White DJ. 2017. Vulnerability of coral reefs to bioerosion from land-based sources of pollution. Journal of Geophysical Research: Oceans **122**:9319–9331.

Pullin AS, Knight TM. 2003. Support for decision making in conservation practice: an evidence-based approach. Journal for Nature Conservation **11**:83–90.

Pulsford SA, Lindenmayer DB, Driscoll DA. 2014. A succession of theories: purging redundancy from disturbance theory. Biological Reviews **91**:148–167.

Purkis SJ, Riegl BM, Dodge RE. 2006. Fractal patterns of coral communities: evidence from remote sensing (Arabian Gulf, Dubai, U.A.E.). Pages 1753–1762 Proceedings of the 10th International Coral Reef Symposium.

R Core Team. 2023. R: A language and environment for statistical computing. R. Foundation for Statistical Computing, R Foundation for Statistical Computing, Vienna, Austria. https://www.R-project.org/.

Raoult V, David PA, Dupont SF, Mathewson CP, O'Neill SJ, Powell NN, Williamson JE. 2016. GoPros^{TM} as an underwater photogrammetry tool for citizen science. PeerJ. DOI: 10.7717/peerj.1960.

Remmers T, Grech A, Roelfsema C, Gordon S, Lechene M, Ferrari R. 2023. Close-range underwater photogrammetry for coral reef ecology: a systematic literature review. Coral Reefs. DOI: 10.1007/s00338-023-02445-w. Springer Berlin Heidelberg.

Richardson LE, Graham NAJ, Hoey AS. 2017. Cross-scale habitat structure driven by coral species composition on tropical reefs. Scientific Reports **7**. Nature Publishing Group.

Richardson LE, Graham NAJ, Hoey AS. 2020. Coral species composition drives key ecosystem function on coral reefs. Proceedings of the Royal Society B: Biological Sciences **287**.

Richaume J, Cheminée A, Drap P, Bonhomme P, Cadene F, Ferrari B, Hartmann V, Michez N, Bianchimani O. 2021. 3D Photogrammetry Modeling Highlights Efficient Reserve Effect Apparition After 5 Years and Stillness After 40 for Red Coral (Corallium rubrum) Conservation in French MPAs. Frontiers in Marine Science. DOI: 10.3389/fmars.2021.639334.

Rietkerk M, van de Koppel J. 2008. Regular pattern formation in real ecosystems. Trends in Ecology and Evolution **23**:169–175.

Risk MJ. 1972. Fish diversity on a coral reef in the Virgin Islands. Atoll Research Bulletin **153**:1–6.

Ritchie EG, Martin JK, Johnson CN, Fox BJ. 2009. Separating the influences of environment and species interactions on patterns of distribution and abundance: competition between large herbivores. Journal of Animal Ecology **78**:724–731.

Rivera HE, Cohen AL, Thompson JR, Baums IB, Fox MD, Meyer-Kaiser KS. 2022. Palau's warmest reefs harbor thermally tolerant corals that thrive across different habitats. Communications Biology **5**:1–12. Springer US.

Roach TNF, Yadav S, Yadav S, Caruso C, Dilworth J, Foley CM, Foley CM, Hancock JR, Huckeba J, Huffmyer AS, Hughes K, Kahkejian VA, Madin EMP, Matsuda SB, McWilliam M, Miller S, Santoro EP, Santoro EP, de Souza MR, de Souza MR, Torres-Pullizaa D, Drury C, Drury C, Madin JS. 2021. A Field Primer for Monitoring Benthic Ecosystems using Structure-from-Motion Photogrammetry. Journal of Visualized Experiments. DOI: 10.3791/61815.

Rodgers KS, Bahr KD, Jokiel PL, Donà AR. 2017. Patterns of bleaching and mortality following widespread warming events in 2014 and 2015 at the Hanauma Bay Nature Preserve, Hawai'i. PeerJ **2017**. PeerJ Inc.

Rodgers KS, Jokiel PL, Brown EK, Hau S, Sparks R. 2015. Over a decade of change in spatial and temporal dynamics of Hawaiian coral reef communities. Pacific Science **69**:1–13. Pacific Science.

Rodgers KS, Richards Donà A, Stender YO, Tsang AO, Han JHJ, Weible RM, Prouty N, Storlazzi C, Graham AT. 2021. Rebounds, regresses, and recovery: A 15-year study of the coral reef community at Pila'a, Kaua'i after decades of natural and anthropogenic stress

events. Marine Pollution Bulletin **171**.

Rodríguez-Casariego JA, Mercado-Molina AE, Garcia-Souto D, Ortiz-Rivera IM, Lopes C, Baums IB, Sabat AM, Eirin-Lopez JM. 2020. Genome-Wide DNA Methylation Analysis Reveals a Conserved Epigenetic Response to Seasonal Environmental Variation in the Staghorn Coral *Acropora cervicornis*. Frontiers in Marine Science **7**:1–17.

Rodriguez C, Amir C, Gray A, Asbury M, Suka R, Lamirand M, Couch C, Oliver T, Rodriguez C, Amir C, Gray A, Asbury M. 2021. Measuring Coral Vital Rates Using Photogrammetry at Fixed Sites : Standard Operating Procedures and Error Estimates Measuring Coral Vital Rates Using Structure-from-Motion Photogrammetry at Fixed Sites : Standard Operating Procedures and Error Estimates.

Rogers A, Harborne AR, Brown CJ, Bozec YM, Castro C, Chollett I, Hock K, Knowland CA, Marshell A, Ortiz JC, Razak T, Roff G, Samper-Villarreal J, Saunders MI, Wolff NH, Mumby PJ. 2015. Anticipative management for coral reef ecosystem services in the 21st century. Global Change Biology **21**:504–514.

Rogers CS. 1993. Hurricanes and coral reefs; the intermediate disturbance hypothesis revisited. Coral Reefs **12**:127–137.

Roik A, Wall M, Dobelmann M, Nietzer S, Brefeld D, Fiesinger A, Reverter M, Schupp PJ, Jackson M, Rutsch M, Strahl J. 2023. Trade-offs in a reef-building coral after six years of thermal acclimation. bioRxiv:2023.07.20.549699.

Rooney JJ, Wessel P, Hoeke R, Weiss J, Baker J, Parrish F, Fletcher CH, Chojnacki J, Garcia M, Brainard R, Vroom P. 2008. Geology and geomorphology of coral reefs in the Northwestern Hawaiian Islands. Pages 519–571 Coral Reefs of the USA. Springer Netherlands.

Roper CD, Donelson JM, Ferguson S, van Oppen MJH, Cantin NE. 2023. Long-term preconditioning of the coral *Pocillopora acuta* does not restore performance in future ocean conditions. Coral Reefs. DOI: 10.1007/s00338-023-02401-8. Springer Berlin Heidelberg.

Rosinski A, Birkeland C, White DJ, Conklin EJ, Williams I, Gove JM, Gorospe K, Oliver TA, Walsh W. 2017. Coral bleaching recovery plan: Identifying management responses to promote coral recovery in Hawai'i.

Ross M. 2015. Environmental and Demographic Drivers of Hawaiian Reef Corals. University of Hawai'i, Manoa.

Ross M, Rodgers K, Jokiel PL. 2010. Quantifying causes of Maui coral decline. Report issued by the Division of Aquatic Resources, Department of Land and Natural Resources, State of Hawai'i.

Ross M, White D, Aiwohi M, Walton M, Sudek M, Lager D, Jokiel P. 2012. Characterization of “dead zones” and population demography of *Porites compressa* along a gradient of anthropogenic nutrient input at Kahekili Beach Park, Maui.

Rossi P, Ponti M, Righi S, Castagnetti C, Simonini R, Mancini F, Agrafiotis P, Bassani L, Bruno F, Cerrano C, Cignoni P, Cignoni P, Corsini M, Drap P, Dubbini M, Garrabou J, Gori A, Gracias N, Ledoux J-BB, Linares C, Mantas TP, Menna F, Nocerino E, Nocerino E, Nocerino E, Palma MA, Pavoni G, Ridolfi A, Rossi S, Skarlatos D, Skarlatos D, Skarlatos D, Treibitz T, Turicchia E, Yuval M, Capra A. 2021. Needs and Gaps in Optical Underwater Technologies and Methods for the Investigation of Marine Animal Forest 3D-Structural Complexity. Frontiers in Marine Science **8**. Frontiers Media S.A.

Runyan H, Petrovic V, Edwards CB, Pedersen N, Alcantar E, Kuester F, Sandin SA. 2022. Automated 2D, 2.5D, and 3D Segmentation of Coral Reef Pointclouds and Orthoprojections. Frontiers in Robotics and AI. DOI: 10.3389/frobt.2022.884317.

Sandin SA, Alcantar E, Clark R, de León R, Dilrosun F, Edwards CB, Estep AJ, Eynaud Y, French BJ, Fox MD, Grenda D, Hamilton SL, Kramp H, Marhaver KL, Miller SD, Roach TNF, Seferina G, Silveira CB, Smith JE, Zgliczynski BJ, Vermeij MJA. 2022. Benthic assemblages are more predictable than fish assemblages at an island scale. Coral Reefs **41**:1031–1043. Springer Berlin Heidelberg.

Sandin SA, Edwards CB, Edwards CB, Pedersen NE, Pedersen NE, Petrovic V, Pavoni G, Alcantar EA, Chancellor KS, Fox MD, Stallings B, Sullivan CJ, Rotjan RD, Ponchio F, Ponchio F, Zgliczynski BJ. 2020. Considering the rates of growth in two taxa of coral across Pacific islands. Pages 167–191 Advances in marine biology. Academic Press.

Sandin SA, McNamara DE. 2012. Spatial dynamics of benthic competition on coral reefs. Oecologia **168**:1079–1090.

Sandin SA, Smith JE, DeMartini EE, Dinsdale EA, Donner SD, Friedlander AM, Konotchick T, Malay M, Maragos JE, Obura D, Pantos O, Paulay G, Richie M, Rohwer F, Schroeder RE, Walsh S, Jackson JBC, Knowlton N, Sala E. 2008. Baselines and degradation of coral reefs in the Northern Line Islands. PLoS ONE **3**.

Santano J, Milton IA, Navarro B, Warren RM, Barber PH, Fong P, Fong CR. 2021. Structural complexity shapes the behavior and abundance of a common herbivorous fish, increasing herbivory on a turf-dominated, fringing reef. Journal of Experimental Marine Biology and Ecology **537**:151515. Elsevier B.V.

Schopmeyer SA, Vroom PS, Kenyon JC. 2011. Spatial and Temporal Comparisons of Benthic Composition at Necker Island, Northwestern Hawaiian Islands. Pacific Science **65**:405–417.

Searle SR, Speed FM, Milliken GA. 1980. Population marginal means in the linear model: An alternative to least squares means. American Statistician **34**:216–221.

Shepard MK, Campbell BA, Bulmer MH, Farr TG, Gaddis LR, Plaut JJ. 2001. The roughness of natural terrain: A planetary and remote sensing perspective. Journal of Geophysical Research E: Planets **106**:32777–32795. American Geophysical Union.

Shlesinger T, van Woesik R. 2023. Oceanic differences in coral bleaching responses to marine heatwaves. Science of the Total Environment **871**:1–12.

Shockley K. 2023. Two faces of vulnerability: Distinguishing susceptibility to harm and system resilience in climate adaptation. WIREs Climate Change **14**:e856.

Shultz JKK, Smith CM, Abbott I, Basch L V. 2004. Comparison of shallow marine algal communities among selected sites of Maui Nui, Hawai'i. University of Hawai'i, Manoa.

Šímová P, Gdulová K. 2012. Landscape indices behavior: A review of scale effects. Applied Geography **34**:385–394. Elsevier Ltd.

Skirving W, Marsh B, De La Cour J, Liu G, Harris A, Maturi E, Geiger E, Mark Eakin C. 2020. Coraltemp and the coral reef watch coral bleaching heat stress product suite version 3.1. Remote Sensing **12**:1–10.

Slocum RK, Parrish CE, Simpson CH. 2020. Combined geometric-radiometric and neural network approach to shallow bathymetric mapping with UAS imagery. ISPRS Journal of Photogrammetry and Remote Sensing **169**:351–363.

Smith EG, Hazzouri KM, Choi JY, Delaney P, Al-Kharafi M, Howells EJ, Aranda M, Burt JA. 2022a. Signatures of selection underpinning rapid coral adaptation to the world's warmest reefs. Science Advances **8**.

Smith HA, Brown DA, Arjunwadkar C V., Fulton SE, Whitman T, Hermanto B, Mastroianni E, Mattocks N, Smith AK, Harrison PL, Boström-Einarsson L, McLeod IM, Bourne DG. 2022b. Removal of macroalgae from degraded reefs enhances coral recruitment. Restoration Ecology **30**.

Smith JE, Brainard R, Carter A, Grillo S, Edwards C, Harris J, Lewis L, Obura D, Rohwer F, Sala E, Vroom PS, Sandin S. 2016. Re-evaluating the health of coral reef communities: Baselines and evidence for human impacts across the central pacific. Proceedings of the Royal Society B: Biological Sciences **283**:1–9. Royal Society of London.

Smith JE, Hunter CL, Smith CM. 2002. Distribution and reproductive characteristics of nonindigenous and invasive marine algae in the Hawaiian Islands. Pacific Science **6**:299–315.

Smith JE, Hunter CL, Smith CM. 2010. The effects of top-down versus bottom-up control on benthic coral reef community structure. Oecologia **163**:497–507.

Smith JE, Runcie JW, Smith CM. 2005. Characterization of a large-scale ephemeral bloom of the green alga Cladophora sericea on the coral reefs of West Maui, Hawai'i. Marine Ecology Progress Series **302**:77–91.

Smith JE, Smith CM, Hunter CL. 2001. An experimental analysis of the effects of herbivory and nutrient enrichment on benthic community dynamics on a Hawaiian reef. Coral Reefs **19**:332–342. Springer Verlag.

Sofiiuk K, Petrov IA, Konushin A. 2022. Reviving Iterative Training With Mask Guidance for Interactive Segmentation. Proceedings - International Conference on Image Processing,

ICIP **1071**:3141–3145.

Sousa WP. 1984. The role of disturbance in natural communities. Annual review of ecology and systematics. Vol. 15:353–391.

Sparks R, Stone K, White D, Ross M. 2015. Maui and Lāna'i Monitoring Report. Report issued by the Division of Aquatic Resources, Department of Land and Natural Resources, State of Hawai'i.

Speaker T, O'Donnell S, Wittemyer G, Bruyere B, Loucks C, Dancer A, Carter M, Fegraus E, Palmer J, Warren E, Solomon J. 2021. A global community-sourced assessment of the state of conservation technology. Conservation Biology. DOI: 10.1111/cobi.13871.

Speare KE, Adam TC, Winslow EM, Lenihan HS, Burkepile DE. 2022. Size-dependent mortality of corals during marine heatwave erodes recovery capacity of a coral reef. Global Change Biology **28**:1342–1358.

Stamski RE, Field ME. 2006. Characterization of sediment trapped by macroalgae on a Hawaiian reef flat. Estuarine, Coastal and Shelf Science **66**:211–216.

Stefanoudis P V, Licuanan WY, Morrison TH, Talma S, Veitayaki J, Woodall LC. 2021. Turning the tide of parachute science. Current Biology. DOI: 10.1016/j.cub.2021.01.029.

Storlazzi CD, Brown EK, Field ME, Rodgers K, Jokiel PL. 2005. A model for wave control on coral breakage and species distribution in the Hawaiian Islands. Coral Reefs **24**:43–55.

Storlazzi CD, Dartnell P, Hatcher GA, Gibbs AE. 2016. End of the chain? Rugosity and fine-scale bathymetry from existing underwater digital imagery using structure-from-motion (SfM) technology. Coral Reefs **35**:889–894. Springer Verlag.

Streit RP, Cumming GS, Bellwood DR. 2019. Patchy delivery of functions undermines functional redundancy in a high diversity system. Functional Ecology **33**:1144–1155.

Sugihara G, May R, Ye H, Hsieh C-H, Deyle E, Fogarty M, Munch S. 2012. Detecting causality in complex ecosystems. Science **338**:496–500.

Sugihara G, May RM. 1990. Applications of fractals in ecology. Trends in Ecology and Evolution **5**:79–86.

Suka RR, Suka R, Asbury M, Gray AE, Gray AE, Winston M, Oliver TA, Couch CS. 2019. Processing Photomosaic Imagery of Coral Reefs Using Structure-from-Motion Standard Operating Procedures. null. DOI: 10.25923/h2q8-jv47.

Sully S, Burkepile DE, Donovan MK, Hodgson G, van Woesik R. 2019. A global analysis of coral bleaching over the past two decades. Nature Communications **10**:1–5. Springer US.

Sully S, Hodgson G, van Woesik R. 2022. Present and future bright and dark spots for coral reefs through climate change. Global Change Biology **28**:4509–4522.

Swetnam TL, Gillian JK, Sankey TT, McClaran MP, Nichols MH, Heilman P, McVay J. 2018. Considerations for Achieving Cross-Platform Point Cloud Data Fusion across Different Dryland Ecosystem Structural States. Frontiers in Plant Science **8**.

Szereday S, Amri AY. 2021. Successive bleaching events (2019-2020) in Northeast Peninsular Malaysia revealed selective thermal acclimatization and susceptibility of hard corals at biophysical reef scale. Preprint (bioRxiv).

Tebbett SB, Connolly SR, Bellwood DR. 2023. Benthic composition changes on coral reefs at global scales. Nature Ecology and Evolution **7**:71–81. Springer US.

Tews J, Brose U, Grimm V, Tielbörger K, Wichmann MC, Schwager M, Jeltsch F. 2004. Animal species diversity driven by habitat heterogeneity/diversity: the importance of keystone structures. Journal of Biogeography **31**:79–92.

Thiault L, Gelcich S, Marshall N, Marshall P, Chlous F, Claudet J. 2019. Operationalizing vulnerability for social–ecological integration in conservation and natural resource management. Conservation Letters **13**:1–13.

Thornton B, Bodenmann A, Pizarro O, Williams SB, Friedman A, Nakajima R, Takai K, Motoki K, Watsuji T, Hirayama H, Matsui Y, Watanabe H, Ura T. 2016. Biometric assessment of deep-sea vent megabenthic communities using multi-resolution 3D image reconstructions. null. DOI: 10.1016/j.dsr.2016.08.009.

Tokeshi M, Arakaki S. 2012. Habitat complexity in aquatic systems: Fractals and beyond.

Topor ZM, Rasher DB, Duffy JE, Brandl SJ. 2019. Marine protected areas enhance coral reef functioning by promoting fish biodiversity. Conservation Letters **12**:1–9.

Turner MG, Baker WL, Peterson CJ, Peet RK. 1998. Factors Influencing Succession: Lessons from Large, Infrequent Natural Disturbances. Ecosystems **1**:511–523.

Turner MG, O'Neill R V, Gardner RH, Milne BT. 1989. Effects of changing spatial scale on the analysis of landscape pattern. Landscape Ecology **3**:153–162. SPB Academic Publishing.

UNEP-WCMC, WRI, TNC. 2021. Global distribution of coral reefs, compiled from multiple sources including the Millenium Coral Reef Mapping Project. Version 4.1, updated by UNEP-WCMC.

Urbina-Barreto I, Elise S, Guilhaumon F, Bruggemann JH, Pinel R, Kulbicki M, Vigliola L, Mou-Tham G, Mahamadaly V, Facon M, Bureau S, Peignon C, Dutrieux E, Garnier R, Penin L, Adjeroud M. 2022. Underwater photogrammetry reveals new links between coral reefscape traits and fishes. Ecosphere **13**.

Urbina-Barreto I, Garnier R, Elise S, Pinel R, Dumas P, Dumas P, Mahamadaly V, Facon M, Bureau S, Peignon C, Peignon C, Quod J-P, Dutrieux E, Penin L, Adjeroud M, Adjeroud M. 2021. Which Method for Which Purpose? A Comparison of Line Intercept Transect and Underwater Photogrammetry Methods for Coral Reef Surveys. Frontiers in Marine Science.

DOI: 10.3389/fmars.2021.636902.

van den Bergh J, Chirayath V, Li A, Torres-Pérez JL, Segal-Rozenhaimer M. 2021. NeMO-Net – Gamifying 3D Labeling of Multi-Modal Reference Datasets to Support Automated Marine Habitat Mapping. Frontiers in Marine Science **8**.

van Hooidonk R, Maynard J, Tamelander J, Gove J, Ahmadia G, Raymundo L, Williams G, Heron SF, Planes S. 2016. Local-scale projections of coral reef futures and implications of the Paris Agreement. Scientific Reports **6**. Nature Publishing Group.

Van Oppen MJH, Oliver JK, Putnam HM, Gates RD. 2015. Building coral reef resilience through assisted evolution. Proceedings of the National Academy of Sciences **112**:2307–2313.

van Woesik R, Shlesinger T, Grottoli AG, Toonen RJ, Thurber RV, Warner ME, Hulver AM, Chapron L, McLachlan RH, Albright R, Crandall E, DeCarlo TM, Donovan MK, Eirin-Lopez JM, Harrison HB, Heron SF, Huang D, Humanes A, Krueger T, Madin JS, Manzello D, McManus LC, Matz M, Muller EM, Rodriguez-Lanetty M, Vega-Rodriguez M, Voolstra C, Zaneveld J. 2022. Coral-bleaching responses to climate change across biological scales. Global Change Biology **00**:1–22.

Vergés A, Vanderklift MA, Doropoulos C, Hyndes GA. 2011. Spatial patterns in herbivory on a coral reef are influenced by structural complexity but not by algal traits. PLoS ONE **6**:1–12.

Vermeij MJA. 2005. Substrate composition and adult distribution determine recruitment patterns in a Caribbean brooding coral. Marine Ecology Progress Series **295**:123–133.

Vermeij MJA, Angly F, Brown EK, Dailer ML, Field ME, Friedlander AM, Gibbs AE, Herzfeld I, Smith CM, Smith JE, Spalding H, Sparks RT, Storlazzi CD, White DJ, Williams ID. 2008. Coral Reefs of Maui: Status, Stressors, and Suggestions.

Vermeij MJA, Dailer ML, Walsh SM, Donovan MK, Smith CM. 2010. The effects of trophic interactions and spatial competition on algal community composition on Hawaiian coral reefs. Marine Ecology **31**:291–299.

Vermeij MJA, Sandin SA, Samhouri JF. 2007. Local habitat distribution determines the relative frequency and interbreeding potential for two Caribbean coral morphospecies. Evolutionary Ecology **21**:27–47.

Villéger S, Miranda JR, Hernández DF, Mouillot D. 2010. Contrasting changes in taxonomic vs. functional diversity of tropical fish communities after habitat degradation. Ecological Applications **20**:1512–1522.

Vo ST, Hua TT, Phan KH. 2019. A study of coral reef resilience and implications of adaptive management and rehabilitation in Khanh Hoa Province, Vietnam. Acta Oceanologica Sinica **38**:112–117.

Voss J, Shilling E, Combs I. 2019. Intervention and fate tracking for corals affected by stony

coral tissue loss disease in the northern Florida Reef Tract. Miami, FL.

Vroom PS, Braun CL. 2010. Benthic composition of a healthy subtropical reef: Baseline species-level cover, with an emphasis on algae, in the Northwestern Hawaiian Islands. PLoS ONE **5**.

Vroom PS, Page KN, Peyton KA, Kukea-Shultz JK. 2005. Spatial heterogeneity of benthic community assemblages with an emphasis on reef algae at French Frigate Shoals, Northwestern Hawaiian Islands. Coral Reefs **24**:574–581.

Vytopil E, Willis BL. 2001. Epifaunal community structure in Acropora spp. (Scleractinia) on the Great Barrier Reef: Implications of coral morphology and habitat complexity. Coral Reefs **20**:281–288.

Walker NS, Nestor V, Golbuu Y, Palumbi SR. 2023. Coral bleaching resistance variation is linked to differential mortality and skeletal growth during recovery. Evolutionary Applications **16**:504–517.

Wall CB, Ricci CA, Wen AD, Ledbetter BE, Delania E, Mydlarz LD, Gates RD, Putnam HM. 2021. Shifting baselines: Physiological legacies contribute to the response of reef corals to frequent heatwaves. Functional Ecology **35**:1366–1378.

Wall CB, Spiegel CJ, Diaz EM, Tran CH, Fabiani A, Broe TY, Sara EP, Mladenov N, Symons CC, Shurin JB. 2023. Fire transforms effects of terrestrial subsidies on aquatic ecosystem structure and function. Global Change Biology **30**:1–16.

Wang X, Blanchet FG, Koper N. 2014. Measuring habitat fragmentation: An evaluation of landscape pattern metrics. Methods in Ecology and Evolution **5**:634–646. British Ecological Society.

Wedding L, Lepczyk C, Pittman S, Friedlander A, Jorgensen S. 2011. Quantifying seascape structure: extending terrestrial spatial pattern metrics to the marine realm. Marine Ecology Progress Series **427**.

Wedding LM, Lecky J, Gove JM, Walecka HR, Donovan MK, Williams GJ, Jouffray JB, Crowder LB, Erickson A, Falinski K, Friedlander AM, Kappel C V., Kittinger JN, McCoy K, Norström A, Nyström M, Oleson KLL, Stamoulis KA, White C, Selkoe KA. 2018. Advancing the integration of spatial data to map human and natural drivers on coral reefs. PLoS ONE **13**. Public Library of Science.

Weeks R, Jupiter SD. 2013. Adaptive comanagement of a marine protected area network in Fiji. Conservation Biology **27**:1234–1244.

Weng KC, Friedlander AM, Gajdzik L, Goodell W, Sparks RT. 2023. Decreased tourism during the COVID-19 pandemic positively affects reef fish in a high use marine protected area. PLoS ONE **18**:1–15.

West JM, Salm R V. 2003. Resistance and Resilience to Coral Bleaching: Implications for Coral

Reef Conservation and Management. Conservation Biology **17**:956–967.

Westoby MJ, Brasington J, Glasser NF, Hambrey MJ, Reynolds JM. 2012. 'Structure-from-Motion' photogrammetry: A low-cost, effective tool for geoscience applications. Geomorphology **179**.

Whittier RB, El-kadi A. 2014. Human Health and Environmental Risk Ranking of On-Site Sewage Disposal Systems for the Hawaiian Islands of Kaua'i, Moloka'i, Maui, and Hawai'i.

Wickham H, François R, Henry L, Müller K, Vaughan D. 2023. dplyr: A grammar of data manipulation.

Wiens JA. 1989. Spatial scaling in ecology. Functional Ecology **3**:385–397.

Williams GJ, Gove JM, Eynaud Y, Zgliczynski BJ, Sandin SA. 2015. Local human impacts decouple natural biophysical relationships on Pacific coral reefs. Ecography **38**:751–761.

Williams GJ, Graham NAJ, Jouffray JB, Norström A V., Nyström M, Gove JM, Heenan A, Wedding LM. 2019. Coral reef ecology in the Anthropocene. Functional Ecology **33**:1014–1022. Blackwell Publishing Ltd.

Williams GJ, Smith JE, Conklin EJ, Gove JM, Sala E, Sandin SA. 2013. Benthic communities at two remote pacific coral reefs: Effects of reef habitat, depth, and wave energy gradients on spatial patterns. PeerJ **2013**:1–26.

Williams ID, White DJ, Sparks RT, Lino KC, Zamzow JP, Kelly ELA, Ramey HL. 2016. Responses of Herbivorous Fishes and Benthos to 6 Years of Protection at the Kahekili Herbivore Fisheries Management Area, Maui. PloS one **11**:e0159100.

Wilson KA, Law EA. 2016. Ethics of conservation triage. Frontiers in Ecology and Evolution **4**:19–26.

Wilson SK, Graham NAJ, Polunin NVC. 2007. Appraisal of visual assessments of habitat complexity and benthic composition on coral reefs. Marine Biology **151**:1069–1076.

Wilson SK, Robinson JPW, Chong-Seng K, Robinson J, Graham NAJ. 2019. Boom and bust of keystone structure on coral reefs. Coral Reefs **38**:625–635. Springer Verlag.

Winston M, Couch CS, Oliver TA, McCarthy OS, Speare K, Donovan MK. (*In Prep*). Signs of resilience: survivorship and growth of corals in Hawai'i two years post-bleaching.

Winston M, Oliver T, Couch C, Donovan MK, Asner GP, Conklin E, Fuller K, Grady BW, Huntington B, Kageyama K, Kindinger TL, Kozar K, Kramer L, Martinez T, McCutcheon A, McKenna S, Rodgers K, Shayler CK ilikea, Vargas-Angel B, Zgliczynski B. 2022. Coral taxonomy and local stressors drive bleaching prevalence across the Hawaiian Archipelago in 2019. PLoS ONE **17**:1–24.

Winter KB, Lincoln NK, Berkes F, Alegado RA, Kurashima N, Frank KL, Pascua P, Rii YM,

Reppun F, Knapp ISS, McClatchey WC, Ticktin T, Smith C, Franklin EC, Oleson K, Price MR, McManus MA, Donahue MJ, Rodgers KS, Bowen BW, Nelson CE, Thomas B, Leong J-A, Madin EMP, Rivera MAJ, Falinski KA, Bremer LL, Deenik JL, Gon III SM, Neilson B, Okano R, Olegario A, Nyberg B, Kawelo AH, Kotubetey K, Kukea-Shultz JK, Toonen RJ. 2020. Ecomimicry in Indigenous resource management: optimizing ecosystem services to achieve resource abundance, with examples from Hawai'i. Ecology and Society **25**.

Witman JD, Dayton PK, Arnold SN, Steneck RS, Birkeland C. 2012. The Revolution of Science through Scuba. Smithsonian Contributions to Marine Sciences **39**:3–11.

Wong AS, Vrontos S, Taylor ML. 2022. An assessment of people living by coral reefs over space and time. Global Change Biology **28**:7139–7153.

Wood SN. 2011. Fast stable restricted maximum likelihood and marginal likelihood estimation of semiparametric generalized linear models. Journal of the Royal Statistical Society (B) **73**:3–36.

Woodhead AJ, Williams GJ, Hicks CC, Norström A V, Graham NAJ. 2019. Coral reef ecosystem services in the Anthropocene. Functional Ecology **33**:1023–1034.

World Economic Outlook. 2022. WEO Groups and Aggregates Information Database. International Monetary Fund.

Yadav S, Roach TNF, McWilliam MJ, Caruso C, de Souza MR, Foley C, Allen C, Dilworth J, Huckeba J, Santoro EP, Wold R, Simpson J, Miller S, Hancock JR, Drury C, Madin JS. 2023. Fine-scale variability in coral bleaching and mortality during a marine heatwave. Frontiers in Marine Science **10**:1–11.

Young GC, Dey S, Rogers AD, Rogers AD, Exton DA. 2017. Cost and time-effective method for multi-scale measures of rugosity, fractal dimension, and vector dispersion from coral reef 3D models. PLOS ONE **12**:1–18. Public Library of Science.

Yuval M, Alonso I, Eyal G, Tchernov D, Loya Y, Tchernov D, Murillo AC, Treibitz T. 2021. Repeatable Semantic Reef-Mapping through Photogrammetry and Label-Augmentation. Remote Sensing. DOI: 10.3390/rs13040659.

Zawada KJA, Madin JS, Baird AH, Bridge TCL, Dornelas M. 2019. Morphological traits can track coral reef responses to the Anthropocene. Functional Ecology **33**:962–975.

APPENDICES

Appendix 1.1: Literature review and coral reef practitioner survey methodology

Literature review

We used the search engine *ResearchRabbit* (Version 2.0, Human Intelligence Technologies Incorporated) to conduct an initial review of coral reef literature that utilized large-area imagery (LAI). Starting with seminal LAI papers in the coral reef field (Burns et al. 2015; Figueira et al. 2015; Leon et al. 2015; Bryson et al. 2017; Edwards et al. 2017; Ferrari et al. 2017; Young et al. 2017; Bayley et al. 2019), we used *ResearchRabbit* to identify additional papers to include based on citations to those original papers. We added papers to this network when studies met our criteria for inclusion and excluded papers suggested by *ResearchRabbit* that did not meet these criteria. These criteria were as follows: 1) the study focused on tropical or subtropical shallow water coral reefs, 2) the study utilized LAI technology, and 3) the study was published between 2010 and 2021. We chose to limit our search to the 2010-2021 timeframe because LAI is still an emerging technology that was not widely used in the coral reef field prior to 2010. We iterated through this process until no new relevant papers were identified.

To check the comprehensiveness of the *ResearchRabbit* approach, we searched Web of Science for relevant papers that might have been missed. We searched for studies published between 2010 and 2021 that used the key word "coral reef" and any of the following key words: Structure from Motion, SfM, photogrammetry, point cloud, orthomosaic, orthoprojection, or photomosaic. We opted to use this broad range of keywords because 1) the terminology used to describe LAI has evolved over time, with "large-area imagery" being a more recent (albeit more appropriate) term, and 2) the point of the Web of Science search was to detect papers that were

missed in the initial *ResearchRabbit* search. We chose to include relevant government reports (n = 7), conference proceedings (n = 8), and book chapters (n = 1) so as not to miss potential applications of LAI technology focused on conservation or resource management. Once papers were identified, we screened each study to identify whether it used LAI to answer some research question related to coral reef science or conservation, and added relevant papers to our *ResearchRabbit* network.

In total, we identified n = 151 relevant studies published from 2010 to 2021. We collated these studies into an excel database and recorded the following metadata for each study: author, publication year, study title and abstract, study location and scale (i.e., whether the study was conducted at the colony scale or site scale, and the number of colonies or sites sampled), DOI, and publication outlet. We also recorded the location (country or territory) where study author institutions were located, and used this information examine trends in authorship between advanced economies in the Global North and emerging or developing economies in the Global South (Table S1.1). Each study was assigned to one of four categories based on the institutional affiliation of the authors: 1) all study authors from institutions based in the Global North, 2) study authors from a mix of Global North and south institutions with a first author based at an institution in the Global North, 3) study authors from a mix of Global North and south institutions with a first author based at an institution in the Global South, and 4) all study authors from institutions based in the Global South. We categorized studies as "methods development" if a portion of the study focused on validating the accuracy of LAI or developing new metrics or components of the LAI pipeline. Finally, each study was assigned to one or more of 33 research topic areas (see Figure 1.3 for list of research topic areas). These topic areas were selected based on common themes that emerged across studies and survey responses. Studies could be assigned

to multiple categories. For example, a hypothetical study that tested the accuracy of a new LAI-based tool for quantifying the 3D structure of corals before and after a hurricane would fall into four categories: methods development, structural complexity, change over time, and storm damage.

Coral reef scientist and practitioner survey

We used the platform *Qualtrics* (Qualtrics, Provo, UT, USA) to develop our survey entitled "Gauging coral reef practitioner awareness of Structure from Motion (SfM) technology". We used the terminology "Structure from Motion" in our survey since it has heretofore been more commonly used in the coral reef literature, even though we now advocate for using the more broad, inclusive, and intuitive term "large-area imaging" throughout the rest of this study. The survey consisted of 25 questions (Appendix 1.2) and was reviewed by the UC San Diego Institutional Review Board (study #801952). We distributed the survey via several listservs and social media channels relevant to coral reef science and conservation. Primary avenues for distribution included coral-list, the Coral Restoration Consortium mailing list, the MPA Help and EBM Help listervs, the Australia Marine Science Association newsletter, the Mideast Coral Reef Society listserv, and twitter. Survey responses were included for analysis as long as respondents answered at least one of the 25 survey questions, and respondents were not required to answer all questions. The survey went live on March 1, 2022 and was closed on June 1, 2022.

We asked respondents to answer demographic questions focused on the respondent's: 1) sector (What type of organization do you work for? [Table S1.7]), 2) region (What country is your organization based in? [Table S1.10]), and 3) experience (How many years of experience in marine conservation do you have? [Table S1.8] AND Have you heard of SfM before this survey? [Table S1.4]). We also asked respondents if they viewed their work as more focused on science

or conservation (Table S1.9). Survey respondents were classified as Global North vs Global South post-hoc based on the country where their organization was based (Table S1.2, Table S1.10).

In addition to demographic questions, respondents were asked to rate their familiarity with SfM applications and software, and to predict their likelihood of using SfM in the future. Respondents were also asked to rate seven potential barriers to SfM adoption (equipment, few applications of SfM, lack of interest, money, opposition from funders or communities, staff capacity, and training/technical expertise) based on the perceived magnitude of those barriers. Respondents were also asked to rank nine potential applications of SfM (archiving reef condition, cost saving and/or efficiency, improving existing monitoring programs, informing conservation decision making, mapping marine habitats, measuring 3D habitat structure, quantifying human impacts, tracking change over time, and visualizing/communicating reef condition) from most to least important/exciting. The order of these options was randomized for each respondent to avoid biasing results. Finally, respondents were asked the following open-ended questions: 1) If capacity, data, and access to the reef were unlimited, what would you most want to know about reef dynamics? AND 2) What ecological functions or processes would be the most useful to have a better scientific understanding of, in terms of informing coral reef conservation? Answers to these questions were categorized according to the same research topic areas used to categorize literature review studies so that research interests could be directly compared between survey respondents and existing LAI literature.

Finally, respondents were given the option to provide their email address so that they could be contacted for an optional 30-minute semistructured follow up interview via the videoconferencing software *Zoom*. Of 135 respondents, 54 indicated that they would like to be

contacted for interviews, and we were able to interview 45 survey respondents. We customized our interview questions based on each respondent's survey responses, but consistently asked the following two questions in all interviews: 1) In your opinion, how can scientists who already use SfM in their work increase the accessibility of this technology for those in the conservation community? AND 2) Do you think that SfM will have an overall positive or negative impact on the field of coral conservation? Video recordings and call transcripts were used to summarize key points and common themes across interviews.

Table S1.1: The categorization of countries and territories as "Global North" or "Global South" used in this study. For our study we define the Global North as advanced economies located primarily in the Northern Hemisphere, with the exception of Australia and New Zealand, that have historically had more access to resources. Global South countries are primarily located in the tropics or southern hemisphere, have historically had less access to resources, and/or been colonized (Haelewaters et al. 2021). To reflect this history of colonization, we consider territories claimed by Global North countries to be Global South for this analysis. Categorizations are based on the World Economic Outlook's classification scheme of advanced economies vs. emerging and developing economies (World Economic Outlook 2022). Only countries and inhabited territories containing tropical coral reefs, or countries that have published coral reef LAI studies, are shown. The number of LAI studies published from 2010 to 2021 is also shown for each country or territory based on the institutional affiliation of the study's first author and co-authors (counts are of studies, not authors; co-authors are not double counted). Finally, the number of survey participants are shown for each country or territory based on the location of their institutional affiliation.

Country or Territory	Region	North vs. South	Coral reefs?	n LAI studies (first author)	n LAI studies (co-author)	n survey participants
American Samoa	Oceania	Global South	Yes	0	0	0
Anguilla	Caribbean	Global South	Yes	0	0	0
Antigua and Barbuda	Caribbean	Global South	Yes	0	0	0
Aruba	Caribbean	Global South	Yes	0	0	0
Australia	Oceania	Global North	Yes	28	36	9
Bahamas	Caribbean	Global South	Yes	0	0	1
Bahrain	Asia	Global South	Yes	0	0	0
Barbados	Caribbean	Global South	Yes	0	0	0
Belgium	Europe	Global North	No	1	0	0
Belize	North America	Global South	Yes	0	0	2
Bermuda	North America	Global South	Yes	0	0	0

Table S1.1: The categorization of countries and territories as "Global North" or "Global South" used in this study (Continued).

Country or Territory	Region	North vs. South	Coral reefs?	n LAI studies (first author)	n LAI studies (co-author)	n survey participants
Bonaire	Caribbean	Global South	Yes	0	0	1
Brazil	South America	Global South	Yes	1	3	1
British Virgin Islands	Caribbean	Global South	Yes	0	0	0
Brunei	Asia	Global South	Yes	0	0	0
Cambodia	Asia	Global South	Yes	0	0	0
Canada	North America	Global North	No	1	4	1
Cayman Islands	Caribbean	Global South	Yes	0	0	1
China	Asia	Global South	Yes	0	1	0
Christmas Island	Asia	Global South	Yes	0	0	0
Cocos Islands	Oceania	Global South	Yes	0	0	0
Colombia	South America	Global South	Yes	0	0	2
Comoros	Africa	Global South	Yes	0	0	0
Cook Islands	Oceania	Global South	Yes	0	0	0
Costa Rica	North America	Global South	Yes	0	0	0
Cuba	Caribbean	Global South	Yes	0	0	0
Curacao	Caribbean	Global South	Yes	0	4	3
Cyprus	Europe	Global North	No	0	1	0
Djibouti	Africa	Global South	Yes	0	0	0
Dominica	Caribbean	Global South	Yes	0	0	0
Dominican Republic	Caribbean	Global South	Yes	0	0	0
Egypt	Africa	Global South	Yes	1	0	1
Eritrea	Africa	Global South	Yes	0	0	0
Federated States of Micronesia	Oceania	Global South	Yes	0	0	0
Fiji	Oceania	Global South	Yes	0	0	0
France	Europe	Global North	No	4	11	0
French Polynesia	Oceania	Global South	Yes	1	2	1
Germany	Europe	Global North	No	3	10	0
Greece	Europe	Global North	No	0	1	0
Grenada	Caribbean	Global South	Yes	0	0	0
Guatemala	North America	Global South	Yes	0	0	0
Haiti	Caribbean	Global South	Yes	0	0	1
Honduras	North America	Global South	Yes	0	1	1
Hong Kong	Asia	Global North	Yes	1	1	1
India	Asia	Global South	Yes	0	0	1
Indonesia	Asia	Global South	Yes	1	2	4
Iran	Asia	Global South	Yes	1	1	1

Table S1.1: The categorization of countries and territories as "Global North" or "Global South" used in this study (Continued).

Country or Territory	Region	North vs. South	Coral reefs?	n LAI studies (first author)	n LAI studies (co-author)	n survey participants
Ireland	Europe	Global North	No	2	3	0
Israel	Asia	Global North	Yes	2	4	0
Italy	Europe	Global North	No	10	15	0
Jamaica	Caribbean	Global South	Yes	0	0	1
Japan	Asia	Global North	Yes	3	4	3
Jordan	Asia	Global South	Yes	0	0	0
Kenya	Africa	Global South	Yes	0	0	1
Kiribati	Oceania	Global South	Yes	0	0	0
Kuwait	Asia	Global South	Yes	0	0	0
Madagascar	Africa	Global South	Yes	0	0	0
Malaysia	Asia	Global South	Yes	3	3	1
Maldives	Asia	Global South	Yes	0	1	0
Marianas Islands/Guam	Oceania	Global South	Yes	0	0	3
Marshall Islands	Oceania	Global South	Yes	0	0	0
Mauritius	Africa	Global South	Yes	0	0	1
Mayotte	Africa	Global South	Yes	0	0	0
Mexico	North America	Global South	Yes	2	2	2
Montserrat	Caribbean	Global South	Yes	0	0	0
Mozambique	Africa	Global South	Yes	0	0	0
Myanmar	Asia	Global South	Yes	0	0	0
Nauru	Oceania	Global South	Yes	0	0	0
Netherlands	Europe	Global North	No	1	4	0
New Caledonia	Oceania	Global South	Yes	0	0	0
Nicaragua	North America	Global South	Yes	0	0	0
Niue	Oceania	Global South	Yes	0	0	0
Oman	Asia	Global South	Yes	0	0	0
Palau	Oceania	Global South	Yes	0	0	0
Panama	North America	Global South	Yes	0	0	0
Papua New Guinea	Oceania	Global South	Yes	0	0	0
Philippines	Asia	Global South	Yes	0	0	0
Pitcairn Islands	Oceania	Global South	Yes	0	0	0
Portugal	Europe	Global North	No	0	2	1
Puerto Rico	Caribbean	Global South	Yes	1	0	1
Qatar	Asia	Global South	Yes	0	0	0
Reunion	Africa	Global South	Yes	3	3	0

Table S1.1: The categorization of countries and territories as "Global North" or "Global South" used in this study (Continued).

Country or Territory	Region	North vs. South	Coral reefs?	n LAI studies (first author)	n LAI studies (co-author)	n survey participants
Saint Barthelemy	Caribbean	Global South	Yes	0	0	0
Saint Kitts and Nevis	Caribbean	Global South	Yes	0	0	0
Saint Lucia	Caribbean	Global South	Yes	0	0	0
Saint Martin	Caribbean	Global South	Yes	0	0	0
Saint Vincent and the Grenadines	Caribbean	Global South	Yes	0	0	0
Samoa	Oceania	Global South	Yes	0	0	0
Saudi Arabia	Asia	Global South	Yes	1	2	0
Seychelles	Africa	Global South	Yes	0	0	1
Singapore	Asia	Global North	Yes	1	1	0
Sint Maarten	Caribbean	Global South	Yes	0	0	0
Solomon Islands	Oceania	Global South	Yes	0	0	0
Somalia	Africa	Global South	Yes	0	0	0
South Africa	Africa	Global South	Yes	0	0	1
Spain	Europe	Global North	No	2	6	0
Sri Lanka	Asia	Global South	Yes	0	0	0
Sudan	Africa	Global South	Yes	0	0	0
Switzerland	Europe	Global North	No	4	5	1
Taiwan	Asia	Global North	Yes	1	1	0
Tanzania	Africa	Global South	Yes	0	0	1
Thailand	Asia	Global South	Yes	0	0	0
Timor Leste	Asia	Global South	Yes	0	0	0
Tokelau	Oceania	Global South	Yes	0	0	0
Tonga	Oceania	Global South	Yes	0	0	0
Trinidad and Tobago	Caribbean	Global South	Yes	0	0	0
Turks and Caicos	Caribbean	Global South	Yes	0	0	0
Tuvalu	Oceania	Global South	Yes	0	0	0
United Arab Emirates	Asia	Global South	Yes	0	0	2
United Kingdom	Europe	Global North	No	10	21	3
United States	North America	Global North	Yes	58	79	32
US Virgin Islands	Caribbean	Global South	Yes	3	3	7
Vanuatu	Oceania	Global South	Yes	0	0	0
Venezuela	South America	Global South	Yes	2	4	0
Vietnam	Asia	Global South	Yes	0	0	0
Wallis and Futuna	Oceania	Global South	Yes	0	0	0
Yemen	Asia	Global South	Yes	0	0	0

Appendix 1.2: Large-area imagery survey questions and results

Study #801952: Gauging coral reef practitioner awareness of Structure from Motion (SfM) technology

Overall research questions that the survey seeks to answer:

1. How familiar are reef conservation practitioners with SfM?
2. What barriers currently limit the application of SfM in the coral reef conservation community?
3. How could SfM be leveraged to add value for reef conservation practitioners?

Content for survey participants begins below this line

Landing page/informed consent statement:

You are invited to participate in a research project about the applications of Structure from Motion technology to coral reef conservation. This online survey should take about 10 minutes to complete. Participation is voluntary, responses will be kept anonymous, and the results of the survey may be published in a scientific paper. You will have the option to voluntarily provide your contact information so that the researchers can follow up with you about your answers, and in this case your responses would be kept confidential to the degree permitted by the technology being used. You have the option to not respond to any questions that you choose.

This research is being conducted by researchers at the Smith and Sandin Labs at the Scripps Institution of Oceanography, UC San Diego. Participation or nonparticipation will not impact your relationship with the Smith or Sandin Labs or UC San Diego.

Submission of the survey will be interpreted as your informed consent to participate and that you affirm that you are at least 18 years of age. If you have any questions about the research, please contact Orion McCarthy or Dr. Jennifer Smith via email [REDACTED]. If you have any questions regarding your rights as a research subject, contact the UC San Diego IRB at 858-246-4777.

By entering survey, you agree to reading the above information and agree to participate in this research project.

Enter survey

Survey questions

Familiarity with SfM

Structure from Motion (SfM) is a technology that can be used to construct 3D models of objects or environments. SfM relies on parallax, the apparent displacement of an object when viewed from multiple different directions, to reconstruct 3D scenes from 2D photographs. If an object is captured in enough photographs from enough angles, it can be accurately rendered in 3D using SfM. This technology has many applications, including in environmental science and marine ecology. Coral reef scientists have used SfM to archive reef condition, visualize reef change over time, and conduct "virtual field work" by collecting ecological data directly from 3D reef models.

While SfM is becoming standard in academic research settings, its application in a conservation context has been more limited. We want to gauge the familiarity of conservation practitioners with SfM, better understand barriers to its adoption, and solicit ideas for how SfM could be best leveraged to add value for reef conservation practitioners.

1. Have you heard of "Structure from Motion" (SfM) before this survey? (Yes/No)

Table S1.2: Survey responses to question 1.

Respondent category		YES (%)	NO (%)	No response (%)	Total (n)
All respondents		60.0%	38.5%	1.5%	135
SfM User?	YES	98.1%	1.9%	0.0%	54
	NO	35.4%	64.6%	0.0%	79
Region	Global North	74.5%	25.5%	0.0%	51
	Global South	70.7%	29.3%	0.0%	41
Focus	Conservation	65.9%	34.1%	0.0%	41
	Science	75.4%	24.5%	0.0%	53
Sector	Academia	75.0%	25.0%	0.0%	36
	Government	73.7%	26.3%	0.0%	19
	Non-profit	76.0%	24.0%	0.0%	25

2. Have you heard of photogrammetry before this survey? (Yes/No)

Table S1.3: Survey responses to question 2.

Respondent category		YES (%)	NO (%)	No response (%)	Total (n)
All respondents		89.6%	8.9%	1.5%	135
SfM User?	YES	100.0%	0.0%	0.0%	54
	NO	84.8%	15.2%	0.0%	79
Region	Global North	96.1%	3.9%	0.0%	51
	Global South	97.6%	2.4%	0.0%	41
Focus	Conservation	100.0%	0.0%	0.0%	41
	Science	94.3%	5.7%	0.0%	53
Sector	Academia	94.4%	5.6%	0.0%	36
	Government	94.7%	5.3%	0.0%	19
	Non-profit	100.0%	0.0%	0.0%	25

3. Have you ever used SfM as part of your work? (Yes/No)

Table S1.4: Survey responses to question 4.

Respondent category		YES (%)	NO (%)	No response (%)	Total (n)
All respondents		40.0%	58.5%	1.5%	135
SfM User?	YES	100.0%	0.0%	0.0%	54
	NO	0.0%	100.0%	0.0%	79
Region	Global North	49.0%	51.0%	0.0%	51
	Global South	46.3%	53.7%	0.0%	41
Focus	Conservation	36.6%	63.4%	0.0%	41
	Science	54.7%	45.3%	0.0%	53
Sector	Academia	41.7%	58.3%	0.0%	36
	Government	47.4%	52.6%	0.0%	19
	Non-profit	56.0%	44.0%	0.0%	25

4. On a scale of 1 to 5, please rate your familiarity with SfM methods and/or software (with 1 being little to no familiarity and 5 being very familiar)
5. On a scale of 1 to 5, please rate your familiarity with SfM applications (with 1 being little to no familiarity and 5 being very familiar)
6. On a scale of 1 to 5, please rate the likelihood that you will use SfM in your work in the future (with 1 being very unlikely and 5 being very likely)

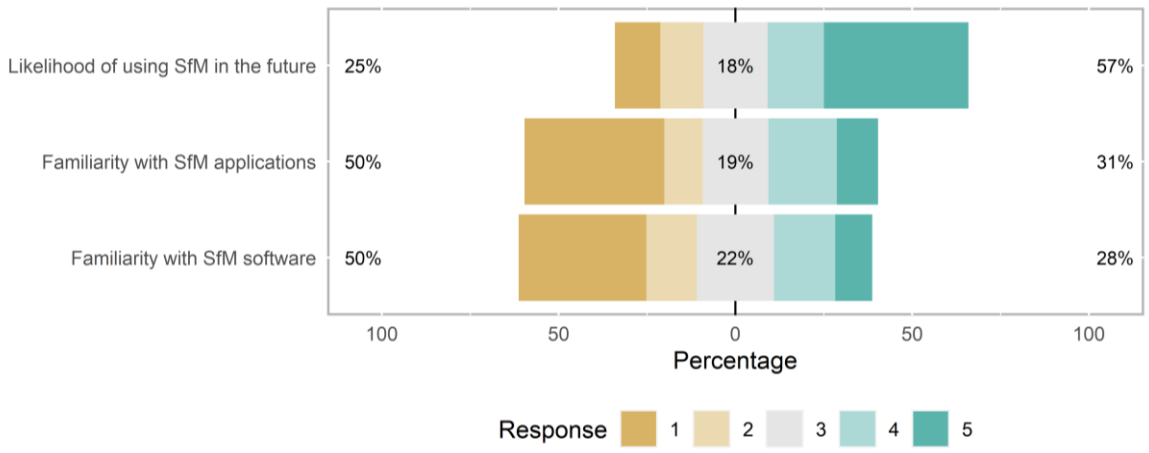

Figure S1.1: Responses to survey questions 4-6 (n = 133 for questions 4 and 6, n = 129 for question 5). Figure S1.4 shows responses to these questions broken down by demographic group (experience, region, sector, and focus).

7. In addition to this survey, we are conducting a literature review to assess how SfM has been applied to study coral reefs. If you have a project or report that uses SfM, please indicate whether you would be willing to share any information about that project. (Yes/No/NA)

Table S1.5: Survey responses to question 7.

Respondent category		YES (%)	NO (%)	NA (%)	Total (n)
All respondents		31.1%	6.7%	62.2%	135
SfM User?	YES	63.0%	5.6%	31.5%	54
	NO	10.1%	7.6%	82.3%	79
Region	Global North	41.2%	5.9%	52.9%	51
	Global South	36.6%	2.4%	70.0%	41
Focus	Conservation	31.7%	7.3%	70.0%	41
	Science	43.4%	3.8%	52.8%	53
Sector	Academia	47.2%	5.6%	47.2%	36
	Government	31.6%	0.0%	68.4%	19
	Non-profit	44.0%	8.0%	48.0%	25

8. If you answered yes, please briefly describe the purpose of your project and how SfM was/will be used (Open ended)

Barriers to adoption

9. We are interested in gauging what factors, if any, might prevent the use of Structure from Motion in a conservation context. Please rate each of the following factors on a scale of 1 to 5, with 1 signifying that the factor is not a barrier to SfM adoption, and 5 signifying that the factor is a major barrier to SfM adoption.

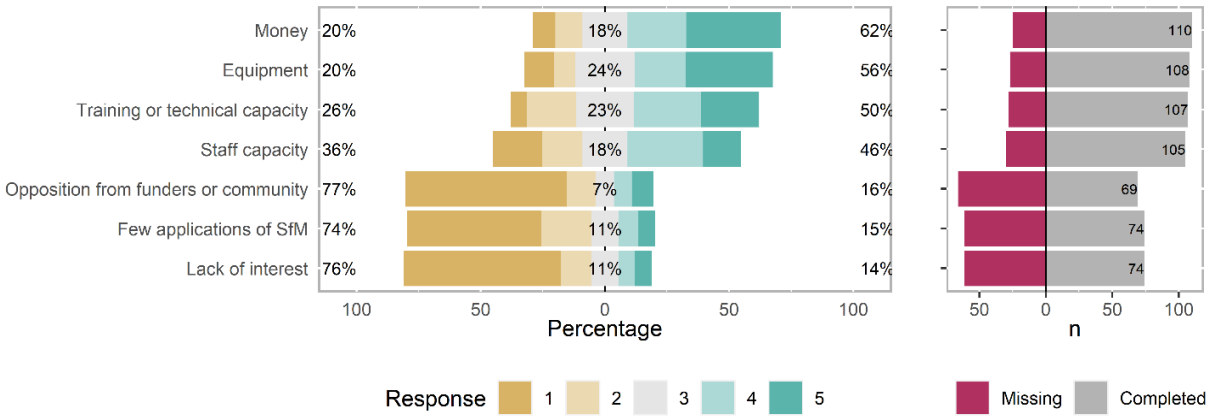

Figure S1.2: Responses to survey question 9. Figure S1.5 shows responses to question 9 broken down by demographic group (experience, region, sector, and focus).

10. Please expand on the barriers to adoption that you think are most significant and relevant to your work? (Open ended)

Potential applications

11. If capacity, data, and access to the reef were unlimited, what would you most want to know about reef dynamics? (Open ended)

12. What ecological functions or processes would be the most useful to have a better scientific understanding of, in terms of informing coral reef conservation? (Open ended)

13. Which of the following applications of SfM do you find the most exciting/important? Please rank the following in order of importance (with 1 being the most important)

14. In your view, how can SfM best add value to coral conservation efforts? (Open ended)

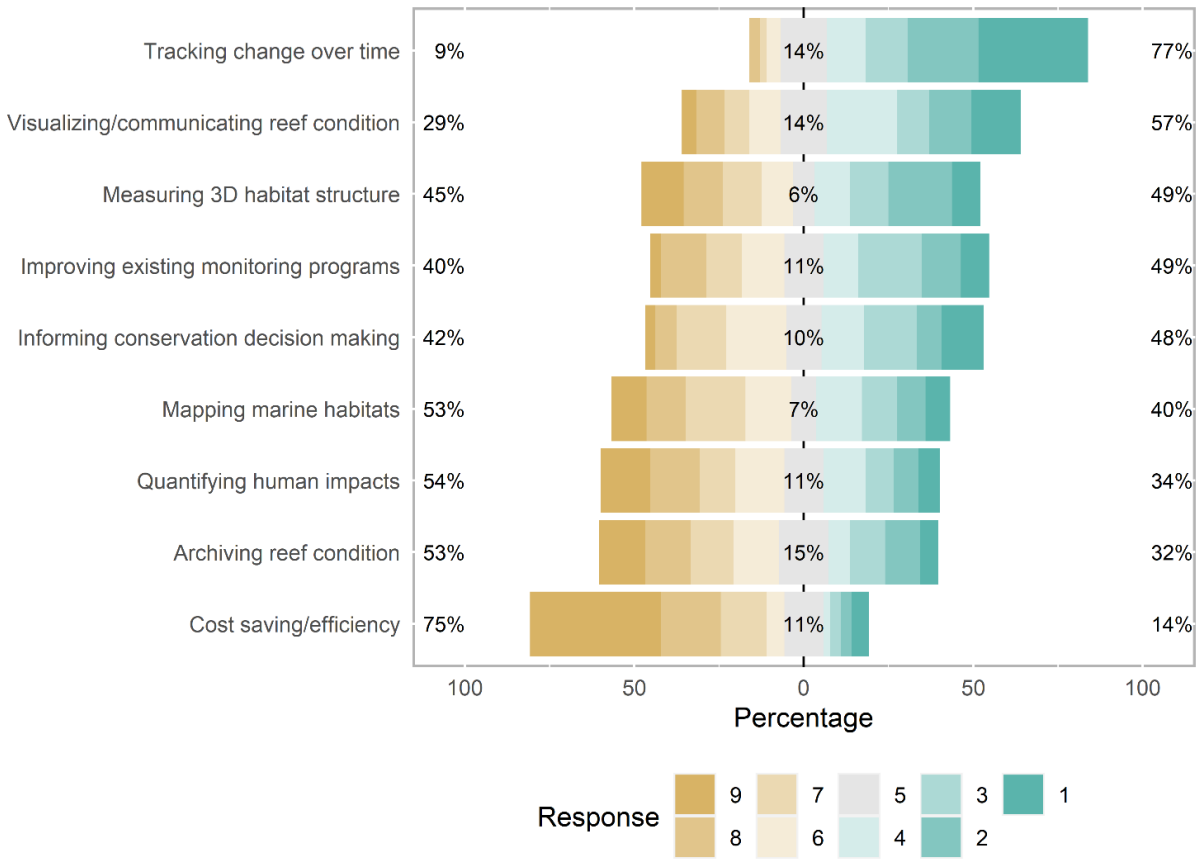

Figure S1.3: Responses to survey question 13 (n = 96). Figure S1.6 shows responses to question 13 broken down by demographic group (experience, region, sector, and focus).

Demographic questions

15. Are you part of the coral reef science or conservation community? (Yes/No)

Table S1.6: Survey responses to question 15.

Respondent category		YES (%)	NO (%)	No response (%)	Total (n)
All respondents		65.9%	5.2%	28.9%	135
SfM User?	YES	77.8%	3.7%	18.5%	54
	NO	59.5%	6.3%	34.2%	79
Region	Global North	94.1%	5.9%	0.0%	51
	Global South	95.1%	4.9%	0.0%	41
Focus	Conservation	95.1%	4.9%	0.0%	41
	Science	92.4%	7.5%	0.0%	53
Sector	Academia	91.7%	8.3%	0.0%	36
	Government	100.0%	0.0%	0.0%	19
	Non-profit	96.0%	4.0%	0.0%	25

16. If you answered no, please describe your relationship to coral reefs (Open ended)

17. What type of organization do you work for?

- Government
- Academia
- Non-profit
- Private sector
- Independent contractor
- Other (please specify)

Table S1.7: Survey responses to question 17.

Respondent category		Acad. (%)	Gov. (%)	Non-profit (%)	Private sector (%)	Ind. cont. (%)	Other (%)	No resp. (%)	Total (n)
All respondents		26.7%	14.1%	18.5%	4.4%	3.7%	2.2%	30.4%	135
SfM User?	YES	27.8%	16.7%	25.9%	5.6%	3.7%	1.9%	18.5%	54
	NO	26.6%	12.7%	13.9%	3.8%	3.8%	2.5%	36.7%	79
Region	North	49.0%	21.6%	13.7%	3.9%	7.8%	3.9%	0.0%	51
	South	24.4%	19.5%	41.5%	9.8%	2.4%	2.4%	0.0%	41
Focus	Conserv.	19.5%	24.4%	41.5%	7.3%	2.4%	2.4%	2.4%	41
	Science	52.8%	15.1%	15.1%	5.7%	7.5%	3.8%	0.0%	53

18. If you selected “Other” for question 17, please specify (Open ended)

19. How many years of experience in marine conservation do you have?

Table S1.8: Survey responses to question 19.

Respondent category		Years (avg.)
All respondents		15.6
SfM User?	YES	13.4
	NO	15.7
Region	Global North	14.6
	Global South	14.9
Focus	Conservation	13.8
	Science	15.0
Sector	Academia	13.5
	Government	16.0
	Non-profit	14.3

20. If you had to choose, would you consider your work to be more focused on science or conservation?

Table S1.9: Survey responses to question 20.

Respondent category		Science (%)	Conservation (%)	No response (%)	Total (n)
All respondents		39.3%	30.4%	30.4%	135
SfM User?	YES	53.7%	27.8%	18.5%	54
	NO	30.4%	32.9%	36.7%	79
Region	Global North	70.6%	27.4%	2.0%	51
	Global South	41.5%	58.5%	0.0%	41
Focus	Conservation	0.0%	100.0%	0.0%	41
	Science	100.0%	0.0%	0.0%	53
Sector	Academia	77.8%	22.2%	0.0%	36
	Government	42.1%	52.6%	2.8%	19
	Non-profit	32.0%	68.0%	0.0%	25

21. What country is your organization based in? (Open Ended)

Table S1.10: Survey responses to question 21.

Count	Country or Territory	Region	North vs. South
32	United States	North America	Global North
2	Mexico	North America	Global South
2	Belize	Caribbean	Global South
1	Canada	North America	Global North
1	Honduras	North America	Global South
7	US Virgin Islands	Caribbean	Global South
3	Curacao	Caribbean	Global South
1	Bahamas	Caribbean	Global South
1	Bonaire	Caribbean	Global South
1	Caribbean	Caribbean	Global South
1	Cayman Islands	Caribbean	Global South
1	Haiti	Caribbean	Global South
1	Jamaica	Caribbean	Global South
1	Puerto Rico	Caribbean	Global South
2	Colombia	South America	Global South
1	Brazil	South America	Global South
1	Egypt	Africa	Global South
1	Kenya	Africa	Global South
1	Mauritius	Africa	Global South
1	Seychelles	Africa	Global South
1	South Africa	Africa	Global South
1	Tanzania	Africa	Global South
3	United Kingdom	Europe	Global North
1	Portugal	Europe	Global North
1	Switzerland	Europe	Global North
4	Indonesia	Asia	Global South
3	Japan	Asia	Global North
2	United Arab Emirates	Asia	Global South
1	Hong Kong	Asia	Global North
1	India	Asia	Global South
1	Iran	Asia	Global South
1	Malaysia	Asia	Global South
9	Australia	Oceania	Global North
3	Marianas Islands/Guam	Oceania	Global South
1	French Polynesia	Oceania	Global South
43	No response	NA	NA

22. How did you hear about this survey?

- coral-list listserv
- Coral Restoration Consortium mailing list
- Mideast Coral Reef Society listserv
- MPA Help or EBM Help listservs
- Social media (i.e., twitter, Facebook, etc.)

Table S1.11: Survey responses to question 22.

Respondent category		coral-list (%)	CRC (%)	MCRS (%)	MPA Help (%)	Soc. media (%)	Other (%)	No resp. (%)	Total (n)
All respondents		21.5%	28.9%	3.0%	1.5%	4.4%	8.1%	32.6%	135
SfM User?	YES	24.1%	35.2%	0.0%	1.9%	3.7%	9.3%	25.9%	54
	NO	20.3%	25.3%	5.1%	1.3%	5.1%	7.6%	35.4%	79
Region	North	31.4%	37.3%	0.0%	2.0%	3.9%	17.6%	7.8%	51
	South	31.7%	46.3%	7.3%	2.4%	7.3%	4.9%	0.0%	41
Focus	Conserv.	22.0%	58.5%	7.3%	0.0%	7.3%	4.9%	0.0%	41
	Science	37.7%	28.3%	1.9%	3.8%	3.8%	17.0%	7.5%	53
Sector	Academia	36.1%	19.4%	5.6%	2.8%	5.6%	22.2%	8.3%	36
	Gov.	36.8%	47.4%	2.8%	0.0%	2.8%	0.0%	2.8%	19
	Non-prof.	16.0%	72.0%	0.0%	0.0%	8.0%	4.0%	0.0%	25

23. If you selected “Other” for question 22, please specify (Open ended)

24. Would you be willing to discuss your survey responses in a 30 min Zoom interview? (Yes/No)

Table S1.12: Survey responses to question 24.

Respondent category		YES (%)	NO (%)	No response (%)	Total (n)
All respondents		40.0%	30.4%	29.6%	135
SfM User?	YES	55.6%	25.9%	18.5%	54
	NO	30.4%	34.2%	35.4%	79
Region	Global North	62.7%	37.3%	0.0%	51
	Global South	53.7%	46.3%	0.0%	41
Focus	Conservation	61.0%	39.0%	0.0%	41
	Science	54.7%	45.3%	0.0%	53
Sector	Academia	47.2%	52.8%	0.0%	36
	Government	47.4%	52.6%	0.0%	19
	Non-profit	64.0%	36.0%	0.0%	25

25. If you answered yes to question 24, please enter your email address

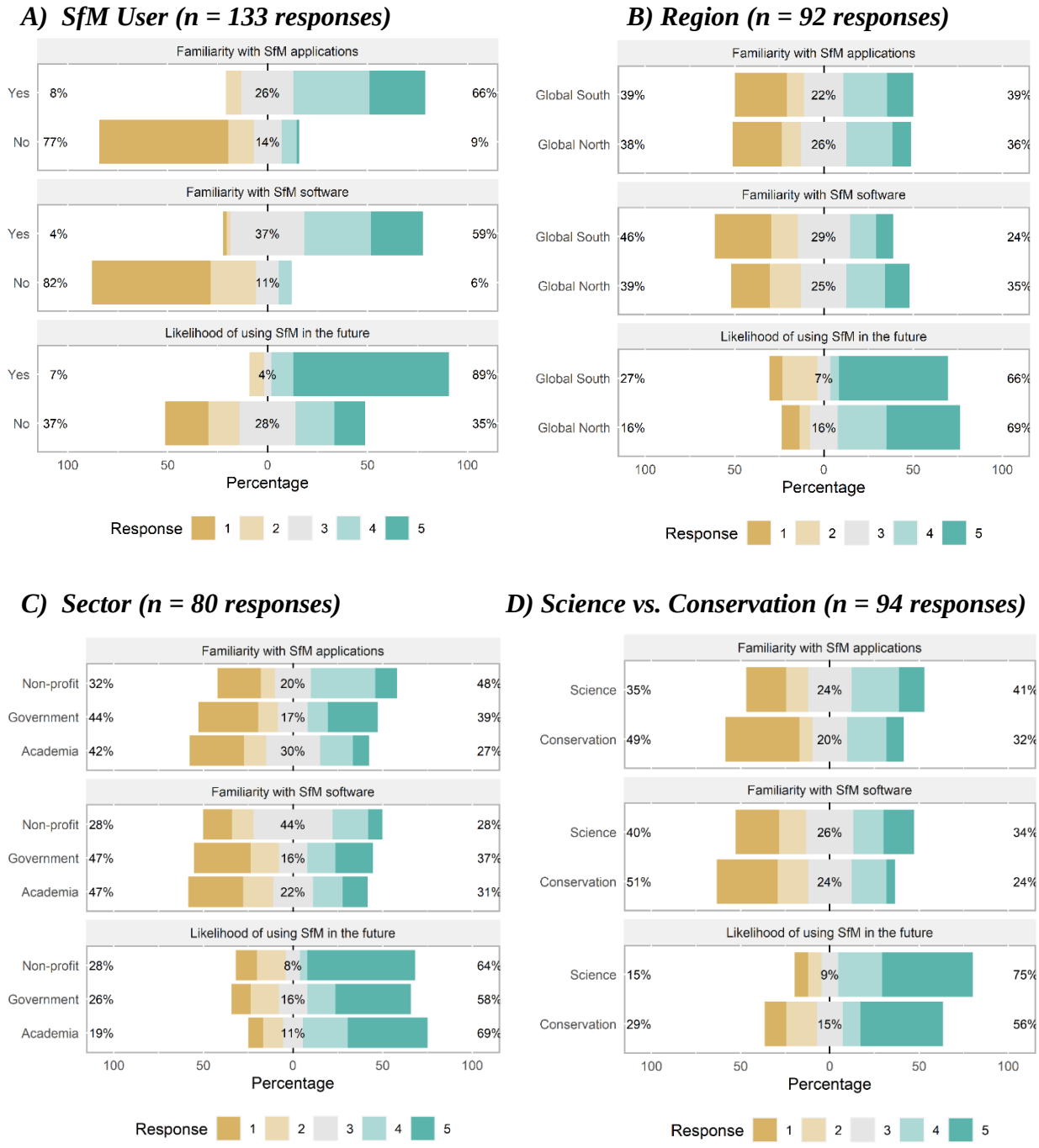

Figure S1.4: Responses to survey questions 4-6 are shown for individual demographic groups: A) prior exposure to Structure from Motion (SfM), B) region (Global North vs. Global South), C) sector (academia, government, or non-profit), and D) focus (conservation or science). Responses are shown on a Likert scale, with 1 indicating low familiarity or low likelihood of using SfM in the future, and 5 indicating high familiarity or high likelihood of using SfM in the future.

A) SfM User

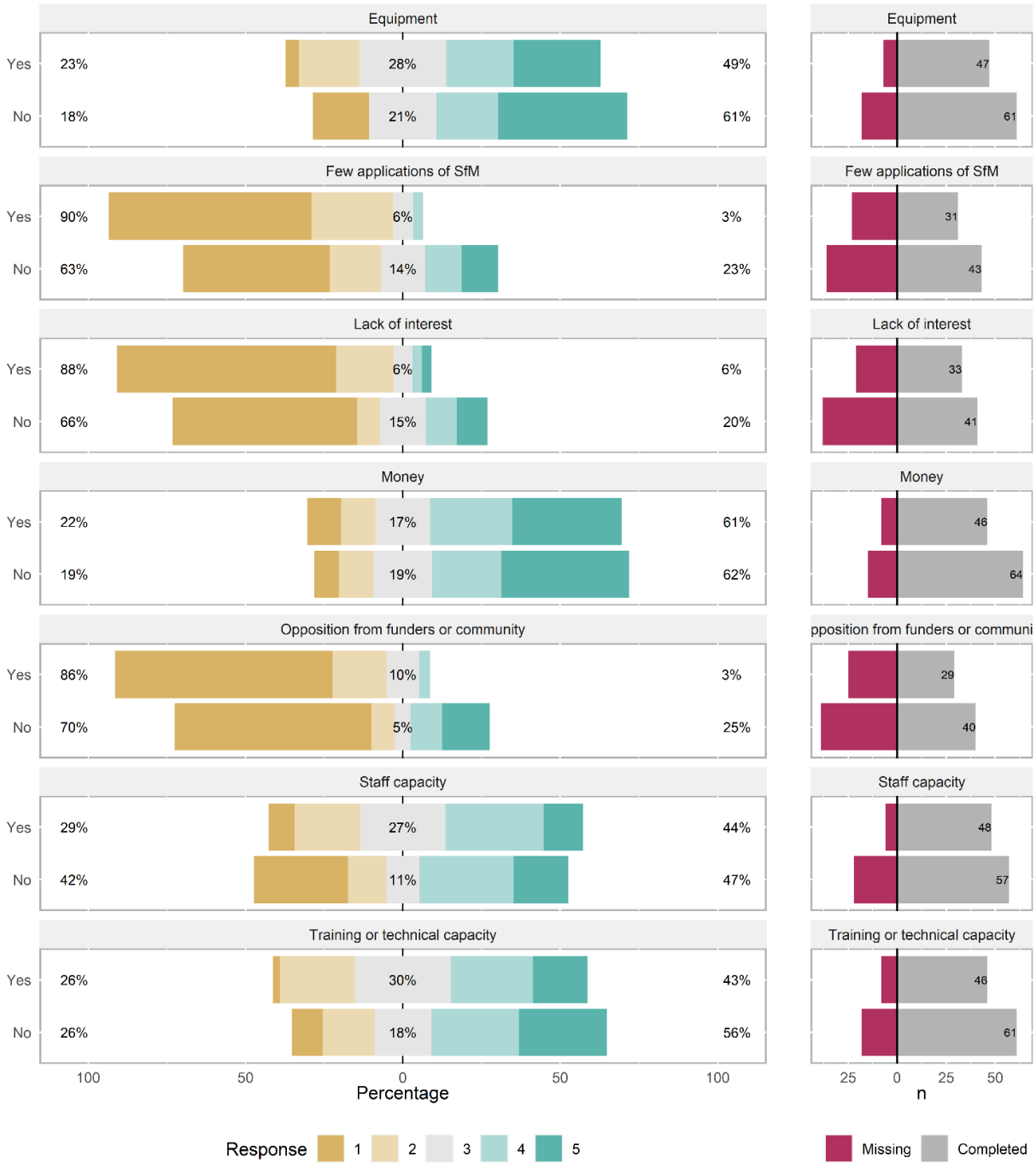

Figure S1.5A: Responses to survey question 9 are shown based on prior exposure to Structure from Motion (SfM). Responses are shown on a Likert scale, with 1 signifying that the factor is not a barrier to SfM adoption, and 5 signifying that the factor is a major barrier to SfM adoption.

B) Region

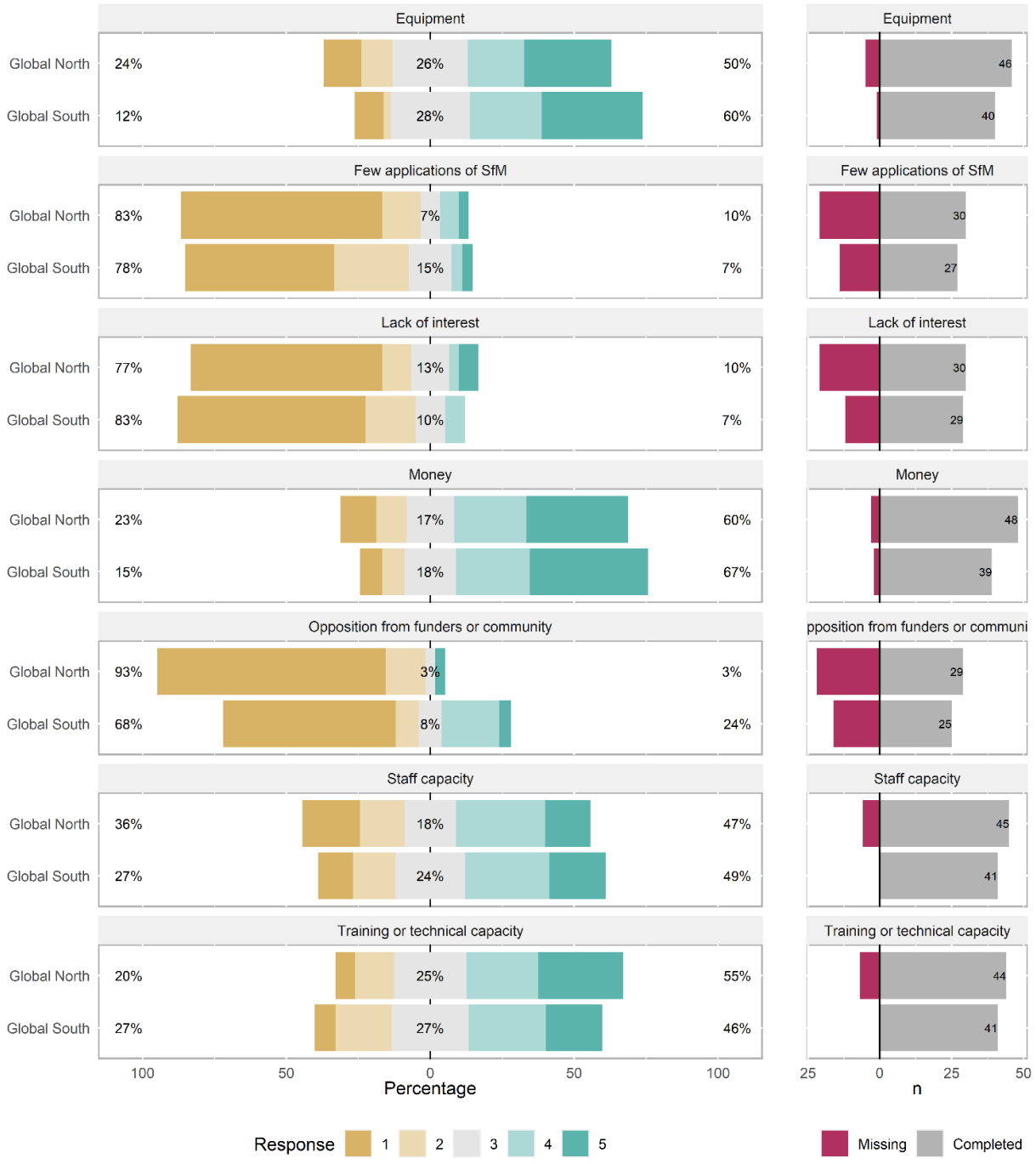

Figure S1.5B: Responses to survey question 9 are shown based on the region (Global North vs. Global South) where the survey respondent worked. Responses are shown on a Likert scale, with 1 signifying that the factor is not a barrier to SfM adoption, and 5 signifying that the factor is a major barrier to SfM adoption.

C) Sector

Figure S1.5C: Responses to survey question 9 are shown based on the sector (academia, government, or non-profit) in which the survey respondent worked. Responses from respondents who worked in the private-sector, as independent contractors, or who listed "other" as their sector are not shown due to small sample sizes. Responses are shown on a Likert scale, with 1 signifying that the factor is not a barrier to SfM adoption, and 5 signifying that the factor is a major barrier to SfM adoption.

D) Science vs. Conservation

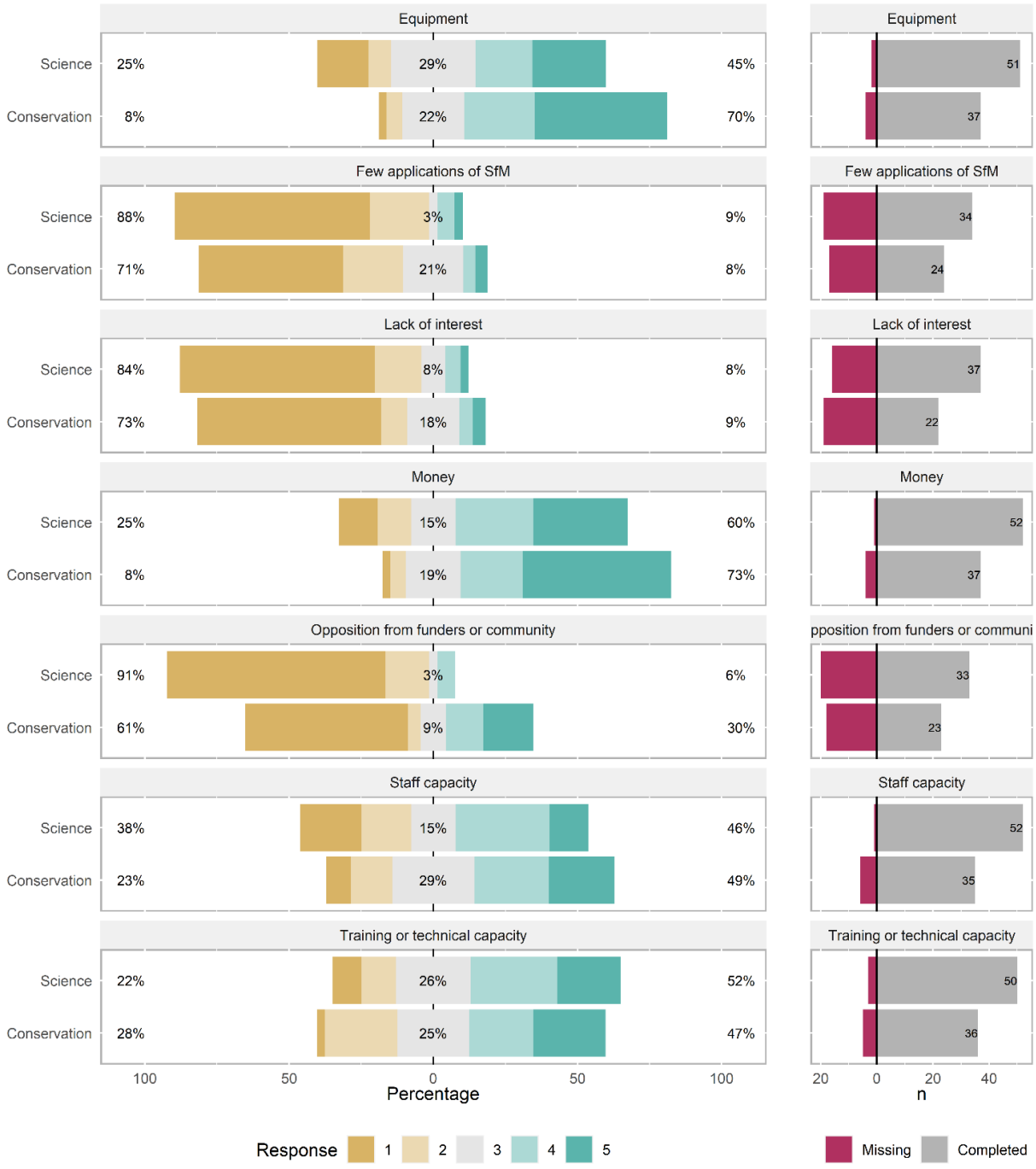

Figure S1.5D: Responses to survey question 9 are shown based on whether respondents classified their work as primarily focused on science or on conservation. Responses are shown on a Likert scale, with 1 signifying that the factor is not a barrier to SfM adoption, and 5 signifying that the factor is a major barrier to SfM adoption.

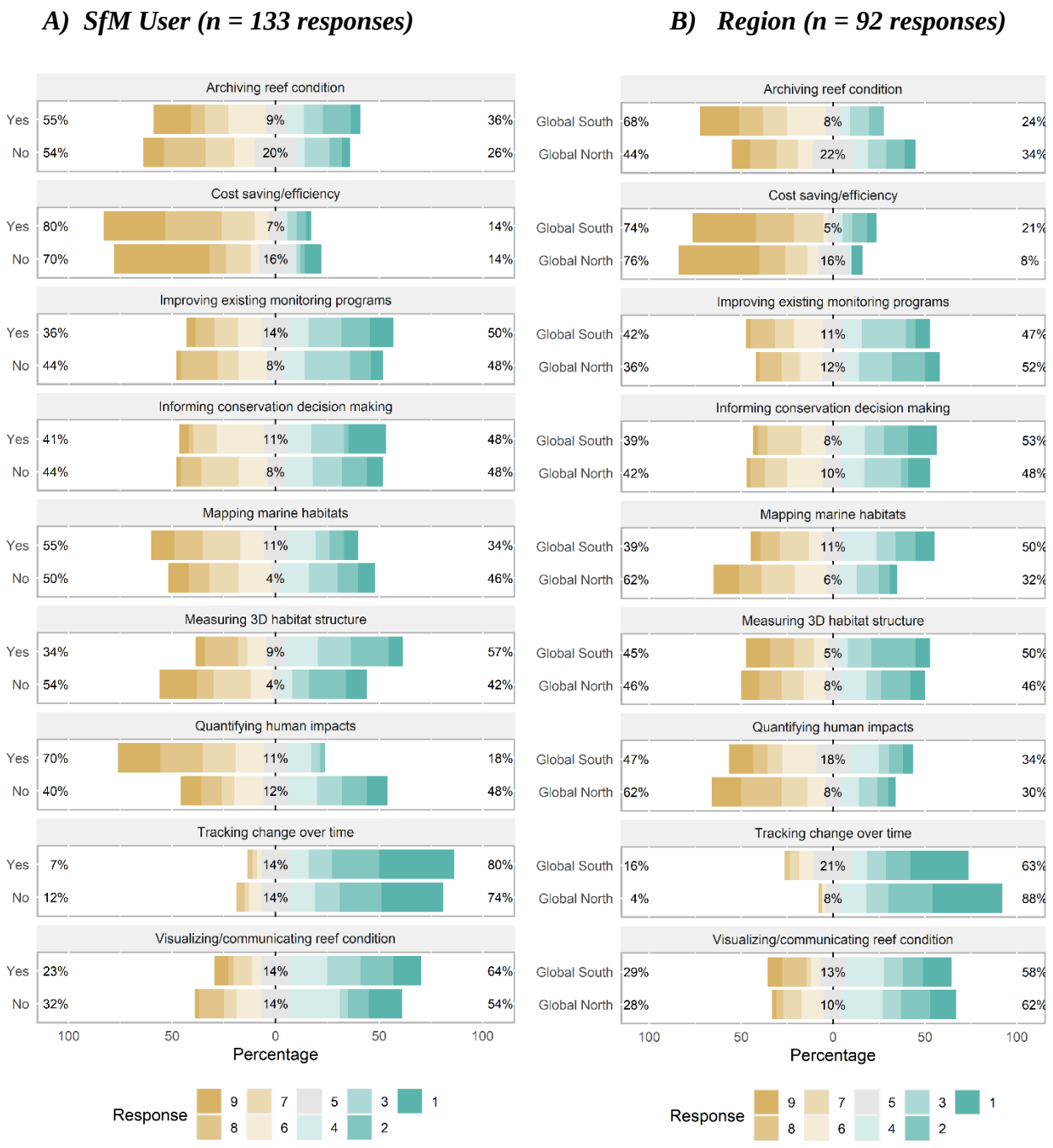

Figure S1.6A-B: Responses to survey question 13 are shown for individual demographic groups: A) prior exposure to Structure from Motion (SfM) and B) region (Global North vs. Global South). Respondents were asked to rank potential applications of SfM from 1 to 9 (with 1 being the most important).

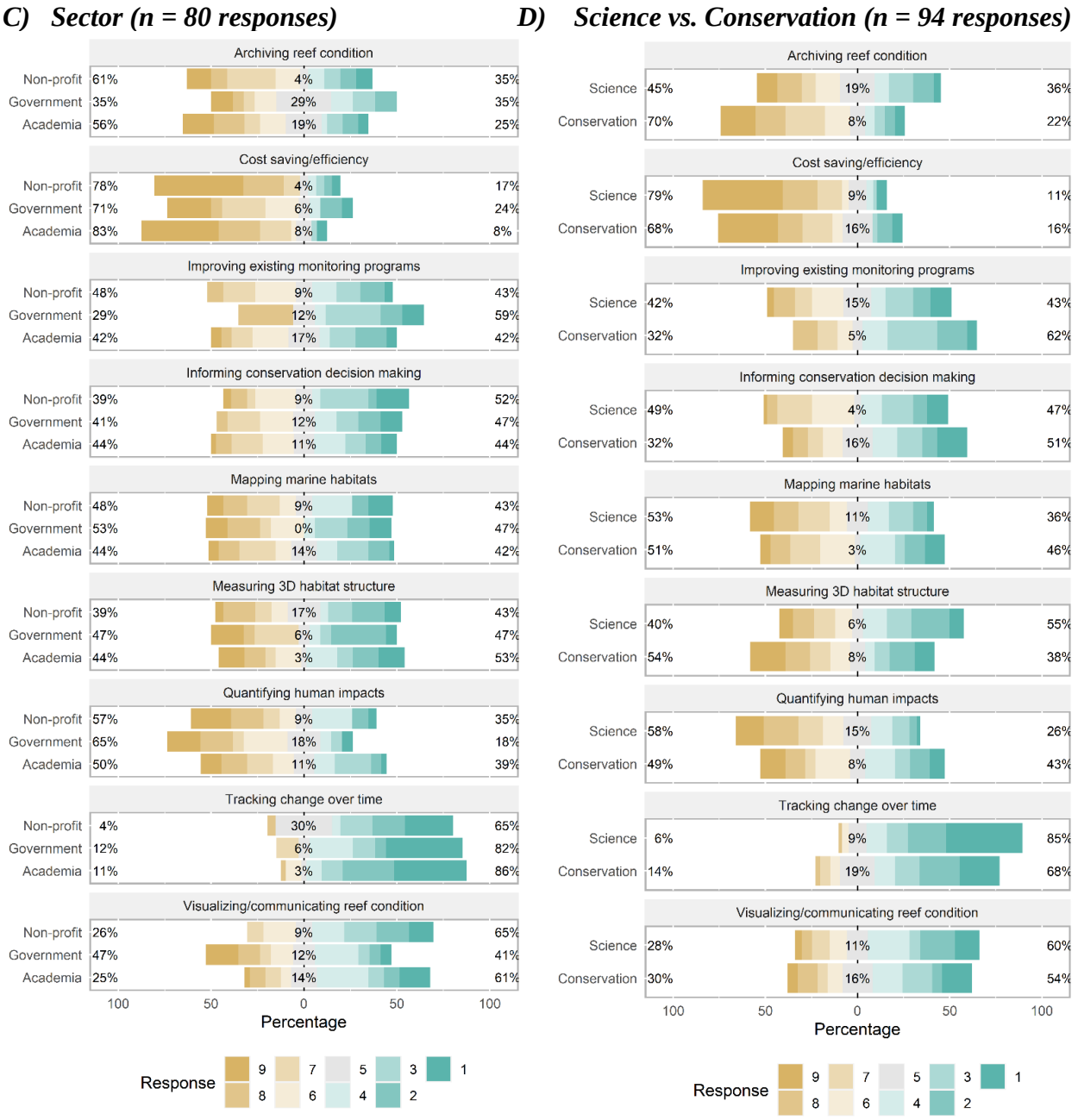

Figure S1.6C-D: Responses to survey question 13 are shown for individual demographic groups: C) respondent sector (academia, government, or non-profit), and D) focus (conservation or science). Respondents were asked to rank potential applications of SfM from 1 to 9 (with 1 being the most important).

Appendix 2: Supplemental Materials for Chapter 2 (Identifying the drivers of structural complexity on Hawaiian coral reefs)

Contents

Sampling design: sites per island

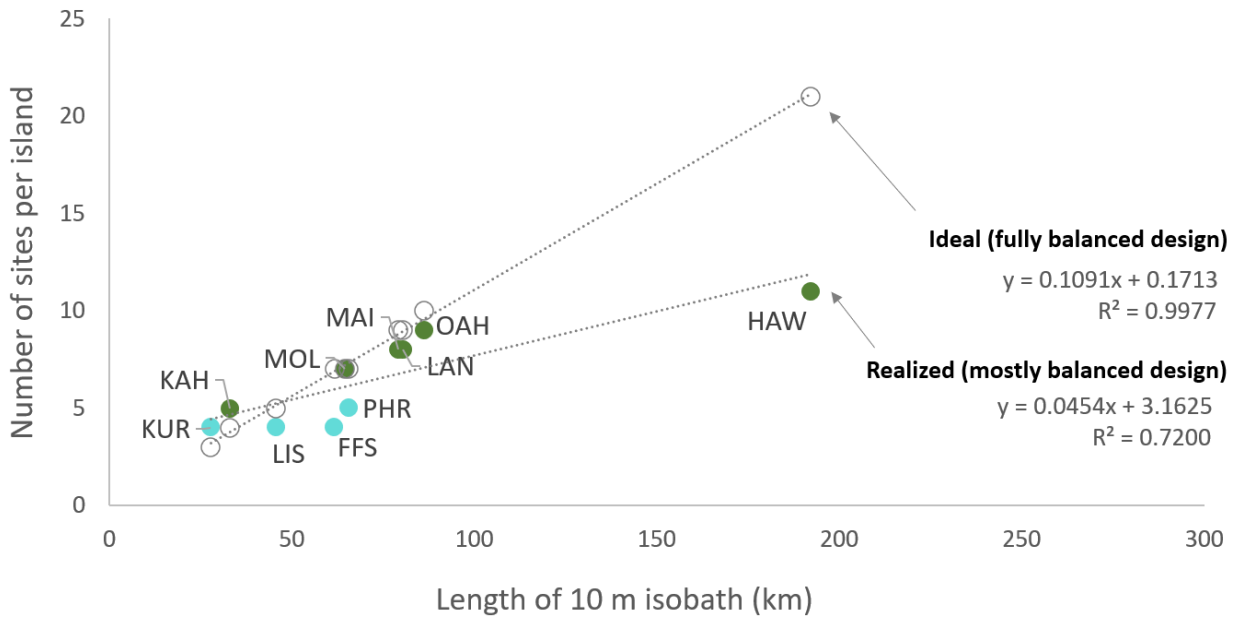

Figure S2.1: The relationship between sampling effort (i.e., the number of sites per island) and the amount of nearshore habitat, represented here by the length of each island's 10 m isobath. For the Main Hawaiian Islands, only leeward coastline was considered since all study sites were located on the leeward side of islands to control for wave energy. Leeward coastline was defined as the length of the continuous 10 m isobath with an average long-term wave energy of < 10 kW/m using data from Wedding et al. 2018. The full length of the 10 m isobath was used for the Northwest Hawaiian Islands since sites were not confined to the leeward side of atolls in this region. Logistical constraints limited sampling effort in the Northwest Hawaiian Islands to 4-5 sites per island. Additional sites from the island of Hawai'i were surveyed, but low image quality necessitated the exclusion of several sites from this analysis. For those reasons, Hawai'i, Pearl and Hermes, French Frigate Shoals, and Lisianski are under-sampled compared to a fully balanced design. Sites were surveyed between July 2016 and August 2017 as part of five separate research expeditions. Scripps researchers, in collaboration with NOAA, surveyed sites in the Northwest Hawaiian Islands as part of the 2016 Hawaiian Archipelago Reef Assessment and Monitoring (HARAMP) cruise from July to September 2016. The 100 Island Challenge team at Scripps surveyed sites on O'ahu in March 2017 and on Moloka'i, Kaho'olawe, and Lāna'i in April 2017. A separate team of researchers from Scripps and The Nature Conservancy surveyed sites along the Kona coast of Hawai'i in April 2017. Finally, researchers from the Smith Lab at Scripps led a research expedition to Maui from July to August 2017 as part of an annual monitoring program. Sites were surveyed using similar methods across research expeditions.

Diagram of site setup in situ

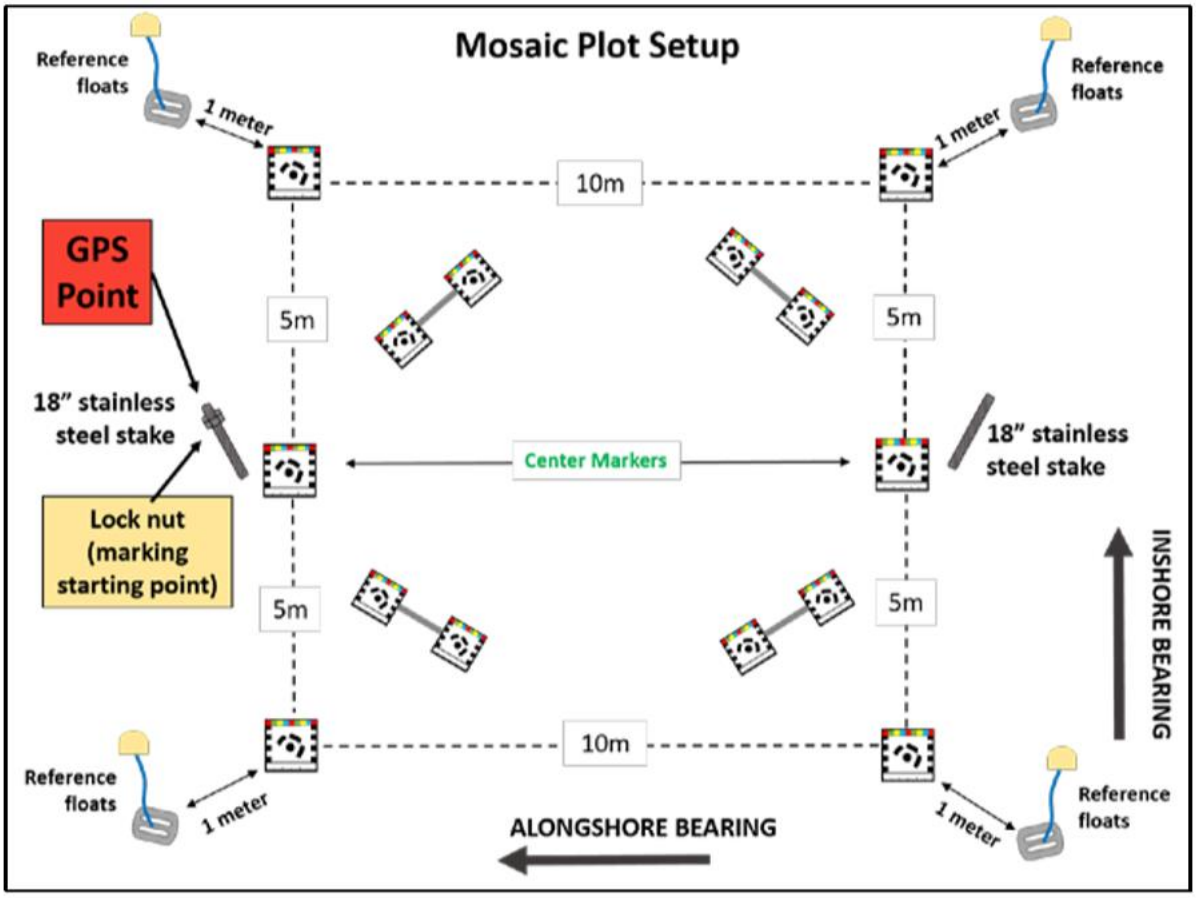

Figure S2.2: A diagrammatic overview of procedures for delineating each site *in situ*. Each site was (typically) marked by two stainless steel pins, one of which corresponded to a GPS point. A diver placed six calibration tiles to delineate the boundaries of a 10 x 10 m site, along with reference floats 1 m away from each corner of the site. These floats marked the boundaries of image collection by the diver, and ensured a minimum 1 m buffer around the edge of the site, which is marked by the calibration tiles. After marking the boundaries of the site, the diver measured the depth of each calibration tile and placed four 50 cm scale bars within the site. These bars were used during model post processing to scale the model, while the depth values taken at each of the calibration tiles were used to orient the model with respect to the sea surface. The second diver swam in a gridded pattern over the site, capturing images while swimming in both the alongshore and inshore directions to ensure maximum photo coverage. Each dive typically lasted about 50 to 60 minutes.

Percent cover power analysis

The Virtual Point Intercept (VPI) tool in Viscore generates a user-determined number of stratified random points within a fixed area. Once these points have been generated, their location is superimposed on the raw imagery used to construct the Structure from Motion point cloud, allowing users to identify benthic taxa directly from high quality photographs. Determining how many stratified random points to use requires a tradeoff between precision of benthic cover estimates and time spent analyzing images. In our experience, it takes a coral and algae ID expert approximately 15 to 20 minutes to identify benthic cover at 100 points. To strike an appropriate balance between precision and analysis time, we conducted a power analysis using fully annotated 3 x 3 m orthoprojections from five sites in Maui. We considered these orthoprojection annotations to be "true" representations of benthic cover on the reef for this exercise. The orthoprojections were sampled in a stratified random manner in R using various VPI point densities, from 1 to 400 points/m^2. This process was repeated 10,000 times. For each VPI point density, we calculated the percent of simulations in which a benthic class wasn't detected, and determined the relationship between this detection probability and percent cover.

Based on our results, we recommend using 25 points/m^2 for research questions focused on quantifying community composition, detecting rare taxa, or documenting benthic change over time. At this point density, we were able to detect taxa with 1.1% cover in 95% of simulations, and would expect VPI analysis to take approximately 6 to 8 hours for one 10 x 10 m site. For studies where a rapid or coarse descriptor of benthic cover is sufficient (i.e., calculating total coral cover or identifying the most dominant taxon on the reef), we suggest 10 points/m^2 as a sufficient tradeoff between precision and efficiency. At this point density, we were able to detect taxa with 3.0% cover in 95% of simulations, and would expect VPI analysis to take only 2.5 to

3.5 hours for one 10 x 10 m site. Since our study deals with large differences in total coral cover across an entire archipelago (sites ranging from 0 to 82% coral cover) rather than more minute differences in coral cover (i.e., from change over time), we felt comfortable with the precision provided by VPI at 10 points/m^2. Past studies have also found that this point density provides qualitative and reliable measures of percent cover (Dumas et al. 2009).

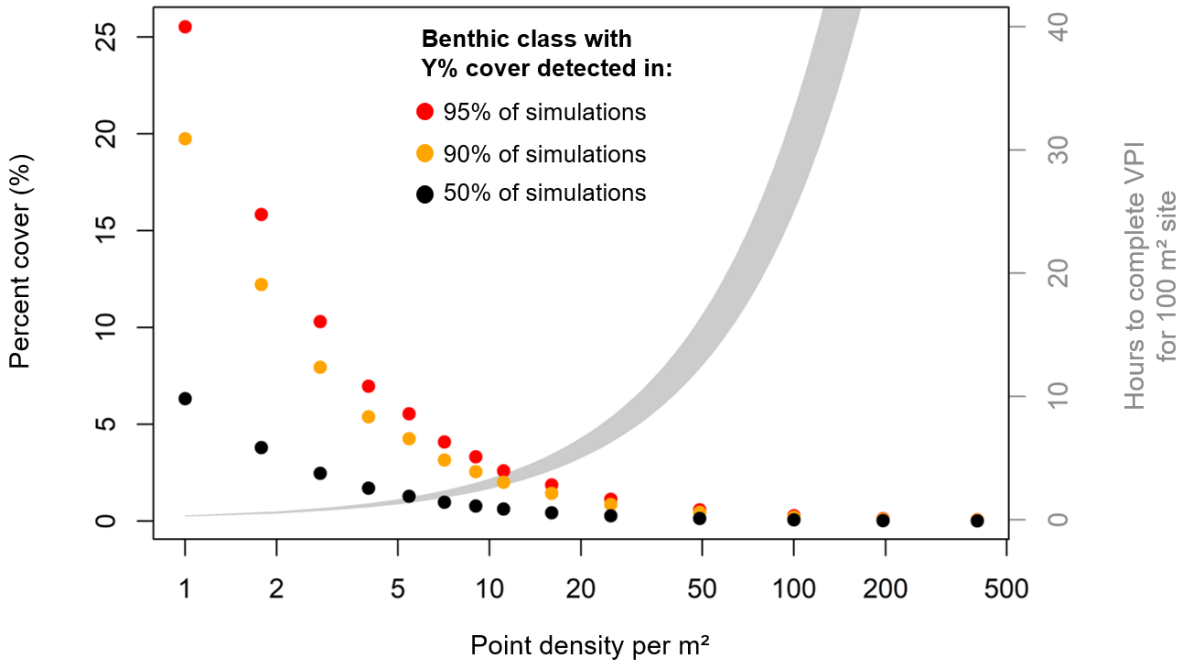

Figure S2.3: Results from a power analysis of percent cover point densities. The probability of detecting a benthic class with Y% cover is shown as a function of VPI point density. For example, a taxon that covers 1.1% of the benthos would be detected 95% of the time using a VPI point density of 25 points/m^2. The shaded gray polygon depicts the estimated amount of time it would take to complete benthic ID for a 100m^2 site as a function of VPI point density.

Data simulation to test fractal dimension approach

To explore the robustness of the fractal dimension approach, we measured the fractal dimension of six simulated reef profiles across 9 scale intervals. Each 10.24 m long profile was simulated using a combination of sine curves meant to generate combinations of fine-, intermediate-, and large-scale structure (Figure S2.4). Fine-scale sine curves were meant to simulate a reef with 25 cm diameter coral colonies and intra-colony features every 6.25 cm (Equation 1), while intermediate-scale sine curves were meant to simulate a reef with 50 cm diameter coral colonies and intra-colony features every 12.5 cm (Equation 2). Large-scale sine curves were meant to simulate underlying landscape topography, and had a period of several meters (Equation 3). For the purposes of the simulation, we interpreted values of D > 1.01 as evidence of reef structure at a given scale interval. We used the maximum value of D across scales (D_{max}) to identify the scale interval with the greatest rate of change in rugosity. Patterns of fractal dimension for these reef profiles provided context to aid in the interpretation of reef profiles obtained using Structure from Motion.

$$\textbf{Eq. 1}: \quad Y = 0.5\left(0.25\left|\sin\left(\frac{x}{16}\right)\right| + 0.05sin\left(\frac{x}{2}\right)\right)$$

$$\textbf{Eq. 2}: \quad Y = 0.5\left(0.25\left|\sin\left(\frac{x}{32}\right)\right| + 0.1\left|\sin\left(\frac{x}{8}\right)\right|\right)$$

$$\textbf{Eq. 3}: \quad Y = \sin\left(\frac{\mathrm{x}}{200}\right) + 0.25\sin\left(\frac{x}{50}\right)$$

The fractal dimension (D) of simulated reef profiles differed depending on the scale of the underlying structures that were simulated (Figure S2.3). The fine-scale sine curve had D > 1.01 at five scale intervals (from 0.5-1 cm to 8-16 cm), and D_{max} occurred at the 2-4 cm scale

interval (D = 1.371). Similarly, the intermediate-scale sine curve had D > 1.01 at six scale intervals (from 0.5-1 cm to 16-32 cm), with D_{max} at the 4-8 cm scale interval (D = 1.139). For the large-scale sine curve, D > 1.01 at five scale intervals (from 8-16 cm to 128-256 cm), and D_{max} occurred at the 128-256 cm scale interval (D = 1.169). The reef profile with no underlying structure never had a value of D > 1.01. Reef profiles with a combination of fine-, intermediate-, and large-scale sine curves had more nuanced patterns of fractal dimension across scales. At the largest scale intervals (between 32 and 256 cm), profiles with large-scale sine curves had nearly identical values of D, regardless of the presence or absence of fine- or intermediate-scale curves. Differences in D were more pronounced between profiles at smaller scales (between 0.5 and 16 cm), although overall trends in D were similar for profiles with fine- and intermediate-scale sine curves regardless of the presence of large-scale sine curves.

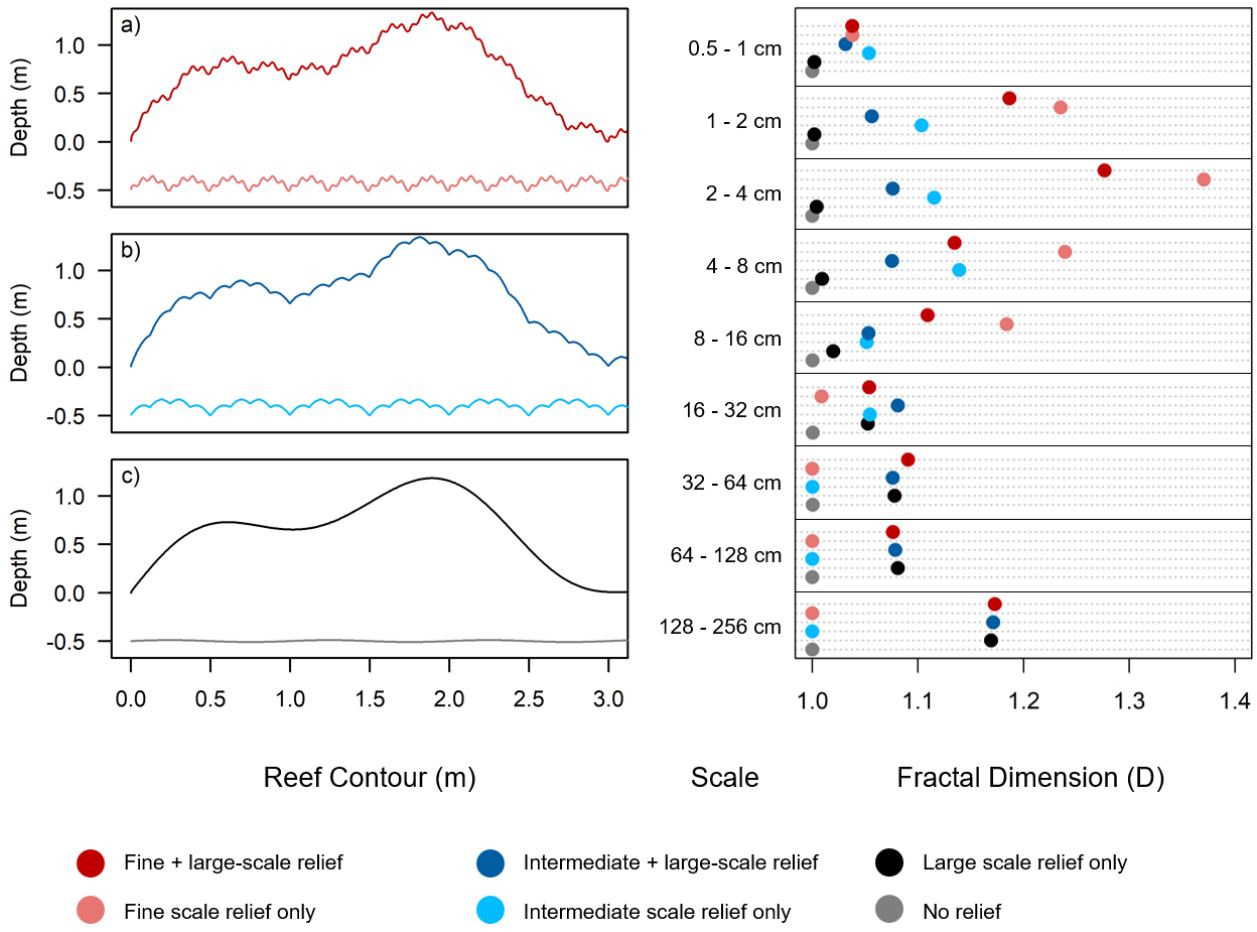

Figure S2.4: Simulated reef profiles with A) fine-scale relief, B) intermediate-scale relief, and C) no fine- or intermediate-scale relief. In each case, an underlying curve was added to one of the two profiles to simulate large-scale relief (red, dark blue, and black profiles respectively). Simulated reef profiles were 10.24 m long, but only the first 3 m are visualized here. D) The fractal dimension of each simulated reef profile is shown across nine scale intervals. Profiles where fine-scale relief were simulated (pink, red) have higher fractal dimension at smaller scale intervals, while the profile with only large-scale relief (black) exhibits a fractal signature only at larger scale intervals.

Overview of the Virtual Profile Gauge tool in Viscore

Viscore's Virtual Profile Gauge tool (VPG) is designed to mimic a profile gauge, a commonly used apparatus for measuring the contour of surfaces that has been used to measure the structural complexity of reefs *in situ* (McCormick 1994). A profile gauge consists of a series of parallel rods in a linear frame. When placed on the substrate, the rods slide independently to rest on the shallowest object beneath, approximating the contour of the substrate along a line. Measuring the substrate along a line is advantageous because it produces an easily interpretable, one-dimensional metric of complexity that can be interrogated to explore cross-scale patterns of 3D structure. One-dimensional measures of 3D structure also have direct analogues to standard *in situ* monitoring tools, such as a chain and tape or profile gauge. Specifically, VPG uses a series of virtual cylindrical rods to measure the vertical height of the point cloud along virtual transects. Viscore allows users to select the number of rods per transect, the length of the transects, the number of transects, and the orientation of the transects with respect to the point cloud (Figure S2.4).

Before VPG analysis can be performed, the point cloud must be scaled and oriented with respect to the surface using measurements made *in situ*. Viscore allows users to manually adjust the scale of the point cloud using *in situ* distance measurements, and to orient the point cloud with respect to the sea surface using four or more *in situ* depth measurements. Following current field protocols for surveying a site, divers place four 50 cm scale bars within the boundaries of the site and record the depth at six points (the four corners of the site and two points midway along the site's inshore boundaries). Point cloud orientation is particularly important because VPG's virtual rods extend orthogonally from the hypothetical sea surface to the model below.

All virtual rods have the same diameter and are directly adjacent to each other so that the height of the point cloud is continuously assessed along the length of each transect (Figure S2.5A).

To determine the position of the substrate under each rod, Viscore records the depth (Z coordinate) of the shallowest point encountered within the diameter of the rod, and uses the center of the rod as the XY coordinates. This approach is necessary because the point cloud is made up of ideal mathematical points separated by empty space. As the diameter of a profile gauge rod approaches zero, the likelihood increases that the rod will fail to encounter any point in the point cloud. In practice, we have found that profile gauge rods with a diameter of ≥0.25 cm are sufficient to avoid this issue. The output of VPG is a .csv file where each row contains the XYZ coordinates of a profile gauge rod terminus, along with its associated transect number, rod number, and rod spacing (i.e., resolution).

Calculating linear rugosity

Linear rugosity is calculated using the .csv output described above. This point data is used to calculate the length of the reef contour along each transect by summing the Euclidean distance between points. For each transect, contour distance is divided by transect length to calculate linear rugosity (Rugosity = Contour Distance / Transect Length). To determine the true length of the transect in three-dimensional space, we calculated transect length in this study as the length of the best fit regression of transect points. This approach allowed us to accounts for the slope of the substrate. However, in other circumstances that approach would not be appropriate, such as when measuring the same location to detect change in rugosity over time. When measuring the same location repeatedly over time, using the “horizontal distance" traversed by the profile gauge in XY space as denominator of linear rugosity would be more advisable since it would create consistent profile gauge lengths in each timestep. Since no single

approach is correct in all circumstances, the choice of how to calculate linear rugosity is dependent on the user's study goals and entirely independent from the mechanics of the VPG tool.

Following the approach in our study, a linear rugosity value of 1 indicates that the substrate has no surface roughness (i.e., that the reef contour is equivalent to the best fit line along the transect), although the substrate may have an overall slope. Values of linear rugosity greater than 1 occur when the reef contour is longer than the overall transect, and progressively higher linear rugosity values correspond to greater levels of structural complexity.

Accounting for missing or erroneous points

Point clouds are approximations of reality, and cannot reliably reconstruct all aspects of the substrate. For example, sections of the substrate that are difficult to photograph or that appear in too few photographs (e.g., holes, crevices, overhangs, or the interstitial space within a coral colony) may not be resolved using Structure from Motion, creating gaps in the point cloud reconstruction. Point cloud gaps may also arise if photographs are taken without enough overlap (i.e., if a diver swam too fast or if camera passes were too far apart). In addition, blurry or low-quality photographs, or the movement of sessile organisms such as macroalgae or gorgonians, may result in low confidence or erroneous "floating points" in point cloud reconstructions.

If a virtual profile gauge rod is positioned over a gap in the point cloud, or if the width of the rod is too small relative to the resolution of the point cloud, that virtual rod will not intersect the point cloud. When this occurs, VPG records a special value to denote the missing point that can be easily identified and filtered in post-processing. When calculating linear rugosity from VPG output data, segments of each transect with missing values are excluded from rugosity calculations (Figure S2.5B). Where VPG encounters floating points, users must manually

identify these instances and replace that point's depth with a special value in the .csv output file to signify a missing point. For this reason, it is not advisable to use VPG to measure rugosity when models have more than a few floating points. In those instances, the photographs that are causing reconstruction errors should be identified, and the model reconstructed without those photos to minimize the number of floating points. Alternatively, if the point cloud was exported from Agisoft Metashape with information about point confidence (i.e., the confidence in the accuracy of each point in the point cloud in 3D space), then this value can be used to automatically filter out points that are likely erroneous.

Sub-setting virtual profile gauges to simulate coarser levels of resolution

Measurements of structural complexity are highly scale dependent, and it is thus important to account for the scale at which linear rugosity is measured. VPG resolution (i.e., the spacing of virtual profile gauge rods) is analogous to the minimum grain size for the purpose of rugosity calculations. The reef contour data that is generated by VPG and used to calculate rugosity can be sub-sampled to simulate rugosity measurements from coarser levels of resolution, which allows users to easily measure linear rugosity of the same surface at multiple scales. To simulate coarser levels of resolution, the user selects a sub-set interval n, which divides each profile gauge into segments of n virtual rods. For example, if the user wishes to simulate 2 cm resolution from a VPG output file with 1 cm resolution, the first two virtual rods on the transect would be joined together, followed by the next two and the next two. The rod with the shallowest depth in each rod pairing would be used as the that segment's new Z coordinate, while the center of the segment would be used for the new XY coordinates. Summing the distance between each segment's new XYZ coordinate generates a sub-sampled

contour distance, which is used in concert with the profile gauge length to calculate linear rugosity at that new resolution.

Accounting for substrate slope

The slope of a forereef is an important component of coral reef benthic structural complexity that has been shown to explain variation in coral reef fish assemblages (Jankowski et al. 2015). However, forereef slope occurs over larger spatial scales (100s of meters to kilometers) than those of interest in this analysis, which focuses on the contribution of biotic and abiotic objects (i.e., coral colonies, boulders, channels, spur and groove formations, etc.) to structural complexity between the scales of 0.5 cm and 2.56 m.

Still, it is important to account for the effect of steep substrate slope on linear rugosity measurements, since a steep substrate slope can obscure the linear rugosity signal of smaller reef structures. This concept is demonstrated in Supplemental Figure 7. If the reef substrate has a non-zero slope, the apparent length of the profile gauge along the substrate will be longer than the horizontal distance covered by that profile gauge. A non-zero substrate slope will inflate the minimum value of rugosity to be greater than 1, assuming the horizontal length of the profile gauge is used as the denominator to calculate rugosity. This "slope effect" will cause the minimum value of rugosity to increase as the substrate slope becomes steeper. For example, a sandy substrate (i.e., otherwise "flat" ecologically) with a slope of 45 degrees would have a rugosity value of 1.41, while the same sandy bottom habitat would have rugosity value close to 1 when the effect of the underlying substrate slope is filtered out.

To account for the slope of the substrate, we measured linear rugosity in the alongshore direction at all sites, which tended to have a more gradual slope than the inshore direction. We also used the distance traversed by the best fit regression of profile gauge points as our measure

of profile gauge length, which incorporates substrate slope into the linear rugosity calculation. This allowed us to focus on smaller-scale processes that create reef structure on the order of magnitude of mm to m.

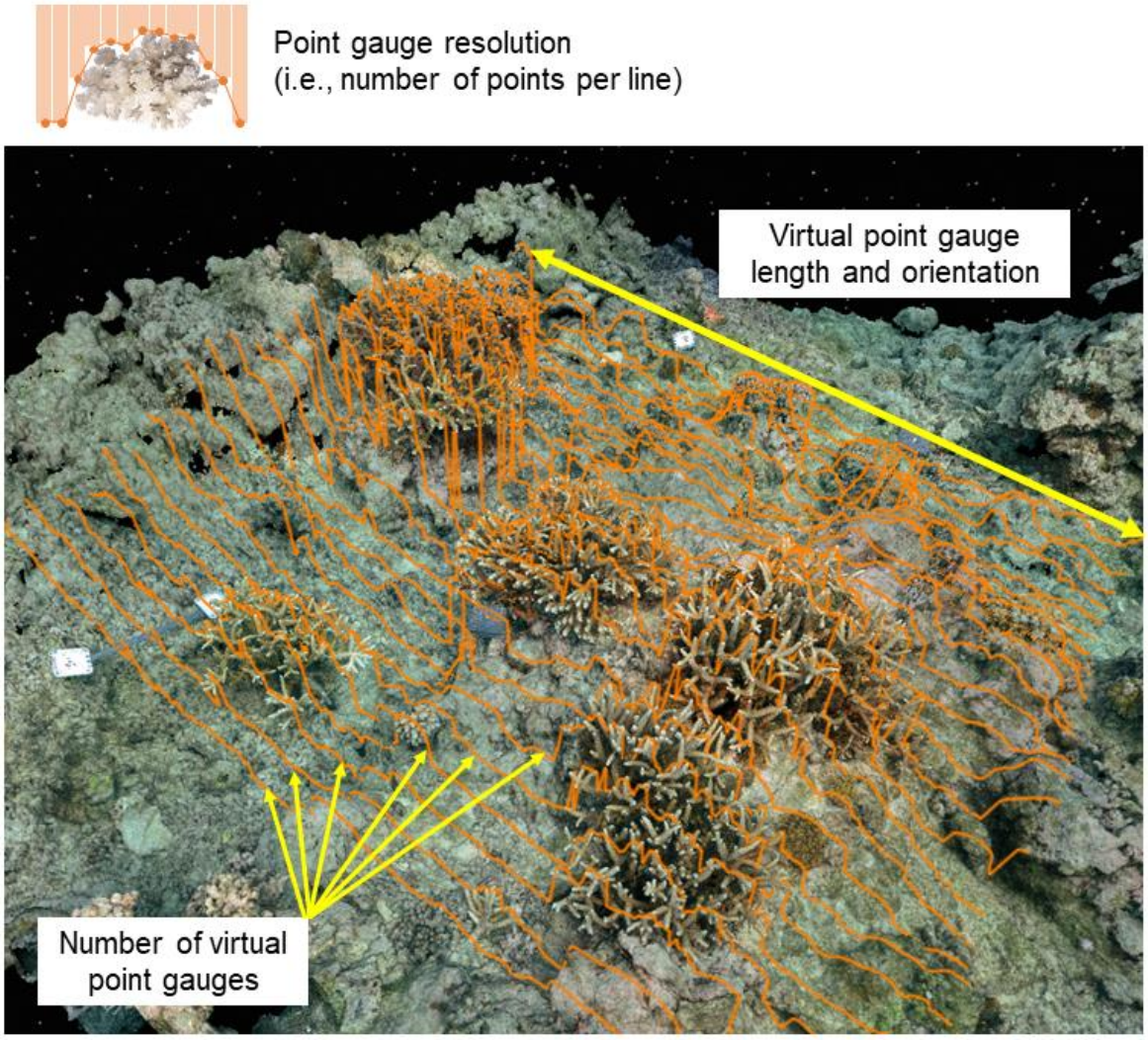

Figure S2.5: An example of Viscore's Virtual Profile Gauge tool (VPG) in action. The tool allows users to measure the linear rugosity of a point cloud along a series of transects, represented here by orange lines. VPG uses virtual rods to measure the depth of the substrate. By determining the coordinates of rod depths in XYZ space, the tool allows users to calculate the distance along the reef contour, which is then divided by the length of the transect. Users select the number of virtual rods per transect (point gauge resolution), the number of transects, and the length and orientation of the transects with respect to the point cloud.

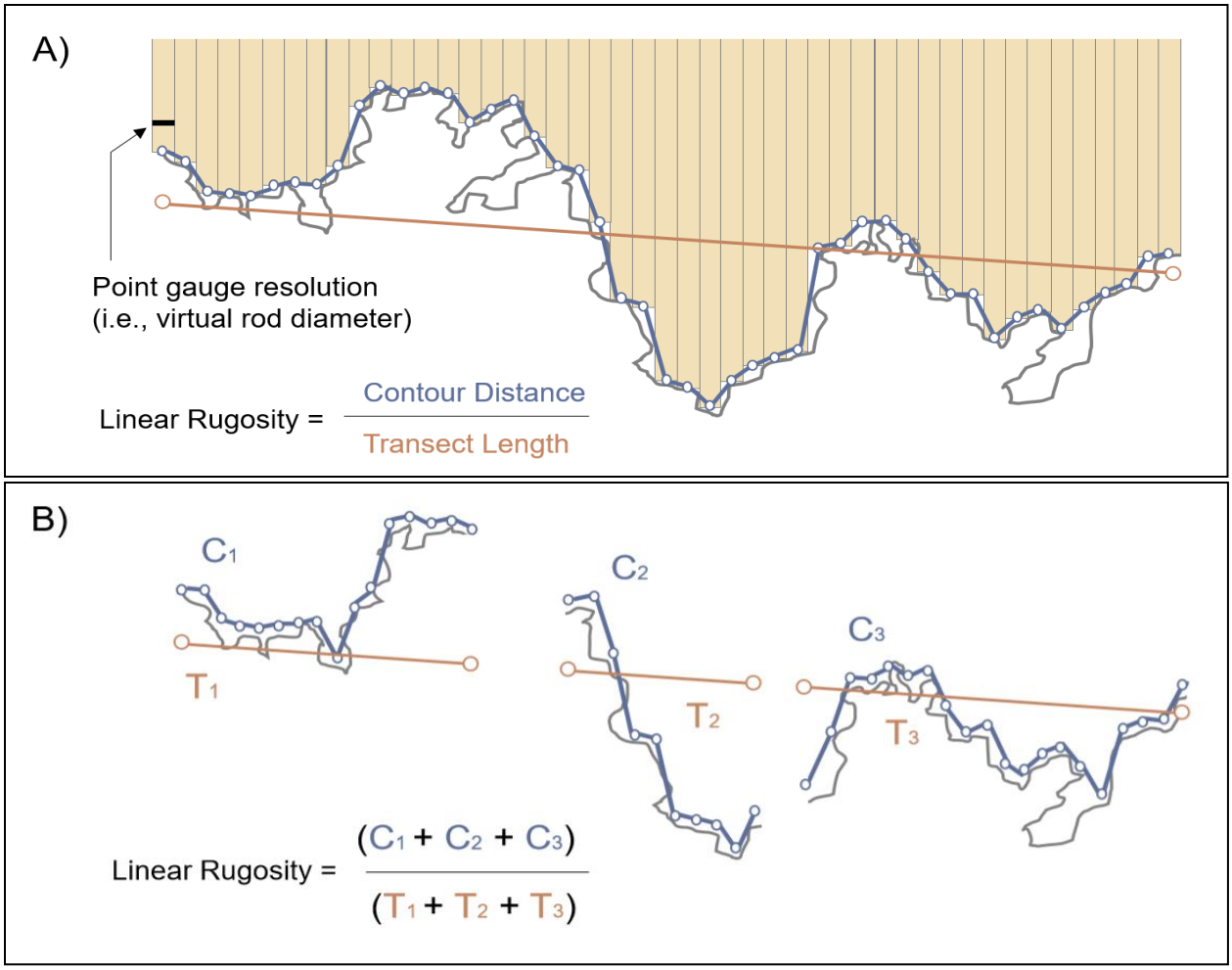

Figure S2.6: A) A conceptual diagram illustrating how the Virtual Profile Gauge tool (VPG) measures the linear rugosity of the point cloud. Each yellow bar represents a virtual rod that is dropped onto the point cloud from above (the diameter of these rods is the VPG resolution). Each rod terminates as soon as it intersects the point cloud, and the Z coordinate of that point is recorded as the depth of the substrate within that rod (represented here by the blue point at the end of each rod). VPG produces an output file with the XYZ coordinates of each rod terminus, where the XY coordinates correspond to the center of each rod. The sum of Euclidean distances between these points is the contour distance (blue line) along the point cloud (gray line). Since the profile gauge rods rest on the shallowest point beneath, the line connecting them rarely intersects with the substrate beneath, although intersections are possible. In this way, the VPG behaves just as a real profile gauge would if it were placed on the substrate *in situ*. In this study, the length of the transect was calculated as the length of the best fit regression of all VPG points (orange line), however it can also be calculated as the horizontal length of the VPG transect. Linear rugosity is calculated as the ratio of contour distance to transect length. B) For models with gaps or missing points, we calculated the contour distance over sections of the point cloud where data exists (i.e., C_1, C_2, C_3). These contours are summed together to generate a total contour distance. The regression through all VPG points is used to determine the full length of the transect, and then the segments of the transect where data exists (i.e., T_1, T_2, T_3) are summed to calculate a transect length that accounts for model gaps.

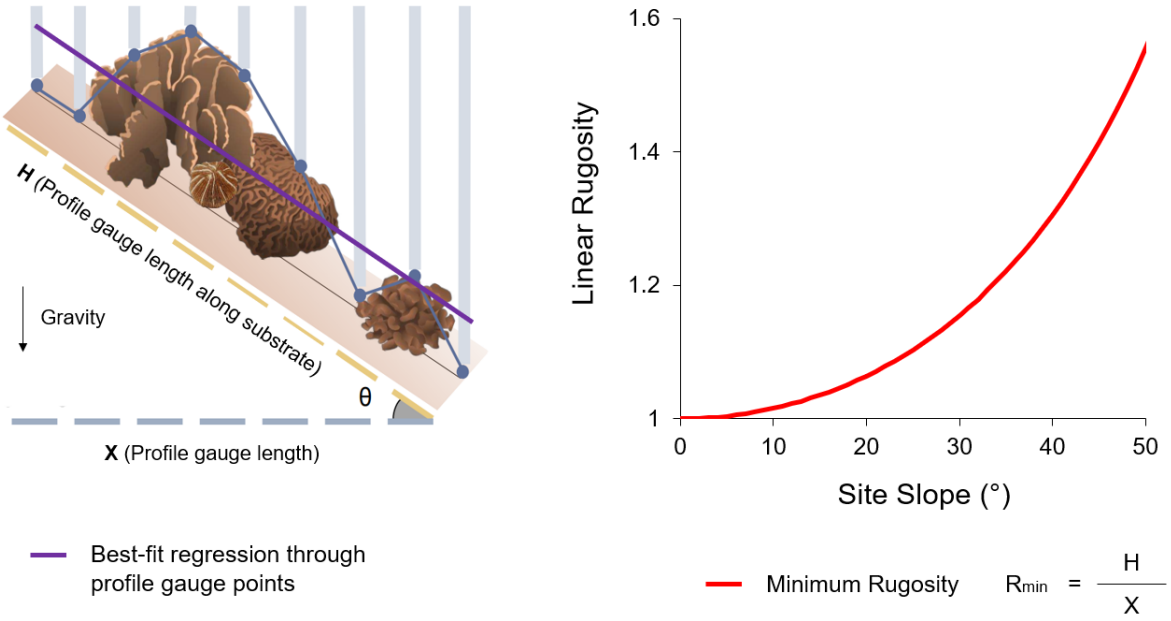

Figure S2.7: The slope of the substrate impacts linear rugosity measurements. If the reef substrate has a non-zero slope, the apparent length of the profile gauge along the substrate (H) will be longer than the horizontal distance covered by that profile gauge (X). A non-zero substrate slope will inflate the minimum value of rugosity (R_{min}) to be greater than 1, assuming the horizontal length of the profile gauge (X) is used as the denominator to calculate rugosity. The red line in the plot to the right shows R_{min} as a function of the substrate's overall slope. The length of the profile gauge along the substrate (H) can be easily calculated as the best fit line through all profile gauge rod termini (shown below as a purple line).

Full results of statistical analyses

Table S2.1: ANOVA results using generalized least squares when sites with >15% coral cover are grouped by their most abundant coral morphotype. Generalized least squares results were considered significant if $p < 0.01$ (n.s. = not significant, * indicates $0.001 < p < 0.01$, ** indicates $0.0001 < p < 0.001$, and *** indicates $p < 0.0001$). Post-hoc letters were determined using Tukey's test of multiple comparisons.

Scale interval (cm)	Df. (among, within)	F value	P value	Sig.	Branching *Montipora* n = 6	Encrusting *Montipora* n = 12	Branching *Porites* n = 13	Massive *Porites* n = 8
0.5 – 1	3, 35	7.4682	0.0007	**	b	ab	c	a
1 – 2	3, 35	9.5801	0.0001	**	b	ab	c	a
2 – 4	3, 35	11.9417	<0.0001	***	ab	b	c	a
4 – 8	3, 35	17.0928	<0.0001	***	a	b	c	ab
8 – 16	3, 35	20.3427	<0.0001	***	a	b	b	a
16 – 32	3, 35	14.8800	<0.0001	***	a	b	b	b
32 – 64	3, 35	5.2195	0.0051	*	a	ab	b	b
64 – 128	3, 35	1.3455	0.2783	n.s.	a	a	a	a
128 – 256	3, 35	1.0952	0.3663	n.s.	a	a	a	a

Table S2.2: Results of the generalized additive model (GAM), where fractal dimension at each scale interval was the response variable and coral cover, root mean square (RMS) height, and latitude were explanatory variables. Explanatory variables were considered to have a significant relationship with fractal dimension if $p < 0.01$ (n.s. = not significant, * indicates $0.001 < p < 0.01$, ** indicates $0.0001 < p < 0.001$, and *** indicates $p < 0.0001$).

Scale interval (cm)	Adj. R^2	Coral Cover			Root Mean Square (RMS) Height			Latitude		
		P value	Df	Sig.	P value	Df	Sig.	P value	Df	Sig.
0.5 – 1	0.5836	<0.0001	2.1113	***	0.0140	1.0000	n.s.	0.0009	2.6615	**
1 – 2	0.6370	<0.0001	2.1715	***	0.0499	1.9602	n.s.	0.0005	2.5051	**
2 – 4	0.6376	<0.0001	2.3361	***	0.1485	2.1711	n.s.	0.0005	2.4602	**
4 – 8	0.6657	<0.0001	2.7236	***	0.2067	2.5544	n.s.	0.0003	2.3098	**
8 – 16	0.6475	<0.0001	3.3048	***	0.1581	2.3157	n.s.	0.0007	2.1093	**
16 – 32	0.5554	0.0394	3.5131	n.s.	0.0021	2.3983	*	0.0042	2.1247	*
32 – 64	0.5110	0.6451	1.1210	n.s.	<0.0001	5.2192	***	0.0052	1.0000	*
64 – 128	0.7083	0.4369	1.0000	n.s.	<0.0001	6.0742	***	0.0279	1.0000	n.s.
128 – 256	0.6405	0.0594	1.0000	n.s.	<0.0001	4.1182	***	0.2850	1.0000	n.s.

Appendix 3: Supplemental Materials for Chapter 3 (Fine-scale variation in community composition shapes ecosystem response to disturbance)

Sensitivity of percent cover estimates using large-area imaging

Using large-area imagery, benthic community composition can be assessed within a single large quadrat (a 100m^2 plot in our study) rather than within small discontinuous quadrats (typically 0.5 to 1m^2), as is typical practice for *in situ* monitoring (Urbina-Barreto et al. 2021; Carneiro et al. 2024). Assessing community composition across a continuous area has advantages. For one, the approach captures information about the arrangement of benthic features, enabling additional metrics such as landscape heterogeneity to be calculated directly from percent cover outputs (Figure S3.4). In addition, structural metrics such as linear rugosity can be collected over the same large area, allowing two different components of the benthic community (percent cover and rugosity) to be compared over the same reef area (McCarthy et al. 2022). However, by using a single large quadrat, we do not have replication to calculate standard error for our percent cover estimates.

There are multiple potential approaches to address this issue of replication. One approach would be to simply state that the area sampled (100m^2) is sufficiently large enough for our point-based estimates of percent cover to be representative of the "true" percent cover across the landscape. Given that we assessed benthic cover at 2,500 points within each site (25 points/m^2), this survey effort is considerably higher than would be achieved using smaller discontinuous quadrats. Another approach would be to subsample percent cover data from the large 10 x 10 m quadrat to create replicate quadrats *a posteriori*. However, these quadrats would likely not represent independent replicates, given their proximity, and this approach would not make use of most of the percent cover data that researchers spent hours collecting. A third approach would be to repeatedly sample the same reef using a fixed 10 x 10 m quadrat, and then calculate the

confidence of our percent cover estimate based on the variance of these repeated samples. While it would take hundreds to thousands of hours to assess percent cover from benthic imagery for the same 10 x 10 m site repeatedly, we can rely on simulations to accomplish this task instead.

Using R, we created an empty 10,000x10,000 raster, where each cell represented 1x1mm. Then we generated a population of coral colonies (represented as circles) where colony area was selected from a log normal distribution, which has been shown to accurately represent coral populations (Bak & Meesters 1998; Rodriguez et al. 2021). We placed a random number of coral colonies in the raster and then calculated the *true* percent cover of corals in this raster. Then, to simulate stratified random sampling with 2,500 points, we aggregated the original raster into a 50x50 cell raster (each cell corresponds to 20x20cm). We randomly sampled one 1x1mm cell from within each aggregated cell, and coded each aggregated cell as either "coral" or "empty". We calculated the *estimated* percent coral cover of the simulated reef based on these aggregated cells, and then calculated the absolute difference between true and estimated percent cover. We repeated this process 10,000 times, each time simulating a new coral population. Finally, we calculated the 95% quantile of the absolute difference in percent cover estimates. This entire process was repeated for coral communities with different mean colony sizes, ranging from $e^{1.75}$ (approximately $5cm^2$) to $e^{4.75}$ (over $100cm^2$). Values were interpolated to produce a 95% confidence estimate of percent cover, visualized a function of true percent cover and coral colony mean size (Figure S3.5).

Based on this simulation, we can confirm that a single $100m^2$ plot is capable of producing robust and consistent estimates of percent cover. The estimate of percent cover was within 1.8% of the true percent cover of the reef in 95% of simulations for most coral size classes. Error was greater for coral populations with smaller size frequency distributions and for reefs where true

percent cover was near 50%. To contextualize our results, we plotted six sites from Maui with available percent cover and coral colony size frequency data to assess what confidence we should have in percent cover estimates for these sites. For Maui, it appears that percent cover estimates should be within 1.6% to 1.8% of true percent cover, using a single 10 x 10 m quadrat with 2,500 stratified random points. One site (Molokini) with higher percent cover and larger colonies is more similar to reefs on Moloka'i and Lāna'i, and was within 1.2% to 1.6% of true percent cover. Based on these results, when assessing change in coral cover over time within a fixed quadrat, we can reasonably conclude that an absolute change of > 3.6% is highly likely to represent actual change in percent cover, and not just sampling error. These findings can be extended to percent cover estimates of other taxa as well, not just estimates of total coral cover.

Quantifying landscape heterogeneity using virtual point intercept data

The arrangement of features in a landscape can provide information about the biotic and abiotic forces that drive spatial patterning, including an ecosystem's history of disturbance (Dietzel et al. 2021), interspecific interactions (Barott et al. 2012; Williams et al. 2013; George et al. 2021), and successional trajectories (Turner et al. 1998). Metrics that quantify the shape and arrangement of habitat patches have been used for decades in terrestrial landscape ecology to study habitat fragmentation and land use change (Krummel et al. 1987; Mcgarigal & Cushman 2002), population connectivity (Kindlmann & Burel 2008), and the impact of disturbance events (Haire & McGarigal 2009).

Over the last decade, landscape ecology metrics have been increasingly applied to seascapes as well (Wedding et al. 2011), including for marine spatial planning (Pittman et al. 2011). On a smaller scale, studies have recently made use of large-area imagery to study the aggregation of individual benthic organisms by applying metrics such as the variance to mean ratio (Edwards et al. 2017; Price et al. 2021). The data used to analyze the spatial patterning of taxa in marine systems include habitat maps derived from aerial or satellite surveys (large scale) to census-based assessments of individual sessile organisms (small scale). There is however a lack of approaches available to study the patch dynamics of benthic taxa at intermediate (i.e., patch-level) scales.

Point intercept data from percent cover surveys could be applied to bridge this gap. Historically, point intercept data has not been applicable for spatial pattern analysis because benthic cover is typically assessed using discontinuous quadrats or along a linear transect. However, using large-area images derived from photogrammetry (i.e., orthoprojections or photomosaics), percent cover can be assessed over a continuous extent using point intercept methods. If sufficient points are used in a percent cover survey, point intercept data can

accurately represent the spatial arrangement of benthic taxa (Figure S3.15). Compared to census-based assessments of individuals, point intercept data can be collected quickly (McCarthy et al. 2022), which enables analysis of more sites or larger extents. More importantly, point intercept data doesn't require researchers to define what constitutes an "individual" organism, and instead facilitates analysis at the patch scale. This is noteworthy because it can be challenging to delineate "individual" organisms for coral species with high fusion/fission dynamics (i.e., *Porites compressa*) or for other benthic taxa (i.e., turf algae, crustose coralline algae). In addition, conducting spatial analyses at the "patch" scale may be more ecologically relevant for certain ecological questions (i.e., questions about how fish and other mobile organisms interact with the benthos) than the organism scale.

While point intercept data won't be suitable for analyzing all types of spatial pattern (especially at very fine-scales), ecological questions that involve habitat fragmentation or the patchiness of benthic community composition at the scale of 10s to 100s of meters may be well suited for this type of analysis. One such application is the study of succession and the response of the benthic community to disturbance. Following the intermediate disturbance hypothesis, we would expect species richness and diversity to peak at intermediate levels of disturbance where weedy, stress tolerant, and competitively dominant taxa can all coexist (Connell 1978; Dollar 1982; Grigg 1983). Much like species diversity, the spatial aggregation of benthic classes should also exhibit characteristic patterns based on the frequency of disturbance or successional stage (Turner et al. 1998). For example, we would expect patches of benthic taxa to be smaller, more dispersed, and/or more fragmented on more diverse reefs where interspecific competition is high, and more aggregation on less diverse reefs, be they highly disturbed degraded reefs or climax communities with high coral cover.

Several studies have shown that landscape metrics are dependent on both the grain and extent of a spatial dataset (Turner et al. 1989; Cushman et al. 2008; Šímová & Gdulová 2012), although some metrics are more dependent on scale than others. In this study, we use the percentage of unlike adjacencies as our metric of landscape heterogeneity (Figure S3.3, Figure S3.4). To test the scale dependence of this metric, we conducted a power analysis using four 10 x 10 m sites from Palmyra Atoll where coral colony boundaries had been previously traced. Using this data as a reference of "true" percent cover, we simulated stratified random sampling using point densities ranging from 1 to 500 points/m^2 (Figure S3.15). We found that the number of patches, mean patch area, and proportion of unlike adjacencies were all scale dependent, but the rank order of sites remained consistent. In other words, the same site always had the highest proportion of unlike adjacencies, regardless of the number of points used to assess percent cover (Figure S3.15). These results suggest that 25 points/m^2 (the current standard of data collection) would be a reasonable point density to use for landscape-level spatial patterning analyses (Figure S3.5).

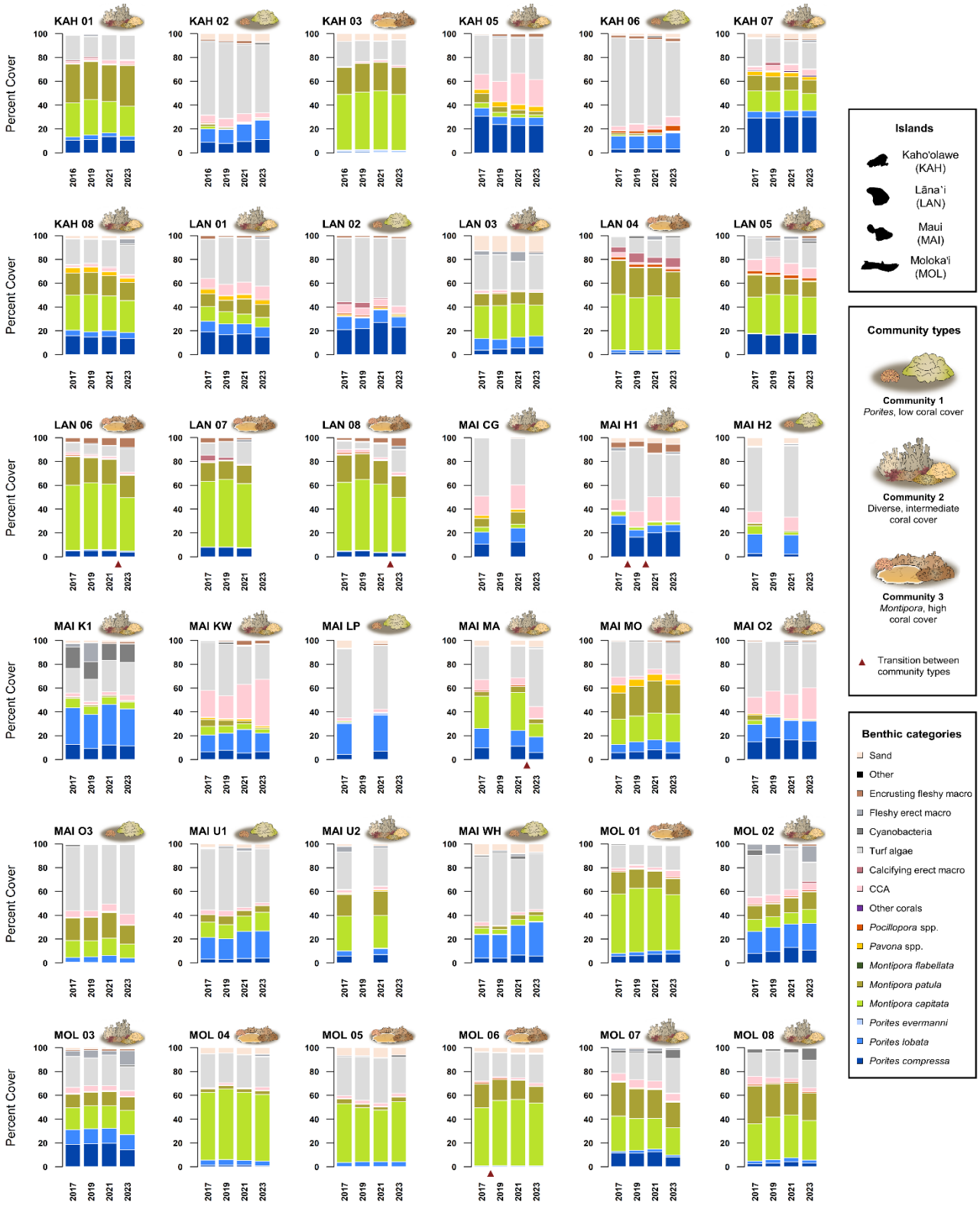

Figure S3.1: Benthic community composition for all sites. Graphics denote each site's community type at the start of the timeseries. Red triangles denote timesteps where a site shifted from one community type to another. Site names correspond to the abbreviations used in Figure 3.4A and Figure S3.10.

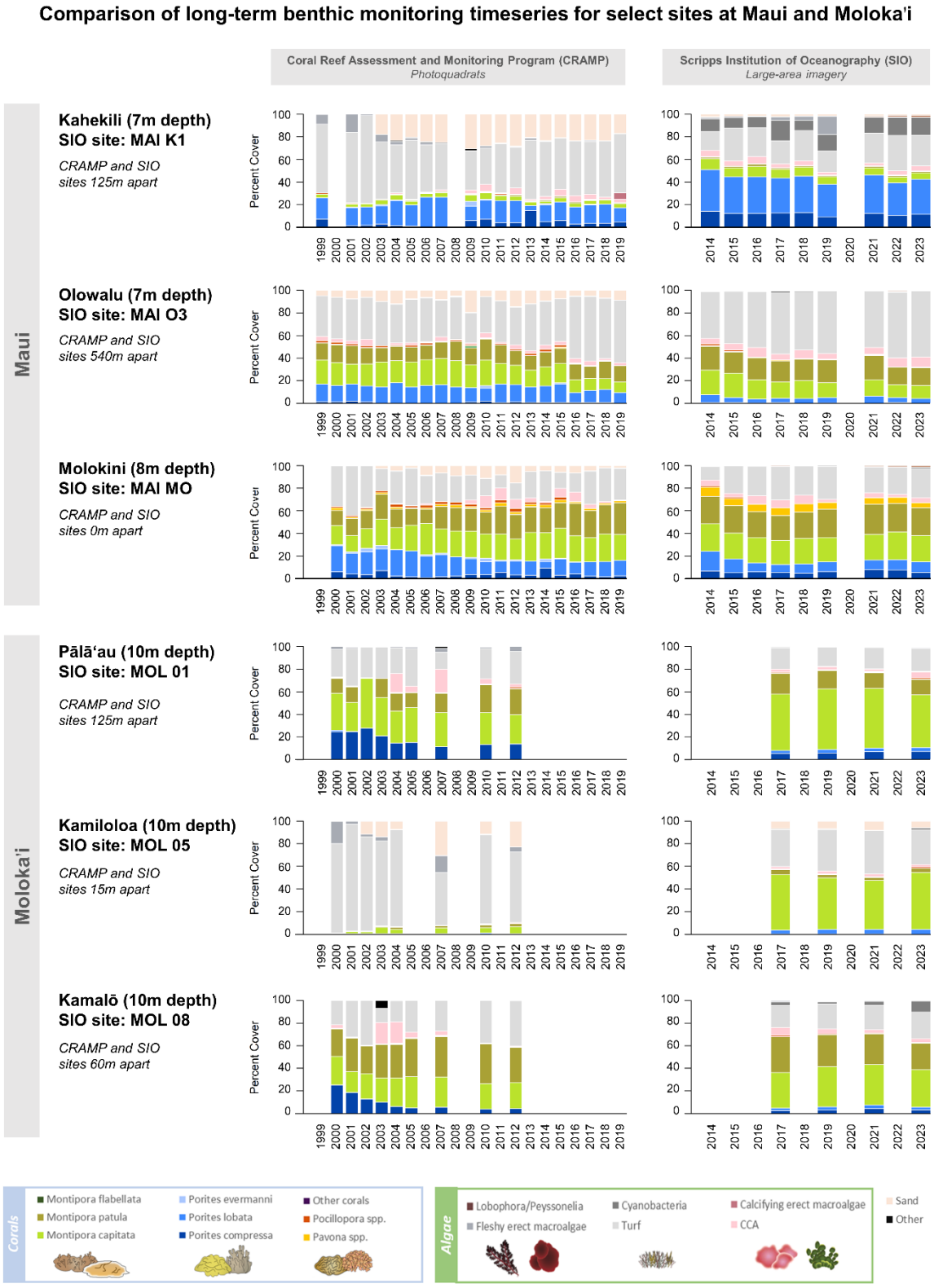

Figure S3.2: A comparison of long-term monitoring data collected at neighboring fixed long-term monitoring sites. SIO data was collected using large-area imagery while CRAMP data was collected using permanent photoquadrats. Colors denote benthic taxa.

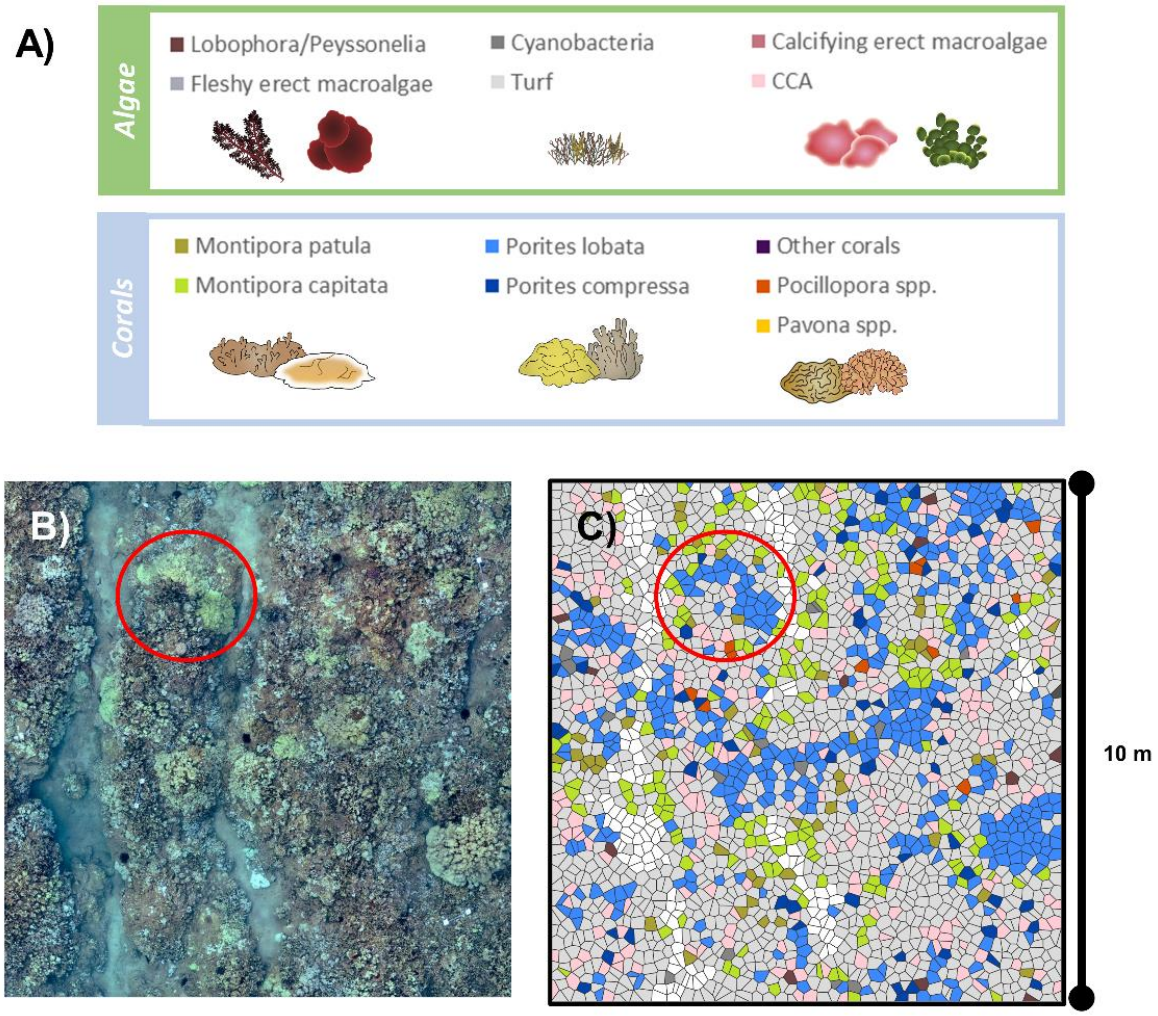

Figure S3.3: A) We identified benthic cover to the finest taxonomic resolution at 2,500 stratified random points per 10 x 10 m site. Coral IDs were assigned to one of seven categories (*Montipora capitata*, *Montipora patula*, *Porites compressa*, *Porites lobata*, *Pocillopora* spp., *Pavona* spp., and other coral), while algae were assigned to one of six functional groups (turf, crustose coralline algae (CCA), calcifying erect macroalgae, fleshy erect macroalgae, fleshy encrusting macroalgae (*Lobophora* or *Peyssonelia*), and cyanobacteria). Remaining points were categorized as either "sand" or "other", which mostly consisted of zoanthids, sponges or tunicates. B) A top-down view of a 10 x 10 m site from Maui, compared with C) benthic cover data from that site, interpolated via a Voronoi tessellation to form a continuous habitat map. The red circle in B) and C) correspond to the same large Porites colony. Use A) as a legend to interpret the benthic categories in C.

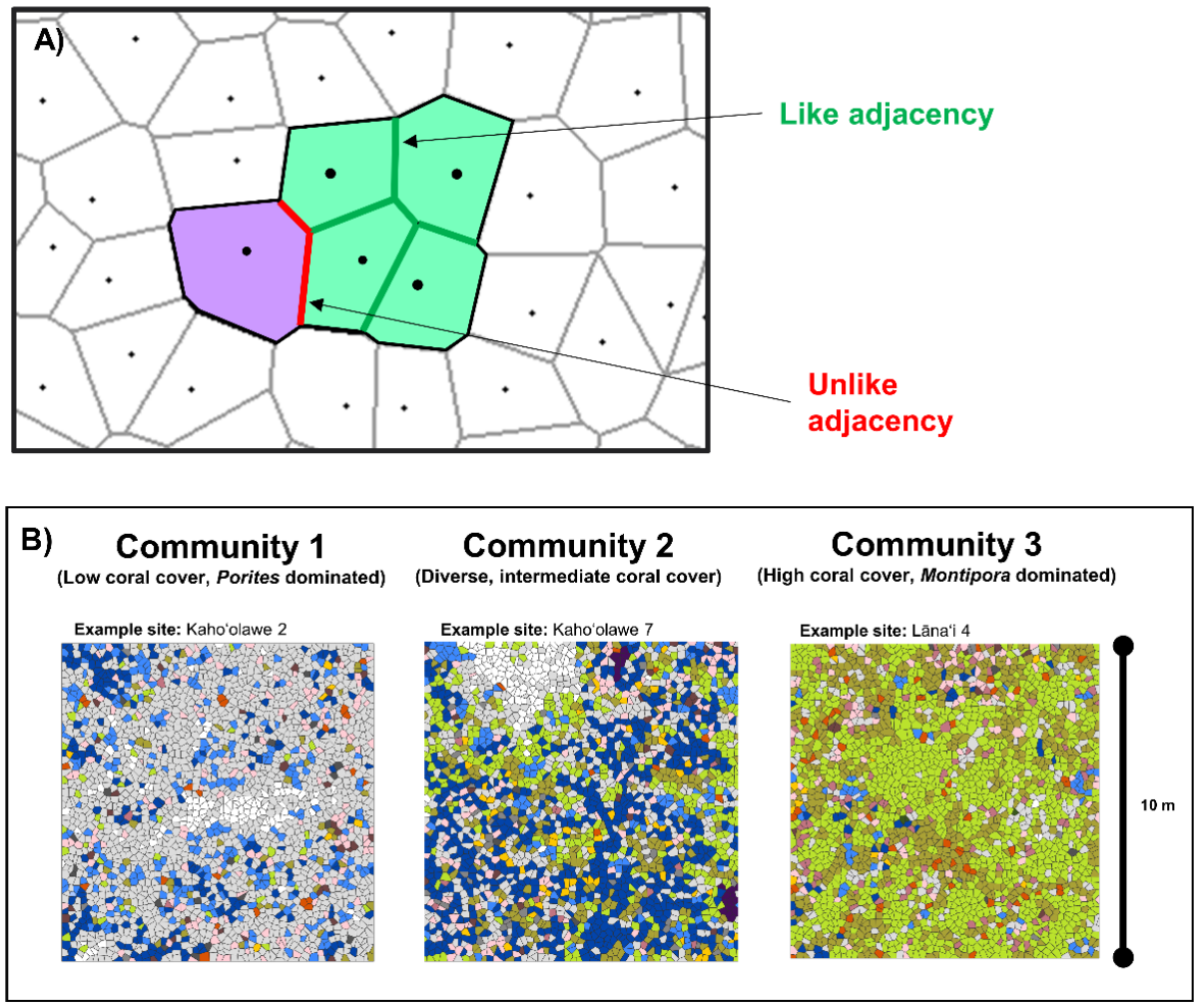

Figure S3.4: A) Landscape heterogeneity is illustrated using a Voronoi tessellation. Points in A) represent stratified random points used for benthic species ID. These point data have been interpolated via a Voronoi tessellation so that each polygon contains one point, and the area inside the polygon is closer to that point than to any other point in the dataset. Points can be considered "adjacent" if their polygons share a boundary. Adjacent points of the same benthic class are termed "like adjacencies", while adjacent points from different classes are termed "unlike adjacencies". We use the number of unlike adjacencies divided by the total number of adjacencies as our metric of landscape heterogeneity. B) Representative Voronoi tessellations for each community type. Most adjacencies in communities 1 and 3 are like adjacencies, reflecting a more compact landscape with large contiguous patches. Community 2 has more unlike adjacencies and thus has smaller patches and more opportunities for interspecific interactions among taxa. Use Figure S3.3 as a legend to interpret the benthic categories here.

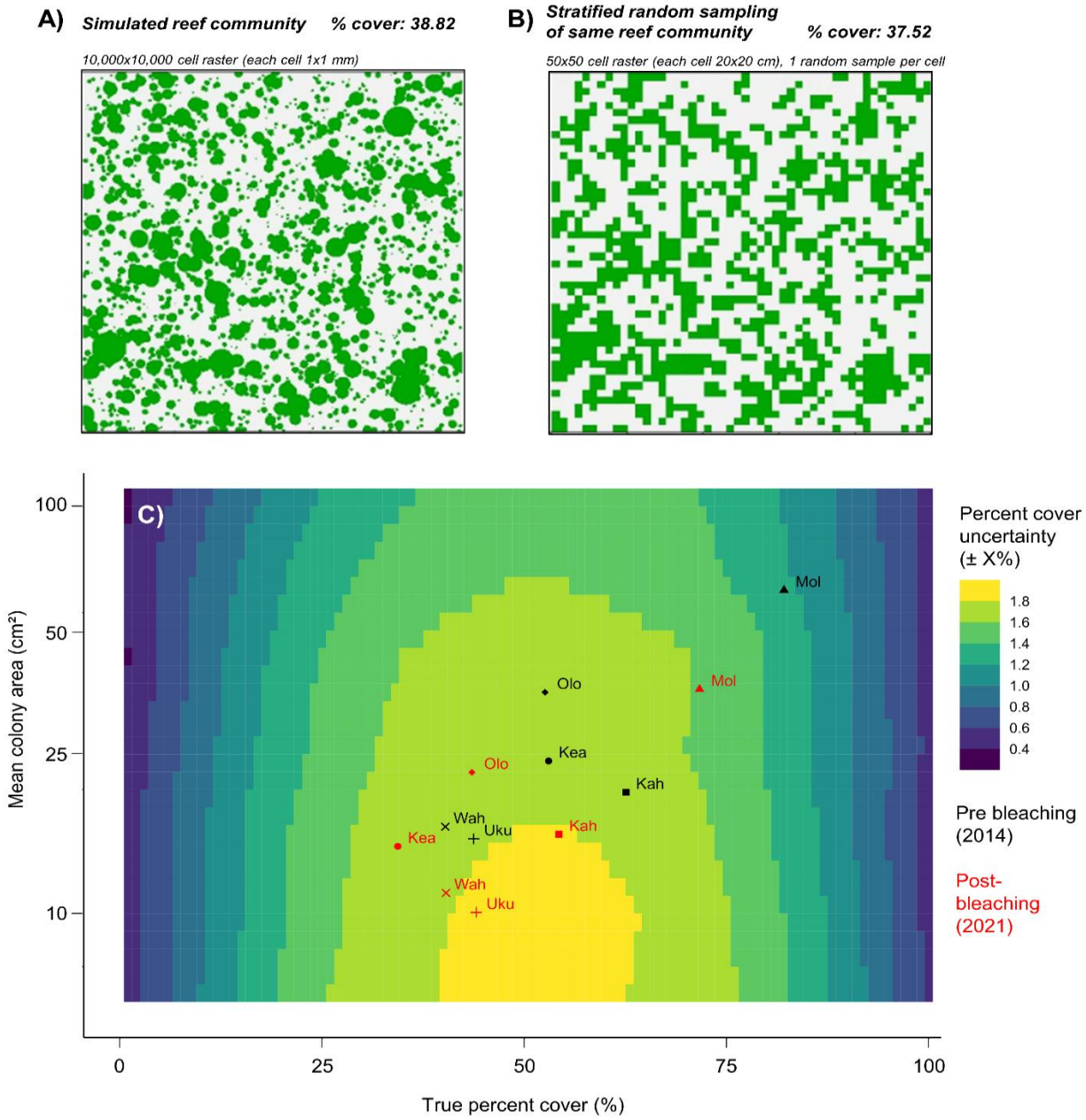

Figure S3.5: An example of A) a simulated coral community where circles represent coral colonies, and B) stratified random sampling of that same community using a 50x50 raster (2,500 points). The difference between estimated percent cover (via stratified random sampling) and true percent cover of the simulated community was calculated for 10,000 simulations, and repeated for various size frequency distributions of corals. C) The 95% quantile of the absolute difference between true and estimated percent cover is shown as a function of colony size frequency and total percent cover. Six sites from Maui with available percent cover and colony size frequency data are plotted, both from before (black) and after (red) bleaching, to illustrate how confidence in percent cover estimates can vary as a function of the spatial and temporal dynamics of benthic communities. Overall, our approach of using a single 10 x 10 m quadrat with 2,500 stratified random points appears to be a highly precise technique for assessing percent cover.

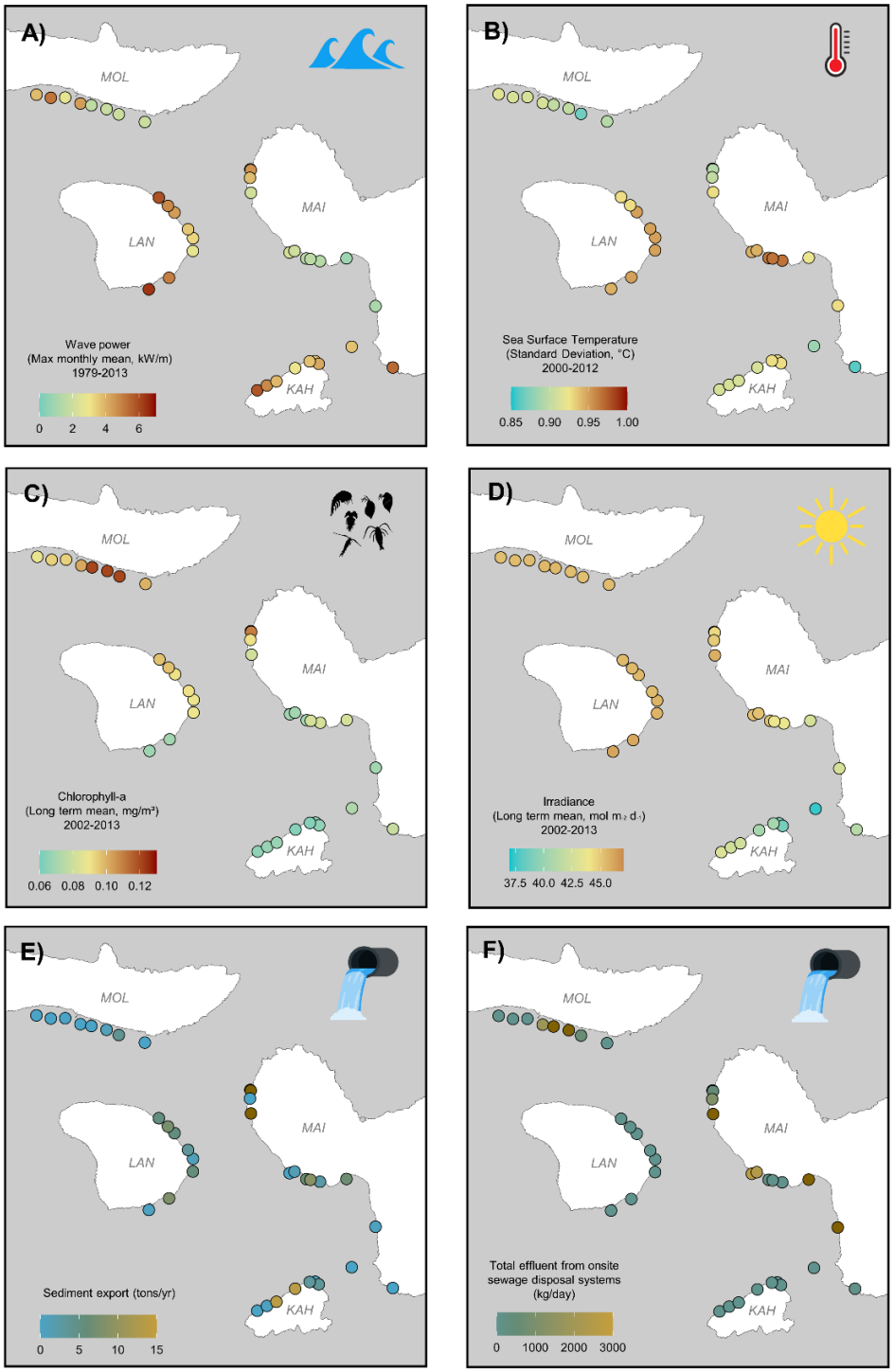

Figure S3.6: A map of environmental drivers used in the PERMANOVA. Data was obtained from the Ocean Tipping Points project (Wedding et al. 2018) and includes A) wave power (max monthly mean, kW/m), B) sea surface temperature (standard deviation, °C), C) chlorophyll-a (mean, mg/m3), D) surface irradiance (mean, mol m^{-2} d^{-1}), E) sediment export (tons/ha/yr), F) effluent (gal/kg^2/day). These data represent the long-term (mean) environmental conditions prior to our timeseries, rather than punctuated (max) conditions associated with disturbance during our timeseries.

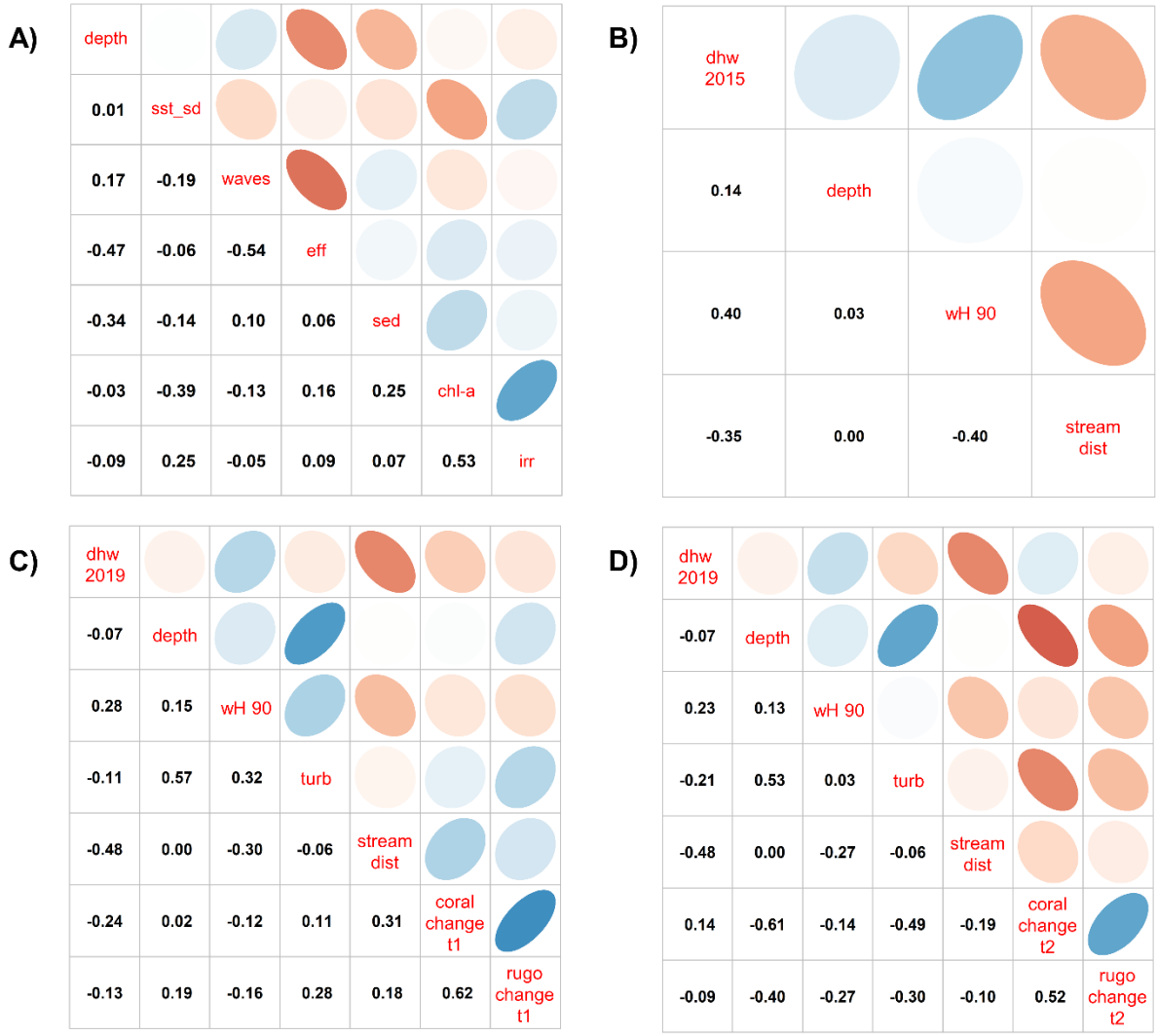

Figure S3.7: A) Correlation plot for long-term environmental data sourced from Ocean Tipping Points. Correlation plots of environmental variables specific to each timestep are also shown for B) 2016/17 to 2019, C) 2019 to 2021, and D) 2021 to 2023. Abbreviations are as follows: dhw = max degree heating weeks, wH 90 = 90th percentile of wave height, turb = mean of quarterly max turbidity, stream dist = distance to the nearest stream (log transformed), eff = total effluent, sed = sediment export, chl-a = chlorophyll-a, irr = surface irradiance.

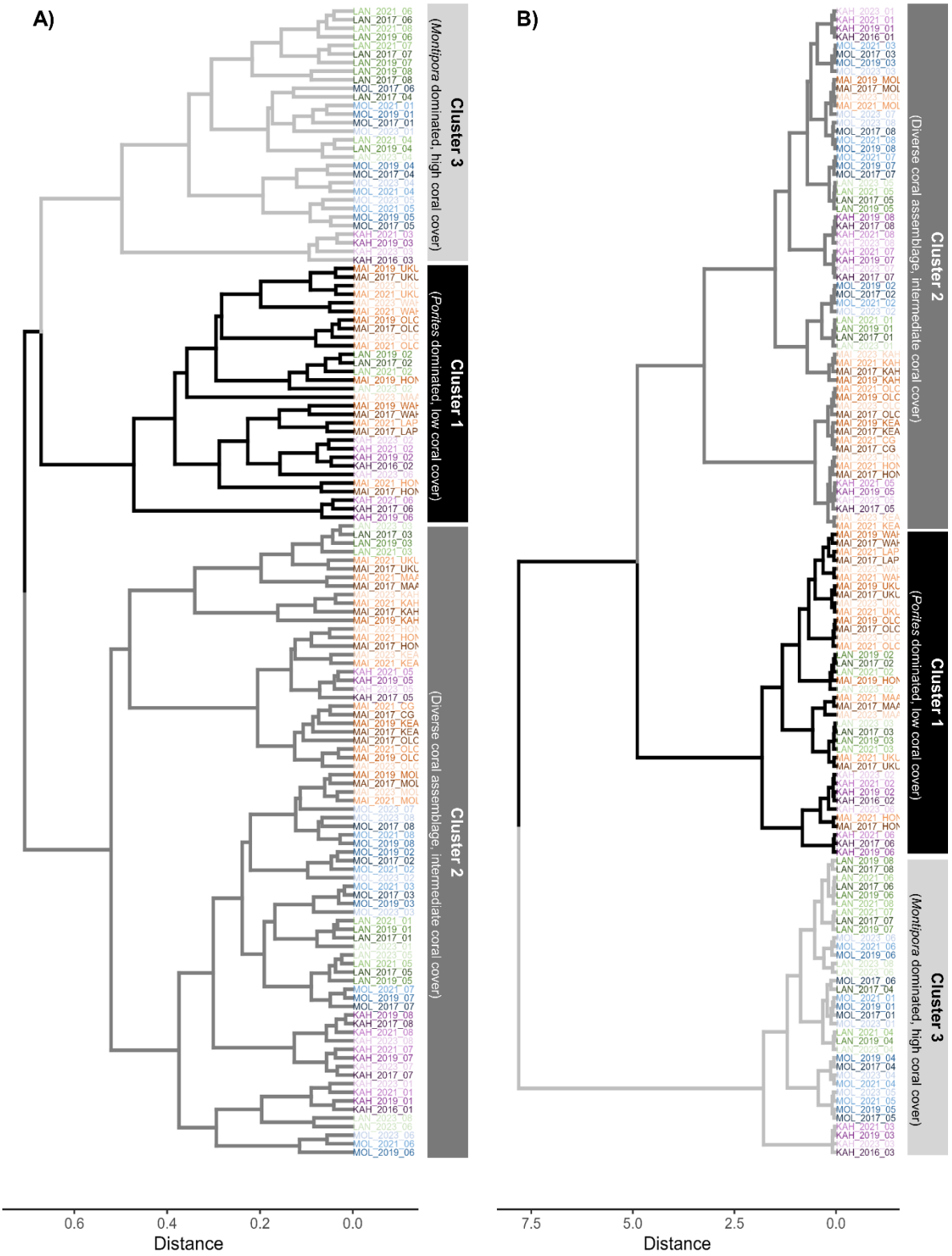

Figure S3.8: Hierarchical clustering results visualized as a dendrogram using A) the complete linkage method and B) Ward's method. The complete linkages method was used for all analyses, but both clustering approaches identified the same three ecological groupings. Text color denotes island and sampling year (same color scheme as Figure S3.10).

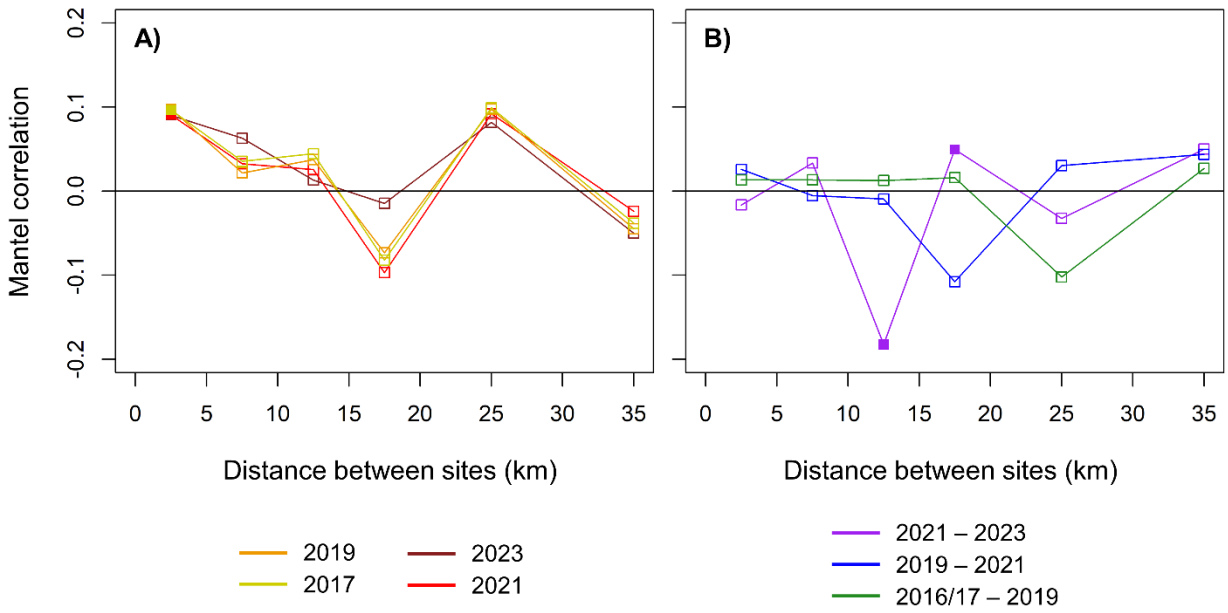

Figure S3.9: Results of multivariate Mantel correlogram (computed using mantel.correlog in the vegan package) show patterns of spatial autocorrelation among sites based on their A) community composition in each year of the timeseries, and B) rates of change in coral cover and rugosity (1cm scale). Multivariate data for A) consists of percent cover of benthic taxa, structural complexity, and landscape heterogeneity (the same 19 variables as used in the PERMANOVA). Multivariate data for B) consists of rates of coral cover and rugosity change (2 variables). We calculated the distance among all sites and dissimilarity among sites, organized site dissimilarities as a function of site distance using 5km bins (0 to 5km, 5 to 10km, etc.), and performed a Mantel correlation for each bin. Significant Mantel correlations are denoted by filled points. A) For each year of our timeseries, we found a significant positive correlation in community composition for sites within 5km of each other, but no significant evidence of spatial autocorrelation at any other scale. B) In terms of change in coral cover and rugosity, we found no evidence for spatial autocorrelation among sites at any scale during the first two timesteps (2016/17 – 2019 and 2019 – 2021). In the final timestep (2021 – 2023), we found a significant negative correlation for sites separated by 10 to 15km, and a significant positive correlation for sites separated by 15 to 20km.

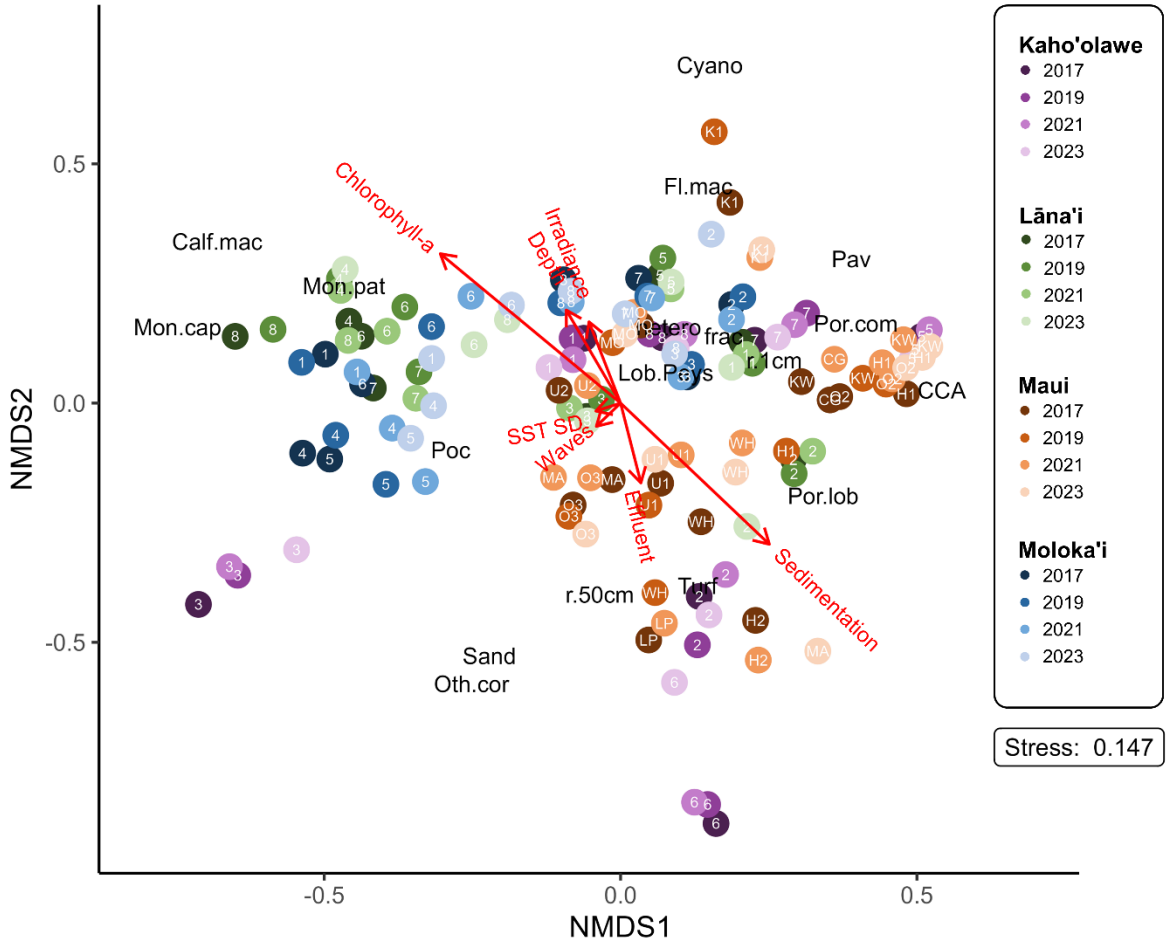

Figure S3.10: Non-metric Multidimensional Scaling (NMDS) ordination of benthic community composition for all sites in all years. Island is symbolized by point color, with lighter shades representing more recent surveys. The label for each point denotes the site name using the same abbreviations as Figure 3.4A and Figure S3.1. Red loadings denote environmental variables used in the PERMANOVA, while black text denotes benthic variables used in the ordination. Benthic variables include percent cover of various benthic taxa, structural complexity (r.1 = rugosity at 1cm resolution; r.50 = rugosity at 50cm resolution; frac = fractal dimension), and landscape heterogeneity (hetero).

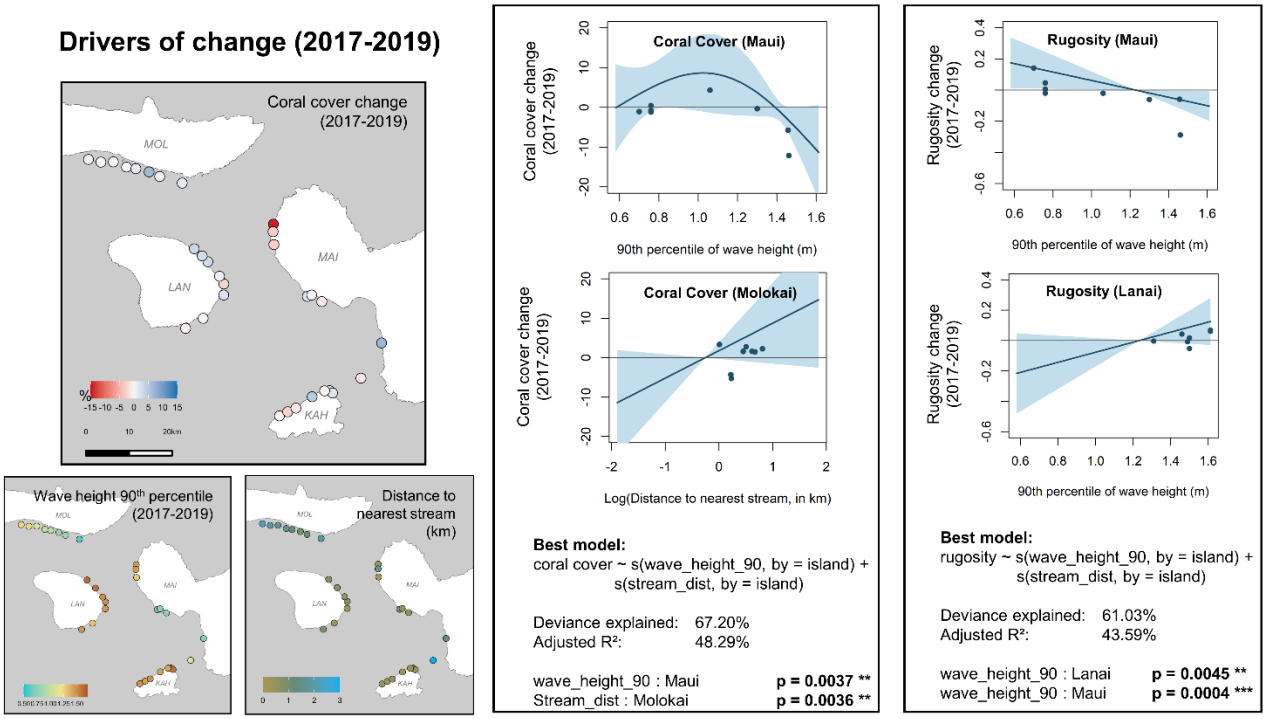

Figure S3.11: Results of the best generalized additive models (GAM) for timestep 1 (2016/17 – 2019). According to these models, reefs on Maui exposed to moderate wave energy were more likely to see coral cover increase, whereas reefs on Moloka'i located further from streams were more likely to see coral cover increase. Increasing wave exposure was associated with positive rugosity change on Lāna'i but negative rugosity change on Maui. A map of absolute change in coral cover during timestep 1 is shown, as well as a map of the best environmental predictors in timestep 1. The formulas for the best models (one for coral cover, one for rugosity), deviance explained, adjusted R^2, and p values (significant terms only) are also shown. The relationship between the response variable and significant model terms are illustrated with partial effects plots (shading denotes 95% confidence estimate).

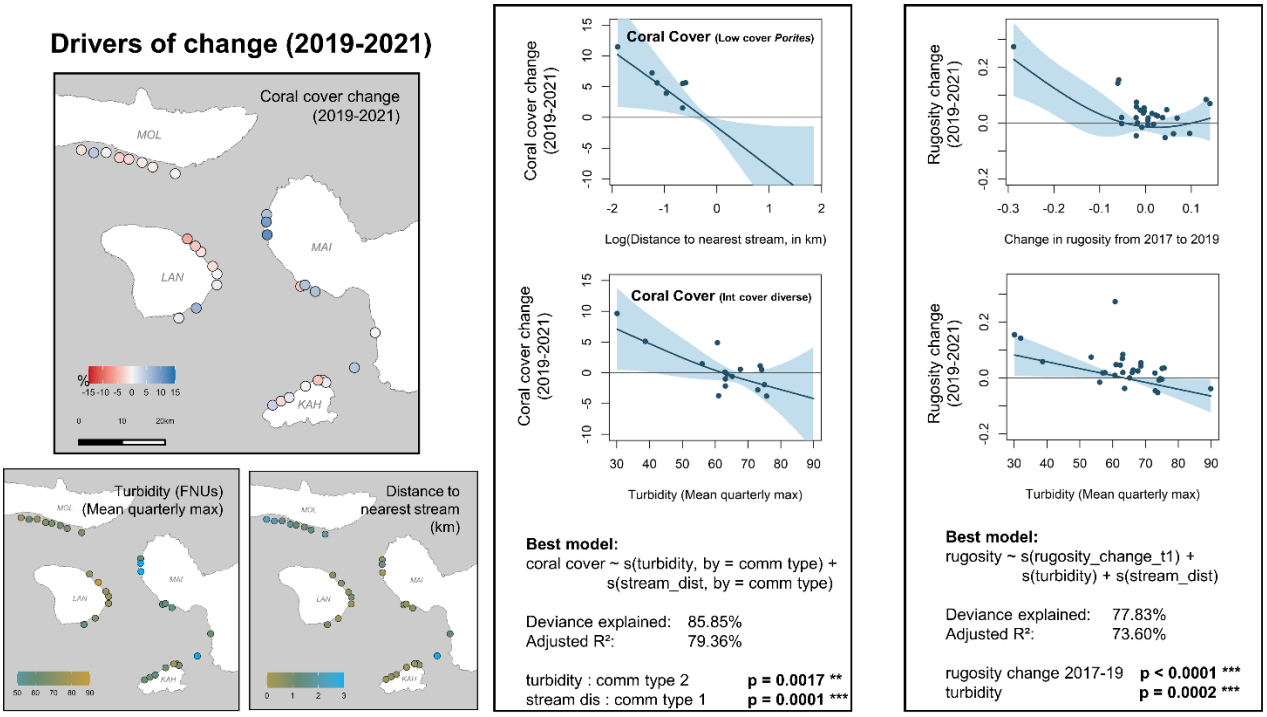

Figure S3.12: Results of the best generalized additive models (GAM) for timestep 2 (2019 – 2021). According to these models, diverse intermediate cover reefs exposed to severe turbidity were more likely to see coral cover decline, while low cover *Porites* reefs close to streams were more likely to see coral cover increase. Reefs that experienced declines in rugosity from 2017 to 2019 and reefs with less exposure to severe turbidity were more likely to see an increase in rugosity from 2019 to 2021. A map of absolute change in coral cover during timestep 2 is shown, as well as a map of the best environmental predictors in timestep 2. The formulas for the best models (one for coral cover, one for rugosity), deviance explained, adjusted R^2, and p values (significant terms only) are also shown. The relationship between the response variable and significant model terms are illustrated with partial effects plots (shading denotes 95% confidence estimate).

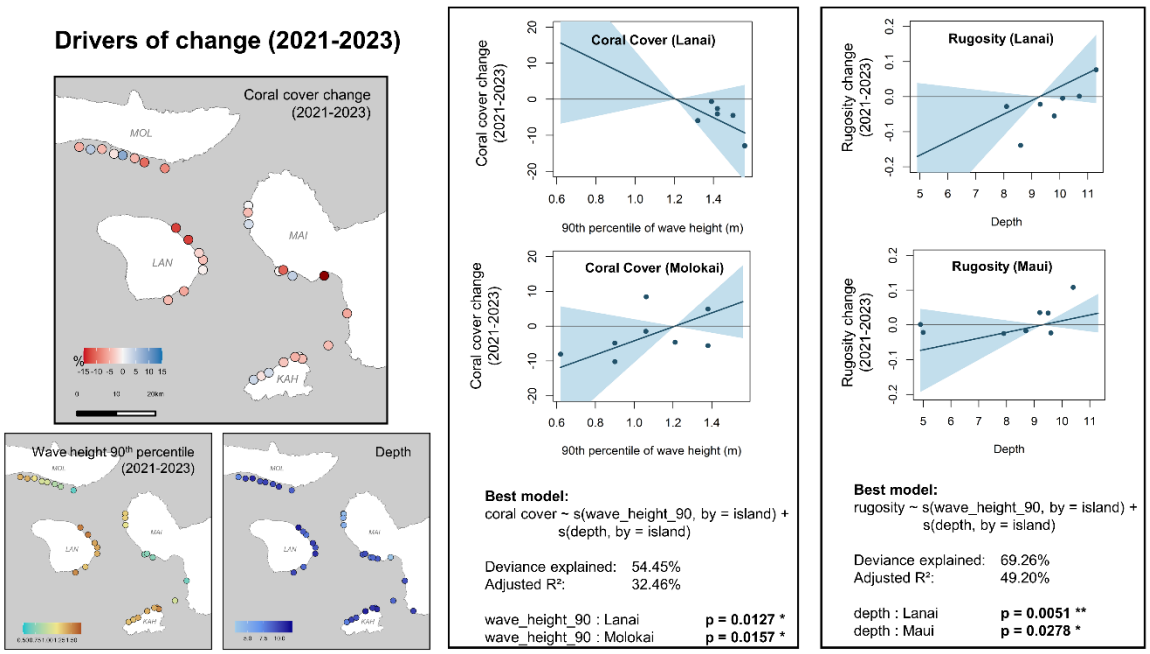

Figure S3.13: Results of the best generalized additive models (GAM) for timestep 3 (2021 – 2023). According to these models, reefs on Lāna'i exposed to higher wave energy were more likely to see declines in coral cover, whereas reefs on Moloka'i exposed to higher wave energy were more likely to see an increase in coral cover. Rugosity was more likely to increase on deeper reefs on both Maui and Lāna'i. A map of absolute change in coral cover during timestep 3 is shown, as well as a map of the best environmental predictors in timestep 3. The formulas for the best models (one for coral cover, one for rugosity), deviance explained, adjusted R^2, and p values (significant terms only) are also shown. The relationship between the response variable and significant model terms are illustrated with partial effects plots (shading denotes 95% confidence estimate).

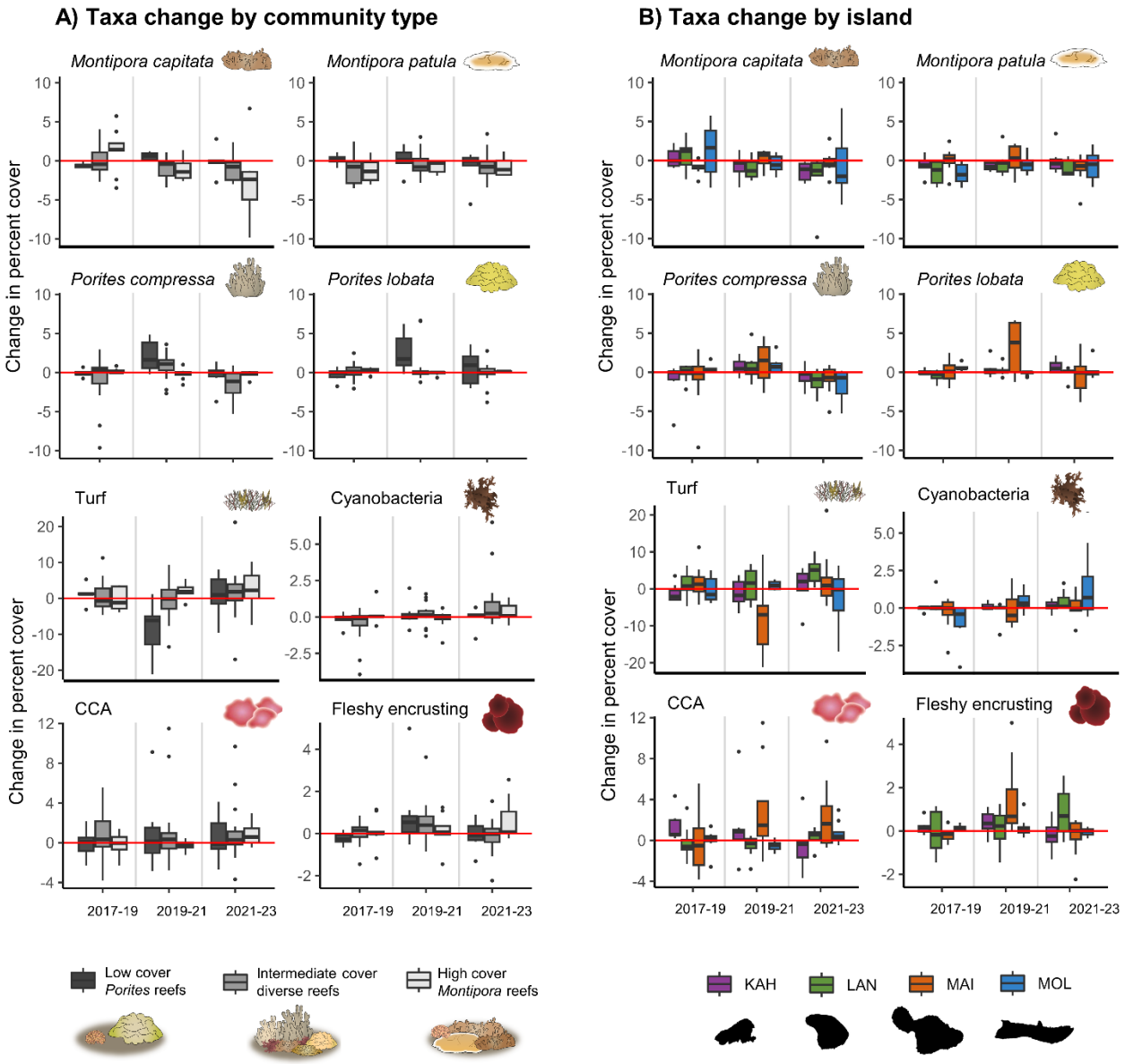

Figure S3.14: Absolute change in percent cover of key coral taxa and algal functional groups, shown in each timestep by A) community type and B) island. Red horizontal line denotes no change during a timestep.

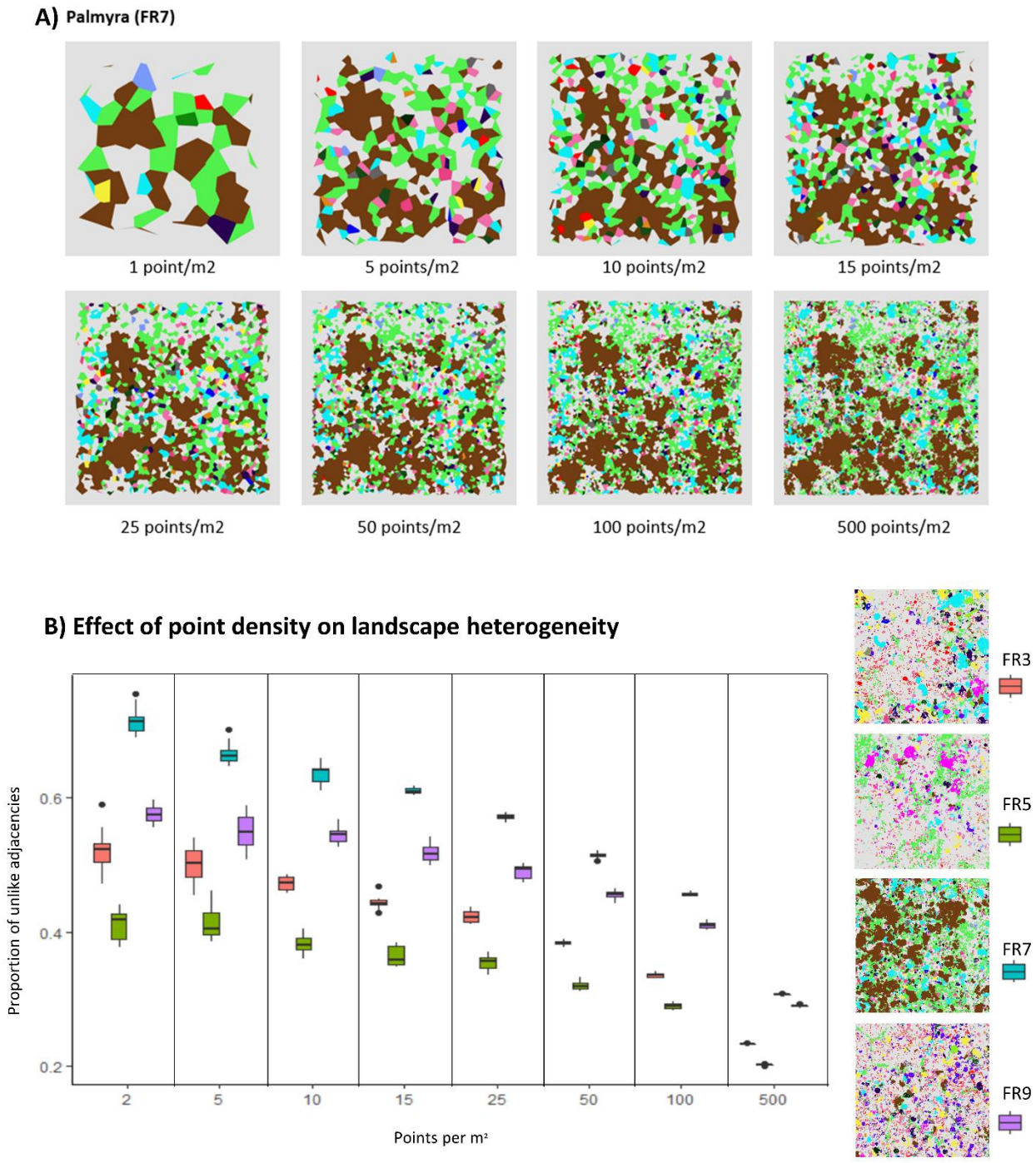

Figure S3.15: A) The effect of point density on Voronoi tessellation resolution. A fully traced 10 x 10 m reef plot from Palmyra Atoll (site FR7) is visualized via Voronoi tessellation using eight different point densities. For reference, we collected percent cover data for Maui Nui sites using 25 points/m^2. B) The effect of point density on landscape heterogeneity (represented here as the proportion of unlike adjacencies) is shown for four sites in Palmyra Atoll. We used stratified random sampling to "virtually" assess percent cover 10 times for each fully traced 10 x 10 m reef plot.

Table S3.1: Results from the repeated-measures PERMANOVA, which we used to explain variance in multivariate community data. The F-statistic, R^2, and p value for eight predictors are shown. For each environmental variable, we compare the range of values at our study sites with the range of values for nearshore environments in the Main Hawaiian Islands, as modeled by the Ocean Tipping Points project (Wedding et al. 2018).

Predictor	***Data descriptor***	***Units***	***Range (our sites)***	***Range (Hawai'i)***	***F statistic***	***R^2***	***p value***
Island	Fixed factor (4 islands)	--	--	--	16.988	0.227	**< 0.001 *****
Wave power	Max monthly mean (1979-2013)	kW/m	0.8 – 6.4	0 – 140	1.836	0.025	0.273
Depth	Depth at site GPS point	m	3.4 – 11.3	--	2.938	0.039	0.109
SST	Standard deviation (2000-2012)	°C	0.86 – 0.97	0.79 – 1.16	-0.316	-0.004	0.999
Chlorophyll-a	Long-term mean (2002-2013)	mg/m^3	0.06 – 0.12	0.05 – 0.14	1.81	0.024	0.287
Total Effluent	Modeled data	kg/day	0 – 16,085	0 – 118,540	1.142	0.015	0.455
Sediment	Modeled data	tons/ha/yr	0 – 55.7	0 – 516	3.226	0.043	0.088
Irradiance	Long-term mean (2002-2013)	mol m^{-2} d^{-1}	37.4 – 46.2	32.4 – 46.2	6.152	0.082	**0.012 ***

Table S3.2: Results from mixed-effects linear modelling, which we used to test if community type or island was a better predictor of coral cover change or fine-scale rugosity change between surveys. Community type was a fixed factor with three levels (low cover *Porites* reefs, diverse intermediate cover reefs, and high cover *Montipora* reefs), while island was a fixed factor with four levels (Kaho'olawe, Lāna'i, Maui, and Moloka'i).

Model formula	**AIC**	**p (intercept)**	**p (main effect)**	**p (interaction)**
coral_change ~ community + community : timestep + (1|site)	-10.06	0.988	0.584	**< 0.001 *****
coral_change ~ island + island : timestep + (1|site)	7.07	0.357	0.637	**0.003 ****
rugo change ~ community + community : timestep + (1|site)	-695.41	**0.020 ***	0.093	**0.005 ****
rugo_change ~ island + island : timestep + (1|site)	-686.90	0.836	0.389	**< 0.001 *****

Table S3.3: Combinations of explanatory variables used for Generalized Additive Model (GAM) multiple regression analysis. Each combination of variables corresponded to a particular hypothesis explaining change in coral cover or change in fine-scale rugosity in each timestep. Some hypotheses were further combined (i.e., wave event and sedimentation hypothesis combined to form major storm hypothesis), and not all combinations of hypotheses are shown here. Timestep abbreviations are as follows: T1 = 2016/17 – 2019, T2 = 2019 – 2021, and T3 = 2021 – 2023. Figures S3.7 – S3.9 show the results of the best GAM for each timestep (p values, AIC, deviance explained, and adjusted R^2 values).

Hypothesis	**Explanatory variable**	Data source	**Timesteps**
Local-scale environmental and/or human impacts	Island	NA	T1, T2, T3
Benthic community composition	Community type	This study	T1, T2, T3
Succession or recovery dynamics	Change in coral cover or rugosity in previous timestep	This study	T2, T3
Thermal stress	DHW (max, °C/weeks)	(NOAA Coral Reef Watch 2020)	2015 Max DHW for T1, 2019 Max DHW for T2 and T3
Wave event	Wave height (90th percentile, m) Depth (m)	(Cheung 2021)	T1, T2, T3
Sedimentation	Turbidity (mean of quarterly max, FNU) Distance to nearest stream (m)	(Dogliotti et al. 2015; Hawai'i Statewide GIS Program 2016; Li et al. 2022)	T1 (stream distance only) T2, T3 (turbidity and stream distance)
Major storm (wave event + sedimentation)	Wave height, depth, turbidity, distance to nearest stream	See above	T1, T2, T3

Appendix 4: Supplemental Materials for Chapter 4 (Corals that survive repeated thermal stress show signs of selection and acclimatization)

Quantifying heat stress

We quantified heat stress at each site using degree heating weeks (DHW), a metric of accumulated heat stress that has been shown to correspond well to coral bleaching thresholds (Liu et al. 2017; Skirving et al. 2020). Widespread coral bleaching is expected above 4 DHW, while widespread coral mortality is expected above 8 DHW (Pandolfi et al. 2011; Kayanne 2017; Couch et al. 2017). DHW for each study site were obtained from NOAA's Coral Reef Watch (CRW) program. DHW values were based on satellite-derived sea surface temperature (SST) data with a 5 km spatial resolution. Most sites were situated far enough apart that they fell into distinct 5 km cells, but two sites (Kahekili and Wahikuli) were close enough that they fell within the same 5 km grid cell and thus had the same DHW values. All sites had zero DHW at the time of sampling in 2014, 2017, and 2021, while sites ranged from 6.75 to 9.40 DHW when sampled in 2015 and from 7.80 to 9.61 DHW when sampled in 2019 (Figure S4.1, Table S4.1).

To corroborate DHW estimates, we compared SST values from the satellite-derived CRW data to SST values modeled using the Regional Ocean Modeling System (ROMS) for the Main Hawaiian Islands. ROMS forecasts sea water temperature at 4 km grid resolution for multiple depth strata, and the model assimilates both satellite and *in situ* ocean temperature data to improve forecasts (Powell 2010). We calculated the difference between SST values obtained from CRW and ROMS at each of our sites (Figure S4.2). SST tracked closely for the duration of both bleaching events, except for the very end of the 2019 bleaching event, where ROMS forecasts cooler SST values than CRW (Figure S4.2). This discrepancy began in November 2019, which is after our 2019 surveys and after DHW peaked for all sites. Thus, this temperature

discrepancy should not explain reductions in bleaching observed in this study. However, if ROMS is picking up on a real drop in temperature that CRW missed, it could help to explain improved coral recovery following bleaching in 2019 compared to 2015.

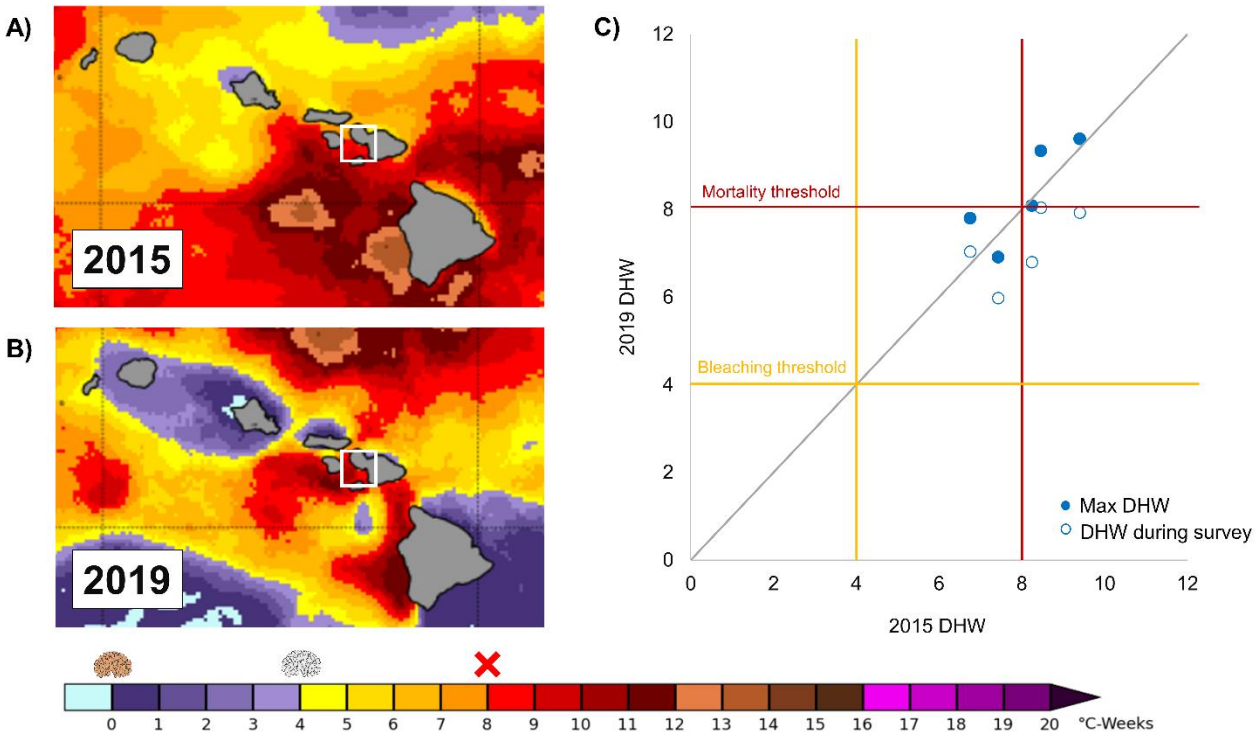

Figure S4.1: The maximum degree heating weeks (DHW) reached in the main Hawaiian Islands in A) 2015 and B) 2019, with leeward Maui denoted by a white box. Widespread coral bleaching is expected above 4 DHW (represented by the white coral in the lower key and the yellow lines in C), while widespread mortality is expected above 8 DHW (represented by the red X in the lower key and the red lines in C). C-D) The maximum DHW at study sites is shown for both 2015 and 2019. Points that fall on the gray diagonal line in C) experienced the same DHW in both 2015 and 2019. Thermal stress was comparable in leeward Maui among sites and between bleaching events. All sites surpassed 4 DHW in 2015 and 2019, indicating that widespread bleaching was expected in both years. Kahekili, Wahikuli, and Ukumehame did not reach the 8 DHW threshold for mortality in 2015 or 2019, while Olowalu, Keawakapu, and Molokini surpassed that threshold in both 2015 and 2019.

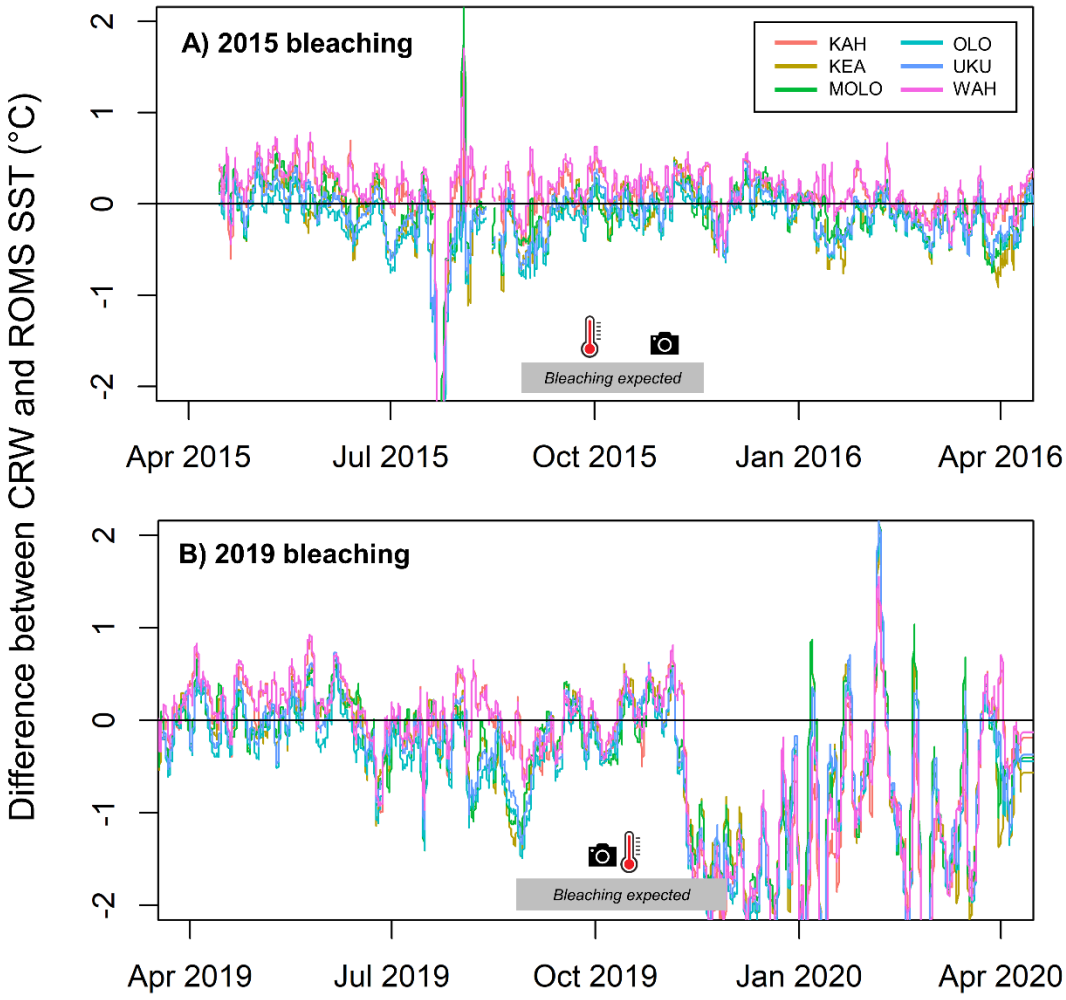

Figure S4.2: A comparison of ocean temperature from Coral Reef Watch (CRW) and the Regional Ocean Modelling System (ROMS) for the duration of the bleaching events in A) 2015 and B) 2019. Temperature timeseries are color coded by site. Positive values indicate that ROMS forecasts were warmer than CRW temperature values, while negative values indicate cooler ROMS forecasts compared to CRW. CRW sea surface temperature is derived from satellites, while ROMS incorporates both satellite and *in situ* data sources into its forecasts. The gray bar indicates the range of dates with > 4 degree heating weeks (DHW), which indicates that bleaching would be expected. The thermometer symbol indicates the date where degree heating weeks peaked, after which DHW plateaued through October before falling in November (same pattern and timing in both years). The camera symbol indicates the date(s) where we resurveyed our long-term monitoring sites.

Comparison of tracing accuracy between annotators and across software platforms

Researchers in this study used two software platforms to trace patches of live coral tissue: TagLab and ArcGIS Pro. The commercially available ArcGIS Pro has a wide variety of geospatial applications, and is the software used in Rodriguez et al. (2021), which is the SOP we used for this study. However, the process of tracing patches of coral tissue in ArcGIS Pro is entirely manual, which necessitates many person-hours for tracing. To expedite our workflow, a subset of researchers explored whether the emerging freeware platform TagLab (Pavoni et al. 2021b) could reduce tracing time without compromising accuracy.

TagLab is a semantic segmentation platform that allows users to delineate the boundaries of benthic organisms and assign species ID. TagLab's "positive-negative click" tool assists the annotator by providing a "best guess" of colony boundaries based on RITM segmentation (Sofiiuk et al. 2022). To do this, the annotator selects several pixels within (+) and outside (-) of a patch of live coral tissue. Each click modifies the "best guess" tracing that TagLab generates, which can be modified with successive positive or negative clicks until the annotator is satisfied with the delineation. In our study, we used the positive-negative click tool as a starting point for tracing, and manually edited coral boundaries as needed.

While seven different annotators traced corals for this project, all annotations were edited and quality checked by a single annotator (OM) for consistency within TagLab. To test for potential differences in accuracy caused by software or annotator identity, we instructed one annotator from SIO and ASU to trace *Pocillopora* at one site (Molokini). Comparing traced boundaries of the same corals, we found no meaningful difference in planar area between the SIO and ASU annotator (Figure S4.3A), which were using their organization's respective software of choice (TagLab for SIO, ArcGIS Pro for ASU).

Comparison of 2D and 3D area measurements

Large-area imagery can be used to generate both 2D and 3D representations of benthic environments (McCarthy et al. 2023). For this study, we used 2D orthoprojections to track the growth and survivorship of corals by tracing patches of live coral tissue in multiple years. Using orthoprojections alone, this approach generated estimates of coral planar area and growth over time. Of course, in reality corals are not flat and instead grow in three-dimensional space. As such it would be preferrable to quantify coral growth by calculating change in colony surface area and volume. This can be done using 3D data products such as digital elevation models (DEMs). DEMs have been used to calculate colony-scale metrics of structural complexity (Miller et al. 2021) and to track changes in live tissue surface area following bleaching (Kopecky et al. 2023). However, the process of generating DEM can present a challenge since some amount of interpolation is usually required to fill in gaps and holes in the "2.5D" reef surface generated via large-area imagery. The choice of settings for interpolation, or even the software used to calculate surface area from DEMs (as we demonstrate here), can lead to downstream consequences and uncertainty.

Comparing tracing results

We used the dataset of *Pocillopora* colonies traced by two annotators in different software platforms to test whether our DEMs produced consistent surface area results between software platforms. We generated a DEM for each site in each year using the software Viscore (Petrovic et al. 2014). The DEMs covered the same 12 x 12 m footprint as the orthoprojections, and were exported at the same resolution (1 pixel per mm). To generate a continuous 3D surface for our DEMs, we used a 5x5cm moving window to interpolate any missing depth values using R. We subsequently loaded the DEMs into TagLab and ArcGIS Pro, where they were co-

registered with the appropriate orthoprojection. We used these DEMs to calculate the surface area and rugosity (surface area / planar area) of *Pocillopora* colonies from Molokini using both TagLab and ArcGIS Pro, and compared surface, planar area, and rugosity calculations between software and annotators.

We found that TagLab and ArcGIS Pro produced inconsistent estimates of coral surface area, despite being given the same DEMs and coral tracing data (Figure S4/3B). ArcGIS Pro tended to produce larger surface area values than TagLab, with increasing discrepancy between software for larger corals. The led to very high rugosity values for some corals using ArcGIS Pro, indicating surface area values were up to 25x greater than planar area values for some corals. Controlling for the effect of software, we found only minor differences in surface area between annotators (Figure S4.3A).

Compared to surface area, we found more consistency in estimates of planar area across software platforms. When given the same tracing shapefile as an input, TagLab and ArcGIS Pro produced identical planar area calculations (Figure S4.3B). This prompted us to forgo surface area and instead use planar area to track coral growth in this study. Coral surface area and volume have been found to scale consistently with planar area (House et al. 2018), which suggests that the 2D estimates of coral growth we use here are still reliable indicators of coral growth over time. Efforts are underway to diagnose these surface area discrepancies between TagLab and ArcGIS Pro. In the meantime, we present this vignette as a cautionary tale for researchers that use DEMs and large-area imagery to calculate 3D metrics of coral growth and structural complexity. Rigorous QA/QC is advised to ensure that methodological choices (i.e., software, interpolation method) are not unduly biasing results.

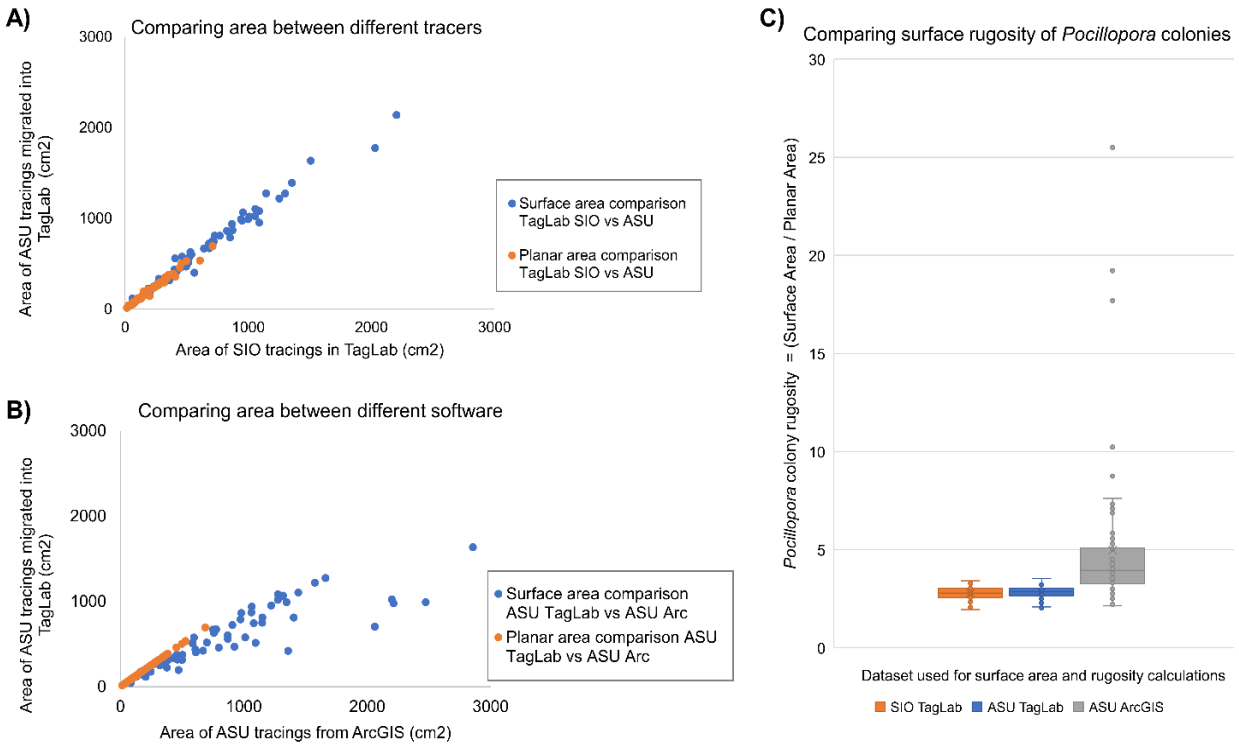

Figure S4.3: *Pocillopora* colony area compared A) between different annotators within TagLab, and B) between ArcGIS Pro and TagLab. Differences between annotators and software are shown both for planar area (orange) and surface area (blue). Values of planar area were identical between ArcGIS Pro and TagLab, but ArcGIS Pro produced higher surface area values than TagLab. C) The ratio of surface area to planar area (rugosity) is shown for *Pocillopora* at a single site. Although we used the same orthoprojection and DEM for this analysis, we found that ArcGIS Pro produced higher rugosity values than TagLab. SIO stands for Scripps Institution of Oceanography; ASU stands for Arizona State University.

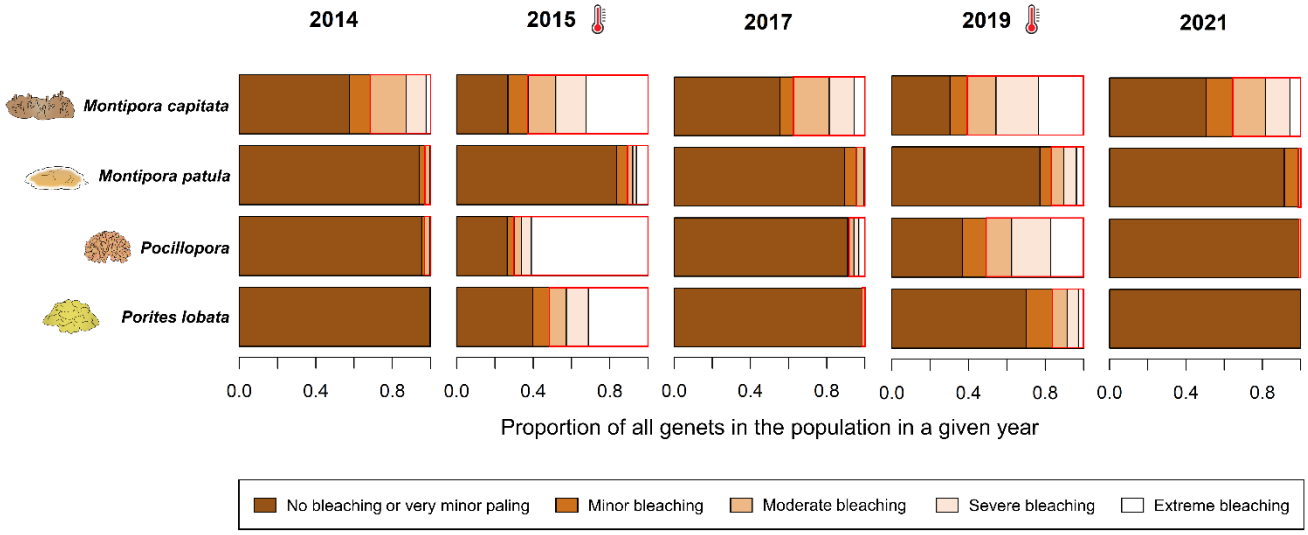

Figure S4.4: The bleaching response of each coral population is shown in each year. All genets are included, not just those that survived to the end of the timeseries. Thermometer icons denote years with documented bleaching events. Red outlines denote the proportion of genets in each population that experienced moderate, severe, or extreme bleaching. These are the genets considered "bleached" (1) for the logarithmic regression presented in Figure 4.3 (genet area vs. bleaching), while genets with no bleaching or minor bleaching were considered "not bleached" (0).

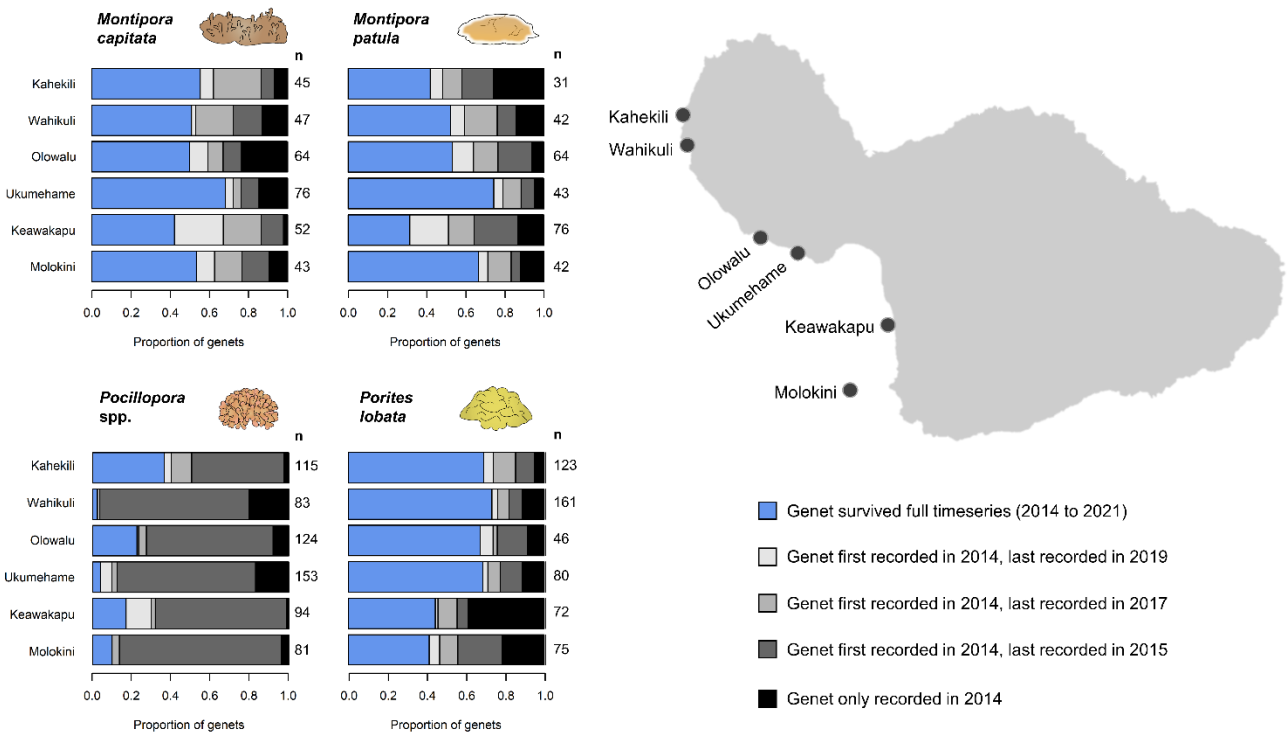

Figure S4.5: All genets are shown for each coral population, with blue representing the proportion of all genets that survived the full duration of the timeseries (2014 to 2021). Genets that did not survive are denoted with shades of grey indicating the last year they were recorded in the timeseries.

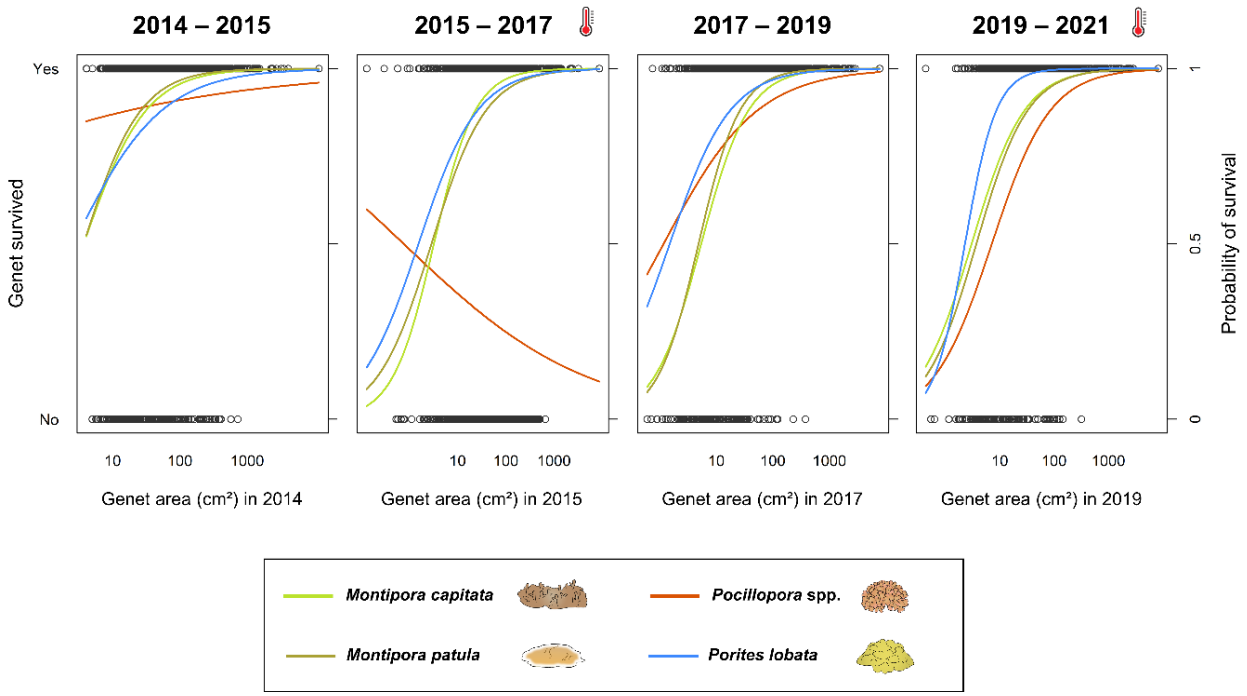

Figure S4.6: The relationship between genet planar area and survivorship is shown for each timestep. Colors denote coral taxa and thermometer icons denote timesteps following documented bleaching events. Survivorship was highest during the first timestep for all taxa, and declined following bleaching in 2015. The relationship between planar area and survivorship for *Pocillopora* inverted multiple times, while for other taxa it remained positive over the entire timeseries.

Table S4.1: Metadata for each study site, including coordinates, depth, distance from shore, coral cover at the start and end of the timeseries, and degree heating weeks (DHW) during 2015 and 2019 (both during our large-area imaging surveys and at the peak of the bleaching event).

Site	Lat.	Long.	Depth (m)	Dist. from shore (m)	2014 coral cover (%)	2021 coral cover (%)	Max DHW (2015)	DHW during survey (2015)	Max DHW (2019)	DHW during survey (2019)
Kahekili	20.9368	-156.6937	5.2	74	62.56	54.26	6.75	6.75	7.8	7.04
Keawakapu	20.7038	-156.4504	10.0	341	52.99	34.34	8.24	8.24	8.09	6.8
Molokini	20.6315	-156.4966	8.7	41	82.09	71.64	9.4	9.4	9.61	7.93
Olowalu	20.8047	-156.6072	9.7	487	52.55	43.51	8.46	8.46	9.34	8.04
Ukumehame	20.7910	-156.5843	8.6	460	43.72	44.03	7.43	7.43	6.91	5.98
Wahikuli	20.9098	-156.6917	4.5	174	40.22	40.30	6.75	6.75	7.8	7.04

Table S4.2: A frequency table showing the sample size of genets for each taxon and site, as well as the number and proportion of those genets that survived until the end of the timeseries (2021). The number of 0.5 m^2 quadrats and the associated survey area is also noted for each population. We did not use quadrats to survey *Pocillopora* (given the low density of this genus on the reef) and instead traced every *Pocillopora* within each 12 x 12 m orthoprojection. Total survey area for *Pocillopora* is lower than 144 m^2 for some populations due to gaps in the orthoprojection in some years. For consistency, when part of an orthoprojection was missing in a given year, we did not trace colonies from that section of reef in other years.

	Site	Genets tracked (n)	Survivors (n)	Proportion surviving	Quadrats (n)	Survey area (m^2)
Montipora capitata	Kahekili	45	25	0.56	10	5
	Keawakapu	52	22	0.42	13	6.5
	Molokini	43	23	0.53	11	5.5
	Olowalu	64	32	0.50	10	5
	Ukumehame	76	52	0.68	10	5
	Wahikuli	47	24	0.51	11	5.5
Montipora patula	Kahekili	31	13	0.42	25	12.5
	Keawakapu	76	24	0.32	13	6.5
	Molokini	42	28	0.67	11	5.5
	Olowalu	64	34	0.53	10	5
	Ukumehame	43	32	0.74	10	5
	Wahikuli	42	22	0.52	20	10
Pocillopora spp.	Kahekili	115	42	0.37	-	144
	Keawakapu	94	16	0.17	-	139
	Molokini	81	8	0.10	-	125
	Olowalu	124	28	0.23	-	143
	Ukumehame	153	6	0.04	-	127
	Wahikuli	83	2	0.02	-	137
Porites lobata	Kahekili	123	85	0.69	10	5
	Keawakapu	72	32	0.44	17	8.5
	Molokini	75	31	0.41	19	9.5
	Olowalu	46	31	0.67	23	11.5
	Ukumehame	80	55	0.69	10	5
	Wahikuli	161	118	0.73	10	5

Table S4.3: Pairwise comparisons of genet survivorship between sites over the timeseries (2014 to 2021). Comparisons are only shown for site pairs that did not exhibit an interaction. P values have been adjusted for multiple comparisons using the Bonferroni method.

	Contrast	Estimate	SE	P value	Sig
Montipora capitata	Kahekili - Keawakapu	0.964	0.473	0.622	n.s.
	Kahekili - Molokini	0.982	0.548	> 0.999	n.s.
	Keawakapu - Ukumehame	-2.353	0.554	**< 0.001**	***
	Keawakapu - Wahikuli	-0.858	0.477	> 0.999	n.s.
	Molokini - Olowalu 3	-0.666	0.527	> 0.999	n.s.
	Molokini - Ukumehame	-2.371	0.620	**0.002**	**
	Olowalu 3 - Ukumehame	-1.706	0.549	**0.028**	*
Montipora patula	Kahekili - Keawakapu	0.631	0.526	> 0.999	n.s.
	Kahekili - Ukumehame	-1.200	0.600	0.681	n.s.
	Kahekili - Wahikuli	-0.432	0.591	> 0.999	n.s.
	Keawakapu - Molokini	-0.878	0.493	> 0.999	n.s.
	Keawakapu - Ukumehame	-1.831	0.471	**0.002**	**
	Keawakapu - Wahikuli	-1.063	0.460	0.312	n.s.
	Molokini - Olowalu 3	0.514	0.518	> 0.999	n.s.
	Ukumehame - Wahikuli	0.768	0.543	> 0.999	n.s.
Pocillopora spp.	Kahekili - Keawakapu	1.204	0.398	**0.037**	*
	Kahekili - Olowalu 3	0.626	0.309	0.637	n.s.
	Kahekili - Ukumehame	2.602	0.475	**< 0.001**	***
	Keawakapu - Olowalu 3	-0.578	0.396	> 0.999	n.s.
	Keawakapu - Ukumehame	1.397	0.536	0.138	n.s.
	Molokini - Wahikuli	1.587	1.135	> 0.999	n.s.
	Olowalu 3 - Ukumehame	1.975	0.474	**< 0.001**	***
Porites lobata	Kahekili - Keawakapu	1.468	0.438	**0.012**	*
	Kahekili - Molokini	2.329	0.453	**< 0.001**	***
	Keawakapu - Molokini	0.862	0.443	0.778	n.s.
	Keawakapu - Ukumehame	-1.282	0.446	0.061	n.s.
	Keawakapu - Wahikuli	-1.602	0.437	**0.004**	**
	Molokini - Ukumehame	-2.144	0.461	**< 0.001**	***
	Molokini - Wahikuli	-2.464	0.452	**< 0.001**	***

Appendix 5: Supplemental Materials for Chapter 5 (Evaluating the predictive capacity of coral reef resilience assessments)

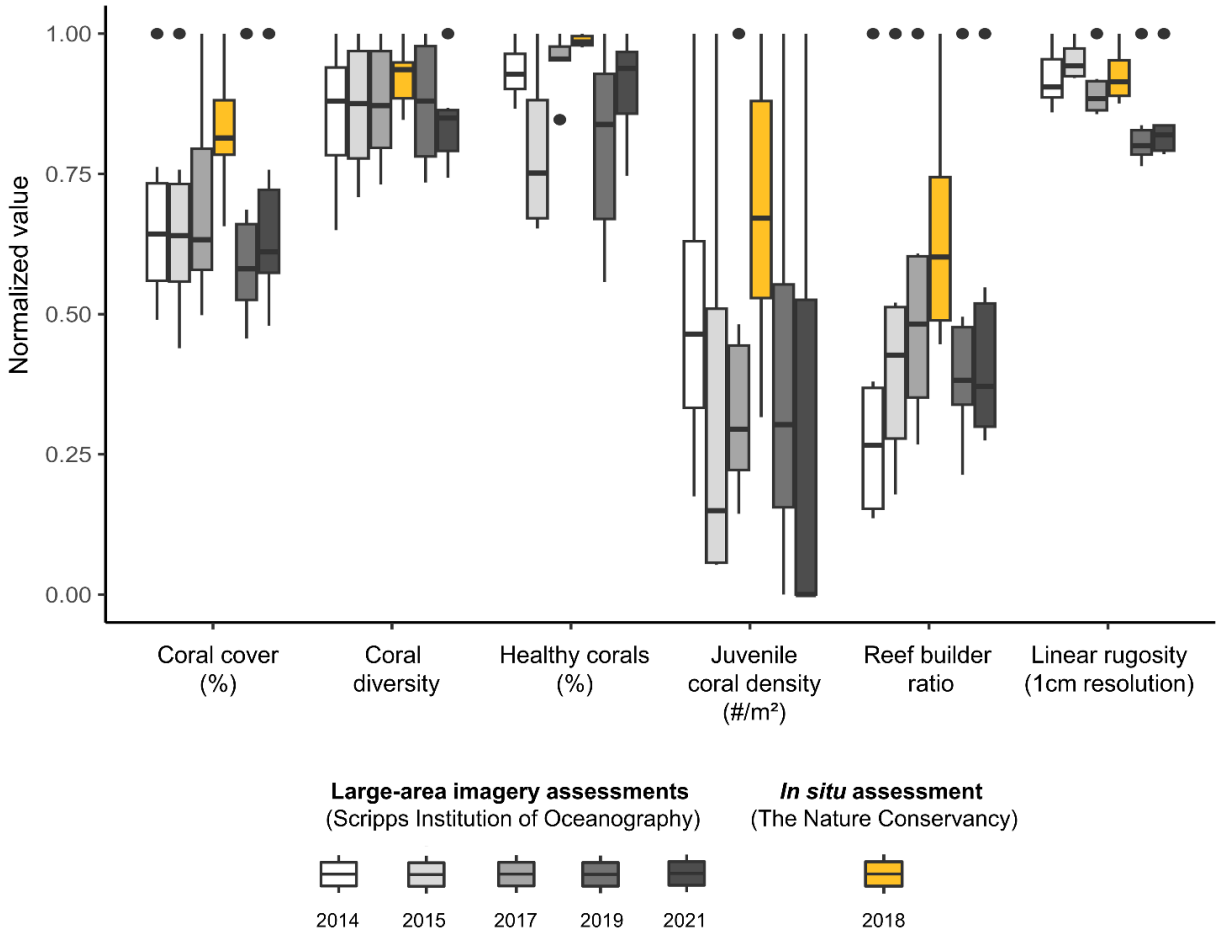

Figure S5.1: Normalized values for six resilience indicators. Boxplot colors denote the year each resilience indicator was assessed. Resilience indicators were assessed at six leeward Maui sites (Kahekili, Keawakapu, Molokini, Olowalu, Ukumehame, and Wahikuli) in six different years (2014, 2015, 2017, 2018, 2019, and 2021).

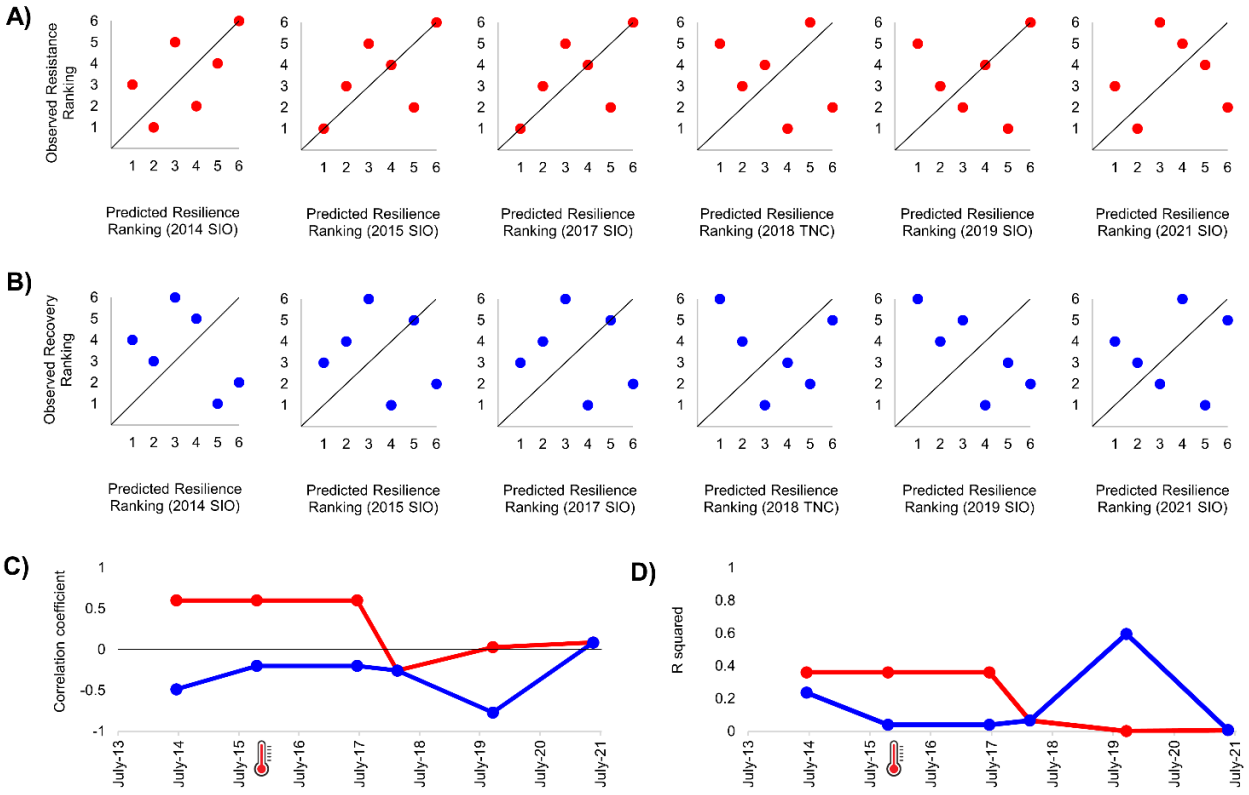

Figure S5.2: Scatterplots show the relationship between resilience rankings (1 = highest resilience, 6 = lowest resilience) and rankings of A) resistance and B) recovery observed over the timeseries. Resilience assessments were conducted by Scripps Institution of Oceanography (SIO) using data from 2014, 2015, 2017, 2019, and 2021, and by the Nature Conservancy (TNC) in 2018. The C) correlation coefficient and D) R squared value for the relationship between predicted resilience and observed resistance (red) and recovery (blue) are shown over time. The 2015 bleaching event is denoted with a thermometer icon in C) and D).

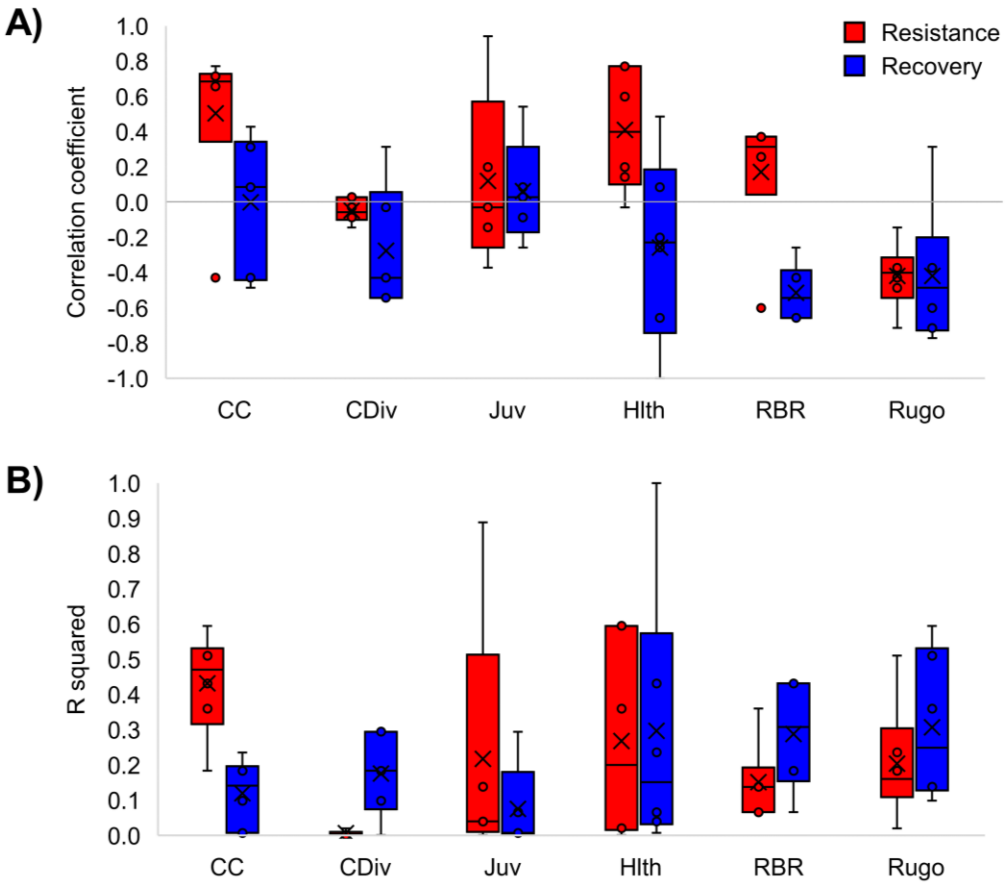

Figure S5.3: We ranked sites based on their coral cover (CC), coral diversity (Cdiv), *Pocillopora* juvenile density (Juv), coral health (Hlth), reef builder ratio (RBR), and rugosity (Rugo) in each resilience assessment year (2014, 2015, 2017, 2018, 2019, and 2021). Here we visualize the strength of the relationship between each resilience indicator and resistance (red) and recovery (blue) based on rank order. The range of A) correlation coefficients and B) R squared values are shown for each indicator across all resilience assessments. Overall, indicators showed low predictive accuracy. Coral cover and coral health were moderately good predictors of resistance, while no indicators accurately predicted recovery.

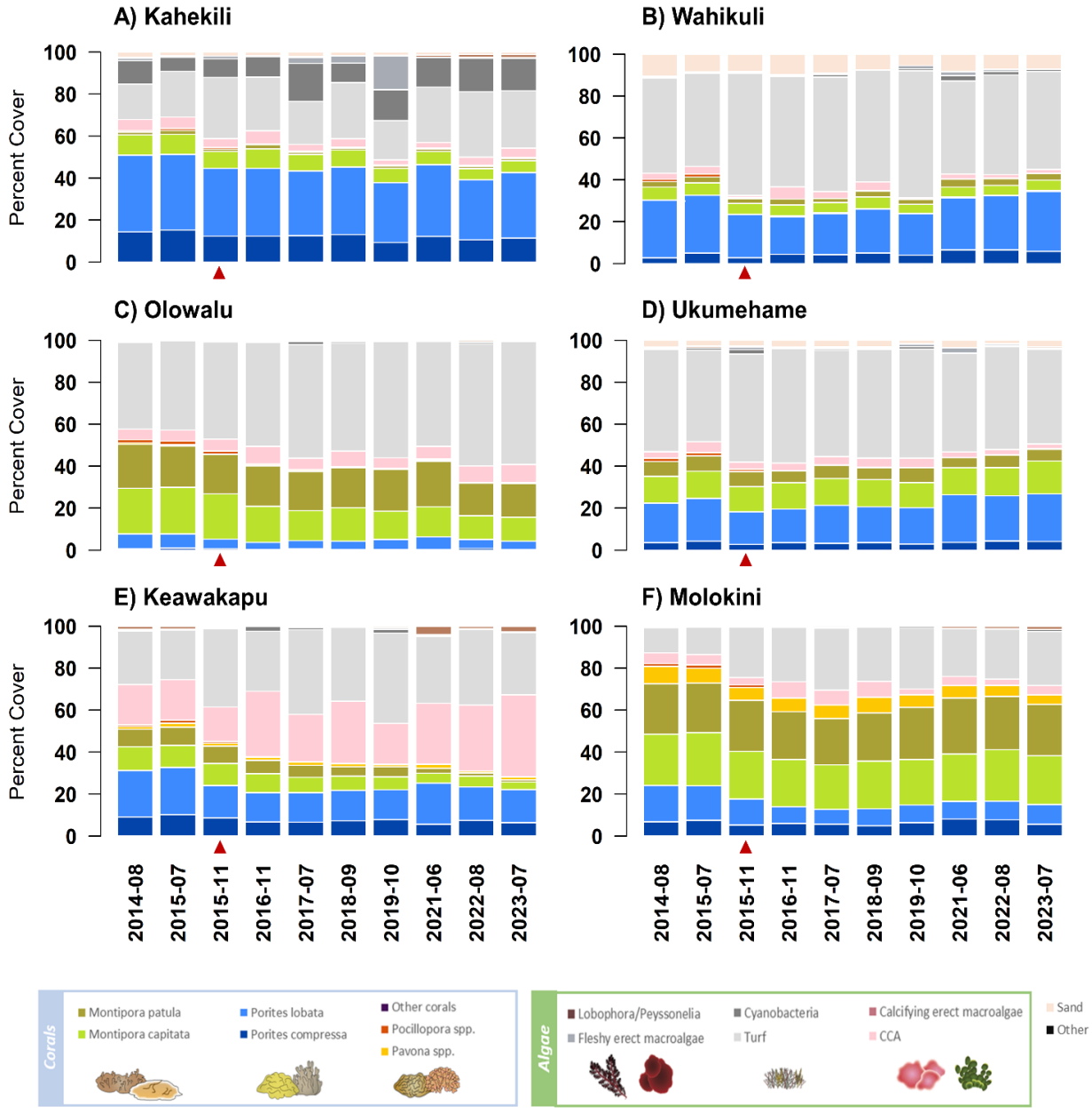

Figure S5.4: Benthic community composition at six resilience assessments sites in leeward Maui. Surveys conducted during the 2015 bleaching event are denoted with a red triangle. *Porites lobata* includes closely related massive *Porites* species that we could not confidently differentiate via imagery, such as *Porites lutea*, *Porites lichen*, *Porites brighami*, and *Porites evermani*. Taxa in the "other coral" category had low abundance (< 0.1% cover) and include *Leptastera* spp. and *Fungia* spp.

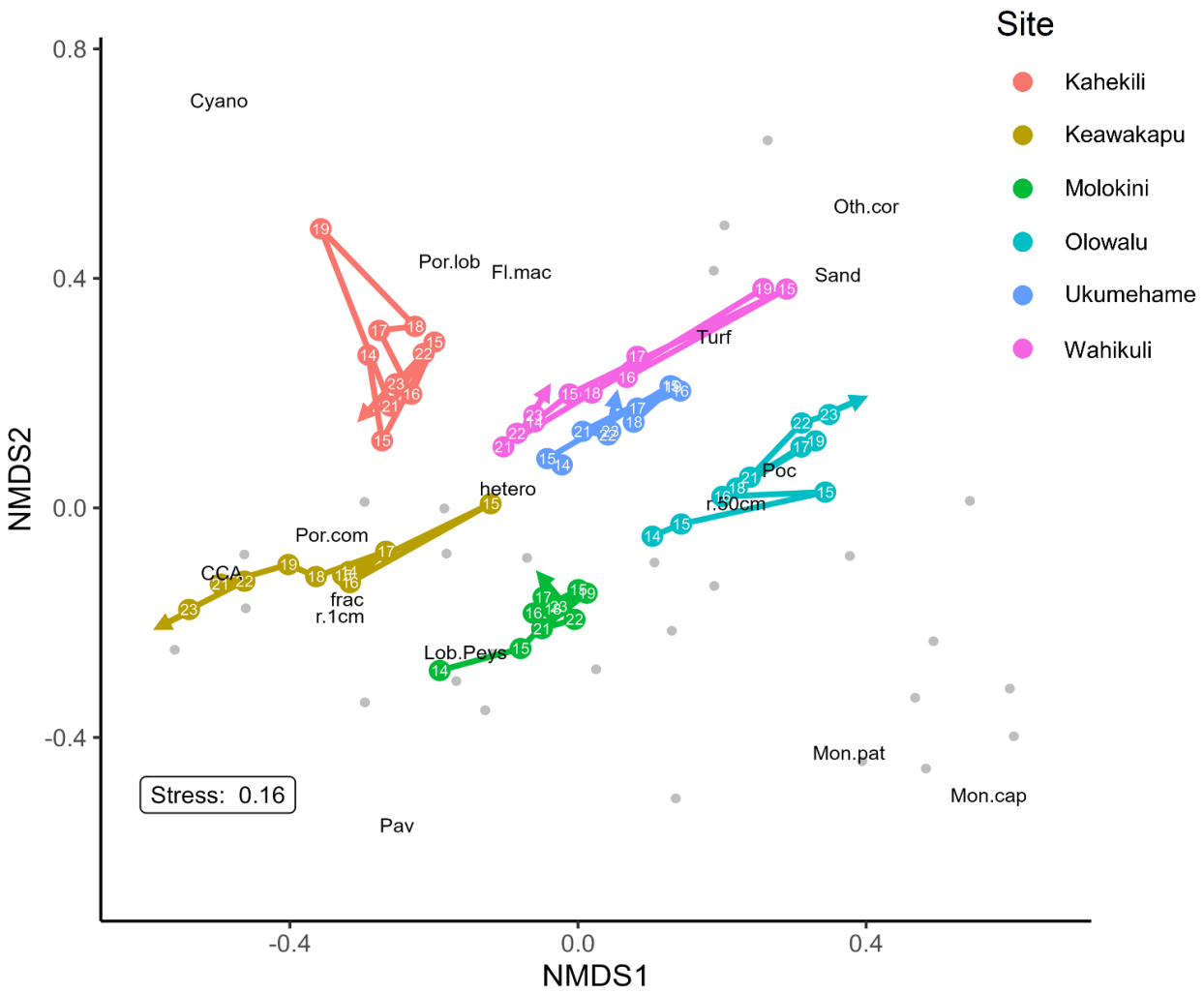

Figure S5.5: Non-metric multidimensional scaling ordination of benthic community composition at six sites in leeward Maui. Each color corresponds to a different site, while the number inside each point corresponds to the year of the survey. Surveys connected in a chronological sequence to form a successional trajectory. Grey dots represent additional sites from the Maui Nui region (surveyed in 2021). Abbreviations correspond to the following benthic variables: Mon.cap = *Montipora capitata*; Mon.pat = *Montipora patula*; Por.com = *Porites compressa*; Por.lob = *Porites lobata*; Poc = *Pocillopora* spp.; Pav = *Pavona* spp.; Oth.cor = other coral taxa; CCA = crustose coralline algae; Turf = turf algae; Cyano = cyanobacteria; Fl.mac = fleshy erect macroalgae; Lob.Peys = fleshy encrusting macroalgae; Sand = sand; r.1cm = linear rugosity measured at 1cm resolution; r.50cm = linear rugosity measured at 50cm resolution; frac = fractal dimension; hetero = landscape heterogeneity.

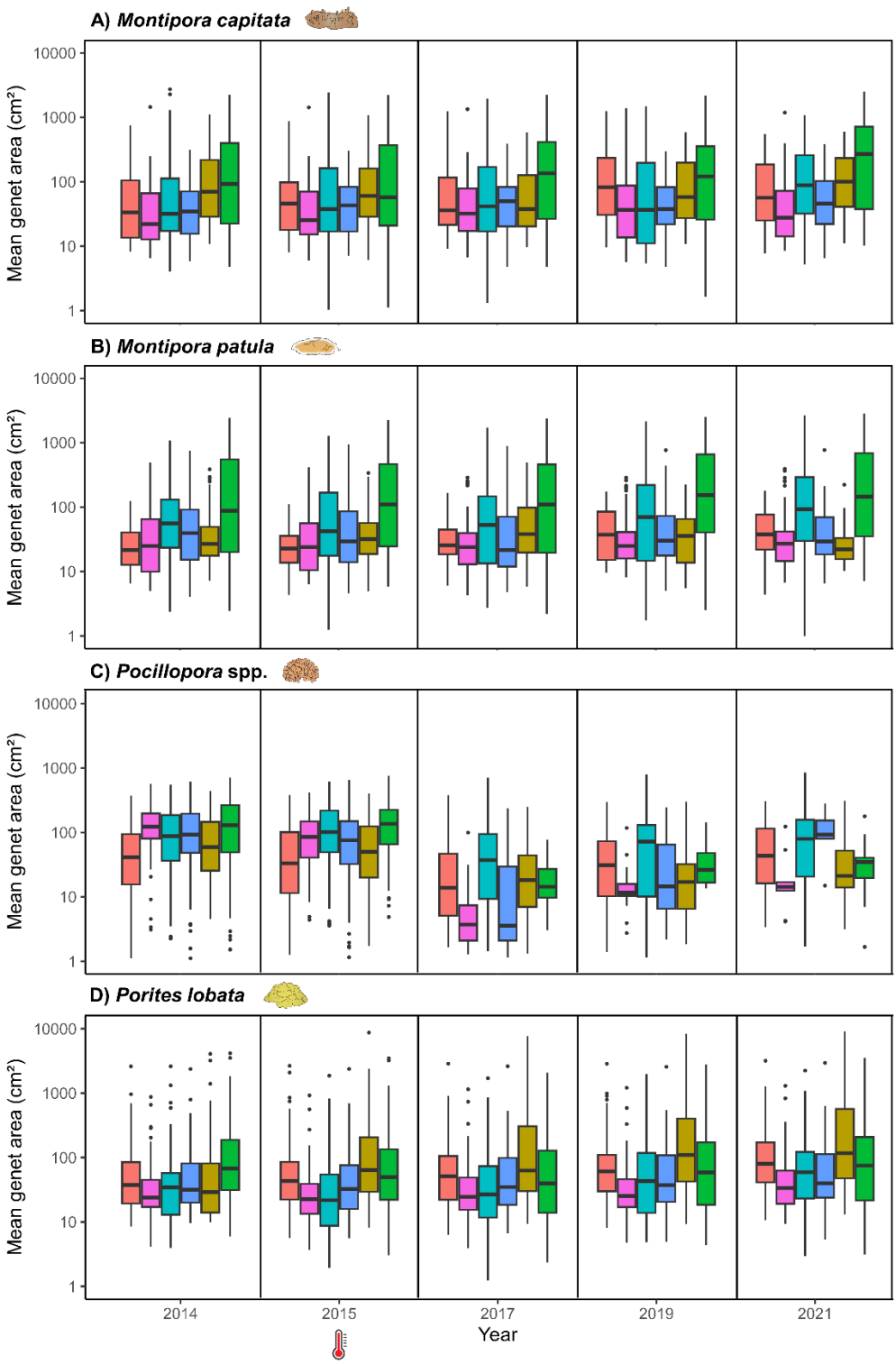

Figure S5.6: Boxplots illustrate the log-transformed planar area of genets for populations of A) *Montipora capitata*, B) *Montipora patula*, C) *Pocillopora* spp., and D) *Porites lobata* at six resilience sites in five different years. A thermometer icon denotes the 2015 bleaching event. Colors denote sites, from left to right: red = Kahekili; magenta = Wahikuli; turquoise = Olowalu; blue = Ukumehame; gold = Keawakapu; green = Molokini.

Table S5.1: The coordinates and depth of resilience sites used in this study. The exact location of sites differed slightly between the original *in situ* resilience assessment (conducted in 2018; see Maynard et al. 2019) and the follow up resilience assessments conducted here (using large-area imagery from Scripps Institution of Oceanography's long-term monitoring sites). The Nature Conservancy surveyed sites in March 2018. The Scripps Institution of Oceanography surveyed sites in July 2014, July 2015, November 2015, November 2016, July 2017, September 2018, October 2019, June 2021, August 2022, and July 2023.

Site	***The Nature Conservancy (TNC)***			***Scripps Institution of Oceanography (SIO)***			**Distance (m) between SIO and TNC sites**
	Latitude	Longitude	Depth (m)	Latitude	Longitude	Depth (m)	
Kahekili	20.93790	-156.69372	6.5	20.93677	-156.69365	5.2	126
Wahikuli	20.90983	-156.69168	3.8	20.90983	-156.69168	4.5	0
Olowalu	20.80605	-156.61222	4.3	20.80465	-156.60721	9.7	542
Ukumehame	20.79098	-156.58437	9.2	20.79098	-156.58437	8.6	0
Keawakapu	20.70482	-156.45037	9.6	20.70482	-156.45036	10.0	1
Molokini	20.63148	-156.49638	6.2	20.63148	-156.49658	8.7	20

Table S5.2: Results from 2-sample Kolmogorov-Smirnov (K-S) tests. Asterisks indicate significant differences in size frequency distributions between 2014 – 2017 (red) and 2017 – 2021 (blue). K-S tests were not conducted for populations < 10 individuals (*Pocillopora* in 2021 at Ukumehame and Wahikuli).

Taxa	Site	Number of genets			P value	
		2014	2017	2021	2014 – 2017	2017 – 2021
Montipora capitata	Kahekili	45	39	29	0.234	0.293
	Keawakapu	52	41	21	0.295	0.059
	Molokini	53	47	34	0.940	0.398
	Olowalu	74	52	40	0.628	0.200
	Ukumehame	76	65	70	0.239	0.835
	Wahikuli	47	25	29	0.088	0.419
Montipora patula	Kahekili	31	32	21	0.165	0.386
	Keawakapu	76	47	30	0.147	0.012 *
	Molokini	52	47	41	0.995	0.697
	Olowalu	78	69	53	0.037 *	0.249
	Ukumehame	43	45	44	0.541	0.569
	Wahikuli	42	43	52	0.838	0.745
Pocillopora	Kahekili	139	115	73	< 0.001 ***	< 0.001 ***
	Keawakapu	101	52	24	< 0.001 ***	0.143
	Molokini	94	17	13	< 0.001 ***	0.014 *
	Olowalu	136	41	40	0.013 *	0.121
	Ukumehame	162	32	7	< 0.001 ***	--
	Wahikuli	87	15	9	< 0.001 ***	--
Porites lobata	Kahekili	123	103	89	0.159	0.005 **
	Keawakapu	72	34	31	0.042 *	0.294
	Molokini	81	54	43	0.006 **	0.174
	Olowalu	63	52	48	0.587	0.011 *
	Ukumehame	80	74	76	0.921	0.306
	Wahikuli	161	140	160	0.779	0.006 **